An Investigation into the Applicability of Inverse Gas Chromatography to Mineral Flotation

Shiva Mohammadi-Jam

Department of Mining and Materials Engineering
McGill University
Montreal, Canada

A thesis submitted to McGill University in partial fulfilment of the requirements of the degree of
Doctor of Philosophy

December 2016

Dedication

To my outstanding husband and my best friend

Reza

Through whom I feel the most amazing expressions of love.

Without whom none of this would be possible.

Abstract

Surface energy is a fundamental thermodynamic characteristic of solids, which governs surface interactions. Surface energy measurements have attracted the attention of researchers in a wide variety of fields due to its importance in physicochemical reactions. Inverse gas chromatography (IGC) is a technique that has been applied to the characterisation of solid surfaces for more than 40 years. It is an analytical technique for evaluating physicochemical properties of materials, including surface energy. The most attractive advantage of the IGC method is its capacity to accurately characterise the surface, and some bulk, properties of materials of various shapes such as powders, particulates, fibres, and films. The technique has been recently expanded to determine the surface energetic heterogeneity of surfaces, which is a useful parameter for characterizing complex surfaces.

Mineral flotation is dependent upon the hydrophilic or hydrophobic characteristic of particles. Surface energy of valuable and gangue minerals plays an important role in the separation process. In other words, the nature and quantity of the excess energies on the surface of ore components has a decisive role in flotation process. Therefore, knowing the surface physicochemical characteristics and their overall reactivity of minerals is useful in understanding the fundamentals of flotation.

This thesis investigates the potential of applying IGC to mineral flotation. Preliminary examinations were undertaken to measure the surface energy of quartz (a naturally hydrophilic mineral) using IGC, and to evaluate the flotation recovery by microflotation tests. The surface energetics of different size ranges of quartz, pre- and post-conditioning with dodecylamine, were determined. The surface chemistry and energetics of the most abundant sulphide mineral (pyrite) was also studied using microflotation experiments and surface characterisation techniques: X-ray photoelectron spectroscopy (XPS) and IGC. The sample's surface characteristics were altered by surface activation with copper to activate the pyrite surface for hydrophobic collector adsorption. The activated and non-activated pyrite was also conditioned with potassium amyl xanthate, a common collector for sulphide minerals. The activation and conditioning processes were conducted at different pH values, which provided an opportunity to evaluate the sensitivity of IGC to the surface alterations. Combining flotation results and IGC measurements, it was verified that the methodology was capable of reliably determining the surface energetics of pure minerals, and the relationship to flotation response. It was shown that a lower surface energy implies a lower degree of hydrophilicity and work of adhesion to water. Meanwhile, it was possible to determine the surface energy heterogeneity profile of minerals, which has been a difficult challenge with conventional techniques. Surface energy heterogeneity is generated as a result of the distribution of surface sites of different energetic levels. It was revealed that surface modification made the surface of mineral particles more homogeneous, as well as decreasing the surface energy.

These findings suggested that the prediction of flotation recovery of pure minerals could be possible by surface characterisation using IGC. The research was extended to a more complicated system: the bench scale flotation of a real ore. It was observed that the floatability of the sulphide ore was directly related to surface energy values. The species with lowest surface energy floated first, and with increasing flotation time, the particles with more energetic surfaces appeared in the overflow. The work of adhesion values, also obtained from IGC analyses, confirmed the same relationship. However, the tailings showed relative low values of surface energy, despite apparent high wettability. The phenomenon was attributed to the high content of coarser particles in the tailings, and hydrodynamic effects.

Résumé

L’énergie de surface est une caractéristique thermodynamique fondamentale qui gouvernent les interactions de surface des solides. La mesure de l’énergie de surface a reçue l’attention de chercheurs provenant de domaines variés considérant l’importance des réactions physicochimiques. La chromatographie en phase gazeuse inverse (CGI) est une technique qui a été appliquée à la caractérisation des surfaces solides depuis plus de 40 ans. Il s’agit d’une technique d’analyse servant à l’évaluation des propriétés physicochimique des matériaux, incluant leurs énergies de surface. L’avantage de la technique CGI est sa capacité à caractériser de façon précise la surface ainsi que certaines propriétés volumique de matériaux ayant des formes variées, tels les poudres, particules, fibres et films. Cette technique a récemment été appliquée à la détermination de l’énergie de surface hétérogène d’une surface, il s’agit d’une caractéristique utile pour la description des surfaces complexes.

La flottation des minéraux dépend de la propriété hydrophile ou hydrophobe des particules. L’énergie de surface des minéraux de valeur et de gangue joue un rôle important dans ce procédé de séparation. Autrement dit, la nature et la quantité de l’excès d’énergie sur la surface des composants d’un minerai joue un rôle décisif sur le procédé de flottation. Il est donc utile de connaître les caractéristiques physicochimiques de surface ainsi que la réactivité des minéraux afin de fondamentalement comprendre la flottation.

Cette thèse cherche à comprendre l’application potentielle de la technique CGI à la flottation des minéraux. Une vérification préliminaire était de mesurer l’énergie de surface du quartz (un minéral naturellement hydrophobe) à l’aide de la technique CGI ainsi que d’évaluer la récupération possible par flottation à l’aide de tests de microflottation. L’énergie de surface de différentes fractions dimensionnelles de quartz avant et après traitement avec un dodécylamine ont été déterminées. La chimie et l’énergie de surface du minéral sulfureux le plus abondant (pyrite) a aussi été étudié à l’aide d’expérience de microflottation ainsi que de caractérisation de surface : la spectroscopie photoélectronique à rayons X (SPX) et la technique CGI. Les caractéristiques de surface des échantillons ont été altérées par l'activation de la surface de la pyrite avec du cuivre pour l'adsorption d'un collecteur hydrophobe.

La pyrite activée et non activée a aussi été conditionnée avec un amyl-xanthate de potassium, un collecteur bien connu pour les minéraux sulfureux. L'activation et le conditionnement ont été réalisés à différents pH, cela a permis d'évaluer la sensibilité de la technique CGI aux altérations de la surface. En combinant les résultats de la flottation aux mesures de la technique CGI, il a été validé que la méthode est capable de déterminer de façon fiable les propriétés énergétiques de surface des minéraux pures ainsi que la relation avec leur réponse à la flottation. Il a été montré qu'une faible énergie de surface implique un faible degré d'hydrophilicité et de travail d'adhérence à l'eau. Plus encore, il a été possible de déterminer le profil d'hétérogénéité de l'énergie de surface des minéraux choisis, qui est un défi complexe lorsque réalisé par des techniques conventionnelles. L'hétérogénéité de l'énergie de surface est le résultat de la distribution des différents niveaux énergétiques des sites surfaciques. Il a été révélé que la modification de la surface des minéraux rend celle-ci plus homogène et réduit leur énergie de surface.

Ces résultats suggèrent que la prédiction de la récupération par flottation de minéraux pures pourrait être possible par la caractérisation de leurs surfaces avec la technique CGI. Les recherches ont été étendues à un système plus complexe : la flottation d'un minerai réel à l'échelle laboratoire. Il a été observé que la flottabilité des minéraux sulfureux est directement reliée à la valeur de l'énergie de surface. Les espèces chimiques ayant l'énergie de surface la plus faible ont flottés en premier et avec une augmentation du temps de flottation, les particules ayant une surface plus énergétique sont apparues dans la surverse. La valeur du travail d'adhérence, aussi obtenu à partir des analyses CGI, a confirmé cette relation. Cependant, les résidus ont montrés de faibles énergies de surfaces en dépit de l'observation d'une grande mouillabilité. Ce phénomène est attribué à la grande fraction de particules grossières dans les résidus ainsi qu'à des effets hydrodynamiques.

Acknowledgements

There have been so many individuals whom I wish to thank for making my doctoral study at McGill an enlightening and productive experience. This academic journey would have not been started nor completed without each and all of the following support.

First and foremost, my sincere gratitude is due to my supervisor, Professor Kristian Edmund Waters for his invaluable guidance and support throughout the course of my doctoral studies. It was only due to his personal generosity and unwavering enthusiasm that I was able to complete my research work in a respectable manner. I especially acknowledge him for the numerous constructive comments and helpful suggestions during various stages of this thesis preparation, as well as the draft manuscripts for publication.

Completing this work would have been all the more difficult were it not for the support and friendship provided by the members of the McGill mineral processing research group and Department of Mining and Materials Engineering. Special thanks go to Darryel Boucher for his outstanding job in translating the Abstract into French. Within our research group, I have had the pleasure of working with Professor James A. Finch whose attitude towards research and life has inspired me and which contributed to my personal development.

I gratefully acknowledge my indebtedness to Dr. Daniel J. Burnett, Dr. Anett Kondor and Mr. Armando Garcia at Surface Measurement Systems for their helpful suggestions regarding SEA and DVS data analysis.

I would like to acknowledge the Natural Sciences and Engineering Research Council of Canada (NSERC) for providing funding for this work through the Collaborative Research and Development (CRD) Grant in conjunction with Vale Base Metals, Teck Resources Ltd., SGS Canada Inc., ChemIQA, Barrick Gold Corp., COREM, XPS Consulting & Testwork Services and Shell Canada for providing their financial support of this research (CRDPJ-445682-12). I would also like to acknowledge the Canada Foundation for Innovation (CFI) for the support in purchasing the Surface Energy Analyser, through the Leadership Opportunity Fund.

I would like to gratefully acknowledge the financial support of McGill University through the McGill Engineering International Tuition Award (MEITA). The Faculty of Engineering is also acknowledged for the Graduate Excellence Award in Engineering. I am also thankful to Department of Mining and Materials Engineering for Graduate Research Excellence Award in Mining and Materials Engineering and Graduate Research Enhancement and Travel (GREAT) Award.

I am especially grateful to all my friends for their friendly and professional support, and for helping me in my adjustment to the new academic and cultural environment.

I am deeply grateful to my wonderful sister and brothers for providing emotional support and encouragements. Thank you for your unconditional love.

I do not know how to thank the most precious thing to me, my sensitive and strong boy, who makes me feel the most blessed woman on the face of the Earth. Thank you Shahab jan for your patience and understanding my absences while I was working towards the completion of this work. I love you with all my heart and soul.

Finally, and most importantly, my deepest appreciation goes to my great source of motivation and inspiration, my beloved parents for their patience, unwavering kindness and grace, and for unending reinforcement throughout my educational endeavours. A special acknowledgement to my mother for the stressing moments I had to put her through whenever having an exam.

With all gratitude and love!

Preface and Contribution of Authors

This thesis is a collection of four manuscripts prepared by the candidate according to the guidelines for a manuscript-based dissertation published by Graduate and Postdoctoral Studies office of McGill University. The first three manuscripts have already been published, while the last one has been submitted, and is currently under consideration for publication.

This thesis is comprised of seven chapters and one appendix.

Chapter 1 includes a general introduction, context and objective of the thesis.

Chapters 2 and 3 provide a literature review and background on mineral processing and inverse gas chromatography (IGC) technique, respectively. Chapter 2 briefly presents mineral processing, definitions, basics and goals. The fundamental operations in mineral processing are introduced, with a focus on the flotation process.

In Chapter 3, inverse gas chromatography (IGC) is introduced. Information concerning the history, instrumentation and applications is discussed. In addition, examples of the many experiments developed for IGC, materials that have been analysed, and the properties that can be determined using IGC are selected and described. The content of this chapter has been published as a review article as follows:

Publication 1: Mohammadi-Jam, S., Waters, K.E. (2014), Inverse gas chromatography applications: A review, *Advances in Colloid and Interface Science*, 212, 21-44.

Chapter 4 discusses the relationship between surface free energy of quartz and flotation recovery. This study has been carried out on quartz mineral of different sizes, before and after surface treatment with dodecylamine, as a collector. The result has been published as a journal article as follows:

Publication 2: Mohammadi-Jam, S., Burnett, D.J., Waters, K.E. (2014), Surface energy of minerals–Applications to flotation, *Minerals Engineering*, 66-68, 112-118.

Chapter 5 details investigations into the effect of surface treatments on the thermodynamic properties of pyrite. The samples were activated and conditioned with copper and xanthate, respectively under different conditions. This work has been published as following journal article:

Publication 3: Mohammadi-Jam, S., Waters, K.E. (2016), Inverse gas chromatography analysis of minerals: pyrite wettability, *Minerals Engineering,* 96-97 (2016) 130-134.

In Chapter 6, the application of surface energy measurements to the flotation recovery of a nickel-copper sulphide ore was investigated. The flotation tests were carried out in a bench scale flotation cell, and the surface energetics were determined by using IGC.

Publication 4: Mohammadi-Jam, S., da Silva, G.R., Waters, K.E., Inverse gas chromatography for bench scale flotation of sulphide ore (manuscript).

Chapter 7 concludes the dissertation, proposes avenues for future research and the contributions of this thesis to original knowledge.

The appendix includes the X-ray photoelectron spectroscopy (XPS) spectra of the pyrite samples (Chapter 5).

All the experiments including material preparations, data collection and analyses were designed and conducted by the candidate. All the manuscripts are co-authored by Professor Kristian E. Waters in his capacity as the candidate’s supervisor. He provided guidance throughout the whole research project, reviewed the manuscripts and contributed to the general layout and discussions. **Dr. Daniel J. Burnett** contributed to the IGC method development for quartz, and provided insightful comments (Publication 2). **Gilberto R. da Silva** contributed to the sulphide ore flotation experiments (Publication 4).

Table of Contents

List of Tables

List of Figures

Nomenclature and Abbreviations

a	Cross sectional area [m^2]
AFM	Atomic force microscopy
AN	Acceptor number
BET	Brunauer-Emmett-Teller
CALB	Candida antarctica lipase B
CGAs	Colloidal gas aphrons
CNCs	Cellulose nanocrystals
CNFs	Carbon nanofibers
CNTs	Carbon nanotubes
CVD	Chemical vapour deposition
DDA	Dodecylamine ($C_{12}H_{27}N$)
DDS	Drug delivery system
DM	Dry milling
DN	Donor number
ECP	Equilibrium capillary pressure
ESO	Epoxidised soybean oil
FC	Finite concentration
F_c	Flow rate of carrier gas [mL min^{-1}]
FID	Flame ionisation detector
FIGC	Frontal inverse gas chromatography
GC	Gas chromatography
GDLs	Gas diffusion layers
HSAGs	High-surface-area graphites
HSP	Hansen solubility parameter [$MPa^{1/2}$]
HSWM	High shear wet milling
HWE	Hot water extractor

ICP	Inductively coupled plasma spectroscopy
ICP-AES	Inductively couples plasma atomic emission spectroscopy
ID	Infinite dilution
IGC	Inverse gas chromatography
IGLC	Inverse gas-liquid chromatography
IGSC	Inverse gas-solid chromatography
ILs	Ionic liquids
j	James-Martin compressibility correction factor
K_A	Acid number
K_B	Base number
LC	Liquid crystal
M	Molar mass [g mol^{-1}]
m_s	Mass [g]
MgSt	Magnesium stearate ($Mg(C_{18}H_{35}O_2)_2$)
MIBC	Methyl isobutyl carbinol (($C_6H_{14}O$))
MWNTs	Multiwalled carbon nanotubes
n	Refractive index
N_A	Avogadro’s number ($6.022140857 \times 10^{23}$ mol^{-1})
NFCs	Nanofibrillated cellulose
PAN	Polyacrylonitrile ($(C_3H_3N)_n$)
PCB	Pyrolytic carbon black
P_{DP}	Deformation polarisation of probe
P_{DS}	Deformation polarisation of solid
PEMA	Poly(ethyl methacrylate) ($(C_6O_2H_{10})_n$)
PE	Polyethylene ($(CH_2CH_2)_n$)
PEMFC	Polymer electrolyte membrane fuel cell
PEO	Poly(ethylene oxide) ($(CH_2CH_2O)_n$)
PMMA	Poly(methyl methacrylate) ($(C_5O_2H_8)_n$)
PVC	Poly(vinyl chloride) ($(C_2H_3Cl)_n$)
R	Gas constant (8.314 J K^{-1} mol^{-1})

RFGC	Reversed-flow gas chromatography
RH	Relative humidity
SBS	Sensor-based sorting
SEA	Surface energy analyser
SEM	Scanning electron microscopy
T	Absolute temperature [K]
t_0	Dead time [min]
TCD	Thermal conductivity detector
T_g	Glass transition temperatures [K]
t_R	Retention time [min]
TWPC	Titanate coupling agent-modified pyrolytic carbon black
V_g^0	Specific retention volume [ml g^{-1}]
V_N	Net retention volume [ml]
W_{adh}	Work of adhesion [J m^{-2}]
W_{co}	Work of cohesion [J m^{-2}]
XPS	X-ray photoelectron spectroscopy
θ	Contact angle
γ^D	Dispersive component of surface free energy [J m^{-2}]
γ_L^D	Dispersive component of surface free energy for liquids [J m^{-2}]
γ_S^D	Dispersive component of surface free energy for solids [J m^{-2}]
γ^{SP}	Specific component of surface free energy [J m^{-2}]
γ^T	Total surface free energy [J m^{-2}]
γ_{CH_2}	Free energy of adsorption of one methylene group (CH_2) (≈ 35.6 J m^{-2})
γ_{LV}	Liquid-vapour interfacial free energy [J m^{-2}]
γ_S^+	Contribution of Lewis acid to the surface free energy [J m^{-2}]
γ_S^-	Contribution of Lewis acid to the surface free energy [J m^{-2}]
γ_{SL}	Solid-liquid interfacial free energy [J m^{-2}]
γ_{SV}	Solid-vapour interfacial free energy [J m^{-2}]
ΔG	Gibbs free energy changes [J]

ΔG_{ad}^{0}	Standard molar Gibbs free energy changes of adsorption [J mol^{-1}]
ΔG_{de}^{0}	Standard molar Gibbs free energy changes of desorption [J mol^{-1}]
ΔG_{ad}^{D}	Dispersive component of Gibbs free energy change of adsorption [J]
ΔG_{ad}^{SP}	Specific component of Gibbs free energy change of adsorption [J]
ΔH	Sorption Enthalpy [J]
ΔS	Sorption Entropy [J K^{-1}]
δ	Hildebrand's solubility parameter [$J^{1/2}$ $m^{-3/2}$]
ρ	Density [g cm^{-3}]
χ_{T}	Topological index

CHAPTER 1

INTRODUCTION

1.1. Introduction

Due to the important role of surface energy in physicochemical interactions, surface energy measurement has attracted the attention of material and surface researchers. Determining the surface energy of liquids (surface tension) is straightforward. It is based on measuring the energy a surface requires to increase its area by one unit. However, the same techniques are not effective for solids due to their resistance against deformation. Contact angle measurement is one of the most widely utilised methods for determining surface energy of solids. However, results for powders are difficult to obtain compared to those of smooth, flat surfaces due to surface roughness, porosity and irregular shapes. A comprehensive review by Buckton [1] discussed the limitations of various methods for measuring the contact angle for powders. Contact angle and surface free energy have also been determined through Washburn [2-4] and equilibrium capillary pressure (ECP) [5, 6] methods. However, particle size, packing time, and pore geometry can all affect these measurements, which are the limitations of liquid-based surface energy techniques. Parsons *et al.* [7] outlined the inherent errors associated with contact angle measurements using liquid penetration. For example, determining the liquid penetration rate through the powder was suggested to be the major source of error in liquid penetration experiments. In addition, it was concluded that the error associated with the choice of perfectly wetting liquid, with a small contact angle, was significant. Furthermore, wetting techniques typically only yield the average surface free energy. The Washburn method, in which the capillary rise of various liquids is monitored, also has limitations because of the absorption of probe liquid into the bulk sample during analysis [8]; this can be particularly challenging for polymers and other organic materials. Hydrophobicity of minerals has also been determined through contact angle measurements by use of time of flight secondary ion mass spectrometry (ToF-SIMS) [9-13]. It is a destructive technique which causes some samples to show different characteristics after being analysed [14]. Accurately determining the surface characteristics of minerals leads to an understanding of the mechanism of interfacial behaviour. All of the above techniques have their merits and limitations in measuring the hydrophobic nature of particles.

Inverse gas chromatography (IGC) is a versatile, powerful, sensitive and relatively fast technique for characterizing the physicochemical properties of materials. Due to its applicability in determining surface properties of solids in any form such as films, fibres and powders of both crystalline and amorphous structures, IGC became a popular technique for surface characterisation, used extensively soon after its development. One of the most appealing features of IGC that led to its popularity among analytical scientists in the early years was its similarity in principle to analytical gas chromatography (GC). The main aspect which distinguishes IGC experiments from conventional GC is the role of mobile and stationary phases. In contrast to conventional GC, the material under investigation is placed in the chromatographic column and a known probe vapour is used to provide information on the surface. Since IGC is a gas-phase technique, it is not affected by the same surface roughness problems of contact angle methods and the bulk absorption phenomenon can be minimised.

Flotation is a physicochemical separation method widely used in various industries such as mineral processing, removing ink from recycled paper, waste water treatment, and recovering silver in metallic form from photographic residues. It separates particles based on their tendency to adhere to either air bubbles or water in slurry. Particles with a higher affinity to water are wetted and stay in the liquid phase, whilst water-repellent particles attach to air bubbles and are carried to the slurry surface to be removed. Flotation is the most commonly used technique applied in mineral processing for separating valuable minerals from waste (gangue). These minerals may be crystalline or amorphous, powders or fibres. Since flotation deals with the hydrophilic or hydrophobic characteristics of a mineral surface, the surface energy of both valuable and gangue minerals plays a significant role in the separation.

1.2. Objectives and Scope

The overriding objective of this research was to link the surface energy to flotation response, in order to use inverse gas chromatography (IGC) technique to further understand the fundamentals behind flotation. To employ this relationship efficiently, the capability of IGC to evaluate the surface energy of mineral particles was examined, first by characterising the surfaces of two different pure minerals of different sizes, using IGC and laboratory scale flotation experiments. The minerals were also surface-treated to change their wettability and examine the IGC potential in detecting the surface energetic changes. The next step was to study a real ore using IGC and bench scale flotation experiments. The separation was improved by modifying the hydrophobicity of certain ore components using a collector.

References

[1] G. Buckton, Contact angle, adsorption and wettability—a review with respect to powders, Powder Technology, 61-3 (1990) 237-249.

[2] E.W. Washburn, The dynamics of capillary flow, Physical Review, 17-3 (1921) 273.

[3] E. Chibowski, L. Holysz, Use of the Washburn equation for surface free energy determination, Langmuir, 8-2 (1992) 710-716.

[4] E. Chibowski, L. Hołysz, On the use of Washburn's equation for contact angle determination, Journal of Adhesion Science and Technology, 11-10 (1997) 1289-1301.

[5] D. Diggins, L.G. Fokkink, J. Ralston, The wetting of angular quartz particles: capillary pressure and contact angles, Colloids and Surfaces, 44 (1990) 299-313.

[6] D. Diggins, J. Ralston, Particle wettability by equilibrium capillary pressure measurements, Coal Preparation, 13-1-2 (1993) 1-19.

[7] G.E. Parsons, G. Buckton, S.M. Chatham, The extent of the errors associated with contact angles obtained using liquid penetration experiments, International Journal of Pharmaceutics, 82-1 (1992) 145-150.

[8] L. Segeren, M. Wouters, M. Bos, J. Van den Berg, G. Vancso, Surface energy characteristics of toner particles by automated inverse gas chromatography, Journal of Chromatography A, 969-1 (2002) 215-227.

[9] S. Brito e Abreu, W. Skinner, Determination of contact angles, silane coverage, and hydrophobicity heterogeneity of methylated quartz surfaces using ToF-SIMS, Langmuir, 28-19 (2012) 7360-7367.

[10] S. Brito e Abreu, C. Brien, W. Skinner, ToF-SIMS as a new method to determine the contact angle of mineral surfaces, Langmuir, 26-11 (2010) 8122-8130.

[11] S. Brito e Abreu, W. Skinner, ToF-SIMS-derived hydrophobicity in DTP flotation of chalcopyrite: Contact angle distributions in flotation streams, International Journal of Mineral Processing, 98-1 (2011) 35-41.

[12] S. Brito e Abreu, W. Skinner, Predicting the surface chemistry contribution to the flotation recovery of chalcopyrite by ToF-SIMS, Minerals Engineering, 24-2 (2011) 160-168.

[13] C. Priest, N. Stevens, R. Sedev, W. Skinner, J. Ralston, Inferring wettability of heterogeneous surfaces by ToF-SIMS, Journal of Colloid and Interface Science, 320-2 (2008) 563-568.

[14] F.C. Krebs, Stability and Degradation of Organic and Polymer Solar Cells, 1st ed., John Wiley & Sons, Ltd, 2012.

CHAPTER 2

MINERAL PROCESSING

2.1. Introduction

Minerals are naturally formed substances in the crust of the earth. Some minerals are rare and precious such as diamond, while others are more abundant and often considered ordinary, such as quartz. The distribution of metals in the earth depends on geologic processes that have taken place. Metals are rarely found in their native or metallic form; gold and platinum principally occur in their pure metallic state, while others are found in the form of sulfides, carbonates, and chlorides. Some are found in both metallic and compound form such as silver, copper and mercury [1]. The main categories of minerals are oxides, carbonates, sulphides, sulphates, phosphates, silicates, halides. Oxides host metals such as aluminium (bauxite), iron (magnetite and hematite), tin (cassiterite), chromium (chromite), manganese (pyrolusite), nickel (laterite) and uranium (uraninite). Carbonates are the source of sodium (soda ash or soda crystal), calcium (limestone) and magnesium (magnesite). Sulphides are the source of metals such as copper (chalcopyrite), zinc (sphalerite), nickel (pentlandite), lead (galena), mercury (cinnabar) and iron (pyrite). Calcium is found as sulphates (gypsum), vanadium as phosphates, and zirconium and aluminium as silicates. Silicate minerals are the largest and most important minerals, making up more than 90% of Earth’s crust. Halides are compounds with chlorine, fluorine, bromine and iodine of sodium and potassium.

Ore deposits are the host of naturally occurring minerals from which the large bulk of structural and functional materials are extracted by mining. Following mining, the ore is prepared for the extraction of valuable contents. The first, major process in extractive metallurgy is to concentrate minerals from their ores is mineral processing, also known as ore beneficiation and mineral dressing. However, mineral processing terminology can be defined as the science and art of extracting valuable commodities, which are not necessarily metals, from raw materials extracted from the earth. Most of the processes involve physical procedures in which the chemical nature of the minerals does not play a significant role. However, some processes are essentially based on the differences in physicochemical surface properties of the components of the ore body.

Mineral processing involves two major operations; liberation to release the grains of valuable mineral from the waste (gangue); and concentration to separate valuable minerals from gangue [1]. A full understanding of these processes and the effective parameters is important for determining the impact of the various conditions on the extraction efficiency and recovery of metals.

2.2. Comminution

The primary operation to liberate the valuable minerals from their interlocked state is the comminution (size reduction) process. Size reduction also produces a greater surface area available for chemical reactions. The process involves crushing and grinding, with size classifiers (such as screens and hydrocyclones) used to control the size distribution of the particles across the various stages of size reduction. Optimum liberation leads to the coarsest possible particle size of the cleanest particles of both valuable minerals and gangue. A good liberation is crucial for subsequent physical separation or chemical extraction. In addition, the final particle size distribution must be the right one from the separation process to be employed.

2.3. Concentration

Concentration involves the separation of valuable minerals from gangue based on differences in colour, density, magnetic susceptibility, electrical conductivity and surface chemistry.

2.3.1. Sorting

Sorting is a separation method based on the visual and fluorescing differences between valuable minerals and gangue. Sorting by hand is the oldest separation method in the history of mineral processing, but is not common today. The visual differentiations have been further exploited in the development of automated systems known as sensor-based ore sorting (SBS) [1]. The electro-optic detectors in these systems collect the data from the response of the particles to UV, visible, IR, X-ray, laser or gamma rays, and facilitate a separation based upon the response.

2.3.2. Gravity Separation

Gravity separation exploits the differences between density values and hydraulic properties of mineral particles which result in the variation of particle movement in a fluid medium. Dense medium separation is a type of gravity concentration in which a suspension of a finely ground heavy mineral is used as a high density fluid to prepare a slurry of particles. The particles having density lower than the medium will float and are separated from the denser particles, which sink.

2.3.3. Magnetic Separation

Magnetic separation separates particles based upon their different magnetic properties. Depending on the type of the magnetic characteristic (ferromagnetic, diamagnetic and paramagnetic), magnetic fields of different intensities are used.

2.3.4. Electrostatic Separation

Electrostatic separation is based on the differential conductivity of minerals using an electrical field. This process is efficiently accomplished by charging the particles. It requires a perfectly dry feed, and the operation has a very low capacity for fine particulates [1].

2.3.5. Froth Flotation

Flotation, or more specifically froth flotation, is the most important method of mineral processing and widely used technique for ore beneficiation. The technology was developed in the early 20th century and was first applied to the separation of sulphide minerals [2]. Despite a century of studies, there remain many aspects of flotation that are poorly understood. In flotation, valuable minerals are separated from gangue based on different physicochemical characteristics of their surfaces. These minerals may be crystalline or amorphous, powders or fibres. In other words, metals, non-sulfide and sulfide minerals can be separated by froth flotation. The particles that are readily wetted and do not attach to bubbles are hydrophilic, and those particles that have a tendency to adhere to bubbles are hydrophobic. In flotation, air is passed through an ore slurry (which may be agitated). The hydrophobic material attaches to an air bubble, rises to the surface, forming a mineralised froth. This froth overflows a lip at the top of the flotation vessel, and is recovered, commonly as the concentrate.

The principle of froth flotation is illustrated in Figure 2.1 [1]. Mechanical flotation cells are usually mechanically agitated by using an impeller to circulate the pulp and keep the particles in suspension, in addition to providing the shear to generate the fine bubble size distribution. This promotes the particle-bubble collisions, resulting in the attachment of hydrophobic particles to bubbles. Air is introduced through the impeller shaft. Floatable components are picked up by air bubbles, and rise through the pulp to the surface, where they are collected as concentrate. Nonfloatable materials are discharged from the base of the column, usually as tailings stream.

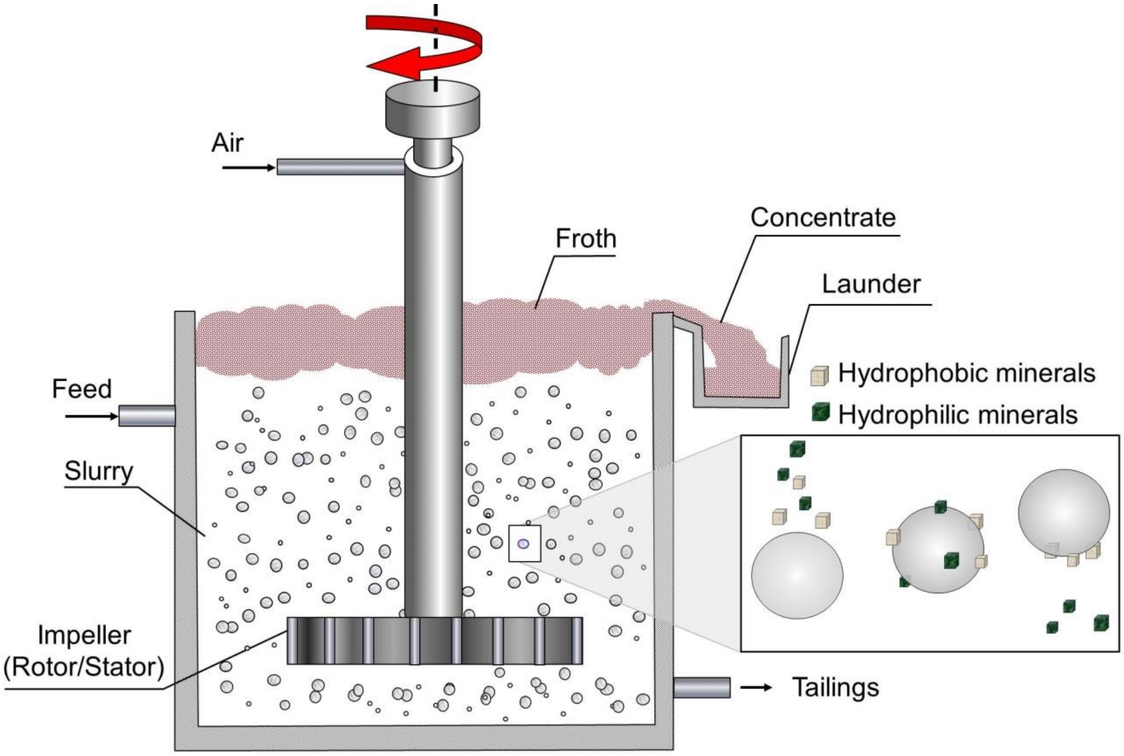

Figure 2.1. Schematic illustration of a mechanical flotation cell [1].

The principle of a three phase contact angle was introduced by Thomas Young [3]. This was further developed into what is known as Young's Equation [4]:

$$\gamma_{SV} = \gamma_{SL} + \gamma_{LV} \cdot \cos\theta \qquad (2-1)$$

where γ_{SV}, γ_{SL} and γ_{LV} are solid-vapour, solid-liquid and liquid-vapour interfacial free energies, respectively. The contact angle, θ, is the angle formed between the solid-liquid interface and the liquid-vapour interface. Hydrophobic particles form a larger contact angle than hydrophilic particles when interacting with bubbles in the flotation process. The efficient capture of desired particles by air bubbles is key to a successful separation by flotation. Naturally hydrophobic minerals such as molybdenite and talc can be directly floated and separated from other minerals. However, most minerals are naturally hydrophilic and need to be hydrophobised to be effectively floated.

Flotation selectivity and recovery (see Section 2.4.2) of valuable minerals are highly dependent on the surface chemistry of the particles, which can be altered by manipulating the surface properties using chemical reagents such as collectors, frothers, modifiers (activators, depressants and pH control reagents) and flocculants. Collectors are surface active reagents which adsorb on mineral surfaces and enhance the particle hydrophobicity. They are classified as being anionic, cationic and non-ionic depending on their ionic charge. The attachment of collectors to a particle's surface can be through a physisorption or chemisorption mechanism. The adsorption of the collectors can be controlled by adding activators or depressants to enhance or prevent the collector adsorption on the mineral particle surface, respectively. The attraction of the collectors can also be manipulated by changing the mineral surface charge or the mechanism of the adsorption. This can be achieved by pH adjustments.

Frothers are surfactants (surface active reagents) used to produce and stabilise small bubbles, by inhibiting coalescence. Frothers also increase flotation recovery by strengthening the froth layer. Moreover, these reagents improve the emulsification of oily collectors [5]. The most common frothers are aliphatic alcohol, containing an O-H group or polyglycols based on ethylene or propylene oxides or a combination of these two types. Methyl isobutyl carbinol or 4-methyl-2-pentanol, known as MIBC is the most well-known of alcohol-based frother.

Flotation recovery is influenced by the surface and interface characteristics of particles and bubbles, particle-bubble collision phenomenon, and froth stability. Therefore, there are numerous parameters that influence the yield and selectivity of this process, such as surface chemistry and reactivity of particles [6-17], particle shape and roughness [18-22], particle size [23-32], froth structure and stability [33-40], pulp chemistry and stability [41-43] and conditioning method (reagents, concentration, time and pH) [15, 44-50].

2.4. Measures of Separation

Complete separation of valuable minerals from gangue, which is the main objective of mineral processing, is rarely possible. Grade and recovery are the important considerations when reporting separation efficiency, and the economic potential of the process.

2.4.1. Grade

Grade refers to the concentration of the component of interest; metal or mineral present within a stream; feed or product of separation. It can be expressed as percentage, parts per million (ppm) or grams per ton (g t^{-1}).

2.4.2. Recovery

The percentage of the total material of interest obtained from the original ore. The recovery of a separation process is a function of both the characteristics of the feed and operating conditions. The relationship between grade and recovery can indicate the operation performance, and from the grade-recovery curves the optimal points can be determined to identify operating conditions that yield improved separation performance. Figure 2.2 compares the copper grade and recovery for a copper-nickel sulphide ore before and after microwave radiation for 120 s [51]. The curve shows that microwave radiation resulted in a noticeable increase in copper recovery and grade, indicating a remarkable improvement on the flotation efficiency.

A serious disadvantage of using grade-recovery curves to compare the performance of different flotation operations is that the curve is very sensitive to variance of feed grade and feed rate [52].

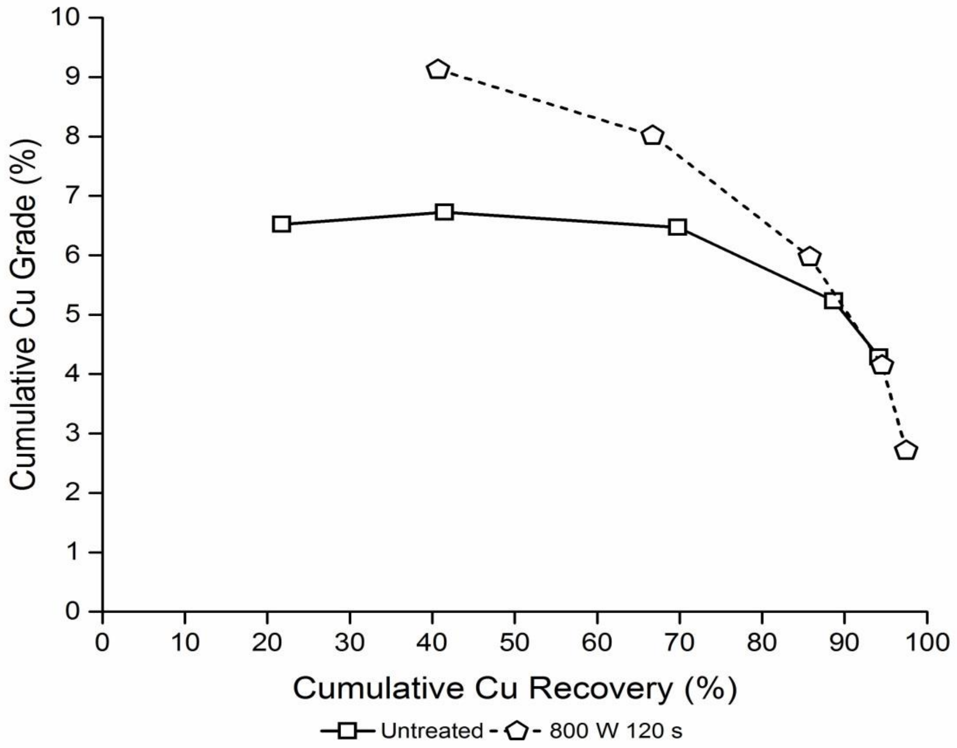

Figure 2.2. Copper grade-recovery curves of the untreated and treated ore with microwave radiation at 800 W, adapted from Marion *et al.* [51].

2.5. Conclusions

Mineral processing is a vital component of the extractive metallurgy, producing a concentration of a valuable metal that is economical to purify using pyro and hydrometallurgical processes. Froth flotation is the most important, most widely used method for concentrating valuable minerals in mineral processing. In order to reach an optimised condition in flotation, it is critical to take all types and values of inter-related parameters into account. Hence, it is difficult to evaluate the effect of all involved parameters individually, and as a result, it has been difficult to develop a predictive model for flotation process. However, fundamental studies on the surface chemistry of particles using new techniques can lead to a better understanding of their flotation behaviour. One such aspect of surface chemistry is surface energy, which is an integral part of Young's Equation, and controls the affinity of a surface to water. The next chapter introduces a powerful technique to determine the surface energy of a material: inverse gas chromatography.

References

[1] B.A. Wills, J.A. Finch, Wills' Mineral Processing Technology: An Introduction to the Practical Aspects of Ore Treatment and Mineral Recovery, 8th ed., Butterworth-Heinemann, 2015.

[2] S.R. Rao, Surface Chemistry of Froth Flotation, Springer Science & Business Media, 2013.

[3] T. Young, An essay on the cohesion of fluids, Philosophical Transactions of the Royal Society of London, 95 (1805) 65-87.

[4] T. Chow, Wetting of rough surfaces, Journal of Physics: Condensed Matter, 10-27 (1998) L445.

[5] J. Laskowski, Coal Flotation and Fine Coal Utilization, Elsevier Science, 2001.

[6] S. Chehreh Chelgani, B. Hart, TOF-SIMS studies of surface chemistry of minerals subjected to flotation separation–A review, Minerals Engineering, 57 (2014) 1-11.

[7] S. Brito e Abreu, W. Skinner, Predicting the surface chemistry contribution to the flotation recovery of chalcopyrite by ToF-SIMS, Minerals Engineering, 24-2 (2011) 160-168.

[8] S. Chander, Electrochemistry of sulfide flotation: Growth characteristics of surface coatings and their properties, with special reference to chalcopyrite and pyrite, International Journal of Mineral Processing, 33-1 (1991) 121-134.

[9] A. Chandra, A. Gerson, A review of the fundamental studies of the copper activation mechanisms for selective flotation of the sulfide minerals, sphalerite and pyrite, Advances in Colloid and Interface Science, 145-1 (2009) 97-110.

[10] A.P. Chandra, L. Puskar, D.J. Simpson, A.R. Gerson, Copper and xanthate adsorption onto pyrite surfaces: Implications for mineral separation through flotation, International Journal of Mineral Processing, 114 (2012) 16-26.

[11] N. Finkelstein, The activation of sulphide minerals for flotation: a review, International Journal of Mineral Processing, 52-2 (1997) 81-120.

[12] T. Khmeleva, W. Skinner, D.A. Beattie, T. Georgiev, The effect of sulphite on the xanthate-induced flotation of copper-activated pyrite, Physicochemical Problems of Mineral Processing, 36 (2002) 185-195.

[13] J. Leppinen, FTIR and flotation investigation of the adsorption of ethyl xanthate on activated and non-activated sulfide minerals, International Journal of Mineral Processing, 30-3 (1990) 245-263.

[14] R. Rath, S. Subramanian, T. Pradeep, Surface chemical studies on pyrite in the presence of polysaccharide-based flotation depressants, Journal of Colloid and Interface Science, 229-1 (2000) 82-91.

[15] R.S. Smart, J. Amarantidis, W.M. Skinner, C.A. Prestidge, L. La Vanier, S.R. Grano, Surface analytical studies of oxidation and collector adsorption in sulfide mineral flotation, Scanning Microscopy, 12-4 (1998) 553-583.

[16] X. Wang, E. Forssberg, N. Bolin, The aqueous and surface chemistry of activation in the flotation of sulphide Minerals—A review. Part I: An electrochemical model, Mineral Procesing and Extractive Metallurgy Review, 4-3-4 (1989) 135-165.

[17] X. Wang, E. Forssberg, N. Bolin, The aqueous and surface chemistry of activation in the flotation of sulphide minerals—A review. Part II: A surface precipitation model, Mineral Procesing and Extractive Metallurgy Review, 4-3-4 (1989) 167-199.

[18] M. Yekeler, U. Ulusoy, C. Hiçyılmaz, Effect of particle shape and roughness of talc mineral ground by different mills on the wettability and floatability, Powder Technology, 140-1 (2004) 68-78.

[19] M.M. Ahmed, Effect of comminution on particle shape and surface roughness and their relation to flotation process, International Journal of Mineral Processing, 94-3 (2010) 180-191.

[20] P. Koh, F. Hao, L. Smith, T. Chau, W. Bruckard, The effect of particle shape and hydrophobicity in flotation, International Journal of Mineral Processing, 93-2 (2009) 128-134.

[21] H. Kursun, U. Ulusoy, Influence of shape characteristics of talc mineral on the column flotation behavior, International Journal of Mineral Processing, 78-4 (2006) 262-268.

[22] D.I. Verrelli, W.J. Bruckard, P.T. Koh, M.P. Schwarz, B. Follink, Particle shape effects in flotation. Part 1: Microscale experimental observations, Minerals Engineering, 58 (2014) 80-89.

[23] B. Awatey, W. Skinner, M. Zanin, Effect of particle size distribution on recovery of coarse chalcopyrite and galena in Denver flotation cell, Canadian Metallurgical Quarterly, 52-4 (2013) 465-472.

[24] W. Trahar, A rational interpretation of the role of particle size in flotation, International Journal of Mineral Processing, 8-4 (1981) 289-327.

[25] D. Feng, C. Aldrich, Effect of particle size on flotation performance of complex sulphide ores, Minerals Engineering, 12-7 (1999) 721-731.

[26] R. Crawford, J. Ralston, The influence of particle size and contact angle in mineral flotation, International Journal of Mineral Processing, 23-1-2 (1988) 1-24.

[27] A. Gaudin, R. Schuhmann Jr, A. Schlechten, Flotation kinetics. II. The effect of size on the behavior of galena particles, The Journal of Physical Chemistry, 46-8 (1942) 902-910.

[28] K. Matis, G. Gallios, K. Kydros, Separation of fines by flotation techniques, Separations Technology, 3-2 (1993) 76-90.

[29] T. Miettinen, J. Ralston, D. Fornasiero, The limits of fine particle flotation, Minerals Engineering, 23-5 (2010) 420-437.

[30] Y. Shi, D. Fornasiero, Effects of particle size and density, and turbulence on flotation recovery, in: Engineering Our Future: Are We up to the Challenge?, Burswood Entertainment Complex. Barton, ACT: Engineers Australia, 27-30 September 2009, pp. 528-536.

[31] R. Sivamohan, The problem of recovering very fine particles in mineral processing—A review, International Journal of Mineral Processing, 28-3 (1990) 247-288.

[32] W. Trahar, L. Warren, The flotability of very fine particles—A review, International Journal of Mineral Processing, 3-2 (1976) 103-131.

[33] A. Dippenaar, The destabilization of froth by solids. I. The mechanism of film rupture, International Journal of Mineral Processing, 9-1 (1982) 1-14.

[34] J.A. Finch, J.E. Nesset, C. Acuña, Role of frother on bubble production and behaviour in flotation, Minerals Engineering, 21-12 (2008) 949-957.

[35] R. Pugh, Experimental techniques for studying the structure of foams and froths, Advances in Colloid and Interface Science, 114 (2005) 239-251.

[36] X. Wang, E. Forssberg, EDTA-induced flotation of sulfide minerals, Journal of Colloid and Interface Science, 140-1 (1990) 217-226.

[37] W. Yuhua, R. Jianwei, The flotation of quartz from iron minerals with a combined quaternary ammonium salt, International Journal of Mineral Processing, 77-2 (2005) 116-122.

[38] J. Finch, S. Gelinas, P. Moyo, Frother-related research at McGill University, Minerals Engineering, 19-6 (2006) 726-733.

[39] Y.S. Cho, J.S. Laskowski, Bubble coalescence and its effect on dynamic foam stability, The Canadian Journal of Chemical Engineering, 80-2 (2002) 299-305.

[40] S. Farrokhpay, The significance of froth stability in mineral flotation—A review, Advances in Colloid and Interface Science, 166-1 (2011) 1-7.

[41] L.K. Koopal, T. Goloub, A. de Keizer, M.P. Sidorova, The effect of cationic surfactants on wetting, colloid stability and flotation of silica, Colloids and Surfaces A: Physicochemical and Engineering Aspects, 151-1 (1999) 15-25.

[42] X.-M. Yuan, B. Pålsson, K. Forssberg, Flotation of a complex sulphide ore II. Influence of grinding environments on CuFe sulphide selectivity and pulp chemistry, International Journal of Mineral Processing, 46-3 (1996) 181-204.

[43] D.J. Bradshaw, A. Buswell, P. Harris, Z. Ekmekci, Interactive effects of the type of milling media and copper sulphate addition on the flotation performance of sulphide minerals from Merensky ore Part I: Pulp chemistry, International Journal of Mineral Processing, 78-3 (2006) 153-163.

[44] R. Mermillod-Blondin, M. Kongolo, P. de Donato, M. Benzaazoua, O. Barrès, B. Bussière, M. Aubertin, Pyrite flotation with xanthate under alkaline conditions-application to environmental desulfurization, in: Centenary of Flotation Symposium, Brisbane, QLD, 2005, pp. 683-692.

[45] M. Monte, F. Lins, J. Oliveira, Selective flotation of gold from pyrite under oxidizing conditions, International Journal of Mineral Processing, 51-1 (1997) 255-267.

[46] C. O'Connor, C. Botha, M. Walls, R. Dunne, The role of copper sulphate in pyrite flotation, Minerals Engineering, 1-3 (1988) 203-212.

[47] A.C. Partridge, G. Smith, Flotation and adsorption characteristics of the hematite-dodecylamine-starch system, Canadian Metallurgical Quarterly, 10-3 (1971) 229-234.

[48] S. Rao, J. Finch, Adsorption of amyl xanthate at pyrrhotite in the presence of nitrogen and implications in flotation, Canadian Metallurgical Quarterly, 30-1 (1991) 1-6.

[49] J. Scott, R. Smith, Diamine flotation of quartz, Minerals Engineering, 4-2 (1991) 141-150.

[50] R. Smith, J. L Scott, Mechanisms of dodecylamine flotation of quartz, Mineral Procesing and Extractive Metallurgy Review, 7-2 (1990) 81-94.

[51] C. Marion, A. Jordens, C. Maloney, R. Langlois, K.E. Waters, Effect of microwave radiation on the processing of a Cu-Ni sulphide ore, The Canadian Journal of Chemical Engineering, 94-1 (2016) 117-127.

[52] S. Neethling, J. Cilliers, Grade-recovery curves: a new approach for analysis of and predicting from plant data, Minerals Engineering, 36 (2012) 105-110.

CHAPTER **3**

INVERSE GAS CHROMATOGRAPHY (IGC)

3.1. Introduction

As detailed in Chapter 2, froth flotation is based on surface chemistry, and involves the interactions between three phases: solid and air, solid and water, and air and water in an aerated slurry. The physicochemical phenomena occurring at the interfaces determine the recovery and grade of flotation. Hydrophobic and hydrophilic particles have different attachment behaviour to a bubble, and a good understanding of wetting behaviour of particles is crucial to predict the surface wettability of particles and control the separation process. Wettability of materials can be evaluated using various surface analytical methods. In mineral processing, wettability has traditionally been evaluated using contact angle measurements. Contact angle is an indicator of hydrophobicity, and is related to the interfacial energies between solid-liquid and solid-vapour through Young's equation (Equation 2-1).

Most common wettability assessments are divided into two main categories: single particle based and bulk powder techniques. The single particle based methods are directly measured by microscopic visualisation of the solid/liquid interface for smooth planar surfaces. Due to direct measurement, accuracy and easy performance, microscopic methods have been widely used in practice [1]. A serious limitation of this technique is that the sample must be perfectly planar, chemically homogeneous, and the surface smoothness must not change upon liquid deposition. This method is not applicable for porous materials and powders. Meanwhile, a single surface cannot be always a good representative of all particles in a pulp. Several different methods have been developed and recommended to accurately determine the contact angle of powders. The most common techniques are sessile drop and capillary penetration. In the sessile drop method, a compressed disc is prepared from the powder, a liquid drop is deposited on the disc surface and the contact angle is measured [1]. The liquid penetration method is conducted by packing the powder in a sample holder, which is a tube with a frit at the bottom, and bringing it into the contact with the liquid. The increase in mass as a function of time is measured, and the contact angle (θ) is calculated using modified Washburn equation [1]:

$$\cos\theta = \frac{\mu}{c.\rho_L^2.\gamma_{LV}}.\frac{m^2}{t} \qquad (3-1)$$

where, μ is the liquid viscosity, c is a constant that accounts for the particles' arrangement and packing conditions, ρ_L is the liquid density, γ_{LV} is the surface tension of the liquid, m is the penetrated liquid mass and t is the penetration time. The measurements are based on three important assumptions: the liquid flow through the sample bulk is laminar; the packing constant and bulk structure remain constant throughout the measurement; and gravity is neglected [2]. Capillary penetration was reported to be inexpensive and straightforward to run. One of the difficulties associated with this method is determining the packed bed constant (c) [1]. The general disadvantage of the contact angle measurement is the generated contact angle hysteresis due to surface roughness, surface heterogeneity and surface immobility at the macromolecular scale [3]. In addition, it was shown that the calculated surface free components from the contact angle determined by Washburn's equation are not necessarily accurate [4, 5].

Time-of-flight secondary ion mass spectrometry (ToF-SIMS) has been also applied to examine the surface wettability of materials [6-12]. It is an analytical method based on focusing a pulsed ion beam onto a sample surface, producing secondary ions from the outermost surface of the sample, and measuring the exact mass of the ejected ions. In order to characterise a sample surface regarding its behaviour towards water, the method applies an excess hydrophobic or hydrophilic fragments to determine the predominant surface species in a sample. A direct relationship between contact angle and ToF-SIMS fragmentation was also suggested by Priest *et al.* [8]. This method is applicable to both flat surfaces and particles, and there is no need for sample preparation or contact with any liquids [12]. However, samples need to be compatible to very low pressure since the technique works under vacuum. The main limitation is that ToF-SIMS is a matrix dependent technique, and the ion concentration on the surface and beam conditions can affect the intensity of the signals from the secondary ions [7, 13-16]. It was reported to be more expensive and time-consuming than other traditional techniques [12]. Also, the technique does not provide quantitative information without standards and calibrations [12, 16]. Meanwhile, finding a representative grain or a good region of the sample for the analysis can be very challenging, similar to other optical techniques.

The limitations of conventional methods have been the motivation for studies on new approaches and experimental methods to assess the wettability of the materials of different shapes and morphology through their inherent parameters. Inverse gas chromatography was introduced in 1941 when Nobel Prize winners Martin & Synge reported using chromatography to measure partition coefficients between two liquids [17]. However, according to Kiselev *et al.* [18] and Conder & Young [19], the pioneers in applying gas chromatography (GC) to physicochemical measurements were Wicke & Voigt (1947) [20], Glueckauf (1947) [21], Cremer & Prior (1951) [22], and James & Phillips (1954) [23] who determined adsorption isotherms from GC. The new method got its name in the early 1960s when the term "inverse gas chromatography" was introduced by Professor A. V. Kiselev at the M. V. Lomonosov Moscow State University [24], who played a significant role in developing surface chemistry and chromatographic science [25]. In a book published in 1967 (translated two years later) [18], Professor Kiselev and co-authors mentioned the capabilities of GC in determining a number of solid surface properties such as activity coefficients, entropies and heats of solution, vapour pressure, molecular weight, diffusion coefficients, adsorption isotherms, surface free energies, heat and entropies of adsorption, activation energies for internal diffusion and boiling points of hydrocarbons; as well as investigations into molecular interactions and gas-liquid interface resistance. This book and other publications [26-33] indicate that the systematic application of GC in measuring the physicochemical properties of solid surfaces was of great interest during the 1960s. Smidsrød & Guillet named GC as a powerful "indispensable analytical instrument" for applications much more than just determining the components of mixtures [28].

Inverse gas chromatography (IGC) became more popular in the 1970s when it was established as a powerful technique for studying the surface and bulk characteristics of polymers, copolymers and their blends [19, 34-47]. IGC in most cases was referred to as a simple, fast and accurate technique for physicochemical measurements, although the term "inverse gas chromatography" was still not commonly used. The number of publications and a wide range of investigations published in the 1980s show that IGC attracted the attention of researchers in a variety of fields [48-51] such as modified silicas [52, 53], glass fibres and silicas (as fillers for polymers) [54, 55], crackers and sweet biscuits [56]. Polymeric research was still the most common use of IGC based upon the large volume of publications [57-65]. IGC provides information about a wide number of important physico-chemical properties such as solubility and thermodynamic interaction parameters; diffusion kinetics; BET surface area; work of cohesion, glass transition temperatures; surface energy heterogeneity; acid-base properties; and polar functionality on the surface of materials as well as characterizing organic adsorbates on particulate surfaces, adsorption isotherms, and work of adhesion. IGC is a useful method for characterizing the surface properties of the powders dissolving in some solvents, for which deficiencies with the Washburn technique were noted, since it determines the interactions between a solid and a liquid without wetting the solid with the liquid [66].

In this chapter, information concerning the history, instrumentation and applications is discussed. Examples of the many experiments developed for IGC method are selected and described. Materials that have been analysed include polymers, pharmaceuticals, minerals, surfactants, and nanomaterials. The properties that can be determined using the IGC technique include enthalpy and entropy of sorption, surface energy (dispersive and specific components), work of co/adhesion, miscibility and solubility parameters, surface heterogeneity, glass transition temperature, and specific surface area.

3.2. Fundamentals

3.2.1. Instrumentation and Methods

Similar to classical GC, an IGC instrument consists of an oven, column, solute reservoir, detector, mass flow controller and a computer as the processor and controller (Figure 3.1). Unlike conventional GC columns, which are coils, an IGC column is a straight glass tube; in some research, stainless steel [67-70], copper [68], and teflon [71] columns have also been used. The main difference between the two setups is the nature of the stationary and mobile phase. In

IGC, the sample of interest is placed into the column, being the stationary phase. The stationary phase may be a crystalline powder, an amorphous compound, a fibrous composition, or viscous liquid. One of the greatest advantages of this method is that no special sample preparation is required. In fact, IGC requires the minimum sample preparation when compared to other surface energy analyzing techniques [72]. Therefore, various forms of solids and even semi-solids can be characterised quickly and efficiently. In the case of the stationary phase being a solid form, the technique is referred to as inverse gas-solid chromatography (IGSC), whilst inverse gas-liquid chromatography (IGLC) refers to liquid samples or a liquid stationary phase. According to Davis & Petersen, IGLC was a valuable approach for "fingerprinting" asphalts [26].

To analyse the stationary phase, a low concentration of a well-characterised single gas or vapour of a volatile substance is injected *via* an inert carrier gas through the stationary phase. This volatile is termed the “probe molecule”. The direction of gas flow is depicted in Figure 3.1. Different probes with known characteristics such as polarity, acidity, molecular area, and electron donor/acceptor number are used. The respective properties of the stationary phase can be determined by analysing the retention data of the interaction of a well-defined probe with the stationary phase.

The probe is carried through the column by the constant flow of a carrier gas which is a high purity inert gas at a set flow rate. The most common carrier gases are helium, argon and nitrogen. In IGC measurements, it is assumed that adsorption and desorption equilibrium of the probe molecule on the stationary phase surface is established. This equilibrium can be achieved using either two pulses or frontal modes [73]. In the pulse technique, a set volume of probe is injected into the carrier gas to be passed through the column, thus coming into contact with the material under investigation. It is applicable for systems that obtain adsorption equilibrium very quickly, whereas for slow rating equilibria, the frontal method is preferred, in which probe solute flows continuously into the carrier gas. This means that a broader peak is eluted due to a longer experiment time [74].

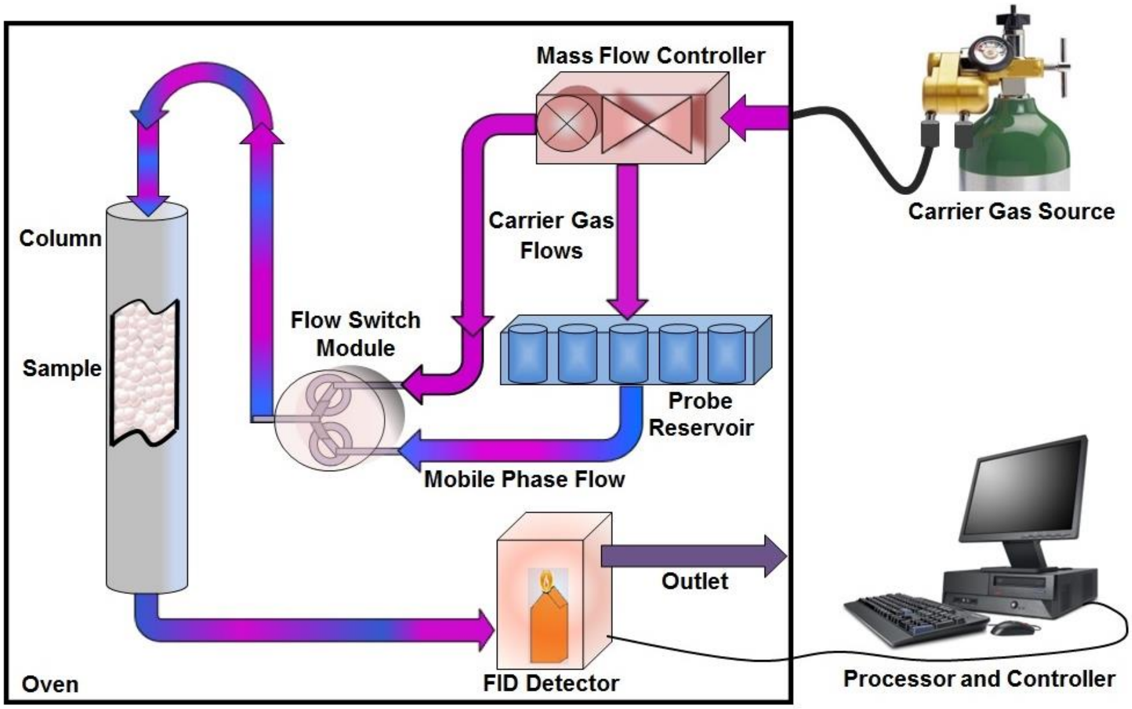

Figure 3.1. Schematic illustration of a typical inverse gas chromatography (IGC) analyser.

Similar to conventional gas chromatography, the interactions between the mobile phase (adsorbate) and the stationary phase (adsorbent) occur when the mobile phase passes through the column. The nature and magnitude of these interactions affects the velocity and, subsequently the retention parameters of the mobile phase. For example, the retention volume is a measure of the quality and quantity of adsorption of the probe molecule on the sample inside the column. Differences between IGC and GC columns and chromatograms are schematically presented in Figure 3.2. In GC, a known volume of a gaseous or liquid mixture under examination (here containing two components) is injected into a very long column with a known stationary phase. Differences between interaction strength of the components with the stationary phase result in their separation while progressing through the column. However, in IGC, the retention behaviour of only a single vapour is detected for every injection into a short column packed with the sample.

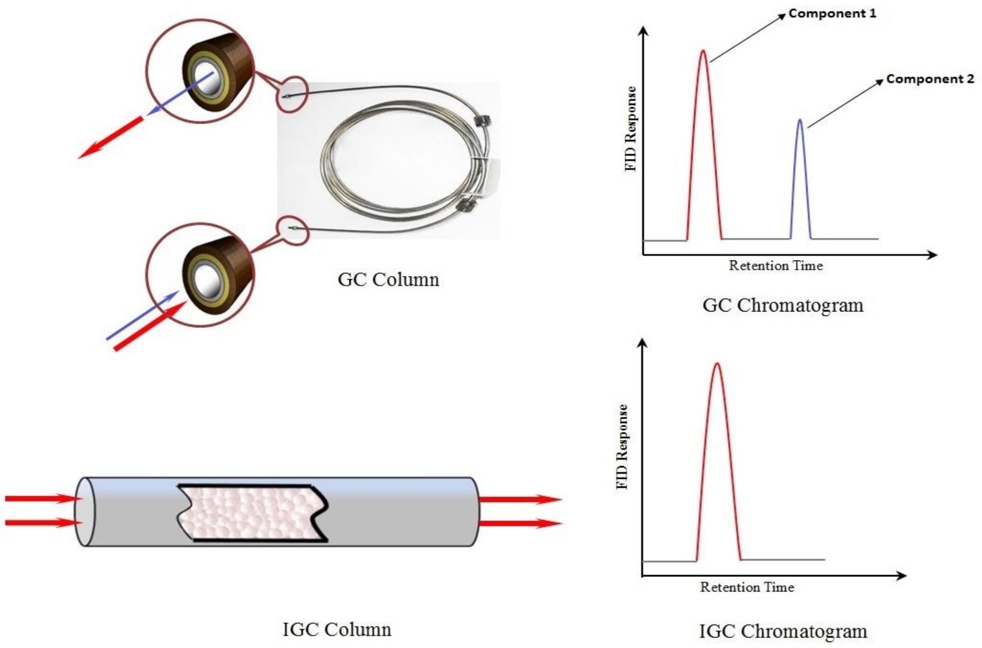

Figure 3.2. Comparison between GC (top) and IGC (bottom) columns and chromatograms.

Selectivity and sensitivity are two important factors for detector selection. The thermal conductivity detector (TCD) works on the basis of thermal conductivity differences between different components of a mixture. Thus, it has the capability of detecting a wide variety of materials. The flame ionisation detector (FID) measures the concentration of organics through their destruction and the formation of ions. It has a high sensitivity to most hydrocarbons; however, water cannot be detected by FID. To benefit from the advantages of both detection methods, the IGC setup may be equipped with a combination of more than one detector. For example, Newell & Buckton [75] operated TCD and FID detectors in series to establish the benefits of high sensitivity in the analysis of an organic probe retention as well as measuring the humidity level in the surface energy of lactose experiments. In recent research, TCD and FID detectors were used together to analyse multi-component probes [76]. FID was used to measure the relative dead time and TCD to measure the retention time of the probe simultaneously. The temporal difference between the two detectors gave the adjusted retention time.

IGC experiments can be conducted under two chromatographic conditions: infinite dilution and finite concentration. Infinite dilution, also called zero surface coverage, was found to be suitable for evaluating the surface energy and heat of sorption of particulates [77]. Infinite dilution refers to very low concentrations of probe and is obtained by introducing a very small quantity of the probe molecule into the system. Since the amount of probe molecule or adsorbate is limited, it is assumed that interactions occur only with the high-energy sites on the surface and therefore interactions with the lower energy sites are negligible. The high sensitivity of IGC detectors (approximately 10^{-9} mole), has made it ideal for experiments at infinite dilution [78]. This mode has the benefit of high sensitivity, which makes it an excellent method for determining thermodynamic parameters [74, 79, 80], and most of the IGC experiments are carried out under this condition. In ideal conditions, no probe-probe interactions are considered and Henry’s Law is obeyed [79]. Hence, a linear adsorption isotherm and a symmetrical (Gaussian) chromatographic peak are expected [74, 81]. A chromatographic diagram of symmetrical peaks for interaction of alkanes with the stationary phase is generated [54]. The measured parameter in this method is net retention time and it has been successfully used to determine the dispersive components of surface free energy [82-84], acid-base properties of surfaces [82, 85-88], surface polarity [89], activity coefficients [90-93], Flory-Huggins thermodynamic interaction parameters [93], free energy of adsorption and surface heterogeneity [94], surface activity and adsorption entropy [53]. Since IGC indicates a high sensitivity at infinite dilution, it has the potential to discriminate between the characteristic differences that are impossible to detect by other techniques such as traditional wettability measurements [74].

Finite concentration inverse gas chromatography has been found to be a reasonable and convenient method for obtaining adsorption isotherms where previous measurement methodologies such as the classical volumetric method [95] have shown inefficiencies. The disadvantage of adsorption studies using volumetric measurements is that using a large quantity of adsorbent (in order to minimise the adsorption effects of the wall) results in more void space and, consequently, uncertainty in minimizing dead space. Finite concentration of the adsorbate is achieved by introducing a high quantity of probe molecule to the chromatographic system, which then interacts with all sites on the surface. It provides complementary information to the results of infinite dilution IGC [96]. The method can be applied to estimate the surface energy heterogeneity of the solids which has been a difficult challenge to overcome [97]. IGC at finite concentration has been applied to study material characteristics such as adsorption enthalpies and entropies [54] as well as the surface area and porosity by measuring adsorption isotherms [77]. It has been applied, in combination with the thermal desorption technique, to distinguish the contributions of micropores from mesopores to the adsorption phenomenon in porous materials [98]. The merit of IGC in comparison to classical volumetric and gravimetric methods is that IGC experiments are able to be conducted over a wide range of temperatures [78]. A comprehensive comparison of inverse gas chromatography and other techniques of characterizing energetics of "real solid surfaces" indicated that IGC is a fast, efficient, and accurate methodology which can function at both low and high pressures of solute vapour [99].

3.2.2. Theory of Surface Energy Measurements by IGC

One of the most interesting and commonly used applications of IGC is in measuring the surface free energy. Regarding the principles of IGC measurements, the fundamental data obtained from this method is either retention time or retention volume. The retention data refers to the required time and carrier gas volume, respectively, to generate a peak as a result of interactions between the probe molecule and the stationary phase. Various characteristics of a material can be calculated by analysing the nature and magnitude of these interactions. The surfaces of solids are described by dispersive and specific (non-dispersive) properties. Dispersive properties are obtained by calculating dispersive components of surface free energy. Specific properties are determined by the parameters which measure surface tendency to be an electron acceptor or electron donor to show Lewis acidity or Lewis basicity properties, respectively. The sum of the dispersive and specific components represents the total solid surface energy [100]. The surface energy of a solid has been defined by the sum of the dispersive component and polar component of the surface energies [101, 102]. Thereafter, acid-base (acceptor-donor) contributions were found to be a more robust term for describing the non-dispersive component [103].

3.2.3. Dispersive Component of Surface Free Energy

Figure 3.3 depicts the IGC chromatogram of a quartz sample (obtained from Ward's Scientific, USA) within the size range (after crushing and grinding) $106 < x < 150$ µm. Every peak corresponds to different surface coverages and peak area or height is proportional to the number of molecules detected by FID. The larger the injections, the greater the deviation from Henry's Law, and consequently the greater the deviation from symmetry of the chromatogram.

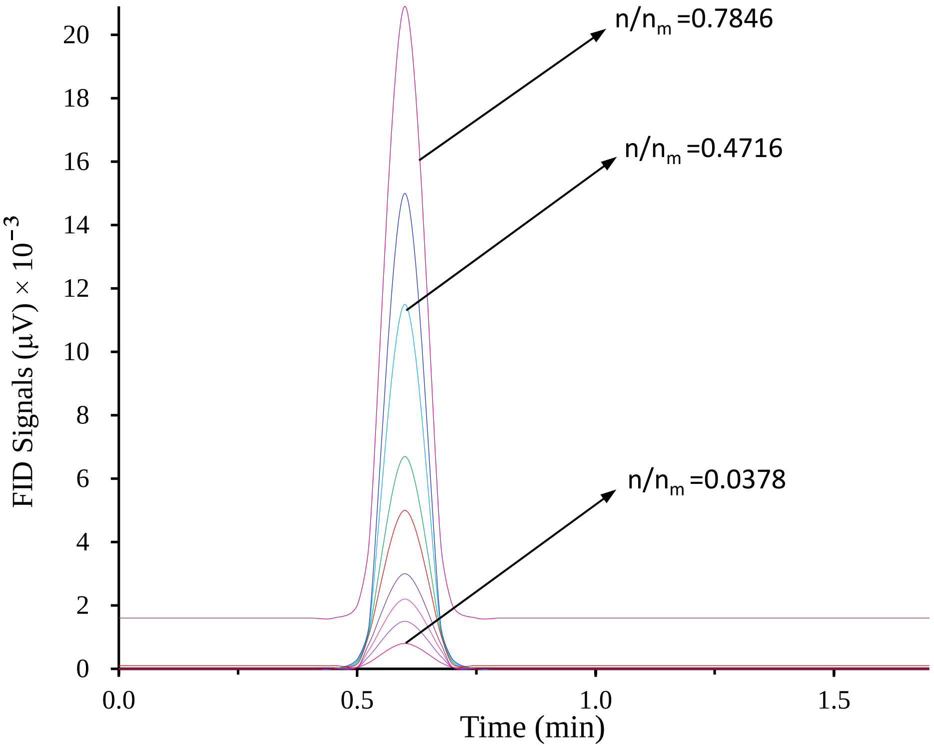

Figure 3.3. A typical IGC chromatogram of n-octane adsorption/desorption on quartz. The n/n_m represents the actual fractional surface coverage.

3.2.3.1. Schultz Method

One of the most commonly applied methods for determining the dispersive component of the surface energy was proposed by Schultz *et al.* [103, 104]. Their calculations were based on the retention parameters of liquid n-alkane probes at infinite dilution. Alkanes were used because there are no acid-base interactions. The dispersive (London) component of surface energy (γ_S^D) is computed from retention parameters obtained at infinite dilution where Henry's Law is obeyed [73]. Under this condition, it is assumed that there are no interactions between adsorbate molecules; consequently a symmetrical Gaussian peak is expected in the IGC chromatogram. After injection into the column, it takes time for the probe molecule to interact with the stationary phase, termed dead-time, t_0. This value is often determined by passing an inert gas through the examined stationary phase. Therefore, the solute exits from the column after a gross retention time, t_R. In order to obtain the net retention time, the dead-time must be deducted from the gross retention time. Hence, net retention volume of the probe (mL) is equal to [105]:

$$V_N = j \cdot F_C \cdot (t_R - t_0) \qquad (3-2)$$

where j and F_c are the James-Martin compressibility correction factor and the flow rate of carrier gas (mL min^{-1}) in the column, respectively. The James-Martin factor corrects the effect of the pressure drop and packing density variation of the stationary phase on the retention time. In some experiments, specific retention volume is used instead of the net retention volume to eliminate the effect of temperature and the quantity of the stationary phase. Specific retention volume is described as [105]:

$$V_g^0 = (\frac{V_N}{m_S}) \cdot (\frac{273.15}{T}) \qquad (3-3)$$

where V_g^0 denotes specific retention volume (mL g^{-1}) at 0 °C, m_s is mass of the sample (g). Hence, specific retention volume can be expressed as [105]:

$$V_g^0 = (\frac{j}{m_S}) \cdot F_C \cdot (t_R - t_0) \cdot (\frac{273.15}{T}) \qquad (3-4)$$

All interactions that occur between adsorbate and adsorbent are either dispersive or specific. Dispersive and specific components of surface free energy are calculated through thermodynamic equations. The standard Gibbs free energy change is defined by the net retention volume, V_N, as [73, 105]:

$$\Delta G_{ad}^{0} = \Delta G_{de}^{0} = R \cdot T . \ln V_N + C \tag{3-5}$$

where ΔG_{ad}^{0} and ΔG_{de}^{0} are standard molar Gibbs free energy changes of adsorption and desorption, respectively. R and T are the gas constant (8.314 J K^{-1} mol^{-1}) and absolute temperature (K), respectively and the constant C is related to the reference states. The free energy of adsorption (ΔG_{ad}^{0}) is the sum of the dispersive and specific (acid-base) components of Gibbs free energy change of adsorption [106]:

$$\Delta G_{ad}^{0} = \Delta G_{ad}^{D} + \Delta G_{ad}^{SP} \tag{3-6}$$

When n-alkanes are used as probes, there are no specific interactions with the stationary phase and hence $\Delta G_{ad}^{0} = \Delta G_{ad}^{D}$ and their quantity depends on the number of carbon atoms in the alkane molecule [73, 107]. The free energy of adsorption is defined as:

$$-\Delta G_{ad}^{0} = N_A \cdot a \cdot W_{adh} \tag{3-7}$$

where N_A is the Avogadro's number ($6.022140857 \times 10^{23}$ mol^{-1}), a is the cross sectional area of the probe molecule (m^2), and W_{adh} is the work of adhesion (mJ m^{-2}) which is related to dispersive free energy of solid and liquid interaction by Fowkes' Equation [108]:

$$W_{adh} = 2 \cdot \sqrt{\gamma_S^D \cdot \gamma_L^D} \tag{3-8}$$

Where γ_S^D and γ_L^D are dispersive components of surface free energy of the solid and probe molecule (mJ m^{-2}), respectively. Combining Equations 3-5, 3-7, and 3-8 yields [75, 103, 104]:

$$R \cdot T \cdot \ln V_N = 2 \cdot N_A \cdot a \cdot \sqrt{\gamma_S^D \cdot \gamma_L^D} + C \tag{3-9}$$

The plot of R.T.lnV_N as a function of $a \cdot \sqrt{\gamma_L^D}$ for a homologous series of n-alkanes is linear of which the gradient gives the dispersive surface free energy of the stationary phase. The graphical illustration of determining γ_S^D for quartz by the Schultz method is depicted in Figure 3.4. The plot is linear and is called the "alkane line" and the slope gives the dispersive surface energy (γ_S^D) of the stationary phase. The calculated dispersive component of surface energy for the diagram depicted in Figure 3.4 was calculated as 52.76 mJ m^{-2} at 5% fractional surface coverage. Polar probe points do not lie on the alkane line and the vertical distance from the alkane line to the polar probe is the Gibbs free energy (Figure 3.5). Therefore, the Schultz method gives both γ_S^D and ΔG^{SP}. As an example, the specific (acid-base) free energy (ΔG^{SP}) of dichloromethane and ethyl acetate adsorption on the quartz (53 µm < x < 75 µm) were calculated through the Schultz concept as 11.05 kJ mol^{-1} and 13.96 kJ mol^{-1}, respectively.

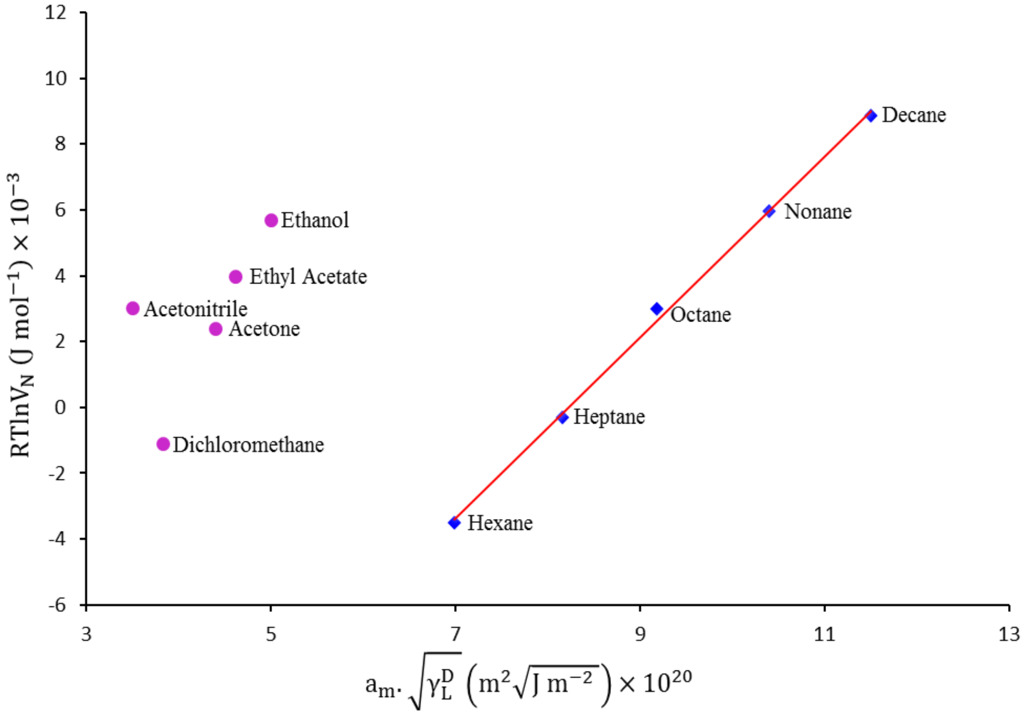

Figure 3.4. The diagram for determining surface free energies for quartz (53 µm < x < 75 µm) by the Schultz method.

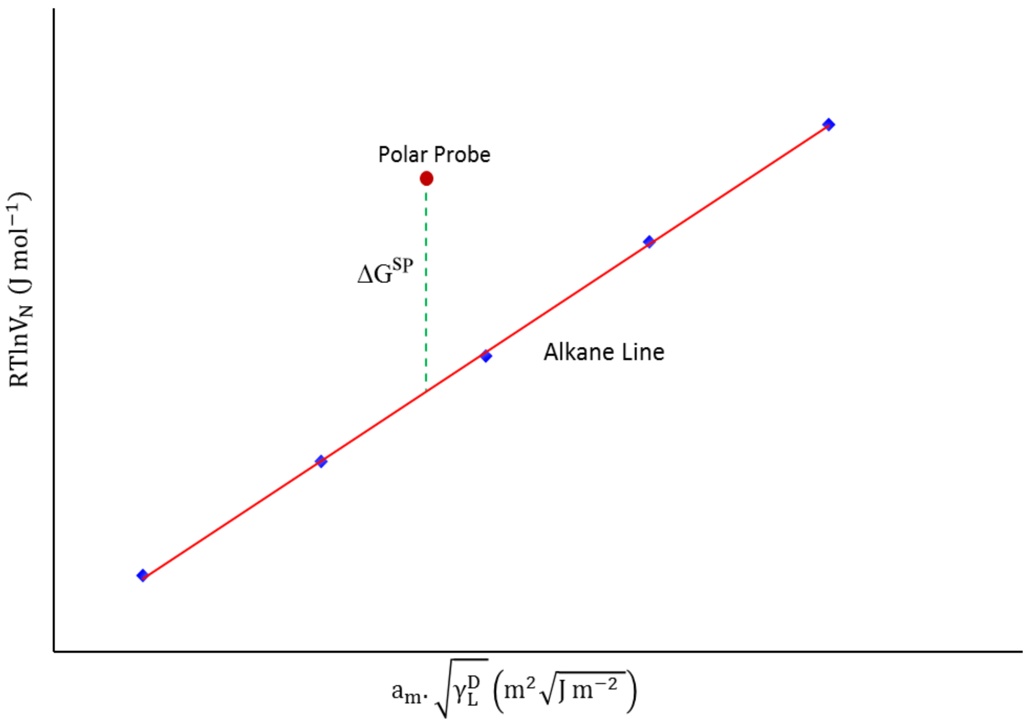

Figure 3.5. The typical diagram for determining Gibbs free energy by the Schultz method.

3.2.3.2. Dorris-Gray Method

Another method for determining the dispersive component of surface free energy, γ_S^D was proposed by Dorris & Gray [109]. They determined the thermodynamics of adsorption for a series of liquid n-alkane at zero coverage conditions (Henry's Law region). The symmetrical peaks of the IGC chromatogram and a constant retention time for different injection volumes confirm the Henry's Law region. Their experiments showed that changes in flow rate did not affect the net retention volume. Dorris & Gray calculated the dispersive component of the surface free energy by considering the contribution of the methylene groups only in the free energy of adsorption, assuming that the Gibbs free energy of desorption per mole of methylene group is equal to the work of adhesion between the stationary phase and hydrocarbon-saturated mobile phases [101]. Hence, the increment per CH_2 in the free energy of adsorption between two alkanes of n and (n+1) carbon atoms can be expressed as:

$$\Delta G_{ad}^{CH_2} = -R \cdot T \cdot \ln \frac{V_{N,C_{n+1}H_{2n+4}}}{V_{N,C_nH_{2n+2}}} \qquad (3-10)$$

According to Equation 3-8, the work of adhesion is described by the dispersive free energy between a CH_2 unit and stationary phase as:

$$W_{CH_2} = 2 \cdot \sqrt{\gamma_S^D \cdot \gamma_{CH_2}^D} \qquad (3-11)$$

Referring to Equation 3-7, the molecular adsorption dispersive free energy change of CH_2:

$$-\Delta G_{CH_2}^0 = N_A \cdot a_{CH_2} \cdot W_{CH_2} \qquad (3-12)$$

Consequently, the contribution of a CH_2 unit to the free energy of adsorption interaction of a series of n-alkane can be described as:

$$-\Delta G_{CH_2}^0 = 2 \cdot (N_A \cdot a_{CH_2} \cdot \sqrt{\gamma_S^D \cdot \gamma_{CH_2}^D}) \qquad (3-13)$$

$$\gamma_S^D = \frac{1}{4 \cdot \gamma_{CH_2}} \cdot \left(\frac{-\Delta G_{CH_2}}{N \cdot a_{CH_2}}\right)^2 \qquad (3-14)$$

where a_{CH_2} is the cross-sectional area of a methylene group (CH_2) (m^2) and γ_{CH_2} is free energy of adsorption of one CH_2 group and is approximately 35.6 mJ m^{-2} [110]; more accurately [111]:

$$\gamma_{CH_2} = 35.6 + 0.058(293 - T) \qquad (3-15)$$

As a result, the ΔG^0 increment per methylene group in the normal alkane series was used to calculate γ_S^D according to the following expression:

$$\gamma_S^D = \frac{\left[R \cdot T \cdot \ln\left[\frac{V_{N,C_{n+1}H_{2n+4}}}{V_{N,C_nH_{2n+2}}} \right] \right]^2}{4 \cdot N^2 \cdot a_{CH_2}^2 \cdot \gamma_{CH_2}} \qquad (3-16)$$

Figure 3.6 is a graphical illustration of determining dispersive surface energy for quartz (53 µm < x < 75 µm) by the Dorris-Gray method. The γ_S^D parameter for this sample was calculated as 52.61 mJ m^{-2}. The slope of the alkane line in the plot of R.T.lnV$_N$ versus the carbon numbers of the n-alkane (probe molecule) gives γ_S^D from Equation 3-17 [112]:

$$\gamma_S^D = \frac{slope^2}{4 \cdot N^2 \cdot a_{CH_2}^2 \cdot \gamma_{CH_2}} \qquad (3-17)$$

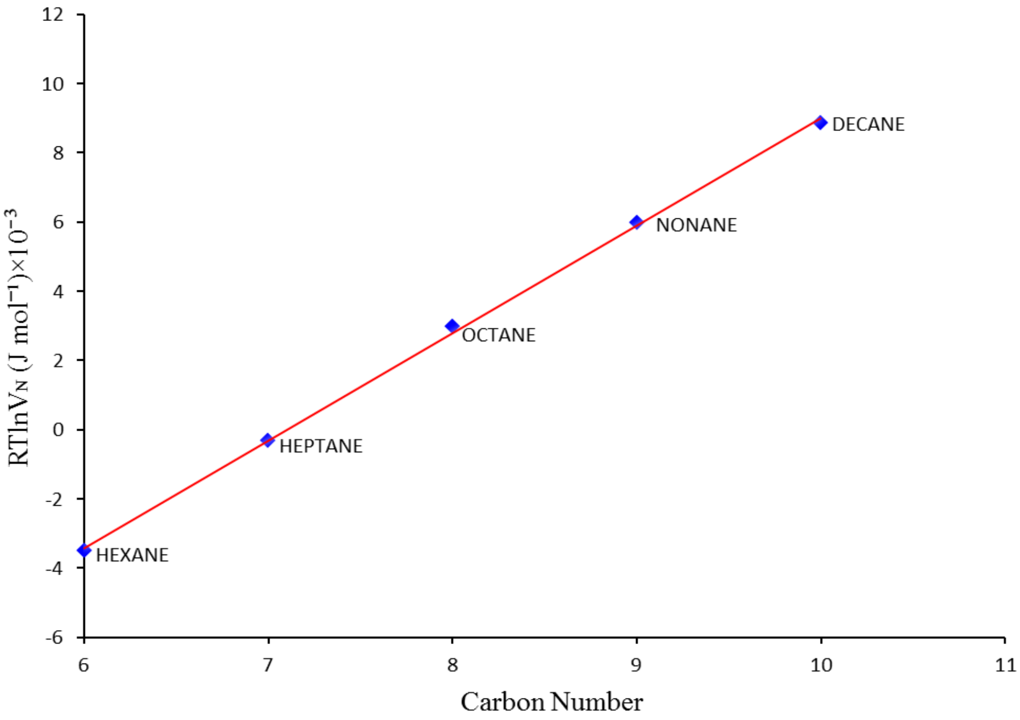

Figure 3.6. The diagram for determining dispersive free energy for quartz (53 µm < x < 75 µm) by the Dorris-Gray method.

As can be seen from Figure 3.6, only the dispersive component (γ_S^D) is calculated in this way. Therefore, when the Dorris-Gray concept is used, the specific component would be calculated using other approaches such as the Polarisation method [113]. In this method, the equation used to calculate γ_S^D is [89]:

$$R \cdot T \cdot \ln V_N + C = C' \cdot P_{DP} \cdot P_{DS} \qquad (3-18)$$

where P_{DP} and P_{DS} are deformation polarisation of probe and solid, respectively. The constants C and C' depend on the chosen reference states. The deformation polarisation (P_D, $cm^3\ mol^{-1}$) is an intrinsic characteristic and is independent from the nature of the probe and is calculated as [89, 114]:

$$P_D = \frac{n^2 - 1}{n^2 + 2} \cdot \frac{M}{\rho} \qquad (3-19)$$

where n, M, and ρ are the refractive index, molar mass (g mol^{-1}), and density (g cm^{-3}) of the probe molecule, respectively. In the plot of $R.T.\ln V_N$ against the molar deformation polarisation of n-alkane probes, the slope of the alkane line is $C'P_{DS}$ which is proportional to dispersive interaction forces. As shown in Figure 3.7, the vertical distance between polar probe points and the alkane line gives specific free energy (ΔG^{SP}) [89]. For quartz (53 µm < x < 75 µm), the specific (acid-base) free energy (ΔG^{SP}) of dichloromethane and ethyl acetate adsorption on the sample were calculated as 11.35 kJ mol^{-1} and 12.53 kJ mol^{-1}, respectively through the Polarisation method.

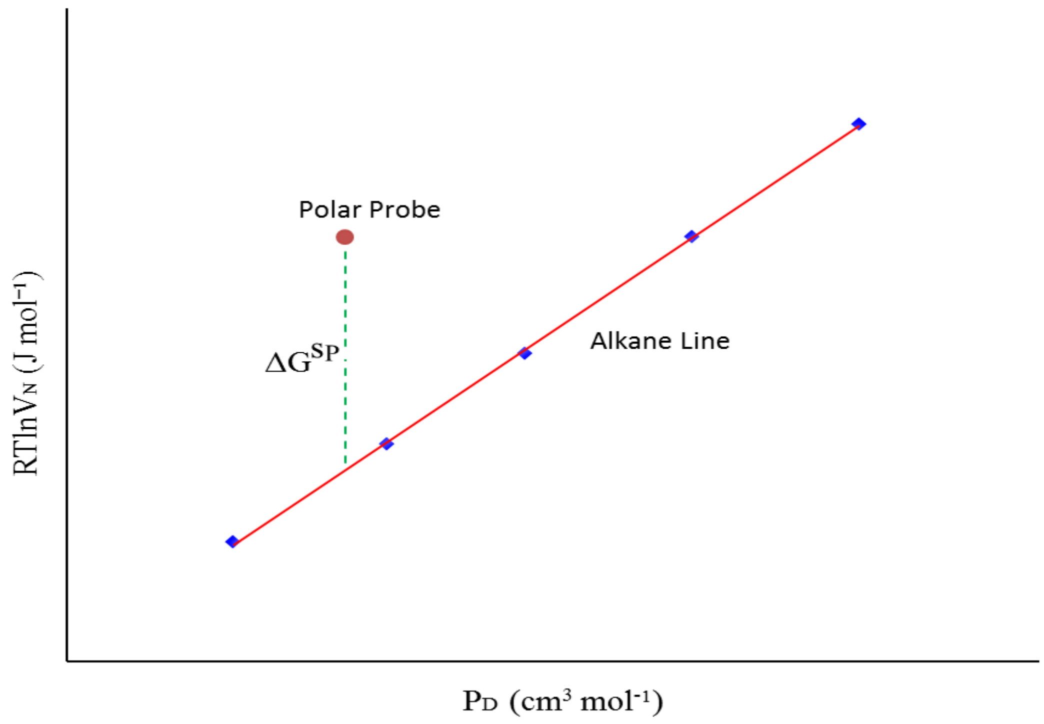

Figure 3.7. The typical diagram for determining the specific free energy by the Polarisation method.

3.2.3.3. Comparison between the Schultz Method and Dorris-Gray Method

Schultz & Lavielle [104] confirmed that the results obtained from the Dorris-Gray procedure were in alignment with their analysis. However, Shi *et al.* [115] calculated the ratio of the dispersive free energy by Dorris-Gray to dispersive free energy proposed by Schultz as the following expression:

$$\frac{\gamma^D_{S,Dorris-Gray}}{\gamma^D_{S,Schultz}} = \frac{\left(a_{n+1} \cdot \sqrt{\gamma_{n+1}} - a_n \cdot \sqrt{\gamma_n}\right)^2}{\gamma_{CH_2} \cdot a^2_{CH_2}} \qquad (3-20)$$

They compared the results obtained from both methods and concluded that $\gamma^D_{S,Dorris-Gray}$ is greater than $\gamma^D_{S,Schultz}$ and the ratio increases with increasing temperature. It was also reported that the calculated parameters through the Schultz method were not in good agreement with the same parameters in the solvents handbook [115]. Another comparison confirmed that the γ_S^D calculated by Dorris-Gray is more accurate compared to the values obtained with the Schultz method [112]. However, some of the reported dispersive surface energies for different hybrid materials do not suggest a definite difference between the γ^D values obtained using the Dorris-Gray and Schultz approaches [116]. Experimentally, little difference was observed for three different samples at 30 ºC (Table 3.1).

Table 3.1. The γ_S^D values calculated by Schultz and Dorris-Gray methods at 5% surface coverage.

Sample	**Particle Size (µm)**	**γ^D (mJ m^{-2})** by **Schultz**	**γ^D (mJ m^{-2})** by **Dorris-Gray**
Quartz	53 < x < 75	52.76	52.61
Talc	53 < x < 75	59.16	59.88
D-mannitol	–	32.79	33.53

3.2.4. Surface Energy Heterogeneity

Surface energy heterogeneity is one of the most useful characteristics provided by IGC. It is, in essence, an energy map which provides important information about energy distribution on the surface and its variation. Surface energy heterogeneity is obtained by plotting surface energy values as a function of surface coverage (surface energy profile). Figure 3.8 shows the dispersive surface energy profile for a quartz sample. It suggests an energetically active surface since the dispersive surface energy decreases dramatically with increasing surface coverage. As a result, there is a notable difference between minimum and maximum dispersive values, ranging from 31 mJ m^{-2} to approximately 60 mJ m^{-2}. This trend is attributed to the fact that at low surface coverages, the high energy sites are first taken up by probe molecules; increasing the surface coverage leads to the occupation of lower energy sites by the probe.

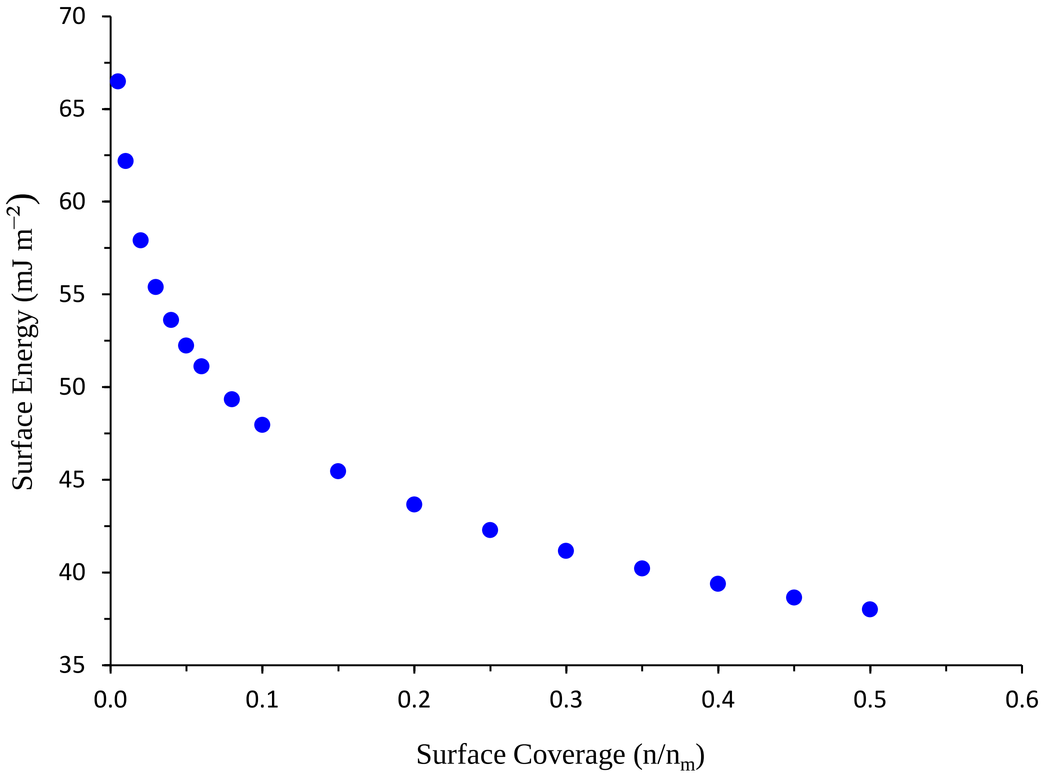

Figure 3. 8. Dispersive surface energy profile of quartz (53 µm < x < 75 µm) by Schultz method, using C6-C10 normal alkanes for surface coverages between 0.5% and 50%.

3.2.5. Specific Component of Surface Free Energy

To determine specific or non-dispersive components, also termed the acid-base interaction parameters of surface free energy, γ_S^{SP} the dispersive component is subtracted from the total free energy of adsorption. Experimentally, it is obtained by calculating the retention data of well-characterised polar solutes. One of the difficulties associated with measuring specific components of surface energy is that the interactions between polar probes and the solid surface are of both types; dispersive and specific. Moreover, specific interactions encompass all categories of interactions such as acid-base, magnetic, metallic, hydrogen-bonding, *etc.* with the exception of London interactions [73].

In the Van Oss description, the specific component of surface free energy can be divided into contribution of Lewis acid (electron acceptor), γ_S^+, and Lewis base (electron donor), γ_S^-, that can be calculated using Equation 3-21 [110]:

$$-\Delta G = 2 \cdot N_A \cdot a \cdot (\sqrt{\gamma_S^+ \cdot \gamma_L^-} + \sqrt{\gamma_S^- \cdot \gamma_L^+}) \qquad (3-21)$$

If monopolar probe molecules are used, γ_S^+ and γ_S^- can be calculated directly from only two probe molecules (one acid and one base), as illustrated in Equations 3-22 and 3-23, using dichloromethane (subscript DCM) as a monopolar acid and ethyl acetate (subscript EthAce) as a monopolar base, for example.

$$\gamma_S^- = (\frac{1}{\gamma_{DCM}^+}) \cdot (\frac{\Delta G_{DCM}}{2 \cdot a_{DCM} \cdot N_A})^2 \qquad (3-22)$$

$$\gamma_S^+ = (\frac{1}{\gamma_{EthAce}^-}) \cdot (\frac{\Delta G_{EthAce}}{2 \cdot a_{EthAce} \cdot N_A})^2 \qquad (3-23)$$

With both γ_S^+ and γ_S^- now known for the solid, one can estimate the acid-base component of the surface energy (γ_S^{SP}) of the solid by using the geometric mean of the γ_S^+ and γ_S^- values. The shortened form of Equation 3-21 proposed by Owens & Wendt makes the measuring of specific component of surface free energy possible by using only two monopolar acidic and basic probes such as dichloromethane (CH_2Cl_2) and ethyl acetate ($C_4H_8O_2$), respectively [110]:

$$\gamma_S^{SP} = 2 \cdot \sqrt{\gamma_S^+ \cdot \gamma_S^-} \qquad (3-24)$$

The total surface energy can then be calculated by adding the specific and dispersive contributions to surface energy:

$$\gamma_S^T = \gamma_S^{SP} + \gamma_S^D \qquad (3-25)$$

3.2.6. Acid-Base Properties

One of the advantages of IGC in investigating acid-base properties of materials is the possibility of studying the variations related to surface group orientations [74]. Different methods are applied to describe the acidic or basic behaviour of a solid. The most commonly applied approach for calculating acid-base contribution of surface energy is the Gutmann concept (or procedure) [73, 74]. In the Gutmann concept, acceptor numbers (AN) and donor numbers (DN) represent the ability of having Lewis acidity (electron acceptor) and Lewis basicity (electron donor) specification, respectively. The enthalpy of a typical acid-base interaction is normalised as [54, 73, 107]:

$$-\Delta H = \frac{AN \cdot DN}{100} \qquad (3-26)$$

According to Papirer *et al.* [54], the main advantage of the Gutmann concept is that it recognises amphoteric probes such as acetone. Amphoteric molecules are able to interact as either an acid or base depending on the nature of the associated substance. Acetone, for example, can act as an electron acceptor due to the electron-deficient carbon of the carbonyl group, and show basicity through sharing the electrons on the oxygen atom. Hence, the specific interactions between solid surface and a polar probe is described by the following [110]:

$$-\Delta G = K_A \cdot DN + K_B \cdot AN \qquad (3-27)$$

$$-\frac{\Delta G}{AN} = K_A \cdot \frac{DN}{AN} + K_B \qquad (3-28)$$

where K_A and K_B are a clear indication of the acid-base or the electron donor-acceptor properties of the sample. the Lewis acid and Lewis base parameters of a series of polar probes, respectively and can be calculated by plotting $-\frac{\Delta G}{AN}$ against $\frac{DN}{AN}$. Figure 3.9 gives an example of calculating the acid-base properties for quartz (53 µm < x < 75 µm) using the Gutmann method. The acid and base constants for this sample were calculated as: $K_A = 0.2119$ and $K_B = 0.2874$; indicating the quartz surface is amphoteric.

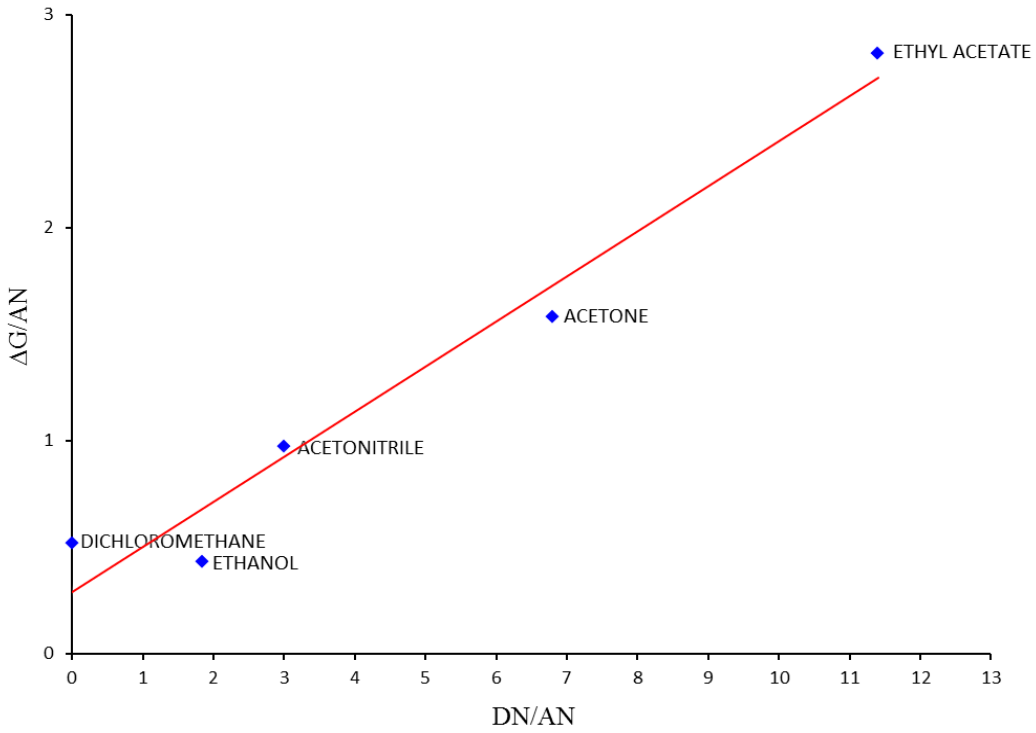

Figure 3.9. The acid-base diagram for quartz (53 µm < x < 75 µm).

3.3. IGC Applications

Soon after IGC was established as a simple and sensitive technique to measure physicochemical properties, a wide variety of materials were investigated by IGC. The most attractive aspect of this technique was the effective application to a wide range of physicochemical characterisation of diverse non-volatile materials in various forms and with different morphologies. Both bulk and surface properties of materials, including dispersive and specific parameters of surface free energy, diffusion coefficients, phase transitions and crystallinity can be characterised by IGC [100, 117, 118]. The activity of a material's surface depends on the nature of the surface, such as surface area, surface free energy, porosity, and acidity-basicity. IGC is a precise surface characterisation technique that can be used to measure these characteristics. It is an excellent method to either determine the production method which affects the surface properties or predict the surface behaviour of the sample in contact with other materials. For example, it was used successfully to predict the effect of milling on the bulk and surface properties of drug compounds [119] which is an important factor in developments for the pharmaceutical industry. In an IGC experiment, bulk interactions arise from diffusion of the probe molecule into the bulk of the stationary phase. Miscibility is one of the most important specifications of the polymerisation process. The solubility parameter and Flory-Huggins interaction parameter can also be determined by IGC. The applicability of IGC in measurements of physicochemical properties of various materials has been described by Voelkel *et al.* [73, 80, 100, 111, 118]. IGC is usually referred to as a physicochemical characterisation technique since physical and chemical properties of materials can be measured simultaneously. However, a new IGC application has been recently introduced in which the structural and chemical characteristics of carbon nanotubes were separately studied by using two different groups of probes with different chemical specifics which were called "structural probes" and "chemical probes" [120].

The following sections cover the use of IGC in analysing the surface properties of a wide variety of materials. These range from pharmaceutical products to naturally occurring minerals indicating the varied applications that can benefit from inverse gas chromatography.

3.3.1. Polymers

Polymers are the most extensively researched materials using IGC. Contact angle measurements are the most widely used traditional methods to characterise polymer surfaces. However, an alternative method was required due to surface heterogeneity and roughness, and also absorption of the liquid into the polymer bulk (instead of adsorption on the surface) that result in inefficiencies of the contact angle method [121]. The popularity of IGC in polymer industries is directly related to its applicability as a technique for the characterisation of the thermodynamic properties of polymer blends, especially the viscous ones [122]. The Flory-Huggins (polymer-polymer and polymer-solvent) interaction parameters, miscibility, Hansen solubility parameters (HSP) (dispersive, polar, hydrogen bonding, and total), and Hildebrand solubility parameter are the bulk properties of polymer blends assessed quickly and accurately by IGC. Guillet & Al-Saigh [123] discussed the application of this technique in characterizing natural and synthetic polymers. The properties they described are the glass transition, degree of crystallinity and rate of crystallisation, diffusion, activity coefficients, solubility parameters, hydrogen bonding, and surface studies such as surface area and energy and adsorption isotherms. The prediction of interactions between a polymeric matrix and a pigment by this technique was also described [117].

The first IGC research to determine the thermodynamic properties of polymers was conducted in 1969 at the University of Toronto [27, 28, 124]. Smidsrød & Guillet [28] determined the glass transition temperature of poly(N-isopropylacrylamide) and noted that the IGC was a fast and valuable technique for assessing the physicochemical properties of polymers. Ansari & Price [125, 126] studied the surface properties of calcined kaolin filled polymers using inverse gas chromatography. They evaluated the different surface energies of two calcined kaolins and calcined kaolin filled polyethylene of which X-ray photoelectron spectroscopy (XPS) was incapable of differentiating [125]. In spite of the similarity between crystallisation specifications and also their XPS results, different surface energies and Lewis acid-base behaviour were observed through IGC. Furthermore, it was examined how the surface energies of different kaolins (as the filler) affected the mechanical properties of Nylon-6 composites [126]. The dispersive components of the surface free energy of the Nylon-6 polyamide, calcined kaolin, and kaolins coated with a coupling agent (aminosilane) were measured by IGC. In spite of the similar enthalpies of adsorption, the dispersive surface energy of uncoated kaolin was remarkably higher than the polyamide, whilst the silane treated sample showed lower surface energy, close to that of the polyamide. In addition, using the coated kaolin resulted in better mechanical properties of Nylon-6 which was correlated to surface energy. Moreover, investigating the specific surface free energy showed a basic surface for Nylon-6 with a high capacity for hydrogen bonding and also suggested an acidic surface for calcined kaolin, which turned to basic after being treated with aminosilane. Voelkel *et al.* [127] used IGC to investigate the dispersive components of the surface free energy of several polymers. The influence of different parameters such as chemical structure, functional group, and heat treatment on the dispersive properties of the polymers was studied. The dispersive component determined by IGC was found to be a useful measure for describing the different behaviours of polymer surfaces of the same chemical characteristics. The diffusivity of solvents in the polymer phase also can be determined through IGC. Diffusivities of water, methanol, and methyl acetate in poly(vinyl acetate) and poly(vinyl alcohol) were measured by IGC and compared to the values from literature [128]. In most experiments, the diffusivity of the solvents in the polymers was highly dependent on the temperature and the concentration of the solvents. In addition, for many experiments, the diffusivity significantly decreased near the glass transition temperatures (T_g). The results were in good agreement with data from gravimetric sorption.

IGC methodology has become the method of choice to evaluate different bulk and surface properties of various polymers and their blends such as polyethylene (PE) [125, 129-131], polyamide [126], polyethers [132], polyesters [132-135], polycarbonates [132], polystyrenes [136-141], poly(vinyl chloride) (PVC) [139, 142-144], poly(ethylene oxide) (PEO) [139, 142], PVC-PEO blends [145], poly(methyl acrylate) [61], poly(ethyl methacrylate) (PEMA) [146, 147], poly(methyl methacrylate) (PMMA) [127, 142-144, 148, 149], PVC-PMMA blend [143], poly(α-n-alkyl) methacrylate [148], poly(vinyl acetate) [61], polyacrylonitrile [150], biopolymers [151], polyimide precursor, and its thermal rearrangement [152]. Cellulose esters, used as biodegradable polymers, were also characterised by IGC [153-157]. There has also been some research into investigating the influence of system parameters on the IGC measurements of polymers. For example, Mayer-Helm & Rauter [158] evaluated column efficiency and the minimum allowable operating temperature of columns containing polysiloxane and polyethylene glycol compounds by inverse gas chromatography. In another study, the impact of carrier gas flow rate on retention volume was studied [159]. The sensitivity of specific retention volume to the flow rate at different temperatures on poly(n-butyl methacrylate) was investigated. Tyagi *et al*. [133] concluded that the changes in specific retention time with flow rate can be linear, nonlinear, or remain unchanged, depending on the column temperature and the flow rate. The work of cohesion (W_{co}) between polymeric matrix microparticles which had been exposed to different conditioning process was determined using IGC, in order to evaluate the flowability of microparticles during production [160]. It was suggested that the flowability improvement could be correlated to the decrease in the interparticle cohesion on which a conditioning process was proposed to improve the microparticle flowability. A large number of polymer matrix materials were introduced to be examined by the same technique; however, the copolymer poly(d,1-lactide-co-glycolide) was proposed to be the preferred compound. The properties of polymers, copolymers, and their blends, as determined by IGC are shown in Table 3.2.

Table 3.2. Physicochemical characteristics of polymers, copolymers and their blends, as determined by IGC.

Parameter	**References**
Solubility parameter component	[130, 134, 154, 156, 161-169]
Flory-Huggins interaction parameter	[58, 61, 62, 71, 130, 134, 136, 141, 143, 145, 146, 161, 163-178]
Miscibility	[58, 61, 136, 145, 171-173, 179]
Activity coefficient	[58, 134, 136, 141, 146, 161-163, 165-170, 173, 174, 177, 179]
Crystallinity	[173, 174, 180-183]
Glass transition temperature (T_g)	[27, 133, 140, 146, 154, 161, 162, 172, 173, 184]
Melting point	[173, 183]
Dispersive surface energy (γ^D)	[125-127, 137, 144, 149, 151, 153, 155, 157, 185-191]
Specific (acid-base) interaction	[79, 125, 126, 185, 187, 189]
Surface area	[36, 138, 177, 192, 193]
Work of cohesion (W_{co})	[160]
Sorption enthalpy (ΔH)	[125, 126, 137, 143, 146, 148, 149, 153, 155, 157, 161, 164-167, 169, 174, 176, 186, 192, 194]
Sorption entropy (ΔS)	[85, 137, 138, 143, 148, 149, 157, 161, 165, 169, 176]
Sorption free energy (ΔG)	[138, 143, 149, 157, 161, 164-166, 169, 176, 186, 189]
Thermodynamics of hydrogen bonding	[194]
Diffusion coefficient	[128, 178, 195, 196]
Partition coefficient	[195]
Acid/base number (K_A, K_B)	[144, 153, 155, 157, 189-191]
Surface nanomorphology	[189]

3.3.2. Pharmaceuticals

After polymers, pharmaceutical powders are the most extensively investigated materials by IGC. The pharmaceutical industry requires a high degree of accuracy when characterizing small quantities of substances in different forms, such as amorphous, polymorphs, hydrates, co-crystals, and solvates. Pharmaceuticals are most commonly formulated with more than one active ingredient and hence understanding the interactions between them in a product is extremely important. Moreover, since pharmaceutical powders are often energetically heterogeneous, their surface energy distribution plays a significant role in product quality. It is believed that traditional methods, such as contact angle measurements for determining interfacial free energy, may lead to the experimental conditions interfering with the results [197]. Therefore, surface characterisation of active pharmaceutical ingredients (APIs), excipients and drug delivery systems (DDS) by IGC has become of significant interest in recent years. IGC was also found to be an effective technique for proposing storage conditions and the shelf life of pharmaceuticals by measuring the crystallisation rates of amorphous dispersions [198]. The pharmaceutically relevant physical and chemical properties of various materials and the influence of different preparation methods, such as milling, dehydration, *etc*. as well as the impact of experimental variables, such as temperature, compaction pressure, water content, and ambient moisture on the product characteristics have been studied [199].

Planinšek & Buckton [200] conducted IGC investigations to characterise various common pharmaceutical excipients in different forms, including amorphous powders, crystalline and highly porous particles ranging from naturally hydrophilic to hydrophobic. They detailed not only the beneficial aspects, but also the potential difficulties of IGC in analyzing amorphous pharmaceuticals. For example, the probability of diffusion of probes (especially polar probes) into amorphous powders such as cellulose was a concern. Moreover, fine materials such as magnesium stearate were found to be difficult to characterise by IGC due to the pressure drop across the column, since the particles tend to aggregate inside the column. Buckton & Gill [201] discussed the significance of powder surface energetics in drug delivery and that IGC was an excellent technique for studying amorphous powders which might crystallise or dissolve during contact angle measurements. Furthermore, it was concluded that IGC was a sensitive enough tool for examining the complexity of powder behaviour *via* their surface interactions. Applications of inverse gas chromatography in pharmaceutical research have been also discussed by Grimsey *et al.* [197]. They mentioned the effect of several parameters such as humidity, sample morphology and particle preparation methods including milling and drying on the results of IGC experiments. The effects of granulation on the surface properties of drug substances and the physicochemical stability of granulated amorphous compounds have also been evaluated by IGC [202]. In addition to various applications of IGC in the pharmaceutical industry, its applicability to studying the anisotropic surface properties of pharmaceuticals was discussed in a recent review by Ho & Heng [105].

IGC has become established as a useful and precise technique to predict changes in the characteristics of pharmaceutical powders due to different industrial processes. For example, surface energy of materials has been evaluated by IGC to assess the thermodynamic impact of particle size and milling [203, 204] or micronisation [110]. More recently, Gamble *et al.* [113] evaluated the efficiency of IGC in analysing the surface heterogeneity of a binary system. They applied IGC to investigate the surface interactions and heterogeneity distributions of drug compounds coated with two different concentrations of silicon dioxide. The results led to the conclusion that the interpretation of IGC results for studying a binary sample's dispersive surface energy was complicated due to different degrees of tendency between coating and bed materials. The dispersive surface energy was derived from contributions of both components on the surface. However, the quantity attributed to each constituent was dependent on its availability and surface energy heterogeneity. Work of cohesion and surface heterogeneity of coarse and micronised lactose were analysed by IGC [205]. The results showed that IGC was able to discriminate between different lactose powders and also to determine the agglomeration due to the storage of powders in a humid environment. The glass transition phenomenon of amorphous lactose was also studied by IGC [206], and it was shown that applying IGC in conjunction with a vapour sorption system provided reliable information about important parameters of amorphous materials, namely: molecular mobility; glass transition temperature (T_g); collapse; and crystallisation. Moreover, the high sensitivity of IGC makes it a powerful technique to detect minor changes in a surface's nature due to processing. Buckton *et al.* [207] applied IGC and isothermal microcalorimetry together to study small variations in the surface properties of saquinavir mesylate powders dried through different techniques. The results indicated a stable, less energetic surface for tray-dried samples than for vacuum-dried and heated samples.

Some of the drugs whose surface properties have been determined by IGC are salbutamol sulphate [208-210], cellulose [199, 211-213], indomethacin [199, 214, 215], lactose [68, 205, 206, 215-228], ibuprofen [229, 230] paracetamol crystal [203], ibipinabant [110], mannitol [219], and dl-propranolol hydrochloride [231]. Furthermore, it has been used in a study of cellulose ether matrix tablets release mechanism of pentoxifylline and vancomycin by determining surface energy parameters of cellulose ether powders [212]. The results indicated that IGC (in combination with other techniques) is a suitable tool to study small differences between the polymers with different substitutions and to predict their behaviour in water.

IGC at infinite dilution can be used to predict the impact of different methods of attrition or cleavage on the powder characteristics. Succinic acid and sucrose were applied as model compounds and the effect of two milling methods, high shear wet milling (HSWM) and dry milling (DM), on their surface properties was studied [119]. It was concluded that the magnitude of the milling effect on the surface energies was highly dependent on the examined compound. If the milling process had a minimal impact on the surface energetics, it resulted in smaller particles but the same atomic arrangement at the surface. In other words, the IGC analysis confirmed significant changes in sucrose surface free energy as a result of the milling process.

The impact of the mixing lubricant and excipient on tablet properties was studied by Otsuka *et al.* [232]. They examined the effects of the type of mixer and mixing time of three types of excipients with magnesium stearate lubricant on particle size, specific surface area and surface morphology of the mixed powders, and also on the tableting compression process by IGC at infinite dilution. The results showed that the surface energy of particles mixed in a twin-shell mixer had less dependency on mixing time than that in the high-speed mixer, although in both cases it decreased with an increase in mixing time. The experiments indicated that the mechanical strength of tablets before adding lubricants could be predicted by the IGC analysis of pharmaceutical ingredients.

Surface energy measurements using IGC were also applied to study the impact of micronisation on the surface of ibuprofen in order to reduce its cohesion [230]. Ibuprofen powder was premixed with amorphous hydrophilic nanosilica; micronisation of the dry coated and uncoated powders was conducted through the same procedure, resulting in powders with different surface energy and flowability. The results revealed a heterogeneous surface and finer particles with a higher surface energy for the uncoated ibuprofen; while dry coating with nanosilica resulted in decreasing the dispersive component of surface energy, producing a homogeneous distribution of surface energy sites, and creation of nanoscale surface roughness which, in turn, resulted in a lower cohesion and improved flowability.

IGC has been also applied to calculate work of adhesion (W_{adh}) and work of cohesion (W_{co}) of pharmaceutical materials. The influence of lubricants in pharmaceutical formulation is directly related to their role in the reduction of cohesive forces between particles or adhesive forces between particles and the container wall [226]. The technique explained how the dispersibility of salbutamol sulphate was improved by magnesium stearate (MgSt) [210]. Determining interactions between non-symmetrical particles using atomic force microscopy (AFM) was found to be difficult due to their variable contact surfaces; therefore, IGC was used to calculate the thermodynamic work of cohesion/adhesion between the sample particles. The work of adhesion (W_{adh}) between salbutamol sulphate and MgSt was significantly smaller than the work of cohesion (W_{co}) between the salbutamol sulphate particles in agglomerates, confirming that magnesium stearate acted as an agglomerate modifier through increasing the particle detachment (and/or packing fraction). The distribution of dispersive, specific and total surface energies of lactose and indomethacin was determined by Das and Stewart in order to study the effect of two different MgSt-addition methods on the surface energy of lactose; the changes in indomethacin surface energy due to micronisation; and the influence of the storage at high relative humidity (RH) on the surface energy of micronised lactose [215]. The results revealed that determining the surface energy heterogeneity was more useful than obtaining only the surface energy value at a determined surface coverage. Mechanofused lactose with MgSt showed a higher decrease in surface energy than the product form mixing in a Turbula, which was in agreement with measurements indicating an improved flowability and dispersibility of the mechanofused sample.

The micronisation process resulted in an increase in the dispersive surface energy and a decrease in the specific and total surface energy of indomethacin. Furthermore, the dispersive, specific, and total surface energy of the micronised lactose decreased after storage for three months at 75% RH. The measured properties of pharmaceutical ingredients and products by IGC method are summarised in Table 3.3.

Table 3.3. Physicochemical characteristics of pharmaceutical materials, as determined by IGC.

Parameter	**References**
Flory-Huggins interaction parameter	[116]
Sorption free energy (ΔG)	[68, 110, 199, 203-205, 208, 209, 217]
Surface energy heterogeneity	[110, 113, 205, 208, 214-216, 219, 228, 233-236]
Dispersive surface energy (γ^D)	[68, 110, 113, 116, 119, 199, 200, 203-205, 207-211, 213-220, 222, 225, 226, 228, 230, 231, 233, 234, 236-247]
Specific free energy (ΔG^{SP})	[69, 110, 119, 199, 203, 205, 208, 209, 214-216, 218, 226, 228, 231, 236-238, 242, 243, 245]
Acid/base number (K_A, K_B)	[68, 69, 116, 199, 200, 202, 203, 207-209, 214, 217, 220, 237, 239, 240, 242, 243, 245, 247]
Work of cohesion (W_{co})	[205, 210, 226, 236]
Work of adhesion (W_{adh})	[210, 236]
Glass transition temperature (T_g)	[199, 206, 248]
Surface structural relaxation	[249-251]
Surface crystallisation	[252]
Hildebrand's solubility parameter (δ)	[236]

3.3.3. Minerals and Inorganic Compounds

Surface characterisation studies of minerals, especially high surface energy compounds, are usually difficult due to their tendency to adsorb water [253]. However, the IGC technique has been successfully applied to characterise such materials. Calcium carbonate ($CaCO_3$) is a high-energy surface filler that was characterised by infinite dilution inverse gas chromatography [253]. It was found that the surface of the $CaCO_3$ was strongly basic and its basicity was reduced dramatically by coating. The high acidity of the coated filler was due to the heterogeneous distribution of coating and more than monolayer surfactant coverage on the surface. Keller and Luner [254] characterised and compared the surface chemistry of synthetic calcium carbonate, marble and chalk, investigating porosity, BET surface area, and chemical composition. The results showed that the physically and chemically adsorbed water at the surface, and within the pores, plays a significant role in the surface energetics of the calcium carbonates. Dehydration of the compound by heating resulted in an increase in surface energy. The IGC showed a high degree of sensitivity in tracking water desorption at sub-monolayer concentrations.

In oil transport, water-wet (hydrophilic) surfaces release more oil than oil-wet (hydrophobic) surfaces; this phenomenon influences oil recovery from reservoirs. In order to enhance/improve the recovery of the inaccessible oil, chemical interactions between oil phase, aqueous phase, and rocks of different origins were studied using IGC [255]. The surface of two natural chalks from a water zone and a gas zone (an analogue for oil saturated chalk) was characterised. It was concluded that the sample from the gas zone was more hydrophobic and the dispersive and specific components of the surface free energy were lower than those of the water zone chalk. Furthermore, it was suggested that the hydrophobicity of the chalk surface was determined by the surface nano-organoclay (hydrocarbons adsorbed clay) rather than the chalk itself.

The study of surface properties of slates by means of inverse gas chromatography was undertaken by Rodriguez *et al.* [256]. The specific and nonspecific surface energy of mesoporous structural slate containing quartz, muscovite and chlorite was characterised at zero surface coverage (infinite dilution) IGC. Consequently, IGC was reported to be a valuable method for determining the properties of the slate surfaces which had been already characterised by chemical analysis, BET N_2-adsorption, XRD, and FTIR.

Surface energy characterisation of rocks by IGC was reported by Arsalan *et al.* [257, 258]. Lifshitz-van der Waals (dispersive) and acid-base components of surface energy of carbonate (calcite and dolomite) and sandstone rocks were determined. For all these minerals, the Lifshitz-van der Waals component decreased with increasing temperature, in contrast to the acid-base properties which increased with increasing temperature. In addition, by determining and comparing the magnitude of the surface interactions between the crude oil-rock and brine-rock they were able to predict whether a reservoir rock would react as a water-wet or oil-wet rock. The influence of polymeric (acrylic) coatings on marbles (and clay) against the corrosive effect of sulphur dioxide (SO_2) was evaluated by a version of IGC called reversed-flow gas chromatography (RFGC) [196]. In the RFGC system, the direction of carrier gas flow is repeatedly reversed for a short time, allowing the measurement of the deposition velocities of SO_2 and the protective efficiency of the coatings on the samples. RFGC was successfully applied to confirm that the examined coating (acrylic copolymer Paraloid B-72) effectively protected the surface of marble (and the clay) from SO_2 corrosion.

The quality of an abrasive material strongly depends on the abrasiveness, its coverage by a wetting agent and the quality of hardening process [259]. Pyrite (FeS_2), calfix ($MgCO_3$+$CaCO_3$), cryolite (Na_3AlF_6), potassium fluoroborate (KBF_4), lithopone (ZnS+$BaSO_4$), and PAF (K_3AlF_6) are compounds that have been characterised as raw fillers for abrasive materials and their semi-products by IGC [260]. Voelkel & Strzemiecka [261] utilised IGC to evaluate the crosslinking extent in the manufacturing of grinding tools. Jurga *et al.* [259] applied IGC to examine the degree of crosslinking of resins in the intermediate-product which is determinative in the stability of abrasive products. Strzemiecka *et al.* [262] used IGC to compare two kinds of abrasive fillers: perlite and zeolite. They used the resulting dispersive and specific components of the surface free energy of the fillers to determine their surface activity and also the Flory-Huggins parameter to examine interaction phenomena between the fillers and phenolic resin.

IGC analyses mainly results in measurements of the adsorption energy. With a slightly different approach, it was shown that even the local adsorption energies are measurable by this technique [263]. Local adsorption isotherms and local specific surface areas for gaseous hydrocarbons on solids including ZnO, PbO and $CaCO_3$ were determined. The terminology "local" refers to those energy sites that are active at a particular time.

The applicability of IGC to flotation in mineral processing was introduced by Ali *et al.* [264]. IGC surface energy analysis and then microflotation experiments were carried out on galena (hydrophobic) and quartz (hydrophilic) minerals. It was shown that there was a correlation between the work of adhesion and the hydrophilic nature of the examined minerals (Figure 3.10), and the subsequent microflotation recovery. In fact, determining work of adhesion using polar and nonpolar solvents makes IGC a fast method for following batch to batch changes in surface characteristics with reproducible results [66]. Hydrophilicity was defined as the ratio of the specific component to the total surface energy by Ho *et al.* [235].

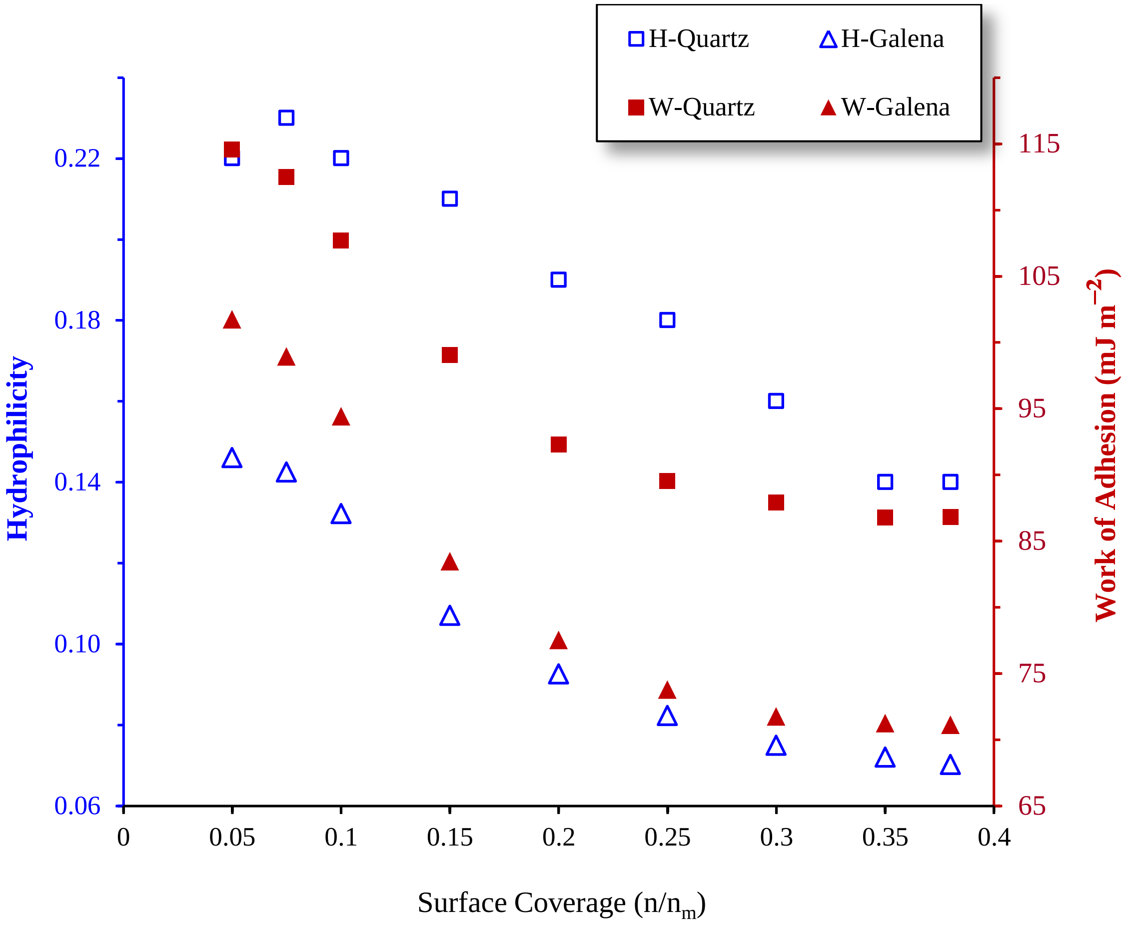

Figure 3.10. Work of adhesion between water and galena (filled in triangles) and quartz (filled in squares); plus the hydrophilicity of galena (empty triangles) and quartz (empty squares), both as a function of surface coverage [264].

3.3.3.1. Silica

Silica is one of the most characterised inorganic compounds, found both in nature and synthesised in different forms including crystal, colloidal, pyrogenic, and porous materials, such as silica gel and aerogel. Surface chemistry of porous silica and the changes due to various modifications have been studied by a number of researchers. The results have shown that the dispersive surface energy of the material functions independently from its specific surface area [265]. The surface of silica modified by an esterification (pyrogenic silica) reaction with alcohols was also investigated for evidence of the degree of coverage by the grafts [266]. In similar research, the surface properties of initial and grafted silica with a C8 alkyl chain [96], methanol [94], and hexadecanol chains [94, 95] were assessed by IGC at finite concentration. In addition, the effect of the degree of coverage of silylated silica was examined by IGC at both finite concentration and infinite dilution [267]. Sidqi *et al.* [268] measured the thermodynamic parameters of the surface of both pure and impure silica samples from different sources. Moreover, modified silicas have been characterised focusing on the influence of the graft carbon numbers on the surface properties [269, 270]. In another study, Pyda & Guiochon [271] characterised silica-based adsorbents by IGC. They believe that their data is dramatically more accurate and precise than other work since they have applied the stationary phase as a coating on the open column wall instead of packing it into the column.

Brendlé & Papirer [272, 273] proposed a topological index (χ_T) for probes in IGC in order to evaluate the surface nanorugosity of solids of various morphologies. Pyrogenic and lamellar crystalline silicas, as well as zirconia (ZrO_2), goethite, and graphite, were characterised using linear, branched, and cyclic alkanes as probes. The study was conducted based on the fact that the interaction between the solid surface and solutes is not only controlled by the surface energy sites' status, but also by the molecular structure and morphology of individual adsorbates. The parameter topological index (χ_T) was successfully used to determine γ^D and the surface roughness (nanomorphology) of the samples using the calculated topological indexes of the probes.

Controlled pore glasses are porous glasses which are prepared with a wide range of textural and porosity properties. Because of its adjustable porosity (therefore adjustable adsorption strength) and its excellent mechanical and chemical stability, it is an attractive material for a diverse range of applications. Rueckriem *et al.* [274] applied IGC to describe how textural properties affect the dispersive surface energy and the specific surface energy. Thermally treated controlled porosity glasses and boron-coated silica gel were also characterised by IGC [275]. The results showed that the dispersive surface energy (γ^D) of the samples was slightly increased due to the surface modification. In contrast, the non-dispersive components of surface free energy (γ^{SP}) changed significantly; this phenomenon was mainly attributed to the existence of hydroxyl groups at the surface.

The changes in glass fibres' surface energy due to treatment with silane and titanate have been studied using IGC [276]. The results demonstrated that in the case of untreated samples, the solid surface was the electron donor and the adsorbed probe was the electron acceptor. However, the treated fibres showed the opposite electron donor/acceptor behaviour, and the electrons transferred from adsorbed molecules to the solid surface. The order of electron transfer ability of the samples was suggested to be: silane-treated < untreated < titanate-treated. Moreover, an improved mechanical performance was observed for the fibre-phenolic resin composites containing silane-treated short glass fibre. This improvement was attributed to an improved matching of surface energy values of the components which resulted in a stronger binding within the composite.

Surface energy, work of adhesion, and hydrophilicity (γ^{SP}/γ^T) of quartz, before and after modification with dodecylamine, was determined using IGC. Microflotation experiments were also conducted to study the correlation between the surface characteristics and flotation response. The results confirmed that the hydrophilic quartz had a relatively high surface energy and the adsorption of the cationic surfactant reduced the surface energy of the hydrophobised quartz. Furthermore, the surface heterogeneity evaluation indicated that the surface of the modified quartz was energetically less active and more homogeneous than the untreated samples. The flotation behaviour of the quartz matched the changes in the surface energy and work of adhesion to water.

Thermodynamic parameters of glass beads with 1 $m^2 g^{-1}$ specific surface area, both untreated and treated with sulfochromic acid, and their proportions of silanol and siloxane surface groups were measured and compared by Comte *et al.* [277]. The carrier gas was used with different relative humidity values, and it was observed that regardless of the humidity, the dispersive component of surface energy for the treated samples was higher than that of untreated beads.

3.3.3.2. Clay Minerals

Clay minerals are attractive compounds for many industrial applications, and as such have been characterised by inverse gas chromatography. Phyllosilicate minerals (smectites) are an important group of minerals for purposes ranging from drilling mud and latex paint to animal litter trays and nail polish. Smectite clays have high specific surface areas and are chemically active; their structural layering allows them to attract a large number of polar molecules, such as water, into their interlamellar structure. Montmorillonite, bentonite, beidellite, saponite, nontronite, and hectorite are the most important clays among this group of minerals. Surface properties of smectites were determined by IGC at infinite dilution by Bandosz *et al.* [88, 278]. They found a relationship between the parameters obtained from IGC and chemical characteristics, surface area, and porosity. The technique was confirmed to be a useful method to study the surface of layered minerals since it complemented conventional characterisation analyses. Kaolinite is another important industrial clay, extensively used as a filler in the polymer industry. Commercial calcined kaolin surfaces, before and after modification with an aminosilane coupling agent, have been analysed by IGC [126, 279]. In these studies, changes in surface free energetics of kaolinite due to calcination and coating with a coupling agent (aminopropyl triethoxysilane) were studied. The authors believe that their results "further validate the use of IGC for the study of the surface properties of finely divided solids" [279]. Additionally, dispersive components of the surface free energy of illites and kaolinites from different sources were studied at different temperatures using infinite dilution IGC [280]. In this work, surface properties of illites and kaolinites from different formation conditions were compared. IGC was capable of differentiating not only illites from kaolinites, but also the species of a given family regarding their origin achieved by analysing a limited number of samples. Sepiolite is another clay mineral that was characterised using IGC under two different conditions [281]. Dispersive components of surface free energy at different temperatures, as well as enthalpies, entropies and the acid-base properties of the sepiolite modified with iron were determined under infinite dilution conditions. Furthermore, specific surface area, pore volume and pore size and adsorption energy distributions were achieved at finite concentrations. It was found to be a useful technique for determining the surface properties of Fe-sepiolite, although the specific surface area calculated by IGC did not show a good agreement with the result obtained from N_2-adsorption isotherms of BET method. The influence of low temperature air plasma treatment on the properties of kaolinite was evaluated by measuring the surface energies through IGC using both the Schultz and Dorris-Gray methods [282]. The dispersive surface energy heterogeneity profiles of untreated and plasma treated samples for different time periods were determined. The calculated γ^D increased after the air plasma treatment. From the γ^D distributions, it was concluded that the surface energy of the sample was activated after a 10 minute treatment; however, increasing the treatment time to 30 minutes showed the opposite effect. Furthermore, the dispersive surface energy profiles confirmed that the air plasma treatment led to a higher average surface energy in a wider surface coverage range for the kaolinite powders.

The isotherm of chlorinated hydrocarbon adsorption on halloysite surface was determined by two IGC methods, peak maximum (PM) and peak division (PD), and the results were compared [283]. In the PM method, several amounts of a single solvent were injected into the IGC column, whilst PD calculation was based on a single chromatographic peak. The adsorption isotherm was obtained quickly, and the results showed little differences. Moreover, the enthalpy of the adsorption of chlorinated hydrocarbons (dichloroethylene, trichloroethylene, tetrachloroethylene) on the halloysite surface was negative and decreased with increasing the number of the chlorine atoms of the adsorbate. The effect of different milling processes on the surface properties of an attapulgite clay (palygorskite) was studied by using IGC, at both infinite dilution (IGC-ID) and finite concentration (IGC-FC) conditions to evaluate the dispersive component of surface energy and the specific surface area, respectively [284]. Three different dry grinding processes (batch ball milling, air jet microniser, and vibratory ball mill) were applied and the changes in surface properties of the ground products were characterised by IGC. It was concluded that the dispersive component of surface energy of the dry-ground samples did not change significantly except for the product from the vibratory ball mill. Moreover, the specific surface area obtained from IGC with octane probe was comparable to BET specific surface area. Some of the determined properties of various clays are summarised in Table 3.4.

Table 3.4. Physicochemical characteristics of clay minerals, as determined by IGC.

Parameter	**References**
Dispersive surface energy (γ^D)	[88, 126, 279, 282, 284, 285]
Specific interaction (ΔG^{SP})	[126]
Sorption entropy (ΔS)	[279]
Sorption enthalpy (ΔH)	[280, 283]
Diffusion coefficient	[196]

3.3.3.3. Zeolites

Natural zeolites have numerous applications including as catalysts, in gas separation, and ion exchange, mostly due to their unique porosity and high specific surface area. This group of minerals is also widely used as molecular sieves with high selectivity to separate different components of a mixture. They are adsorbents in water treatment and purification of other industrial fluids. The specific and dispersive components of surface free energy as well as free energy and enthalpy of adsorption of zeolites have been measured by inverse gas chromatography [286]. IGC was applied to characterise a variety of zeolites [287-289]. These experiments used IGC to investigate the effect of storage conditions, including humidity, on zeolite surfaces [287]. The results showed that the surface acidity and basicity had a direct relationship with the relative humidity of the carrier gas, although the respective parameters of fine and thick zeolites could not be measured due to their very high activity. Furthermore, applying IGC provided the possibility of studying the use of zeolites in producing abrasive materials without manufacturing a trial product, very important in time- and cost-efficient production [288]. The effect of impregnation with acetic and succinic acid, aqueous solutions of 1,2,3-propanetriol (glycerol), propane-1,3-diol, butane-2,3-diol, and model post-fermentation broth on the surface properties of Zeolite 5A was investigated by IGC and compared to the other sorbents, Amberlite XAD7HP, Zeolite 5A, and Diaion SK116 [289]. The acid and base numbers suggested that the most acidic surface among the examined samples was Zeolite 5A, and a high decrease in dispersive surface energy occurred as a result of blockage of the zeolite active sites due to the strong adsorption of water during the impregnation.

Since the BET technique proved inadequate for surface characterisation and prediction of adsorption behaviour, IGC was used to comprehensively investigate the adsorption of fragrances onto the natural and synthetic zeolites [290]. In other interesting research, Thielmann *et al.* [77, 98] combined thermal desorption methods with IGC to examine the surface of 3A and 13X zeolites. They succeeded in distinguishing between micropore and mesopore contributions from adsorption phenomena due to differences between adsorption mechanisms.

3.3.4. Surfactants

Surfactants are surface active agents, their function being based on their adsorption at interfaces and lowering the surface tension between interfaces. According to the nature of the polar group, they are classified as cationic, anionic or non-ionic surfactants. Interaction parameters of anhydrous cationic surfactants and their mixtures were determined by inverse gas chromatography [291-294]. The results showed that a surfactant’s interactive miscibility depends on the differences in temperature, chain length, and the component ratio of the surfactant mixtures. Furthermore, solubility parameters of non-ionic surfactants have been determined by IGC [295-299]. The results indicated that thermodynamic properties of these surfactants were governed by temperature, molecular structure, molecular weight, chain length, component ratio, polarity, and hydrogen bonding components. Voelkel *et al.* [300] applied IGC to determine the binary parameters resulting from hydrogen bonding and polarity of oxyethylene derivatives of 1-hexadecanol. By using two groups of polar probes with the capacity to form hydrogen and polar bonds, it was concluded that the structure of the liquid stationary phase (oxyethylate) and the temperature of the IGC column might be responsible for the hydrogen bonding and polar binary parameter changes. However, no general link between these two parameters and column temperature was reported. Table 3.5 summarises the examined characteristics of surfactants by IGC and some of the studied compounds.

Table 3.5. Physicochemical characteristics of surfactants, as determined by IGC.

Parameter	**References**
Miscibility	[291, 292, 294]
Flory-Huggins interaction parameter	[291, 292, 295-297]
Activity coefficient	[293, 295]
Solubility parameters	[295-299]

3.3.5. Nanomaterials

Nanomaterials may belong to one of the above mentioned material types, but with nanostructures. However, their chemical and physical properties such as electronic properties and surface energy may be different from bulk material characteristics due to particle size. Inverse gas chromatography applications in this area have mostly focused on carbon nanoparticles. Menzel *et al.* [120] studied the physicochemical surface properties of carbon nanotubes (CNTs) such as dispersive surface energy and surface heterogeneity by inverse gas chromatography. The novelty of their work was applying IGC to the investigation of solids' surface structure and surface chemistry separately, to avoid convoluting these two characteristics. IGC was also reported to be a powerful tool for characterizing the surfaces of chemical vapour deposition (CVD)-grown, multiwalled carbon nanotubes (CNTs) [301].

Dispersive surface energy (γ^D), acid and base numbers (K_A and K_B), and specific free energy (ΔG^{SP}) for various as-received (commercial), in-house (prepared), and surface-modified CNTs by high temperature annealing, thermal oxidation, and grafting with methyl methacrylate were determined and compared. The IGC results were shown to be in good agreement with the obtained values from conventional surface characterisation techniques, including Bohm's titration, scanning electron microscopy (SEM), and X-ray photoelectron spectroscopy (XPS). The results revealed a high dispersive surface for the as-received CNT samples and a higher polar component for the commercial CNT surface than the graphitic in-house materials. In addition, it was indicated that the modification of the surface by high temperature annealing resulted in a decrease in surface polarity, while the thermal oxidation increased the polarity of the CNT surface. Furthermore, grafting small amounts of methyl methacrylate was found to have a remarkable influence on the surface properties of the examined carbon nanotubes by lowering the surface energy and adsorption capacity. IGC was also applied to study the mechanism of adsorption of organic chemicals on to carbon nanotubes [302]. Properties such as the dispersive component of surface free energy and acid-base parameters of multiwalled carbon nanotubes (MWNTs) were determined at infinite dilution in order to investigate their changes due to chemical modifications [301, 303]. The examination of the dispersive and specific surface free energy values of a composite as a gas diffusion layer for proton exchange membrane fuel cell by IGC was also reported [304]. IGC was noted to be an excellent technique for characterizing the surface energy of the microporous layer containing nanocarbon chain and fibrous nanocarbon. Nanostructured nonmicroporous carbons were also studied using IGC. Three different kinds of carbon including carbon nanofibres (CNFs), multiwalled carbon nanotubes (CNTs), and high-surface-area graphites (HSAGs) have been characterised [305]. Surface free energy and its dispersive and specific components, free energy and enthalpy of adsorption of the compounds were evaluated by IGC to investigate their capacity for adsorption of n-alkanes; the adsorption on HSAGs surface was indicated to be the most energetically favourable. Few-layer graphene and graphite nanopowders were also characterised using IGC [306]. The isosteric adsorption enthalpies of acetone to the powders as a function of surface coverage were calculated and the variation of the enthalpies was explained based on the face and edge of single- and multi-layer samples. For example, the determined enthalpy of adsorption at very low surface coverage was attributed to the surface steps and edge cavities; whereas the enthalpy obtained at higher surface coverages ($\geq$ 4%) was considered to be the result of the adsorption to flat surfaces. In addition, the graphite nanopowders indicated many more high energy sites than the graphene powder [285]. The adsorption enthalpies of different probes (acetone, acetonitrile, dichloromethane, ethanol, ethyl acetate, hexane, and toluene) on graphene flakes were also determined and the results were in excellent agreement with the calculated enthalpies of adsorption through *ab initio* molecular dynamics [307].

The impact of different drying methods on the surface properties of cellulose nanofibrils including nanofibrillated cellulose (NFCs) and cellulose nanocrystals (CNCs), was evaluated using IGC [308]. The dispersive component of surface energy at different temperatures and acid-base parameters were determined for NFC and CNC samples dried though various drying methods. Supercritical-drying NFCs showed the highest γ^D, and the freeze-dried NFCs and CNCs showed the lowest γ^D, and different γ^D values were attributed to different degrees of agglomeration due to different drying methods. Furthermore, applying the same drying method led to a higher acid/base number ratio for NFCs.

Both IGC conditions, finite concentration and infinite dilution, were applied to study the effect of milling media on the surface heterogeneity of graphites [309]. The samples were first ground for different times and with different oxygen contents. Then the dispersive component of surface energy of the milled graphites was characterised by IGC. It was concluded that the graphite surface became more energetic as the result of the milling process, and the number of high energy sites increased considerably with increased milling time. IGC was also used to analyse the surface properties of other inorganic materials at the nano scale, including metal oxides. Dispersive components of the surface free energy as well as specific surface area of zinc oxide nanoparticles were determined, in order to study and compare zinc oxides of different morphologies, sizes, and specific surface area [310]. The spherical zinc oxide with a high specific surface area and the highest structure deficiency showed the highest value of dispersive surface energy. In addition, the coated zinc oxide with itaconic (methylenesuccinic) acid showed lower surface energy with fewer tendencies to specific interactions.

3.3.6. Planar Materials

In order to characterise the surface of planar materials such as polymer films by means of inverse gas chromatography, different methods have been applied to introducing the sample to the IGC system. Some of them were deposited on the wall of the chromatographic column [41, 311, 312]. Poly(ethylene terephthalate) film was characterised through IGC [121]. Small disks of the polyester were packed into the chromatographic column, and the dispersive component of surface energy and the Gibbs energy of adsorption (ΔG_{ad}) of the film at three temperatures (15 ºC, 26.5 ºC, and 40 ºC) were determined. The γ^D values were in good agreement with contact angle measurements. Cellophane film was also studied using IGC by Katz & Gray [102, 313, 314]. Partition coefficients for a series of n-alkanes, surface free energy (ΔG_{ad}), entropy (ΔS_{ad}), and enthalpy (ΔH_{ad}) of adsorption were determined by packing cellophane disks into the IGC column. They investigated in detail the adsorption of hydrocarbons on cellophane, which is regenerated cellulose. In this research, the surface characteristics of cellophane and the influence of humidity on the surface interactions were examined. The surface free energy and the adsorption isotherms obtained from IGC were compared to the contact angle measurement and BET analysis results, respectively; the IGC results were in good agreement with the results from conventional methods. In another study [315], the column was filled with strips of food packaging polymer films to investigate aroma scalping through them. Similarly, IGC analysis of cellulosic paper was conducted by cutting the paper to into small pieces, and was then was introduced into a "U" shape stainless steel column under vacuum [67].

However, none of the above mentioned methods is considered to be the ideal route for introducing film samples in to the IGC system. New IGC instruments can be equipped with a film/monolithic sample holder for characterizing thin films, strips and wafers. This has the capability of accommodating a wide range of planar samples and being connected to the IGC instrument externally.

3.3.7. Other Applications

Since inverse gas chromatography became a well-established method for investigating the properties of a wide variety of materials, there are some examples other than those outlined previously which are worth mentioning.

3.3.7.1. Carbon

Activated carbon is a widely used material in various industries. Surface chemical properties and pore-size distribution of different activated carbons were investigated using IGC [86, 316] in order to evaluate the influence of various treatments on their characteristics. The analysing the IGC data indicated an increase in the adsorption energy of alkanes on activated carbon due to the oxidation from nitric acid; it clearly demonstrated a correlation between surface chemistry and adsorption thermodynamics. Activated carbon was used to test the capability of a modified inverse gas chromatography in determining the thermodynamics of porous materials [76]. The dispersive component of the surface free energy, specific component of adsorption energy for the adsorption of polar probes, specific components of enthalpy of adsorption of two active carbons with different BET surface areas, and molar free energy of adsorption of one methylene group on the active carbons were determined by using multi-component probes in one injection. An external capillary column was used to separate the components of the probe before entering the IGC column. Meanwhile, applying both FID and TCD at the same time ensured that the measurements were sensitive and fast. The activated carbon with the higher BET area showed lower dispersive surface energy.

Compared to the conventional IGC, the modified IGC was reported to be a convenient and quick method to characterise the surface properties of porous solids. The specific interaction, acid (K_A) and base (K_B) numbers, nanomorphology, and electron donor (DN) and acceptor (AN) properties of natural and heat treated graphite were determined through the calculated topological index (χ_T) for used probes in IGC [273]. It was concluded that $\Delta\chi_T$ was independent of temperature for the natural sample, and the acidic properties of the graphite surface decreased after heat treatment. Surface energy heterogeneity of electro-graphite and synthetic graphite was determined by Thielmann & Pearse using finite concentration IGC [317]. It was shown that the adsorption of different probes at solid surfaces occurs through different mechanisms that could be useful for blend quality control improvements through understanding the intermolecular interactions.

3.3.7.2. Ionic Liquids (ILs)

Thermodynamic characteristics of ionic liquids (ILs) and their complexes were successfully determined by inverse gas chromatography [90-92, 318-322]. Ionic liquids are widely used as scavengers in chemical industries, solvents in cellulose processing, dispersing agents in paints, transport media for reactive gases, electrolyte media in nuclear fuel recovery, and electrolyte in electric batteries. By determining the activity coefficients, the interaction between an ionic liquid and different solvents is predictable, and by calculating the selectivity parameter from activity coefficients, the efficiency of an IL for a certain separation process would be predictable [319]. The studies demonstrated the effect of substitutions in ionic liquid selectivity in the separation of aliphatic and aromatic hydrocarbons, as well as the effect of the alkyl chain length on the activity coefficient of the ionic liquids. IGC was also used to study miscibility in isosteric solvents mixtures [323]. In this work, the Flory–Huggins interaction parameters between isosteric solvents were calculated to examine solvent-solvent interactions. The effects of probe concentration and temperature on their interactions were studied. The results showed that an increase in temperature resulted in a decrease in the Flory–Huggins interaction parameter and this effect was more significant for polar solutes than nonpolar solvents. Activity coefficients, selectivities, and partial molar excess enthalpies for four new dicationic ionic liquids based on morpholine were measured by IGC [320, 321]. The results showed that the examined ILs can be efficiently used as extracting solvents for separating aromatic from aliphatic compounds.

3.3.7.3. Fibres

Natural and synthetic fibres have also been characterised by IGC. Wool fibres (untreated and chlorinated) were characterised using C_1-C_5 n-alcohols as probes [324]. The chlorinated wool was shown to contain less sulfonic groups at the surface and a macromolecular rearrangement was demonstrated to happen during wetting and drying processes. IGC was used to study the surface properties of pitch based and polyacrylonitrile (PAN) carbon fibres [85, 103, 104, 325-

327]. Dispersive components and specific interactions of pitch based carbon fibres were measured before and after modification by thermal treatments and anodic oxidations, to evaluate the adhesion between matrix and fibres [325]. The surface of thermo-final treated fibres was found to be electron donor (basic) in nature, with a relatively high γ^D. Both K_A and K_D were high for aniodic-treated fibres, indicating a better adhesiveness to matrix than non-treated fibres. High strength PAN based carbon fibres were also characterised using IGC. It was shown that the shear strength of the interface determined through a fragmentation technique is correlated with the acid-base interaction parameter obtained from IGC experiments [103, 104]. Comparing the measured acid-base properties of different fibres indicated that coated fibres were both more acidic and more basic than oxidised and untreated fibres. The study resulted in the proposal of a third parameter (K) which reflects the amphoteric character of solids such as oxides or carbon fibres [85]. Surface energies (γ^D, γ^{SP}, γ^T) of PAN-based carbon fibres collected at three stages of production (carbonisation, electrolytic surface oxidation, and epoxy sizing) were examined using IGC. The remarkably high γ^D values of unoxidised and oxidised samples reflected the graphitic nature of carbon fibre. Oxidised fibres demonstrated the highest γ^{SP}, most likely due to oxygen and nitrogen interactions on the surface. Epoxy-sized fibres showed the highest surface polarity or hydrophilicity (γ^{SP}/γ^T), this was consistent with the known fact that epoxy sizing increase the wettability of carbon fibres [326]. Surface energy heterogeneity (γ^D, γ^{SP}, γ^T) of high, standard, and intermediate modulus fibres was also studied [327]. The fibres from different stages of production indicated different distributions of energy at the surface. The sized fibre surface was energetically homogeneous, and the heterogeneity of unoxidised and oxidised fibres was suggested to be about 15% and 30% of the surfaces, respectively.

Different kinds of lignocellulosic fibres including flax, hemp, kenaf, agave, agave hybrid, sisal and pineapple were treated with two modifiers: sodium hydroxyl and a cereal protein called zein. Thereafter, acid-base characteristics and dispersive surface energy of the untreated and modified lignocellulosic fibres were measured by IGC [328]. Chemical composition, crystallinity and morphology of the natural fibres were shown to be the determining parameters in their dispersive surface energy values. In addition, measuring the specific free energy indicated a basic surface for natural fibres, contrary to an acidic surface of alkaline treated fibres. Surface characteristics of cellulose fibres were also studied by Belgacem *et al.* and Czeremuszkin *et al.* [329, 330]. IGC was used to follow the effect of purification of the fibres by thorough removal of surface impurities through acetone treatment as well as the effect of corona treatment on the cellulose fibres. Cellulose showed a 50% increase in the dispersive surface energy, both after purification with acetone and treating with a corona; due to both methods removing impurities from the fibre surface, confirmed by XPS analysis [330]. The impact of particle size of flax fibres on the surface properties showed that the dispersive component of surface energy of flax fibre was lower after grinding, and increased with decreasing the particle size since more functional groups are available at the ground sample's surface. Combining IGC and XRD, it was concluded that crystallinity did not have a significant influence on the γ^D values [331].

3.3.7.4. Pulps

Kraft pulps from different origins were analysed for changes in the dispersive components of surface energy, specific components of work of adhesion to several polar probes of the pulps, before and after extraction with hot water (HWE) [332]. It was suggested that the HWE sample prepared from E. globulus chips, which showed a higher acid-base interaction affinity, was not suitable for paper production, compared to kraft pulps from sugar maple chips. However, using it as a reinforcement material would improve the adhesion of composites to polymers. Bagasse paper handsheets were also characterised, prepared from raw and HWE bagasse fibres, using two dry–strength agents: chitosan and cationic starch [333]. The surface heterogeneity profile, calculated ΔG^{SP}, γ^D, K_A, K_B, and K_A/K_B ratio confirmed the positive impact of the dry–strength agents on paper handsheets by forming a film on their surfaces.

3.3.7.5. Biomaterials and Environment

The influence and impact of IGC is also noticeable in environmental and biotechnology fields. Pyrolytic carbon black (PCB) is one of the key products from the pyrolysis of waste tires. It can be used to replace the commercial semi-reinforcing carbon black after demineralisation and modification with titanate coupling agent (TWPC). The rubber containing PCB was analysed by IGC, to evaluate the interaction between natural rubber and TWPC in comparison with commercial carbon black [334]. IGC has found its way even into biological reactions, although these groups of materials have not been widely examined by IGC. Enzymes are one of the most important biological molecules; the proteins which are interpreted as being biological catalysts. They are applied in diverse industries including food and fuel production, health, paper and cleaning industry. As with other catalysts, enzymes increase the rate of reactions significantly by lowering the activation energy for biochemical reactions. Marton *et al.* [335] studied the dispersive surface energy and acid-base properties of lipase by IGC. Conducting IGC experiments allowed them to successfully determine the adsorption of substrates at the enzyme surface in competition with that of water molecules. In another study, IGC was applied to study the adsorption mechanism of organic substrates and water on enantioselectivity of candida antarctica lipase B (CALB) at infinite dilution by determining the adsorption enthalpy [336]. Enantioselectivity of lipases is a crucial characteristic in their applications and is affected by various parameters, considered to be a complex phenomenon to investigate. IGC experiments suggested that the mechanism through which water influenced CALB enantioselectivity was highly dependent on its surface hydration. At low hydration, the inhibitive role of water on enantioselectivity towards secondary alcohols was serious, whilst the high hydration caused polar groups to be fully taken up by water and hence its effect became negligible.

3.3.7.6. Metal Oxides

Metal oxide surfaces were also characterised using IGC. The effect of heat treatment on the surface properties of different hematites was studied through evaluation of free energy of adsorption of CH_2 group, morphology, and acid-base properties of sample surfaces [337]. The existence of an oxyhydroxide layer on the hematite surface was suggested and it was showed that for the treated samples above 350 °C, the rehydration was nearly impossible due to the reconstruction of the surface layer. The impact of the thermal treatment on the surface properties of nickel oxide was studied by Papirer *et al.* [70]. IGC was used to evaluate the surface nanomorphology of the sample as well as the dispersive component of surface free energy (γ^D), specific interaction parameter (I_{SP}), and surface energetic heterogeneity of NiO. The hydrated surface irreversibly destroyed upon the heat treatment and became highly heterogeneous due to increased number of the high-energy sites at the surface.

IGC was also used to predict the interactions between the air pollutants and metal oxide surfaces by Abatzoglu *et al.* [338]. In this work, the effects of gaseous hydrocarbons and dimethyl sulphide on Cr_2O_3 and ZnO and of dimethyl sulphide $(CH_3)_2S$ on marble particles from archaeological samples were studied before and after exposure to nitrogen dioxide (NO_2) as the second air pollutant factor. The results revealed that the physicochemical parameters of the solid surfaces in the majority of experiments changed in the presence of nitrogen dioxide. Moreover, it was suggested that the mechanism of this effect (which had been unknown before) was related to the blocking or creating an active site of the gas adsorption by NO_2.

In order to study the surface of plutonium dioxide, the surface of its non-radioactive surrogate, ceria, was investigated by IGC at infinite dilution (IGC-ID) and finite solute concentration (IGC-FC) [339]. The plot of energy site distribution, obtained from IGC-FC, revealed a high heterogeneous surface with three types of energy site for isopropanol adsorption. The γ^D was determined for different treated and calcined samples at different temperatures through IGC-ID, and the results indicated that the interaction of the ceria surface with the probe molecules increased remarkably after hydration. Moreover, the hydration reactivity of the surface was affected by the calcination temperature, and at 800 ºC a significant regeneration of the surface occurred.

3.3.7.7. Human Hair

Surface energetics, surface heterogeneity, and Gutmann's acid-base constants (K_A, K_B) of virgin and delipidised human hair (entire strands) were determined using IGC [340]. The results indicated a greater dispersive surface energy for virgin than delipidised hair since fewer lipids on the hair surface result in fewer interactions between the surface and probes. In addition, various types of lipid species caused the surface of virgin hair to be more energetically heterogeneous (for the dispersive component). The quantity of acid-base (specific) component of surface energy did not change significantly after delipidisation; however, the distribution profile of acid-base component of surface energy was broader than that of virgin sample due to more polar interactions, probably as a result of the lipid removal from the surface and the exposure of protein chains. Moreover, the surface of delipidised hair was shown to be more acidic (higher K_A

and lower K_B) due to the existence of pendant groups on amino acids at the surface of delipidised hair.

3.3.7.8. Food

The food industry has also benefited from inverse gas chromatography. Interactions between aroma substances and carbohydrates were directly investigated by passing the flavour compounds (probes) through maltodextrin and starches (stationary phase) [341]. It was concluded that IGC was useful for evaluating the aroma-carbohydrate interactions, although the technique showed restrictions due to the dehydration of the starch caused by using a dry carrier gas and the lack of humidity control of the stationary phase. Apostolopoulos & Gilbert [342, 343] described the mechanism of sorption of water on coffee by using a modified gas chromatography called frontal inverse gas chromatography (FIGC) in which the "matrix" of the stationary phase was referred to instead of the "surface", and "sorption" than "adsorption". Determining thermodynamic parameters (entropy, enthalpy, and free energy), it was shown that freeze-dried coffee is highly hydrophilic. The sorption isotherm showed that once the first water molecules penetrated the coffee matrix, these sorbed molecules favoured sorption of more water molecules and, consequently, in a humid environment, the moisture sorption of the coffee increased. Since FIGC analysis required a shorter time to be completed, it was introduced a suitable method for examining moisture-sensitive foods.

3.3.7.9. Oils

The use of IGC in evaluating mixing properties of mineral and synthetic base oils of different polarities was discussed by Fall *et al.* [344]. The Flory–Huggins interaction parameters and consequently miscibility of a mineral oil, poly-α-olefins, diesters, and their mixtures to produce semi-synthetic oils were determined. Epoxidised soybean oil (ESO), an important additive in poly(vinyl chloride) (PVC) industry, was characterised by IGC to study the correlation between the solubility parameter of epoxidised soybean oil and temperature [345]. The enthalpy of adsorption of probes, the Flory–Huggins interaction parameter, solubility parameter, and mass fraction activity coefficients of the probes were measured at different temperatures. The solubility parameter of the sample decreased with increasing temperature. The dispersive component of surface free energy (γ^D), free energy of adsorption (ΔG), and acid-base properties of ESO were also determined by IGC [346]. The γ^D decreased with increasing temperature, and the values of K_A and K_B, their ratio, specific free energy, and enthalpy of adsorption indicated an amphoteric nature for ESO with predominant basicity. IGC was found to be an easy, inexpensive, and useful technique for characterizing the thermodynamics of epoxidised soybean oil.

3.3.7.10. Liquid crystals (LC)

Liquid crystals (LCs) can also be analysed using inverse gas chromatography. One of the pioneering works in this field was carried out on phase transitions in low molecular weight liquid crystals [347]. Thermodynamic interaction parameters of a liquid crystal with a liquid copolymer were determined by IGC for the first time [348]. In this study, to examine the stability of the liquid crystal dispersion in the polymeric matrix, the solvent independent liquid crystal-polymer interaction parameter was measured. In other work [349], in order to quantify the interactions between LC and a polysiloxane fluid, a mixture of a low molar mass hexyloxycyanobiphenyl liquid crystal and linear poly(dimethyl siloxane) was characterised by IGC and the Flory-Huggins interaction parameter, as well as transition temperatures, were studied. Price *et al.* [350] determined different characteristic parameters of a series of LC systems, including activity coefficients, mass fraction crystallinity, enthalpies and entropies of solution for different probes as well as the Flory–Huggins interaction parameters and glass transition temperature. They showed that subtle changes in retention data could be monitored with accuracy. The obtained fundamental information was applied to design. This suggests a more efficient binary stationary phase for analytical purposes in classical GC.

3.3.7.11. Petroleum Residues

Separated components of petroleum vacuum distillation residues were also characterised by IGC [351]. The Flory-Huggins interaction parameter of different fractions was applied to identify similar components separated from different kinds of petroleum. High values for the parameter signalled a poor solvent, whilst a very low value suggested strong intermolecular interactions and consequently a high solubility. Therefore, it was concluded that alcohols and nitro-compounds were not soluble in the examined oil fractions (heptane, aromatic, and resins) and the solubility of benzene and 1,4-dioxane was very low. However, the negative values of the Flory-Huggins interaction parameter for n-alkane probes on the fractions indicated their nonpolar surfaces. Bitumens are viscous mixtures of petroleum refining residues that are mostly used in the construction of roads. The dispersive surface energy, specific interaction parameter, and glass transition temperature of two bituminous binders with different asphaltene contents were measured [352]. As a result, the compound containing more asphaltene exhibited a higher value of γ^D. Both binders had strong acidity and the binder with less asphaltene value was more acidic. In addition, the glass transition temperature for this sample was reported to be 6 ºC more than the binder with a higher asphaltene content with T_g = -27 ºC.

3.3.7.12. Fuel Cells

The performance of a fuel cell can be evaluated by studying water agglomerations within gas diffusion layers (GDLs). IGC was applied to investigate the water agglomerations within a polymer electrolyte membrane fuel cell gas diffusion layer (PEMFC GDL) [353]. The γ^D and ΔG^{SP} were used to calculate the contact angle of water on the GDL, and the obtained wetting properties were used as the input data for simulating the behaviour of water on the GDL surface during fuel cell operation.

3.3.7.13. Powder Coating

Surface energy is a dominating parameter in cohesion/adhesion between particles, and cohesion/adhesion forces, in turn, significantly affect the flowability of materials. Fine aluminium powders, which are used in various industries, were also characterised using IGC [69, 228, 354, 355]. The dispersive surface energy of aluminium powders was determined, to compare the results of two techniques of reducing cohesiveness and enhancing flowability: surface silanisation and dry particle coating with silica [354]. Treating with silane caused a remarkable decrease in powder surface energy and surface roughness, whilst dry coating with silica resulted in some reduction in surface energy and surface roughness. Silane treatment showed an excellent effect on improving flowability; however, applying silica with smaller particles having a surface energy comparable to silane treated sample caused a remarkable decrease in surface roughness and a significant increase in flowability, confirming that the cohesiveness reduction was highly attributed to a decrease in the dispersive surface energy and in comparison to surface roughness, surface energy had a stronger impact on flowability. As a result, dry coating with nanosilica was considered to be a more economic and environmentally friendly technique to improve aluminium powder flowability. In other work [355], the flowability and reactivity of raw aluminium powder was compared to modified powders through different methods: surface silanisation, dry coating with silica, titania, and carbon black nanoparticles. The results showed lower dispersive surface energies for modified powders than the raw materials. In addition, the flowability of modified samples improved compared to raw powder due to a reduction in cohesiveness. For silane treated powder, which had a remarkable decrease in surface energy, a significant flowability improvement was observed, confirming the substantial role of the surface energy, and surface roughness, in flowability improvement of treated samples.

3.4. Conclusions

Inverse gas chromatography (IGC) as an independent field of study has certainly proven beneficial to many industries. Despite a long history and several hundred publications in the last 50 years, it is still evolving and considered a modern technique that is quite attractive to chemical engineers, analytical chemists and material scientists in various fields. Results of a large quantity of research experiments on a wide range of materials have evidenced that IGC is successfully applied to characterizing different surface and bulk properties of solids in different shapes and morphologies. Its versatility as well as high accuracy and simplicity can establish its position as an indispensable part of analytical laboratories.

This chapter detailed the theory behind IGC, and the many applications of this technique. As noted in Section 3.3.3, Ali *et al.* [264] introduced the potential of using IGC in flotation research; where they investigated galena and quartz. The following chapters detail further research into the application of IGC to enhance our understanding of flotation. This includes IGC analyses and flotation experiments on minerals treated with flotation reagents.

References

[1] M. Lazghab, K. Saleh, I. Pezron, P. Guigon, L. Komunjer, Wettability assessment of finely divided solids, Powder Technology, 157-1 (2005) 79-91.

[2] U. Teipel, I. Mikonsaari, Determining contact angles of powders by liquid penetration, Particle & Particle Systems Characterization, 21-4 (2004) 255-260.

[3] W. Anderson, Wettability literature survey-Part 2: Wettability measurement, Journal of Petroleum Technology, 38-11 (1986) 1,246-241,262.

[4] E. Chibowski, L. Hołysz, On the use of Washburn's equation for contact angle determination, Journal of Adhesion Science and Technology, 11-10 (1997) 1289-1301.

[5] E. Chibowski, R. Perea-Carpio, Problems of contact angle and solid surface free energy determination, Advances in Colloid and Interface Science, 98-2 (2002) 245-264.

[6] A. Boulton, D. Fornasiero, J. Ralston, Characterisation of sphalerite and pyrite flotation samples by XPS and ToF-SIMS, International Journal of Mineral Processing, 70-1 (2003) 205-219.

[7] S. Chehreh Chelgani, B. Hart, TOF-SIMS studies of surface chemistry of minerals subjected to flotation separation–A review, Minerals Engineering, 57 (2014) 1-11.

[8] C. Priest, N. Stevens, R. Sedev, W. Skinner, J. Ralston, Inferring wettability of heterogeneous surfaces by ToF-SIMS, Journal of Colloid and Interface Science, 320-2 (2008) 563-568.

[9] C. Piantadosi, R.S.C. Smart, Statistical comparison of hydrophobic and hydrophilic species on galena and pyrite particles in flotation concentrates and tails from TOF-SIMS evidence, International Journal of Mineral Processing, 64-1 (2002) 43-54.

[10] S. Brito e Abreu, W. Skinner, Determination of contact angles, silane coverage, and hydrophobicity heterogeneity of methylated quartz surfaces using ToF-SIMS, Langmuir, 28-19 (2012) 7360-7367.

[11] S. Brito e Abreu, W. Skinner, ToF-SIMS-derived hydrophobicity in DTP flotation of chalcopyrite: Contact angle distributions in flotation streams, International Journal of Mineral Processing, 98-1 (2011) 35-41.

[12] S. Brito e Abreu, C. Brien, W. Skinner, ToF-SIMS as a new method to determine the contact angle of mineral surfaces, Langmuir, 26-11 (2010) 8122-8130.

[13] M.S. Wagner, S.L. McArthur, M. Shen, T.A. Horbett, D.G. Castner, Limits of detection for time of flight secondary ion mass spectrometry (ToF-SIMS) and X-ray photoelectron spectroscopy (XPS): detection of low amounts of adsorbed protein, Journal of Biomaterials Science, Polymer Edition, 13-4 (2002) 407-428.

[14] A. Benninghoven, R.J. Colton, D.S. Simons, H.W. Werner, Secondary Ion Mass Spectrometry SIMS V: Proceedings of the Fifth International Conference, Washington, DC, September 30–October 4, 1985, Springer Science & Business Media, 2012.

[15] A. Benninghoven, Chemical analysis of inorganic and organic surfaces and thin films by static time-of-flight secondary ion mass spectrometry (TOF-SIMS), Angewandte Chemie International Edition in English, 33-10 (1994) 1023-1043.

[16] S. Ferrari, B.D. Ratner, ToF-SIMS quantification of albumin adsorbed on plasma-deposited fluoropolymers by partial least-squares regression, Surface and Interface Analysis, 29-12 (2000) 837-844.

[17] Nobel Laureates in Chemistry, 1901-1992, Wiley-VCH, 1993.

[18] A.V. Kiselev, Y.I. Yashin, J. Bradley, Gas-Adsorption Chromatography, Plenum Press, New York, 1969.

[19] J.R. Conder, C.L. Young, Physicochemical Measurement by Gas Chromatography, 1st ed., John Wiley & Sons, Ltd, New York, 1979.

[20] E. Wicke, U. Voigt, Bedeutung der Oberflächendiffusion für die Nutzung poröser Kontakte. II. Oberflächendiffusion bei geringen Drücken, Angewandte Chemie, 19-4 (1947) 94-96.

[21] E. Glueckauf, Theory of chromatography. Part II. Chromatograms of a single solute, Journal of the Chemical Society (Resumed), (1947) 1302-1308.

[22] E. Cremer, F. Prior, Anwendung der chromatographischen Methode zur Trennung von Gasen und zur Bestimmung von Adsorptionsenergien, Zeitschrift für Elektrochemie, 55 (1951) 66-70.

[23] D. James, C. Phillips, The chromatography of gases and vapours. Part III. The determination of adsorption isotherms, Journal of the Chemical Society (Resumed), (1954) 1066-1070.

[24] D. Butler, D.R. Williams, Particulate characterization: Inverse gas chromatography, in: I.D. Wilson (Ed.) Encyclopedia of Separation Science, Elsevier Science Ltd., 2000, pp. 3609-3614.

[25] K. Shcherbakova, Y.I. Yashin, V. Andrej, Kiselev's contributions to the science of adsorption, molecular interaction and chromatography, Pure & Applied Chemistry, 61 (1989) 1829-1834.

[26] T. Davis, J. Petersen, W. Haines, Inverse gas-liquid chromatography. A new approach for studying petroleum asphalts, Analytical Chemistry, 38-2 (1966) 241-243.

[27] A. Lavoie, J. Guillet, Estimation of glass transition on temperatures from gas chromatographic studies on polymers, Macromolecules, 2-4 (1969) 443-446.

[28] O. Smidsrød, J. Guillet, Study of polymer-solute interactions by gas chromatography, Macromolecules, 2-3 (1969) 272-277.

[29] J.R. Conder, D.C. Locke, J.H. Purnell, Concurrent solution and adsorption phenomena in chromatography. 1. General considerations, The Journal of Physical Chemistry, 73-3 (1969) 700-708.

[30] J. Conder, J. Purnell, Gas chromatography at finite concentrations. Part 2.—A generalised retention theory, Transactions of the Faraday Society, 64 (1968) 3100-3111.

[31] J. Conder, J. Purnell, Gas chromatography at finite concentrations. Part 3.—Theory of frontal and elution techniques of thermodynamic measurement, Transactions of the Faraday Society, 65 (1969) 824-838.

[32] J. Conder, J. Purnell, Gas chromatography at finite concentrations. Part 4.—Experimental evaluation of methods for thermodynamic study of solutions, Transactions of the Faraday Society, 65 (1969) 839-848.

[33] J. Conder, J. Purnell, Gas chromatography at finite concentrations. Part 1.—Effect of gas imperfection on calculation of the activity coefficient in solution from experimental data, Transactions of the Faraday Society, 64 (1968) 1505-1512.

[34] J.E. Guillet, Molecular probes in the study of polymer structure, Journal of Macromolecular Science—Chemistry, 4-7 (1970) 1669-1674.

[35] O. Olabisi, Polymer compatibility by gas-liquid chromatography, Macromolecules, 8-3 (1975) 316-322.

[36] D. Gray, J. Guillet, A gas chromatographic method for the study of sorption on polymers, Macromolecules, 5-3 (1972) 316-321.

[37] A. Lavoie, J. Guillet, Estimation of glass transition temperatures from gas chromatographic studies on polymers, Rubber Chemistry and Technology, 46-1 (1973) 1-6.

[38] J. Hradil, J. Stamberg, A.L. Kaganov, P. Synek, Investigation of the surface structure of polymers by chromatographic methods. I. Hydrophilized polyethylene capillaries for medical applications, Journal of Polymer Science: Polymer Symposia, 47-1 (1974) 123-129.

[39] J.M. Braun, J. Guillet, Determination of crystallinity of olefin copolymers and polyolefin powders by inverse gas chromatography, Journal of Polymer Science: Polymer Chemistry Edition, 13-5 (1975) 1119-1131.

[40] I. Schneider, C. Elena-Maria, The estimation of phase modifications in polymers by the method of "molecular probes" in gas chromatography—III. Glass transition behaviour and compatibility in mixtures of poly(methyl methacrylate) with poly(vinyl chloride), European Polymer Journal, 11-12 (1975) 861-863.

[41] J.-M. Braun, J. Guillet, Study of polymers by inverse gas chromatography, in: Mechanisms of Polyreactions-Polymer Characterization, University of Toronto, 1976, pp. 107-145.

[42] J.-M. Braun, J. Guillet, Inverse gas chromatography in the vivinity of T_g. Effects of the probe molecule, Macromolecules, 9-2 (1976) 340-344.

[43] G.J. Courval, D.G. Gray, Surface and kinetic effects in gas chromatographic studies of polystyrene, Canadian Journal of Chemistry, 54-22 (1976) 3496-3507.

[44] M. Evans, R. Newton, Inverse gas chromatography in the study of polymer degradation. Part I. Oxidation of squalene as a model for the oxidative degradation of natural rubber, Chromatographia, 9-11 (1976) 561-566.

[45] K. Shoji, K. Nakamura, R. Endo, M. Takeda, Melting behavior of poly(ethylene oxide)-polystyrene-poly(ethylene oxide) triblock copolymer by gas chromatography, Polymer Journal, 8-5 (1976) 471-473.

[46] A.M. Abushihada, F.E. Shunbo, F. Al-Hajjar, Y.Y. Al-Sultan, Determination of the glass transition temperature of polystyrene, poly(vinyl chloride) and poly(methyl methacrylate) using gas chromatography, Journal of High Resolution Chromatography, 2-8 (1979) 512-516.

[47] K. Ito, J. Guillet, Estimation of solubility parameters for some olefin polymers and copolymers by inverse gas chromatography, Macromolecules, 12-6 (1979) 1163-1167.

[48] T.W. Card, Z.Y. Al-Saigh, P. Munk, Inverse gas chromatography. 2. The role of" inert" support, Macromolecules, 18-5 (1985) 1030-1034.

[49] P. Demertzis, K. Riganakos, M. Kontominas, Water sorption isotherms of crystalline raffinose by inverse gas chromatography, International Journal of Food Science & Technology, 24-6 (1989) 629-636.

[50] Inverse Gas Chromatography, American Chemical Society, Washington, DC (USA), 1989.

[51] G.J. Price, D.R. Lloyd, T.C. Ward, H.P. Schreiber, Calculation of solubility parameters by inverse gas chromatography, in: ACS Symposium Series, ACS Publications, 1989, pp. 48-58.

[52] E. Papirer, H. Balard, Y. Rahmani, A. Legrand, L. Facchini, H. Hommel, Characterization by inverse gas chromatography of the surface properties of silicas modified by poly(ethylene glycols) and their models (oligomers, diols), Chromatographia, 23-9 (1987) 639-647.

[53] A. Vidal, E. Papirer, W.M. Jiao, J. Donnet, Modification of silica surfaces by grafting of alkyl chains. I-Characterization of silica surfaces by inverse gas-solid chromatography at zero surface coverage, Chromatographia, 23-2 (1987) 121-128.

[54] E. Papirer, H. Balard, A. Vidal, Inverse gas chromatography: a valuable method for the surface characterization of fillers for polymers (glass fibres and silicas), European Polymer Journal, 24-8 (1988) 783-790.

[55] M. Nardin, E. Papirer, Relationship between vapor pressure and surface energy of liquids: application to inverse gas chromatography, Journal of Colloid and Interface Science, 137-2 (1990) 534-545.

[56] H. Helen, S. Gilbert, Moisture sorption of dry bakery products by inverse gas chromatography, Journal of Food Science, 50-2 (1985) 454-458.

[57] K. Ito, N. Usami, Y. Yamashita, Syntheses of methyl methacrylate-stearyl methacrylate graft copolymers and characterization by inverse gas chromatography, Macromolecules, 13-2 (1980) 216-221.

[58] G. DiPaola-Baranyi, Thermodynamic miscibility of various solutes with styrene-butyl methacrylate polymers and copolymers, Macromolecules, 14-3 (1981) 683-687.

[59] T. Ward, D. Sheehy, J. McGrath, J. Riffle, Inverse gas chromatography studies of poly(dimethylsiloxane)-polycarbonate copolymers and blends, Macromolecules, 14-6 (1981) 1791-1797.

[60] Z.Y. Al-Saigh, P. Munk, Study of polymer-polymer interaction coefficients in polymer blends using inverse gas chromatography, Macromolecules, 17-4 (1984) 803-809.

[61] A.K. Nandi, B.M. Mandal, S.N. Bhattacharyya, Miscibility of poly(methyl acrylate) and poly(vinyl acetate): Incompatibility in solution and thermodynamic characterization by inverse gas chromatography, Macromolecules, 18-7 (1985) 1454-1460.

[62] C.T. Chen, Z.Y. Al-Saigh, Characterization of semicrystalline polymers by inverse gas chromatography. 1. Poly(vinylidene fluoride), Macromolecules, 22-7 (1989) 2974-2981.

[63] J.E. Guillet, M. Romansky, G.J. Price, R. van der Mark, Studies of polymer structure and interactions by automated inverse gas chromatography, in: Inverse Gas Chromatography: Characterization of Polymers and Other Materials, American Chemical Society, Washington, DC, 1989, pp. 20-32.

[64] R.H. Schuster, H. Gräter, H.J. Cantow, Thermodynamic studies on polystyrene-solvent systems by gas chromatography, Macromolecules, 17-4 (1984) 619-625.

[65] M. Öner, S. Dincer, Thermophysical properties of polymer-probe pairs by gas chromatography, Polymer, 28-2 (1987) 279-282.

[66] J. Litster, B. Ennis, Wetting, nucleation and binder distribution, in: The Science and Engineering of Granulation Processes, Springer, 2004, pp. 37-74.

[67] J. Santos, M. Gil, A. Portugal, J. Guthrie, Characterisation of the surface of a cellulosic multi-purpose office paper by inverse gas chromatography, Cellulose, 8-3 (2001) 217-224.

[68] O. Planinšek, J. Zadnik, Š. Rozman, M. Kunaver, R. Dreu, S. Srčič, Influence of inverse gas chromatography measurement conditions on surface energy parameters of lactose monohydrate, International Journal of Pharmaceutics, 256-1 (2003) 17-23.

[69] L.J. Jallo, Y. Chen, J. Bowen, F. Etzler, R. Dave, Prediction of inter-particle adhesion force from surface energy and surface roughness, Journal of Adhesion Science and Technology, 25-4-5 (2011) 367-384.

[70] E. Papirer, E. Brendlé, H. Balard, J. Dentzer, Variation of the surface properties of nickel oxide upon heat treatment evidenced by temperature programmed desorption and inverse gas chromatography studies, Journal of Materials Science, 35 (2000) 3573-3577.

[71] K. Milczewska, A. Voelkel, K. Piędzia, Interactions in PEG/Aerosil and PLA/Aerosil composites described by IGC-determined Flory-Huggins χ_{23} parameter, Journal of Polymer Research, 21-4 (2014) 1-7.

[72] J. Stapley, G. Buckton, D. Merrifield, Investigation to find a suitable reference material for use as an inverse gas chromatography system suitability test, International Journal of Pharmaceutics, 318-1 (2006) 22-27.

[73] A. Voelkel, Physicochemical measurements (inverse gas chromatography), in: C. Poole (Ed.) Gas Chromatography, Elsevier, 2012, pp. 477-494.

[74] F. Thielmann, Introduction into the characterisation of porous materials by inverse gas chromatography, Journal of Chromatography A, 1037-1 (2004) 115-123.

[75] H.E. Newell, G. Buckton, D.A. Butler, F. Thielmann, D.R. Williams, The use of inverse phase gas chromatography to measure the surface energy of crystalline, amorphous, and recently milled lactose, Pharmaceutical Research, 18-5 (2001) 662-666.

[76] W. Wang, Q. Hua, Y. Sha, D. Wu, S. Zheng, B. Liu, Surface properties of solid materials measured by modified inverse gas chromatography, Talanta, 112 (2013) 69-72.

[77] F. Thielmann, D. Butler, D. Williams, E. Baumgarten, Characterisation of microporous materials by dynamic sorption methods, Studies in Surface Science and Catalysis, 129 (2000) 633-638.

[78] A. Sen, Inverse Gas Chromatography, Defence Scientific Information & Documentation Centre, Defence Research & Development Organisation, Ministry of Defence, UK., New Delhi, 2005.

[79] P. Mukhopadhyay, H. Schreiber, Aspects of acid-base interactions and use of inverse gas chromatography, Colloids and Surfaces A: Physicochemical and Engineering Aspects, 100 (1995) 47-71.

[80] A. Voelkel, Inverse gas chromatography: characterization of polymers, fibers, modified silicas, and surfactants, Critical Reviews in Analytical Chemistry, 22-5 (1991) 411-439.

[81] F. Thielmann, E. Baumgarten, Characterization of microporous aluminas by inverse gas chromatography, Journal of Colloid and Interface Science, 229-2 (2000) 418-422.

[82] M.M. Chehimi, M.-L. Abel, C. Perruchot, M. Delamar, S.F. Lascelles, S.P. Armes, The determination of the surface energy of conducting polymers by inverse gas chromatography at infinite dilution, Synthetic Metals, 104-1 (1999) 51-59.

[83] J. Donnet, S. Park, H. Balard, Evaluation of specific interactions of solid surfaces by inverse gas chromatography, Chromatographia, 31-9 (1991) 434-440.

[84] E. Papirer, E. Brendle, F. Ozil, H. Balard, Comparison of the surface properties of graphite, carbon black and fullerene samples, measured by inverse gas chromatography, Carbon, 37-8 (1999) 1265-1274.

[85] T. Hamieh, M.-B. Fadlallah, J. Schultz, New approach to characterise physicochemical properties of solid substrates by inverse gas chromatography at infinite dilution: III. Determination of the acid–base properties of some solid substrates (polymers, oxides and carbon fibres): a new model, Journal of Chromatography A, 969-1 (2002) 37-47.

[86] J. Jagiełło, T.J. Bandosz, J.A. Schwarz, Application of inverse gas chromatography at infinite dilution to study the effects of oxidation of activated carbons, Carbon, 30-1 (1992) 63-69.

[87] M.M. Chehimi, E. Pigois-Landureau, Determination of acid–base properties of solid materials by inverse gas chromatography at infinite dilution. A novel empirical method based on the dispersive contribution to the heat of vaporization of probes, Journal of Materials Chemistry, 4-5 (1994) 741-745.

[88] T.J. Bandosz, J. Jagiello, B. Andersen, J.A. Schwarz, Inverse gas chromatography study of modified smectite surfaces, Clays and Clay Minerals, 40-3 (1992) 306-310.

[89] S. Dong, M. Brendle, J. Donnet, Study of solid surface polarity by inverse gas chromatography at infinite dilution, Chromatographia, 28-9 (1989) 469-472.

[90] F. Mutelet, J.-N. Jaubert, M. Rogalski, J. Harmand, M. Sindt, J.-L. Mieloszynski, Activity coefficients at infinite dilution of organic compounds in 1-(meth)acryloyloxyalkyl-3-methylimidazolium bromide using inverse gas chromatography, The Journal of Physical Chemistry B, 112-12 (2008) 3773-3785.

[91] F. Mutelet, J.-N. Jaubert, M. Rogalski, M. Boukherissa, A. Dicko, Thermodynamic properties of mixtures containing ionic liquids: Activity coefficients at infinite dilution of organic compounds in 1-propyl boronic acid-3-alkylimidazolium bromide and 1-propenyl-3-

alkylimidazolium bromide using inverse gas chromatography, Journal of Chemical & Engineering Data, 51-4 (2006) 1274-1279.

[92] A.-L. Revelli, L.M. Sprunger, J. Gibbs, W.E. Acree Jr, G.A. Baker, F. Mutelet, Activity coefficients at infinite dilution of organic compounds in trihexyl(tetradecyl)phosphonium bis(trifluoromethylsulfonyl)imide using inverse gas chromatography, Journal of Chemical & Engineering Data, 54-3 (2009) 977-985.

[93] M.K. Kozłowska, U. Domańska, M. Lempert, M. Rogalski, Determination of thermodynamic properties of isotactic poly(1-butene) at infinite dilution using density and inverse gas chromatography, Journal of Chromatography A, 1068-2 (2005) 297-305.

[94] E. Papirer, A. Vidal, W.M. Jiao, J. Donnet, Modification of silica surfaces by grafting of alkyl chains. II-Characterization of silica surfaces by inverse gas-solid chromatography at finite concentration, Chromatographia, 23-4 (1987) 279-285.

[95] J. Jagiełło, G. Ligner, E. Papirer, Characterization of silicas by inverse gas chromatography at finite concentration: Determination of the adsorption energy distribution function, Journal of Colloid and Interface Science, 137-1 (1990) 128-136.

[96] I. Tijburg, J. Jagiello, A. Vidal, E. Papirer, Inverse gas chromatographic studies on silica: Infinite dilution and finite concentration measurements, Langmuir, 7-10 (1991) 2243-2247.

[97] H. Balard, Estimation of the surface energetic heterogeneity of a solid by inverse gas chromatography, Langmuir, 13-5 (1997) 1260-1269.

[98] F. Thielmann, D. Butler, D. Williams, Characterization of porous materials by finite concentration inverse gas chromatography, Colloids and Surfaces A: Physicochemical and Engineering Aspects, 187 (2001) 267-272.

[99] B. Charmas, R. Leboda, Effect of surface heterogeneity on adsorption on solid surfaces: Application of inverse gas chromatography in the studies of energetic heterogeneity of adsorbents, Journal of Chromatography A, 886-1 (2000) 133-152.

[100] A. Voelkel, B. Strzemiecka, K. Adamska, K. Milczewska, Inverse gas chromatography as a source of physiochemical data, Journal of Chromatography A, 1216-10 (2009) 1551-1566.

[101] A.J. Vukov, D.G. Gray, Properties of carbon fiber surfaces, in: D.R. Lloyd, M.S. Wagner, H. Schiavone (Eds.) Inverse Gas Chromatography, ACS Symposium Series, ACS Publications, 1988, pp. 168–184.

[102] S. Katz, D.G. Gray, The adsorption of hydrocarbons on cellophane: I. Zero coverage limit, Journal of Colloid and Interface Science, 82-2 (1981) 318-325.

[103] J. Schultz, L. Lavielle, C. Martin, The role of the interface in carbon fibre-epoxy composites, The Journal of Adhesion, 23-1 (1987) 45-60.

[104] J. Schultz, L. Lavielle, Interfacial properties of carbon fiber-epoxy matrix composites, in: Inverse Gas Chromatography Characterisation of Polymers and Other Materials, ACS Symposium Ser, ACS Publications, 1989, pp. 185-202.

[105] R. Ho, J.Y.Y. Heng, A Review of inverse gas chromatography and its development as a tool to characterize anisotropic surface properties of pharmaceutical solids, KONA Powder and Particle Journal, -30 (2013) 164-180.

[106] H. Balard, E. Brendlé, E. Papirer, Determination of the acid–base properties of solid surfaces using inverse gas chromatography: advantages and limitations, in: K. Mittal (Ed.) Acid-Base Interactions: Relevance to Adhesion Science and Technology, CRC Press, 2000, pp. 299-316.

[107] A. Voelkel, Inverse gas chromatography in the examination of acid-base and some other properties of solid materials, Studies in Surface Science and Catalysis, 99 (1996) 465-477.

[108] F.M. Fowkes, Attractive forces at interfaces, Industrial & Engineering Chemistry, 56-12 (1964) 40-52.

[109] G.M. Dorris, D.G. Gray, Adsorption of n-alkanes at zero surface coverage on cellulose paper and wood fibers, Journal of Colloid and Interface Science, 77-2 (1980) 353-362.

[110] J.F. Gamble, M. Leane, D. Olusanmi, M. Tobyn, E. Šupuk, J. Khoo, M. Naderi, Surface energy analysis as a tool to probe the surface energy characteristics of micronized materials-A comparison with inverse gas chromatography, International Journal of Pharmaceutics, 422 (2011) 238-244.

[111] A. Voelkel, Inverse gas chromatography in characterization of surface, Chemometrics and Intelligent Laboratory Systems, 72-2 (2004) 205-207.

[112] P.P. Ylä-Mäihäniemi, J.Y. Heng, F. Thielmann, D.R. Williams, Inverse gas chromatographic method for measuring the dispersive surface energy distribution for particulates, Langmuir, 24-17 (2008) 9551-9557.

[113] J.F. Gamble, R.N. Davé, S. Kiang, M.M. Leane, M. Tobyn, S.S. Wang, Investigating the applicability of inverse gas chromatography to binary powdered systems: An application of surface heterogeneity profiles to understanding preferential probe-surface interactions, International Journal of Pharmaceutics, 445 (2013) 39-46.

[114] M.D. Jones, P. Young, D. Traini, The use of inverse gas chromatography for the study of lactose and pharmaceutical materials used in dry powder inhalers, Advanced Drug Delivery Reviews, 64-3 (2012) 285-293.

[115] B. Shi, Y. Wang, L. Jia, Comparison of Dorris–Gray and Schultz methods for the calculation of surface dispersive free energy by inverse gas chromatography, Journal of Chromatography A, 1218-6 (2011) 860-862.

[116] J. Kołodziejek, A. Voelkel, K. Heberger, Characterization of hybrid materials by means of inverse gas chromatography and chemometrics, Journal of Pharmaceutical Sciences, 102 (2013) 1524-1531.

[117] M. Kunaver, J. Zadnik, O. Planinsek, S. Srcic, Inverse gas chromatography-A different approach to characterization of solids and liquids, Acta Chimica Slovenica, 51-3 (2004) 373-394.

[118] A. Voelkel, K. Adamska, Properties of materials as determined by inverse gas chromatography, Annales UMCS, Chemistry, 64-12 (2009) 169-183.

[119] P.E. Luner, Y. Zhang, Y.A. Abramov, M.T. Carvajal, Evaluation of milling method on the surface energetics of molecular crystals using inverse gas chromatography, Crystal Growth & Design, 12-11 (2012) 5271-5282.

[120] R. Menzel, A. Bismarck, M.S. Shaffer, Deconvolution of the structural and chemical surface properties of carbon nanotubes by inverse gas chromatography, Carbon, 50 (2012) 3416-3421.

[121] J. Anhang, D.G. Gray, Surface characterization of poly(ethylene terephthalate) film by inverse gas chromatography, Journal of Applied Polymer Science, 27-1 (1982) 71-78.

[122] Z.Y. Al-Saigh, Review: Inverse gas chromatography for the characterization of polymer blends, International Journal of Polymer Analysis and Characterization, 3-3 (1997) 249-291.

[123] J. Guillet, Z.Y. Al-Saigh, Inverse gas chromatography in analysis of polymers, in: Encyclopedia of Analytical Chemistry, 2006, pp. 1-34.

[124] J. Guillet, A. Stein, Study of crystallinity in polymers by use of "molecular probes", Macromolecules, 3-1 (1970) 102-105.

[125] D.M. Ansari, G.J. Price, Chromatographic estimation of filler surface energies and correlation with photodegradation of kaolin filled polyethylene, Polymer, 45-6 (2004) 1823-1831.

[126] D.M. Ansari, G.J. Price, Correlation of mechanical properties of clay filled polyamide mouldings with chromatographically measured surface energies, Polymer, 45-11 (2004) 3663-3670.

[127] A. Voelkel, E. Andrzejewska, R. Maga, M. Andrzejewski, Examination of surfaces of solid polymers by inverse gas chromatography: 1. Dispersive properties, Polymer, 37-3 (1996) 455-462.

[128] J.M. Zielinski, M. Hamedi, I.M. Balashova, R.P. Danner, Diffusion of solvents in poly(vinyl acetate) and partially and fully hydrolyzed poly(vinyl alcohol), Polymer International, 63-2 (2013) 221-227.

[129] M. Ghaemy, M. Hadjmohammadi, R. Tabaraki, Study of crystallinity of high-density polyethylene by inverse gas chromatography, Iranian Polymer Journal, 9 (2000) 117-124.

[130] Y. Ren, P. Zhu, Application of inverse gas chromatography to solid propellants, Journal of Chromatography, 457 (1988) 354-361.

[131] D. Patterson, Y. Tewari, H. Schreiber, J. Guillet, Application of gas-liquid chromatography to the thermodynamics of polymer solutions, Macromolecules, 4-3 (1971) 356-359.

[132] A. Edelman, A. Fradet, Inverse gas chromatography study of some triacetin-polymer systems, Polymer, 30-2 (1989) 317-323.

[133] L. Segeren, M. Wouters, M. Bos, J. Van den Berg, G. Vancso, Surface energy characteristics of toner particles by automated inverse gas chromatography, Journal of Chromatography A, 969-1 (2002) 215-227.

[134] G. Dritsas, K. Karatasos, C. Panayiotou, Investigation of thermodynamic properties of hyperbranched aliphatic polyesters by inverse gas chromatography, Journal of Chromatography A, 1216-51 (2009) 8979-8985.

[135] G.J. Vancso, Z. Tan, Solvent clustering, polar network density, and thermodynamic interactions in coordination polymers: an inverse gas chromatography study of metal-ion-

containing polyesters of poly(diethylene glycol-co-succinic acid), Canadian Journal of Chemistry, 73-11 (1995) 1855-1861.

[136] S. Klotz, R.H. Schuster, H.J. Cantow, Compatibility of polymers in polymer blends investigated by gas chromatography, Die Makromolekulare Chemie, 187-6 (1986) 1491-1500.

[137] M. Kontominas, R. Gavara, J. Giacin, Gas-solid chromatographic study of polymer surfaces: Adsorption on polystyrene, European Polymer Journal, 30-2 (1994) 271-277.

[138] M. Kontominas, R. Gavara, J. Giacin, The adsorption of hydrocarbons on polystyrene by inverse gas chromatography: Infinite dilution concentration region, European Polymer Journal, 30-2 (1994) 265-269.

[139] Y. Murakami, T. Inui, Y. Takegami, Dispersion states of porous inorganic materials in polymer blends observed by inverse gas chromatography, Polymer, 24-12 (1983) 1596-1600.

[140] M. Minagawa, H. Kanoh, S. Tanno, Y. Nishimoto, Glass-transition temperature (T_g) of free-radically prepared polyacrylonitrile by inverse gas chromatography, 1. A study on T_g of atactic monodisperse polystyrenes, Macromolecular Chemistry and Physics, 203-17 (2003) 2475-2480.

[141] E. Özdemir, M. Coşlkun, A. Açlikses, Estimation of thermodynamic parameters of polystyrene-n_hydrocarbons systems using inverse gas chromatography, Macromolecular Reports, 28-S2 (1991) 129-136.

[142] Y. Murakami, R. Enoki, Y. Ogoma, Y. Kondo, Studies on interaction between silica gel and polymer blend by inverse gas chromatography, Polymer Journal, 30-6 (1998) 520-525.

[143] İ. Kaya, Determination of thermodynamic interactions of the PVC-PMMA blend system by inverse gas chromatography, Polymer-Plastics Technology and Engineering, 38-2 (1999) 385-396.

[144] M.-L. Abel, M.M. Chehimi, F. Fricker, M. Delamar, A.M. Brown, J.F. Watts, Adsorption of poly(methyl methacrylate) and poly(vinyl chloride) blends onto polypyrrole: Study by X-ray photoelectron spectroscopy, time-of-flight static secondary ion mass spectroscopy, and inverse gas chromatography, Journal of Chromatography A, 969-1 (2002) 273-285.

[145] A. Etxeberria, J. Elorza, J. Iruin, C. Marco, M. Gomez, J. Fatou, Miscibility of poly(vinyl chloride)/poly(ethylene oxide) blends—II. An inverse gas chromatography study, European Polymer Journal, 29-11 (1993) 1483-1487.

[146] İ. Kaya, E. Özdemir, Thermodynamic interactions and characterization of poly(ethyl methacrylate) by inverse gas chromatography, Journal of Macromolecular Science, Part A: Pure and Applied Chemistry, 32-S3 (1995) 377-383.

[147] C.-T. Chen, Z.Y. Al-Saigh, Characterization of poly(ethyl methacrylate) by inverse gas chromatography, Polymer, 31-6 (1990) 1170-1176.

[148] T. Hamieh, Study of the specific entropy of poly(α-n-alkyl) methacrylates adsorbed on alumina or silica by inverse gas chromatography (IGC), Soft Materials, 9-1 (2010) 15-31.

[149] A. Onjia, S. Milonjić, N. Jovanović, S. Jovanović, An inverse gas chromatography study of macroporous copolymers based on methyl and glycidyl methacrylate, Reactive and Functional Polymers, 43-3 (2000) 269-277.

[150] İ. Kaya, D. Şenol, Study of changes in polymer–probe interactions with stabilization temperature of a column contained polyacrylonitrile by using inverse gas chromatography, Polymer-Plastics Technology and Engineering, 43-1 (2004) 273-283.

[151] D. Cava, R. Gavara, J. Lagaron, A. Voelkel, Surface characterization of poly(lactic acid) and polycaprolactone by inverse gas chromatography, Journal of Chromatography A, 1148-1 (2007) 86-91.

[152] N.A. Belov, Y.A. Nizhegorodova, S. Kim, S.H. Han, Y.P. Yampolskii, Y.M. Lee, Inverse gas chromatographic study of sorption thermodynamics in thermally rearranged polymer based on 2, 2-bis(3-amino-4-hydroxyphenyl)-hexafluoropropane and 4, 4′-hexafluoroisopropylidene diphthalic anhydride, Industrial & Engineering Chemistry Research, 52 (2013) 10467-10475.

[153] A.S. Reddy, P.R. Rani, K.S. Reddy, Lewis acid–base properties of cellulose acetate phthalate-polycaprolactonediol blend by inverse gas chromatography, Polymer Engineering & Science, 53-8 (2013) 1780-1785.

[154] A.S. Reddy, S. Ramanaiah, K.S. Reddy, Hansen solubility parameters of a cellulose acetate propionate-poly(caprolactone)diol blend by inverse gas chromatography, International Journal of Polymer Analysis and Characterization, 18-3 (2013) 172-180.

[155] P.R. Rani, S. Ramanaiah, B.P. Kumar, K.S. Reddy, Lewis acid-base properties of cellulose acetate butyrate-poly(caprolactonediol) blend by inverse gas chromatography, Polymer-Plastics Technology and Engineering, 52-12 (2013) 1228-1234.

[156] S. Ramanaiah, A.S. Reddy, K.S. Reddy, Hansen solubility parameters of cellulose acetate butyrate–poly(caprolactone) diol blend by inverse gas chromatography, Polymer Bulletin, 70 (2013) 1303-1312.

[157] B.P. Kumar, S. Ramanaiah, T.M. Reddy, K.S. Reddy, Surface characterization of cellulose acetate propionate by inverse gas chromatography, Polymer Bulletin, 71-1 (2014) 125-132.

[158] B.X. Mayer-Helm, W. Rauter, Determination of the minimum allowable operating temperature of stationary phases in capillary columns by inverse gas chromatography, Analyst, 130-4 (2005) 502-507.

[159] O. Tyagi, D. Deshpande, Inverse gas chromatography of poly(n-butyl methacrylate): Effect of flow rate on specific retention volume and detection of glass transition temperature, Journal of Applied Polymer Science, 34-7 (2003) 2377-2388.

[160] J.M. Ramstack, S.G. Wright, D.A. Dickason, Preparation of microparticles having improved flowability, in, Europe, 2013.

[161] İ. Kaya, Z. İlter, D. Şenol, Thermodynamic interactions and characterisation of poly[(glycidyl methacrylate-co-methyl, ethyl, butyl) methacrylate] by inverse gas chromatography, Polymer, 43-24 (2002) 6455-6463.

[162] İ. Kaya, K. Demirelli, Determination of thermodynamic properties of poly[2-(3-methyl-3-phenylcyclobutyl)-2-hydroxyethylmethacrylate] and its copolymers at infinite dilution using inverse gas chromatography, Polymer, 41-8 (2000) 2855-2863.

[163] A. Polese, C. Mio, A. Bertucco, Infinite-dilution activity coefficients of polar and nonpolar solvents in solutions of hyperbranched polymers, Journal of Chemical & Engineering Data, 44-4 (1999) 839-845.

[164] İ. Kaya, E. Özdemir, Thermodynamic interactions and characterisation of poly(isobornyl methacrylate) by inverse gas chromatography at various temperatures, Polymer, 40-9 (1999) 2405-2410.

[165] M.H. Karagöz, Ö.S. Zorer, Z. İlter, Analysis of physical and thermodynamic properties of poly(2-phenyl-1, 3-dioxolane-4-Yl-methyl-methacrylate-co-styrene) polymer with inverse gas chromatography, Polymer-Plastics Technology and Engineering, 45-7 (2006) 785-789.

[166] S.K. Papadopoulou, C. Panayiotou, Assessment of the thermodynamic properties of poly(2, 2, 2-trifluoroethyl methacrylate) by inverse gas chromatography, Journal of Chromatography A, 1324 (2013) 207-214.

[167] O.K. Duaij, A. Alghamdi, Z.Y. Al-Saigh, Solubility and surface thermodynamics of conducting polymers by inverse gas chromatography. III: Polypyrrole chloride, Journal of Chromatography A, 1291 (2013) 137-145.

[168] J. Camacho, E. Díez, G. Ovejero, I. Díaz, Thermodynamic interactions of EVA copolymer-solvent systems by inverse gas chromatography measurements, Journal of Applied Polymer Science, 128-1 (2013) 481-486.

[169] Z. İlter, İ. Kaya, A. Açİkses, Determination of poly[(2-phenyl-1, 3-dioxolane-4-yl) methyl methacrylate-co-glycidyl methacrylate]-probe interactions by inverse gas chromatography, Polymer-Plastics Technology and Engineering, 43-1 (2004) 229-243.

[170] K. Demirelli, İ. Kaya, M. Coşkun, 3, 4-Dichlorobenzyl methacrylate and ethyl methacrylate system: monomer reactivity ratios and determination of thermodynamic properties at infinite dilution by using inverse gas chromatography, Polymer, 42-12 (2001) 5181-5188.

[171] M.J. El-Hibri, W. Cheng, P. Munk, Inverse gas chromatography. 6. Thermodynamics of poly(ϵ-caprolactone)-polyepichlorohydrin blends, Macromolecules, 21-12 (1988) 3458-3463.

[172] F. Cakar, O. Cankurtaran, F. Karaman, Relaxation and miscibility of the blends of a poly(ether imide)(Ultem) and a phenol-A-based copolyester (Ardel) by inverse gas chromatography, Chromatographia, 75 (2012) 1157–1164.

[173] G. DiPaola-Baranyi, S. Fletcher, P. Degre, Gas chromatographic investigation of poly(vinylidene fluoride)-poly(methyl methacrylate) blends, Macromolecules, 15-3 (1982) 885-889.

[174] A. Sarac, D. Şakar, O. Cankurtaran, F.Y. Karaman, The ratio of crystallinity and thermodynamical interactions of polycaprolactone with some aliphatic esters and aromatic solvents by inverse gas chromatography, Polymer Bulletin, 53-5 (2005) 349-357.

[175] D. Deshpande, D. Patterson, H. Schreiber, C. Su, Thermodynamic interactions in polymer systems by gas-liquid chromatography. IV. interactions between components in a mixed stationary phase, Macromolecules, 7-4 (1974) 530-535.

[176] İ. Kaya, D. Şenol, Investigation of thermodynamic properties of PIBMA-PVC (50%/50%) and P-4-t-BS-PVC (50%/50%) blends systems by inverse gas chromatography, Polymer-Plastics Technology and Engineering, 44-5 (2005) 981-992.

[177] M. Galin, M. Rupprecht, Study by gas-liquid chromatography of the interactions between linear or branched polystyrenes and solvents in the temperature range 60°–200° C, Polymer, 19-5 (1978) 506-512.

[178] R.P. Danner, Measuring and correlating diffusivity in polymer–solvent systems using free-volume theory, Fluid Phase Equilibria, 362 (2014) 19-27.

[179] J. Iribarren, M. Iriarte, C. Uriarte, J. Iruin, Phenoxy resin: characterization, solution properties, and inverse gas chromatography investigation of its potential miscibility with other polymers, Journal of Applied Polymer Science, 37-12 (2003) 3459-3470.

[180] G. Courval, D. Gray, The effect of surface adsorption on gas chromatographic measurements near polymer melting transitions, Macromolecules, 8-3 (1975) 326-331.

[181] D. Gray, J. Guillet, The application of the molecular probe technique to a study of polymer crystallization rates, Macromolecules, 4-1 (1971) 129-133.

[182] W. Orts, M. Romansky, J. Guillet, Measurement of the crystallinity of poly(β-hydroxybutyrate-co-β-hydroxyvalerate) copolymers by inverse gas chromatography, Macromolecules, 25-2 (1992) 949-953.

[183] E. Fernandez-Sanchez, A. Fernandez-Torres, J. Garcia-Dominguez, M. Salvador-Moya, Gas chromatographic comparative study of superox 20m immobilized in different ways, Journal of Chromatography A, 556-1 (1991) 485-493.

[184] A.B. Nastasović, A.E. Onjia, Determination of glass temperature of polymers by inverse gas chromatography, Journal of Chromatography A, 1195-1 (2008) 1-15.

[185] A. Ben Slimane, K. Boukerma, M. Chabut, M.M. Chehimi, An inverse gas chromatographic characterization of polypyrrole-coated poly(vinyl chloride) powder particles, Colloids and Surfaces A: Physicochemical and Engineering Aspects, 240-1 (2004) 45-53.

[186] M. Chehimi, S. Lascelles, P. Armes, Characterization of surface thermodynamic properties of p-toluene sulfonate-doped polypyrrole by inverse gas chromatography, Chromatographia, 41-11 (1995) 671-677.

[187] P. Mukhopadhyay, H. Schreiber, Inverse gas chromatography for polymer surface characterization above and below T_g, Macromolecules, 26-24 (1993) 6391-6396.

[188] R. Calvet, S. Del Confetto, H. Balard, E. Brendlé, J.-B. Donnet, Study of the interaction polybutadiene/fillers using inverse gas chromatography, Journal of Chromatography A, 1253 (2012) 164-170.

[189] E. Papirer, E. Brendle, H. Balard, C. Vergelati, Inverse gas chromatography investigation of the surface properties of cellulose, Journal of Adhesion Science and Technology, 14-3 (2000) 321-337.

[190] R.H. Mills, D.J. Gardner, R. Wimmer, Inverse gas chromatography for determining the dispersive surface free energy and acid–base interactions of sheet molding compound—Part II. 14 Ligno-cellulosic fiber types for possible composite reinforcement, Journal of Applied Polymer Science, 110-6 (2008) 3880-3888.

[191] R.H. Mills, W.T. Tze, D.J. Gardner, A. van Heiningen, Inverse gas chromatography for the determination of the dispersive surface free energy and acid–base interactions of a sheet molding compound. I. Matrix material and glass, Journal of Applied Polymer Science, 109-6 (2008) 3519-3524.

[192] A. Vega, F.V. Díez, P. Hurtado, J. Coca, Characterization of polyarylamide fibers by inverse gas chromatography, Journal of Chromatography A, 962-1 (2002) 153-160.

[193] U. Mohlin, D. Gray, Gas chromatography on polymer surfaces: Adsorption on cellulose, Journal of Colloid and Interface Science, 47-3 (1974) 747-754.

[194] G. DiPaola-Baranyi, J.E. Guillet, H.E. Jeberien, J. Klein, Thermodynamics of hydrogen bonding polymer-solute interactions by inverse gas chromatography, Die Makromolekulare Chemie, 181-1 (1980) 215-226.

[195] F. Tihminlioglu, R.K. Surana, R.P. Danner, J. Duda, Finite concentration inverse gas chromatography: diffusion and partition measurements, Journal of Polymer Science Part B: Polymer Physics, 35-8 (1997) 1279-1290.

[196] N. Bakaoukas, D. Sevastos, J. Kapolos, A. Koliadima, G. Karaiskakis, Characterization of polymeric coatings in terms of their ability to protect marbles and clays against corrosion from sulfur dioxide by inverse gas chromatography, International Journal of Polymer Analysis and Characterization, 18 (2013) 401-4013.

[197] I.M. Grimsey, J.C. Feeley, P. York, Analysis of the surface energy of pharmaceutical powders by inverse gas chromatography, Journal of Pharmaceutical Sciences, 91-2 (2002) 571-583.

[198] Y. Guo, E. Shalaev, S. Smith, Solid-state analysis and amorphous dispersions in assessing the physical stability of pharmaceutical formulations, Trends in Analytical Chemistry, 49 (2013) 137-144.

[199] S.P. Chamarthy, The Different Roles of Surface and Bulk Effects on the Functionality of Pharmaceutical Materials, ProQuest, 2007.

[200] O. Planinšek, G. Buckton, Inverse gas chromatography: Considerations about appropriate use for amorphous and crystalline powders, Journal of Pharmaceutical Sciences, 92-6 (2003) 1286-1294.

[201] G. Buckton, H. Gill, The importance of surface energetics of powders for drug delivery and the establishment of inverse gas chromatography, Advanced Drug Delivery Reviews, 59-14 (2007) 1474-1479.

[202] Y. Yokoi, E. Yonemochi, K. Terada, Changes in surface properties by granulation and physicochemical stability of granulated amorphous cefditoren pivoxil with additives, International Journal of Pharmaceutics, 280-1 (2004) 67-75.

[203] J.Y. Heng, F. Thielmann, D.R. Williams, The effects of milling on the surface properties of form I paracetamol crystals, Pharmaceutical Research, 23-8 (2006) 1918-1927.

[204] S.P. Chamarthy, R. Pinal, The nature of crystal disorder in milled pharmaceutical materials, Colloids and Surfaces A: Physicochemical and Engineering Aspects, 331-1 (2008) 68-75.

[205] S. Das, I. Larson, P. Young, P. Stewart, Understanding lactose behaviour during storage by monitoring surface energy change using inverse gas chromatography, Dairy Science & Technology, 90-2 (2010) 271-285.

[206] A.V. Ambarkhane, K. Pincott, G. Buckton, The use of inverse gas chromatography and gravimetric vapour sorption to study transitions in amorphous lactose, International Journal of Pharmaceutics, 294-1 (2005) 129-135.

[207] G. Buckton, J.W. Dove, P. Davies, Isothermal microcalorimetry and inverse phase gas chromatography to study small changes in powder surface properties, International Journal of Pharmaceutics, 193-1 (1999) 13-19.

[208] M.J. Davies, T.D. Kerry, L. Seton, M.F. Murphy, P. Gibbons, J. Khoo, M. Naderi, The crystal engineering of salbutamol sulphate via simulated pulmonary surfactant monolayers, International Journal of Pharmaceutics, 446 (2013) 34-45.

[209] M. Ticehurst, R. Rowe, P. York, Determination of the surface properties of two batches of salbutamol sulphate by inverse gas chromatography, International Journal of Pharmaceutics, 111-3 (1994) 241-249.

[210] T. Tay, S. Das, P. Stewart, Magnesium stearate increases salbutamol sulphate dispersion: What is the mechanism?, International Journal of Pharmaceutics, 383-1 (2010) 62-69.

[211] D.F. Steele, R.C. Moreton, J.N. Staniforth, P.M. Young, M.J. Tobyn, S. Edge, Surface energy of microcrystalline cellulose determined by capillary intrusion and inverse gas chromatography, The AAPS Journal, 10-3 (2008) 494-503.

[212] B. Saša, P. Odon, S. Stane, K. Julijana, Analysis of surface properties of cellulose ethers and drug release from their matrix tablets, European Journal of Pharmaceutical Sciences, 27-4 (2006) 375-383.

[213] D. Zhang, J. Flory, S. Panmai, U. Batra, M. Kaufman, Wettability of pharmaceutical solids: its measurement and influence on wet granulation, Colloids and Surfaces A: Physicochemical and Engineering Aspects, 206-1 (2002) 547-554.

[214] D. Burnett, J. Khoo, M. Naderi, J.Y. Heng, G. Wang, F. Thielmann, Effect of processing route on the surface properties of amorphous indomethacin measured by inverse gas chromatography, AAPS PharmSciTech, 13-4 (2012) 1511-1517.

[215] S.C. Das, P.J. Stewart, Characterising surface energy of pharmaceutical powders by inverse gas chromatography at finite dilution, Journal of Pharmacy and Pharmacology, 64-9 (2012) 1337-1348.

[216] F. Thielmann, D.J. Burnett, J.Y. Heng, Determination of the surface energy distributions of different processed lactose, Drug Development and Industrial Pharmacy, 33-11 (2007) 1240-1253.

[217] I. Saleem, H. Smyth, M. Telko, Prediction of dry powder inhaler formulation performance from surface energetics and blending dynamics, Drug Development and Industrial Pharmacy, 34-9 (2008) 1002-1010.

[218] M. Ticehurst, P. York, R. Rowe, S. Dwivedi, Characterisation of the surface properties of α-lactose monohydrate with inverse gas chromatography, used to detect batch variation, International Journal of Pharmaceutics, 141-1 (1996) 93-99.

[219] A.E. Jefferson, D.R. Williams, J.Y. Heng, Computing the surface energy distributions of heterogeneous crystalline powders, Journal of Adhesion Science and Technology, 25-4-5 (2011) 339-355.

[220] M.J. Telko, A.J. Hickey, Critical assessment of inverse gas chromatography as means of assessing surface free energy and acid–base interaction of pharmaceutical powders, Journal of Pharmaceutical Sciences, 96-10 (2007) 2647-2654.

[221] M. Kumon, M. Suzuki, A. Kusai, E. Yonemochi, K. Terada, Novel approach to DPI carrier lactose with mechanofusion process with additives and evaluation by IGC, Chemical and Pharmaceutical Bulletin, 54-11 (2006) 1508-1514.

[222] H.E. Newell, G. Buckton, Inverse gas chromatography: Investigating whether the technique preferentially probes high energy sites for mixtures of crystalline and amorphous lactose, Pharmaceutical Research, 21-8 (2004) 1440-1444.

[223] G. Pilcer, N. Wauthoz, K. Amighi, Lactose characteristics and the generation of the aerosol, Advanced Drug Delivery Reviews, 64-3 (2012) 233-256.

[224] Q.T. Zhou, D.A. Morton, Drug–lactose binding aspects in adhesive mixtures: controlling performance in dry powder inhaler formulations by altering lactose carrier surfaces, Advanced Drug Delivery Reviews, 64-3 (2012) 275-284.

[225] A.J. Hickey, H.M. Mansour, M.J. Telko, Z. Xu, H.D. Smyth, T. Mulder, R. McLean, J. Langridge, D. Papadopoulos, Physical characterization of component particles included in dry powder inhalers. I. Strategy review and static characteristics, Journal of Pharmaceutical Sciences, 96-5 (2007) 1282-1301.

[226] Q.T. Zhou, J.A. Denman, T. Gengenbach, S. Das, L. Qu, H. Zhang, I. Larson, P.J. Stewart, D.A. Morton, Characterization of the surface properties of a model pharmaceutical fine powder

modified with a pharmaceutical lubricant to improve flow via a mechanical dry coating approach, Journal of Pharmaceutical Sciences, 100-8 (2011) 3421-3430.

[227] S. Apte, Excipient-API interactions in dry powder inhalers, Journal of Excipients and Food Chemicals, 3-4 (2012) 129-142.

[228] S.C. Das, Q. Zhou, D.A. Morton, I. Larson, P.J. Stewart, Use of surface energy distributions by inverse gas chromatography to understand mechanofusion processing and functionality of lactose coated with magnesium stearate, European Journal of Pharmaceutical Sciences, 43-4 (2011) 325-333.

[229] M. Capece, Z. Huang, D. To, M. Aloia, C. Muchira, R. Davé, A. Yu, Prediction of porosity from particle scale interactions: Surface modification of fine cohesive powders, Powder Technology, 254 (2014) 103-113.

[230] X. Han, L. Jallo, D. To, C. Ghoroi, R. Davé, Passivation of high-surface-energy sites of milled ibuprofen crystals via dry coating for reduced cohesion and improved flowability, Journal of Pharmaceutical Sciences, 102-7 (2013) 2282-2296.

[231] P. York, M. Ticehurst, J. Osborn, R. Roberts, R. Rowe, Characterisation of the surface energetics of milled dl-propranolol hydrochloride using inverse gas chromatography and molecular modelling, International Journal of Pharmaceutics, 174-1 (1998) 179-186.

[232] M. Otsuka, I. Yamane, Y. Matsuda, Effects of lubricant mixing on compression properties of various kinds of direct compression excipients and physical properties of the tablets, Advanced Powder Technology, 15-4 (2004) 477-493.

[233] R. Ho, M. Naderi, J.Y. Heng, D.R. Williams, F. Thielmann, P. Bouza, A.R. Keith, G. Thiele, D.J. Burnett, Effect of milling on particle shape and surface energy heterogeneity of needle-shaped crystals, Pharmaceutical Research, 29 (2012) 2806-2816.

[234] R. Ho, D.A. Wilson, J.Y. Heng, Crystal habits and the variation in surface energy heterogeneity, Crystal Growth & Design, 9-11 (2009) 4907-4911.

[235] R. Ho, S.J. Hinder, J.F. Watts, S.E. Dilworth, D.R. Williams, J.Y. Heng, Determination of surface heterogeneity of D-mannitol by sessile drop contact angle and finite concentration inverse gas chromatography, International Journal of Pharmaceutics, 387-1 (2010) 79-86.

[236] L. Lapčík, E. Otyepková, B. Lapčíková, M. Otyepka, Surface energy analysis (SEA) study of hyaluronan powders, Colloids and Surfaces A: Physicochemical and Engineering Aspects, 436 (2013) 1170-1174.

[237] M. Ohta, G. Buckton, Determination of the changes in surface energetics of cefditoren pivoxil as a consequence of processing induced disorder and equilibration to different relative humidities, International Journal of Pharmaceutics, 269-1 (2004) 81-88.

[238] J. Dove, G. Buckton, C. Doherty, A comparison of two contact angle measurement methods and inverse gas chromatography to assess the surface energies of theophylline and caffeine, International Journal of Pharmaceutics, 138-2 (1996) 199-206.

[239] P. Tang, H.-K. Chan, H. Chiou, K. Ogawa, M. Jones, H. Adi, G. Buckton, R. Prud'homme, J. Raper, Characterisation and aerosolisation of mannitol particles produced via confined liquid impinging jets, International Journal of Pharmaceutics, 367-1 (2009) 51-57.

[240] A. Columbano, G. Buckton, P. Wikeley, Characterisation of surface modified salbutamol sulphate-alkylpolyglycoside microparticles prepared by spray drying, International Journal of Pharmaceutics, 253-1 (2003) 61-70.

[241] H.E. Newell, G. Buckton, D.A. Butler, F. Thielmann, D.R. Williams, The use of inverse phase gas chromatography to study the change of surface energy of amorphous lactose as a function of relative humidity and the processes of collapse and crystallisation, International Journal of Pharmaceutics, 217-1 (2001) 45-56.

[242] N.M. Ahfat, G. Buckton, R. Burrows, M.D. Ticehurst, An exploration of inter-relationships between contact angle, inverse phase gas chromatography and triboelectric charging data, European Journal of Pharmaceutical Sciences, 9-3 (2000) 271-276.

[243] A. Alhalaweh, W. Kaialy, G. Buckton, H. Gill, A. Nokhodchi, S.P. Velaga, Theophylline cocrystals prepared by spray drying: Physicochemical properties and aerosolization performance, AAPS PharmSciTech, 14 (2013) 265-276.

[244] K. Stank, H. Steckel, Physico-chemical characterisation of surface modified particles for inhalation, International Journal of Pharmaceutics, 448 (2013) 9–18.

[245] J. Raula, F. Thielmann, M. Naderi, V.P. Lehto, E.I. Kauppinen, Investigations on particle surface characteristics vs. dispersion behaviour of L-leucine coated carrier-free inhalable powders, International Journal of Pharmaceutics, 385-1 (2010) 79-85.

[246] M. Shyamala, S.P. Ranjan, J. Sharma, Pharmaceutical applications of inverse gas chromatography, International Journal of Pharma Sciences, 3-2 (2013) 201-204.

[247] H. Schiavone, S. Palakodaty, A. Clark, P. York, S.T. Tzannis, Evaluation of SCF-engineered particle-based lactose blends in passive dry powder inhalers, International Journal of Pharmaceutics, 281-1 (2004) 55-66.

[248] G. Buckton, A. Ambarkhane, K. Pincott, The use of inverse phase gas chromatography to study the glass transition temperature of a powder surface, Pharmaceutical Research, 21-9 (2004) 1554-1557.

[249] P. Ke, S. Hasegawa, H. Al-Obaidi, G. Buckton, Investigation of preparation methods on surface/bulk structural relaxation and glass fragility of amorphous solid dispersions, International Journal of Pharmaceutics, 422-1 (2012) 170-178.

[250] S. Hasegawa, P. Ke, G. Buckton, Determination of the structural relaxation at the surface of amorphous solid dispersion using inverse gas chromatography, Journal of Pharmaceutical Sciences, 98-6 (2009) 2133-2139.

[251] N. Furuyama, S. Hasegawa, S. Yada, T. Hamaura, N. Wakiyama, E. Yonemochi, K. Terada, G. Buckton, Do amorphous troglitazones prepared from two diastereomer-pairs have the same molecular mobility and crystallization rate at the surface?, Chemical and Pharmaceutical Bulletin, 59-12 (2011) 1452-1457.

[252] H. Miyanishi, T. Nemoto, M. Mizuno, H. Mimura, S. Kitamura, Y. Iwao, S. Noguchi, S. Itai, Evaluation of crystallization behavior on the surface of nifedipine solid dispersion powder using inverse gas chromatography, Pharmaceutical Research, 30-2 (2013) 502-511.

[253] E. Fekete, J. Móczó, B. Pukánszky, Determination of the surface characteristics of particulate fillers by inverse gas chromatography at infinite dilution: a critical approach, Journal of Colloid and Interface Science, 269-1 (2004) 143-152.

[254] D.S. Keller, P. Luner, Surface energetics of calcium carbonates using inverse gas chromatography, Colloids and Surfaces A: Physicochemical and Engineering Aspects, 161-3 (2000) 401-415.

[255] L. Skovbjerg, D. Okhrimenko, J. Khoo, K.N. Dalby, T. Hassenkam, E. Makovicky, S. Stipp, Preferential adsorption of hydrocarbons to nanometer-sized clay on chalk particle surfaces, Energy & Fuels, 27-7 (2013) 3642-3652.

[256] M. Rodriguez, J. Rubio, F. Rubio, M. Liso, J. Oteo, Application of inverse gas chromatography to the study of the surface properties of slates, Clays and Clay Minerals, 45-5 (1997) 670-680.

[257] N. Arsalan, S.S. Palayangoda, D.J. Burnett, J.J. Buiting, Q.P. Nguyen, Surface energy characterization of carbonate rocks, Colloids and Surfaces A: Physicochemical and Engineering Aspects, 436 (2013) 139-147.

[258] N. Arsalan, S.S. Palayangoda, D.J. Burnett, J.J. Buiting, Q.P. Nguyen, Surface energy characterization of sandstone rocks, Journal of Physics and Chemistry of Solids, 74 (2013) 1069-1077.

[259] J. Jurga, A. Voelkel, B. Strzemiecka, Application of different analytical methods used in the study of the cross-linking of resins in intermediate-product used in manufacturing of abrasive articles, Journal of Applied Polymer Science, 112-6 (2009) 3305-3312.

[260] A. Voelkel, B. Strzemiecka, Characterization of fillers used in abrasive articles by means of inverse gas chromatography and principal component analysis, International Journal of Adhesion and Adhesives, 27-3 (2007) 188-194.

[261] A. Voelkel, B. Strzemiecka, Inverse gas chromatographic evaluation of the extent of cross-linking of resins in grinding tools, Acta Chromatographica, 16 (2006) 140.

[262] B. Strzemiecka, K. Héberger, A. Voelkel, Similarity and grouping of perlite and zeolite abrasive fillers: A replacement test, Journal of Applied Polymer Science, 127 (2012) 3839-3847.

[263] N. Katsanos, E. Arvanitopoulou, F. Roubani-Kalantzopoulou, A. Kalantzopoulos, Time distribution of adsorption energies, local monolayer capacities, and local isotherms on heterogeneous surfaces by inverse gas chromatography, The Journal of Physical Chemistry B, 103-7 (1999) 1152-1157.

[264] S.S. Ali, J.Y. Heng, A. Nikolaev, K.E. Waters, Introducing inverse gas chromatography as a method of determining the surface heterogeneity of minerals for flotation, Powder Technology, 249 (2013) 373-377.

[265] M. Rückriem, A. Inayat, D. Enke, R. Gläser, W.-D. Einicke, R. Rockmann, Inverse gas chromatography for determining the dispersive surface energy of porous silica, Colloids and Surfaces A: Physicochemical and Engineering Aspects, 357-1 (2010) 21-26.

[266] H. Balard, M. Sidqi, E. Papirer, J. Donnet, A. Tuel, H. Hommel, A. Legrand, Study of modified silicas by inverse gas chromatography part II: Influence of chain length on surface properties of silicas grafted with α−ω diols, Chromatographia, 25-8 (1988) 712-716.

[267] J.-B. Donnet, H. Balard, N. Nedjari, B. Hamdi, H. Barthel, T. Gottschalk-Gaudig, Influence of specific surface area of pyrogenic silicas on their heat of immersion in water and on their surface properties assessed using inverse gas chromatography, Journal of Colloid and Interface Science, 328 (2008) 15-19.

[268] M. Sidqi, G. Ligner, J. Jagiello, H. Balard, E. Papirer, Characterization of specific interaction capacity of solid surfaces by adsorption of alkanes and alkenes. Part I: Adsorption on open surfaces, Chromatographia, 28-11 (1989) 588-592.

[269] M. Sidqi, H. Balard, E. Papirer, A. Tuel, H. Hommel, A. Legrand, Study of modified silicas by inverse gas chromatography. Influence of chain length on the conformation of n-alcohols grafted on a pyrogenic silica, Chromatographia, 27-7 (1989) 311-315.

[270] H. Balard, M. Sidqi, E. Papirer, J. Donnet, A. Tuel, H. Hommel, A. Legrand, Study of modified silicas by inverse gas chromatography. Part I: Influence of chain length on grafting ratio, Chromatographia, 25-8 (1988) 707-711.

[271] M. Pyda, G. Guiochon, Surface properties of silica-based adsorbents measured by inverse gas-solid chromatography at finite concentration, Langmuir, 13-5 (1997) 1020-1025.

[272] E. Brendlé, E. Papirer, A new topological index for molecular probes used in inverse gas chromatography for the surface nanorugosity evaluation, Journal of Colloid and Interface Science, 194-1 (1997) 207-216.

[273] E. Brendlé, E. Papirer, A new topological index for molecular probes used in inverse gas chromatography, Journal of Colloid and Interface Science, 194-1 (1997) 217-224.

[274] M. Rueckriem, T. Hahn, D. Enke, Inverse gas chromatographic studies on porous glass, Optica Applicata, 42-2 (2012) 295-306.

[275] B. Biliński, W. Wójcik, A.L. Dawidowicz, Investigation of the surface free energy components of thermally treated controlled porosity glasses by inverse gas chromatography, Applied Surface Science, 47-1 (1991) 99-108.

[276] C. Saint Flour, E. Papirer, Gas-solid chromatography: A quick method of estimating surface free energy variations induced by the treatment of short glass fibers, Journal of Colloid and Interface Science, 91-1 (1983) 69-75.

[277] S. Comte, R. Calvet, J. Dodds, H. Balard, Surface properties of low specific surface powders using inverse gas chromatography, Powder Technology, 157-1 (2005) 39-47.

[278] T.J. Bandosz, K. Putyera, J. Jagiełło, J.A. Schwarz, Application of inverse gas chromatography to the study of the surface properties of modified layered minerals, Microporous Materials, 1-1 (1993) 73-79.

[279] G.J. Price, D.M. Ansari, An inverse gas chromatography study of calcination and surface modification of kaolinite clays, Physical Chemistry Chemical Physics, 5-24 (2003) 5552-5557.

[280] A. Saada, E. Papirer, H. Balard, B. Siffert, Determination of the surface properties of illites and kaolinites by inverse gas chromatography, Journal of Colloid and Interface Science, 175-1 (1995) 212-218.

[281] S. Lazarević, I. Janković-Častvan, A. Onjia, J. Krstić, D. Janaćković, R. Petrović, Surface characterization of iron-modified sepiolite by inverse gas chromatography, Industrial & Engineering Chemistry Research, 50-20 (2011) 11467-11475.

[282] L. Lapčík, B. Lapčíková, I. Krásny, I. Kupská, R.W. Greenwood, K.E. Waters, Effect of low temperature air plasma treatment on wetting and flow properties of kaolinite powders, Plasma Chemistry and Plasma Processing, 32-4 (2012) 845-858.

[283] K. Czech, P. Słomkiewicz, Determination of adsorption isotherms of chlorinated hydrocarbons on halloysite adsorbent by inverse gas chromatography, Journal of Chromatography A, 1288 (2013) 96-100.

[284] L. Boudriche, A. Chamayou, R. Calvet, B. Hamdi, H. Balard, Influence of different dry milling processes on the properties of an attapulgite clay, contribution of inverse gas chromatography, Powder Technology, 254 (2014) 352-363.

[285] C. Bilgiç, D. Topaloğlu Yazıcı, N. Karakehya, H. Çetinkaya, A. Singh, M.M. Chehimi, Surface and interface physicochemical aspects of intercalated organo-bentonite, International Journal of Adhesion and Adhesives, 50 (2014) 204-210.

[286] E. Díaz, S. Ordóñez, A. Vega, J. Coca, Evaluation of adsorption properties of zeolites using inverse gas chromatography: comparison with immersion calorimetry, Thermochimica Acta, 434-1 (2005) 9-14.

[287] B. Strzemiecka, J. Kołodziejek, M. Kasperkowiak, A. Voelkel, Influence of relative humidity on the properties of examined materials by means of Inverse Gas Chromatography, Journal of Chromatography A, 1271 (2012) 201-206.

[288] B. Strzemiecka, A. Voelkel, M. Kasperkowiak, Characterization of zeolites as potential new generation fillers in abrasive articles. Physicochemical properties of zeolites and their interactions with resins, Colloids and Surfaces A: Physicochemical and Engineering Aspects, 372-1 (2010) 80-85.

[289] M. Kasperkowiak, J. Kołodziejek, B. Strzemiecka, A. Voelkel, Effect of impregnating agent and relative humidity on surface characteristics of sorbents determined by inverse gas chromatography, Journal of Chromatography A, 1288 (2013) 101-104.

[290] B. Strzemiecka, M. Kasperkowiak, M. Łożyński, D. Paukszta, A. Voelkel, Examination of zeolites as fragrance carriers, Microporous and Mesoporous Materials, 161 (2012) 106-114.

[291] S. Bardavid, P. Schulz, E. Arancibia, Miscibility of anhydrous cationic surfactant mixtures, Journal of Molecular Liquids, 156-2 (2010) 165-170.

[292] S. Bardavid, P. Schulz, E. Arancibia, Interaction parameters of anhydrous cationic surfactant mixtures by inverse gas chromatography, Journal of Solution Chemistry, 41 (2012) 1197-1209.

[293] S. Bardavid, P. Schulz, E. Arancibia, IGC studies of binary cationic surfactant mixtures, Journal of Colloid and Interface Science, 316-1 (2007) 114-119.

[294] E.L. Arancibia, P.C. Schulz, S.M. Bardavid, Interaction parameters of surfactant mixtures by inverse gas chromatography, in: R. Davarnejad, M. Jafarkhani (Eds.) Applications of Gas Chromatography, InTech, 2012, pp. 132.

[295] C. de Schaefer, M. de Ruiz Holgado, E. Arancibia, Effective solubility parameters of sucrose monoester surfactants obtained by inverse gas chromatography, Fluid Phase Equilibria, 272-1 (2008) 53-59.

[296] K. Adamska, A. Voelkel, Hansen solubility parameters for polyethylene glycols by inverse gas chromatography, Journal of Chromatography A, 1132-1 (2006) 260-267.

[297] C.R. de Schaefer, M.E.F. de Ruiz Holgado, E.L. Arancibia, Sucrose derivative surfactants studied by inverse gas chromatography, Journal of Colloid and Interface Science, 239-1 (2001) 222-225.

[298] A. Voelkel, J. Janas, Solubility parameters of broad and narrow distributed oxyethylates of fatty alcohols, Journal of Chromatography A, 645-1 (1993) 141-151.

[299] P. Choi, T. Kavassalis, A. Rudin, Measurement of three-dimensional solubility parameters of nonyl phenol ethoxylates using inverse gas chromatography, Journal of Colloid and Interface Science, 180-1 (1996) 1-8.

[300] A. Voelkel, J. Janas, J. Garcia-Dominguez, Inverse gas chromatography in characterization of surfactants: determination of binary parameter, Journal of Chromatography A, 654-1 (1993) 135-141.

[301] R. Menzel, A. Lee, A. Bismarck, M.S. Shaffer, Inverse gas chromatography of as-received and modified carbon nanotubes, Langmuir, 25-14 (2009) 8340-8348.

[302] Y.-h. Shih, M.-s. Li, Adsorption of selected volatile organic vapors on multiwall carbon nanotubes, Journal of Hazardous Materials, 154-1 (2008) 21-28.

[303] X. Zhang, D. Yang, P. Xu, C. Wang, Q. Du, Characterizing the surface properties of carbon nanotubes by inverse gas chromatography, Journal of Materials Science, 42-17 (2007) 7069-7075.

[304] A.M. Kannan, L. Munukutla, Carbon nano-chain and carbon nano-fibers based gas diffusion layers for proton exchange membrane fuel cells, Journal of Power Sources, 167-2 (2007) 330-335.

[305] E. Díaz, S. Ordóñez, A. Vega, Adsorption of volatile organic compounds onto carbon nanotubes, carbon nanofibers, and high-surface-area graphites, Journal of Colloid and Interface Science, 305-1 (2007) 7-16.

[306] P. Lazar, E. Otyepková, P. Banáš, A. Fargašová, K. Šafářová, L. Lapčík, J. Pechoušek, R. Zbořil, M. Otyepka, The nature of high surface energy sites in graphene and graphite, Carbon, 73 (2014) 448-453.

[307] P. Lazar, F. Karlický, P. Jurečka, M. Kocman, E. Otyepková, K. Šafářová, M. Otyepka, Adsorption of small organic molecules on graphene, Journal of the American Chemical Society, 135-16 (2013) 6372-6377.

[308] Y. Peng, D.J. Gardner, Y. Han, Z. Cai, M.A. Tshabalala, Influence of drying method on the surface energy of cellulose nanofibrils determined by inverse gas chromatography, Journal of Colloid and Interface Science, 405 (2013) 85-95.

[309] H. Balard, D. Maafa, A. Santini, J. Donnet, Study by inverse gas chromatography of the surface properties of milled graphites, Journal of Chromatography A, 1198 (2008) 173-180.

[310] M. Przybyszewska, A. Krzywania, M. Zaborski, M.I. Szynkowska, Surface properties of zinc oxide nanoparticles studied by inverse gas chromatography, Journal of Chromatography A, 1216-27 (2009) 5284-5291.

[311] I.H. Romdhane, R.P. Danner, J. Duda, Influence of the glass transition on solute diffusion in polymers by inverse gas chromatography, Industrial & Engineering Chemistry Research, 34-8 (1995) 2833-2840.

[312] R.K. Surana, R.P. Danner, J.L. Duda, Diffusion and equilibrium measurements in ternary polymer-solvent-solvent systems using inverse gas chromatography, Industrial & Engineering Chemistry Research, 37-8 (1998) 3203-3207.

[313] S. Katz, D.G. Gray, The adsorption of hydrocarbons on cellophane: II. Finite coverage region, Journal of Colloid and Interface Science, 82-2 (1981) 326-338.

[314] S. Katz, D.G. Gray, The adsorption of hydrocarbons on cellophane: III. Effect of relative humidity, Journal of Colloid and Interface Science, 82-2 (1981) 339-351.

[315] R. Gavara, R. Catalá, P. Hernández-Muñoz, Study of aroma scalping through thermosealable polymers used in food packaging by inverse gas chromatography, Food Additives & Contaminants, 14-6-7 (1997) 609-616.

[316] J. Jagiełło, T.J. Bandosz, J.A. Schwarz, Inverse gas chromatographic study of activated carbons: The effect of controlled oxidation on microstructure and surface chemical functionality, Journal of Colloid and Interface Science, 151-2 (1992) 433-445.

[317] F. Thielmann, D. Pearse, Determination of surface heterogeneity profiles on graphite by finite concentration inverse gas chromatography, Journal of Chromatography A, 969-1 (2002) 323-327.

[318] Q. Wang, Y. Chen, L. Deng, J. Tang, Z. Zhang, Determination of the solubility parameter of ionic liquid 1-allyl-3-methylimidazolium chloride by inverse gas chromatography, Journal of Molecular Liquids, 180 (2013) 135-138.

[319] M. Rogalski, A. Modaressi, P. Magri, F. Mutelet, A. Grydziuszko, M. Wlazło, U. Domańska, Physico-chemical properties and phase Behavior of the ionic liquid-β-cyclodextrin complexes, International Journal of Molecular Sciences, 14-8 (2013) 16638-16655.

[320] K.T. Heydar, M. Nazifi, A. Sharifi, M. Mirzaei, H. Gharavi, S.H. Ahmadi, Determination of activity coefficients at infinite dilution of solutes in new dicationic ionic liquids based on morpholine using gas–liquid chromatography, Chromatographia, 76-3-4 (2013) 165-175.

[321] M. Królikowski, M. Królikowska, The study of activity coefficients at infinite dilution for organic solutes and water in 1-butyl-4-methylpyridinium dicyanamide, [B^{4}MPy][DCA] using GLC, The Journal of Chemical Thermodynamics, 68 (2014) 138-144.

[322] M. Królikowska, M. Karpińska, M. Królikowski, Measurements of activity coefficients at infinite dilution for organic solutes and water in N-hexylisoquinolinium thiocyanate, [HiQuin][SCN] using GLC, The Journal of Chemical Thermodynamics, 62 (2013) 1-7.

[323] T.V.M. Sreekanth, K.S. Reddy, Analysis of solvent–solvent interactions in mixed isosteric solvents by inverse gas chromatography, Chromatographia, 65-5 (2007) 325-330.

[324] J. McLaughlin, C. Pope, Inverse gas chromatography of wool, Journal of Applied Polymer Science, 27-5 (1982) 1643-1654.

[325] J.B. Donnet, S.J. Park, Surface characteristics of pitch-based carbon fibers by inverse gas chromatography method, Carbon, 29-7 (1991) 955-961.

[326] A. Kafi, L. Henderson, L. Servinis, M. Huson, T. Gengenbach, J. Khoo, C. Garschke, B. Fox, New surface treatments for low cost carbon fiber, in: Society for the Advancement of Material and Process Engineering, SAMPE, Long Beach, California, 2013, pp. 456-469.

[327] M.G. Huson, J.S. Church, A.A. Kafi, A.L. Woodhead, J. Khoo, M. Kiran, J.E. Bradby, B.L. Fox, Heterogeneity of carbon fibre, Carbon, 68 (2014) 240-249.

[328] N. Cordeiro, C. Gouveia, M.J. John, Investigation of surface properties of physico-chemically modified natural fibres using inverse gas chromatography, Industrial Crops and Products, 33-1 (2011) 108-115.

[329] G. Czeremuszkin, P. Mukhopadhyay, S. Sapieha, Elution behavior of chemically different probes on the evaluation of surface properties of cellulose by inverse gas chromatography, Journal of Colloid and Interface Science, 194-1 (1997) 127-137.

[330] M. Belgacem, G. Czeremuszkin, S. Sapieha, A. Gandini, Surface characterization of cellulose fibres by XPS and inverse gas chromatography, Cellulose, 2-3 (1995) 145-157.

[331] E. Csiszár, E. Fekete, A. Tóth, É. Bandi, B. Koczka, I. Sajó, Effect of particle size on the surface properties and morphology of ground flax, Carbohydrate Polymers, 94 (2013) 927-933.

[332] J.A. Gamelas, G.V. Duarte, P.J. Ferreira, Inverse gas chromatography and XPS of extracted kraft pulps, Holzforschung, 67-3 (2013) 273-276.

[333] A. Ashori, N. Cordeiro, M. Faria, Y. Hamzeh, Effect of chitosan and cationic starch on the surface chemistry properties of bagasse paper, International Journal of Biological Macromolecules, 58 (2013) 343-348.

[334] J. Zhou, T. Yu, S. Wu, Z. Xie, Y. Yang, Inverse gas chromatography investigation of rubber reinforcement by modified pyrolytic carbon black from scrap tires, Industrial & Engineering Chemistry Research, 49-4 (2010) 1691-1696.

[335] Z. Marton, L. Chaput, G. Pierre, M. Graber, Lipase hydration state in the gas phase: Sorption isotherm measurements and inverse gas chromatography, Biotechnology Journal, 5-11 (2010) 1216-1225.

[336] V. Léonard-Nevers, Z. Marton, S. Lamare, K. Hult, M. Graber, Understanding water effect on Candida antarctica lipase B activity and enantioselectivity towards secondary alcohols, Journal of Molecular Catalysis B: Enzymatic, 59-1 (2009) 90-95.

[337] E. Brendlé, J. Dentzer, E. Papirer, Variation of the surface properties of hematite upon heat treatment evidenced by inverse gas chromatography and temperature programmed desorption techniques: Influence of surface impurities and surface reconstruction, Journal of Colloid and Interface Science, 199-1 (1998) 63-76.

[338] C. Abatzoglou, E. Iliopoulou, N. Katsanos, F. Roubani-Kalantzopoulou, A. Kalantzopoulos, Deposition parameters of air pollutants on solid surfaces, measured in the presence of surface and gaseous reactions, with a simultaneous determination of the experimental isotherms, Journal of Chromatography A, 775-1-2 (1997) 211-224.

[339] J. Gaillard, L. Venault, R. Calvet, S. Del Confetto, N. Clavier, R. Podor, M. Odorico, J.-L. Pellequer, N. Vigier, P. Moisy, Effect of hydration and thermal treatment on ceria surface using non-intrusive techniques, Journal of Nuclear Materials, 444-1 (2014) 359-367.

[340] R.L. McMullen, D. Laura, S. Chen, D. Koelmel, G. Zhang, T. Gillece, Determination of physicochemical properties of delipidized hair, Journal of Cosmetic Science, 64-5 (2013) 355-370.

[341] J. Delarue, P. Giampaoli, Study of interaction phenomena between aroma compounds and carbohydrate matrixes by inverse gas chromatography, Journal of Agricultural and Food Chemistry, 48-6 (2000) 2372-2375.

[342] D. Apostolopoulos, S.G. Gilbert, Frontal inverse gas chromatography as used in studying water sorption of coffee solubles, Journal of Food Science, 53-3 (1988) 882-884.

[343] D. Apostolopoulos, S.G. Gilbert, Water sorption of coffee solubles by frontal inverse gas chromatography: Thermodynamic considerations, Journal of Food Science, 55-2 (1990) 475-487.

[344] J. Fall, K. Milczewska, A. Voelkel, Characterisation of mineral oil–polyester, mineral oil–poly-α-olefin mixtures by inverse gas chromatography, Journal of Materials Chemistry, 11-4 (2001) 1042-1046.

[345] Q. Wang, Y. Chen, J. Tang, Z. Zhang, Determination of the solubility parameter of epoxidized soybean oil by inverse gas chromatography, Journal of Macromolecular Science, Part B: Physics, 52-10 (2013) 1405-1413.

[346] Y. Chen, Q. Wang, J. Tang, Z. Zhang, Determination of surface characteristics of epoxidized soybean oil by inverse GC, Chromatographia, 76-1-2 (2013) 91-96.

[347] G.J. Price, I.M. Shillcock, Investigation of mesophase transitions in liquid crystals using inverse gas chromatography, Canadian Journal of Chemistry, 73-11 (1995) 1883-1892.

[348] S. Coskun, B.B. Eran, O. Cankurtaran, F. Karaman, Thermodynamics of the mixture of a liquid crystal and a copolymer of dimethylsiloxane, Journal of Optoelectronic and Biomedical Materials, 1-1 (2009) 91-102.

[349] I.M. Shillcock, G.J. Price, Inverse gas chromatography study of poly(dimethyl siloxane)—liquid crystal mixtures, Polymer, 44-4 (2003) 1027-1034.

[350] G.J. Price, S.J. Hickling, I.M. Shillcock, Applications of inverse gas chromatography in the study of liquid crystalline stationary phases, Journal of Chromatography A, 969-1 (2002) 193-205.

[351] A. Voelkel, J. Fall, Inverse gas chromatography for the examination of fractions separated from oil vacuum distillation residues, Journal of Chromatography A, 768-2 (1997) 271-281.

[352] C. Puig, H. Meijer, M. Michels, L. Segeren, G.J. Vancso, Characterization of glass transition temperature and surface energy of bituminous binders by inverse gas chromatography, Energy & Fuels, 18-1 (2004) 63-67.

[353] K. Seidenberger, F. Wilhelm, J. Haußmann, H. Markötter, I. Manke, J. Scholta, Grand canonical Monte Carlo study on water agglomerations within a polymer electrolyte membrane fuel cell gas diffusion layer, Journal of Power Sources, 239 (2013) 628-641.

[354] Y. Chen, L. Jallo, M.A. Quintanilla, R. Dave, Characterization of particle and bulk level cohesion reduction of surface modified fine aluminum powders, Colloids and Surfaces A: Physicochemical and Engineering Aspects, 361-1 (2010) 66-80.

[355] L.J. Jallo, M. Schoenitz, E.L. Dreizin, R.N. Dave, C.E. Johnson, The effect of surface modification of aluminum powder on its flowability, combustion and reactivity, Powder Technology, 204-1 (2010) 63-70.

CHAPTER **4**

SURFACE ENERGY OF QUARTZ: APPLICATIONS TO FLOTATION

Abstract

Inverse gas chromatography (IGC) is a versatile and powerful technique for characterizing physicochemical properties of materials. One such property, the surface energy, plays an important role in the adhesiveness, wettability, and consequently flotation of minerals. In this work, quartz was chosen as a naturally hydrophilic mineral, and dodecylamine was used to hydrophobise the surface. To study the correlation between the surface properties as measured from IGC experiments and flotation, microflotation experiments were also conducted. It was shown that with treatment by dodecylamine, the surface energy decreased, as did the work of adhesion to water. The recovery of quartz increased after the treatment, indicating a correlation between surface energy and flotation response. The results indicate that IGC has the capability to determine the thermodynamic properties of quartz, pre- and post-conditioning. Relating the hydrophobicity and flotation of minerals to the surface energy can be observed from combining the results of IGC and microflotation experiments.

4.1. Introduction

The interfacial behaviour of a material is an important characteristic, controlled mainly by surface properties, one of the most important of which is the surface free energy. Thermodynamically, the surface free energy of a solid is the work required to reversibly create a unit area of a surface. It is an excess energy on the material surface, which arises from fewer bonds between surface molecules comparing to bulk molecules. This energy is analogous to the surface tension of a liquid, in which the atoms are able to move from the higher-energy surface to the lower-energy bulk, resulting in changes in the surface area. However, geometry and the mechanical state of solids affect the apparent values of surface energy [1], therefore making its measurement more complex than that of liquid surface tension. The surface energy of solids plays a key role in industrial processes that rely on wetting phenomena and coating, such as polymers, pharmaceuticals, surfactants, and mineral processing. Understanding the surface characteristics of minerals and the effect of collectors and depressants on mineral surface chemistry is a necessity of modern flotation. In an aqueous suspension, different phenomena occur as a result of different interfacial reactions between molecules. For example, the wetting process occurs when the adhesion force between a solid and liquid is greater than the cohesion force between the liquid's molecules. The applicability of IGC to flotation was introduced by Ali *et al.* [2]. It was shown that IGC is a powerful technique for determining the surface energy of galena and quartz at different surface coverages; however, the effect of reagent addition was not investigated.

The surface energy of solids is defined as the sum of dispersive and specific (acid–base) components. The dispersive component, also called non-specific interactions, is attributed to molecular interactions due to London (van der Waals) forces. The specific component (also termed acid–base interactions) results from polar interactions such as hydrogen bonding and electron donor–acceptor behaviour [3-5]. However, for a real solid, a single value is not considered as the energy of the whole surface of the solid; rather, there is a range of energetic sites of different levels. Altering the distribution of the energetic sites of higher and lower energy on a solid surface causes surface energy heterogeneity, which affects intermolecular interactions between surfaces. Different parameters related to surface heterogeneity have been studied, including the ratio of hydrophilic and hydrophobic sites on the surface [6]; existence of hetero atoms and functional groups on the surface [7]; also impurities, oxidised surfaces, and crystal orientation.

Inverse gas chromatography provides important information such as surface area, surface energetics, work of adhesion, and surface energy heterogeneity. In this method, the sample is placed in a column (most commonly a glass tube) and characterised by passing solutes (called molecular probes) through the column. Adsorption and desorption phenomena occur at the sample which result in delayed exit of the probe from the column (retention). Therefore the fundamental data obtained from IGC provides a plot of the detector signals as a function of retention time. The retention time refers to the time the probe molecules require to generate a peak as a result of interactions with the stationary phase. Various characteristics of materials can be calculated by analysing the nature and quantity of these interactions.

The surface energy of a solid can be obtained from IGC by applying various relationships. The two commonly used approaches for characterizing surface energetics of materials are the Dorris–Gray and Schultz methods. Dorris & Gray [8] developed their method based on the contribution of CH_2 groups in the free energy of desorption of n-alkane at zero surface coverage. Schultz *et al.* [9, 10] proposed a method for determining the dispersive component of a solid's surface energy on the base of applying n-alkanes as probe molecules at zero surface coverage . Once the surface energy is calculated, the work of adhesion can be determined by:

$$W_{adh} = 2 \cdot \sqrt{\gamma_1^D \cdot \gamma_2^D} + 2 \cdot \sqrt{\gamma_1^{SP} \cdot \gamma_2^{SP}} \qquad (4-1)$$

where the subscripts 1 and 2 represent any two materials. The work of adhesion (W_{adh}) is the difference in interfacial energy between adhering and individual phases, such as a liquid on a solid. Equation 4-2 shows the relationship between W_{adh} and the surface tension at an interface [11, 12].

$$W_{adh} = \gamma \cdot (1 + \cos\theta) \qquad (4-2)$$

where γ is surface energy between water and air, or the water surface tension (mJ m^{-2}) and θ is the angle formed between the solid surface and air (contact angle). Any changes to the surface lead to changes in the work of adhesion. Therefore, determining this parameter provides useful information to investigate the surface energetics of materials, and thus wettability.

In the present study, IGC was used to characterise the surface energy of quartz by injecting a series of probe vapours at a specific surface coverage. The surface energy heterogeneity was observed by injecting the probe vapours at different surface coverages. The surfaces were changed by treatment with dodecylamine to induce hydrophobicity. The correlation between surface energy and flotation recovery of the samples was investigated through microflotation.

4.2. Experimental

4.2.1. Materials

The material used was quartz (Ward’s Scientific, USA) as a naturally hydrophilic mineral in three sizes (after crushing and grinding); -75 +53 µm (Quartz I), -106 +75 µm (Quartz II), and -150 +106 µm (Quartz III). The size fractions were obtained through sieving. The alkanes used in the surface energy experiments were decane, nonane, octane, and heptane, and the polar probe molecules were toluene and dichloromethane. All reagents used were HPLC grade (>99.5% purity) purchased from Sigma-Aldrich (USA). In order to change the degree of hydrophobicity, the examined minerals were conditioned by applying a solution of dodecylamine (DDA) as collector for quartz. Methyl isobutyl carbinol (MIBC) solution was used as the frother in microflotation experiments.

4.2.2. Methods

BET surface area of the samples was determined by Surface Area and Porosity Analyser (Micromeritics TriStar, USA). The N_2 sorptions were measured at 77 K and the samples were degassed under N_2 flow for approximately 2 hours at 200 ˚C prior to the analysis.

In order to modify the quartz surface, a 0.01 M solution of dodecylamine (DDA) and acetic acid (molar ratio: 1/4) in water was prepared. 50 ml of this solution was added to 5 g of quartz in a 150 ml beaker and stirred with a magnetic stirrer for two hours. The suspension was centrifuged for 30 min at 4,500 rpm. Then the solid phase was separated from the liquid, redispersed in toluene for washing, and centrifuged again for 15 min at 4,500 rpm. Finally, the solid was dried in air at room temperature overnight.

Microflotation experiments were conducted using a modified Smith-Partridge cell [13, 14] consisting of a 60 mL glass column with a launder on the top (Figure 4.1). Air was introduced at a controlled rate through a sintered glass frit at the bottom of the cell. Approximately 6 mg L^{-1} of MIBC added to the suspension and the rate of air flow was kept constant at approximately 37 ml

min^{-1}. The microflotation experiments were conducted for 1 min after bubbles appeared and the process was operated under batch conditions. During the microflotation, constant stirring was maintained by use of a magnetic stirrer to keep the particles in suspension.

Figure 4. 1. Microflotation cell

Surface energy measurements were carried out using the Surface Energy Analyser, SEA (Surface Measurements System Ltd., UK). The inert carrier gas used was helium and the measurements were carried out at 30 ˚C and 0% RH. The chromatography columns were presilanised glass tubes with 6 mm outer diameter, 4 mm inner diameter, and 30 cm long. Approximately 2-3 g of the sample powder was packed into the column, 5 minutes vertical tapping was applied to give a consistent packing density. Measurements were conducted with carrier gas flow rate of 7 mL min^{-1}.

4.3. Results and Discussion

The mean particle size and BET surface area of the samples are given in Table 4.1.

Table 4.1. Particle size and specific surface area of the examined quartz samples.

Sample	**Particle Size Range** (μm)	**Specific Surface Area** ($m^2\ g^{-1}$)
Quartz I	-75 +53	0.0445
Quartz II	-106 +75	0.0112
Quartz III	-150 +106	0.0055

The recovery percentage of the three quartz samples as a function of dispersive surface energy measured at 5% surface coverage is shown in Figure 4.2. It can be clearly observed that untreated quartz has a relatively high surface energy and, as expected, none of the untreated samples floated. However, the adsorption of the cationic surfactant at the sample resulted in a significant increase in recovery. This was expected, as adsorption of dodecylamine conferred hydrophobic properties to the quartz, due to the formation of hydrogen bonds between silanol groups and nitrogen, and the laying of dodecyl chains on the surface [15].

From the flotation behaviour, it was expected that the surface energy would decrease after modification with the collector, which is seen in Figure 4.2. It shows the surface energy at a coverage of 5%. However, for a heterogeneous surface, the surface energy will change as the surface is covered to a greater extent. This is because the probe molecules will adsorb preferentially to the higher energy sites when very few probe molecules are present and after these sites are taken up, the lower energy sites are covered by the probe. The 5% coverage shown here will allow the probe molecules to cover the sites on the surface that have the highest surface energy, therefore a map of the surface heterogeneity is required.

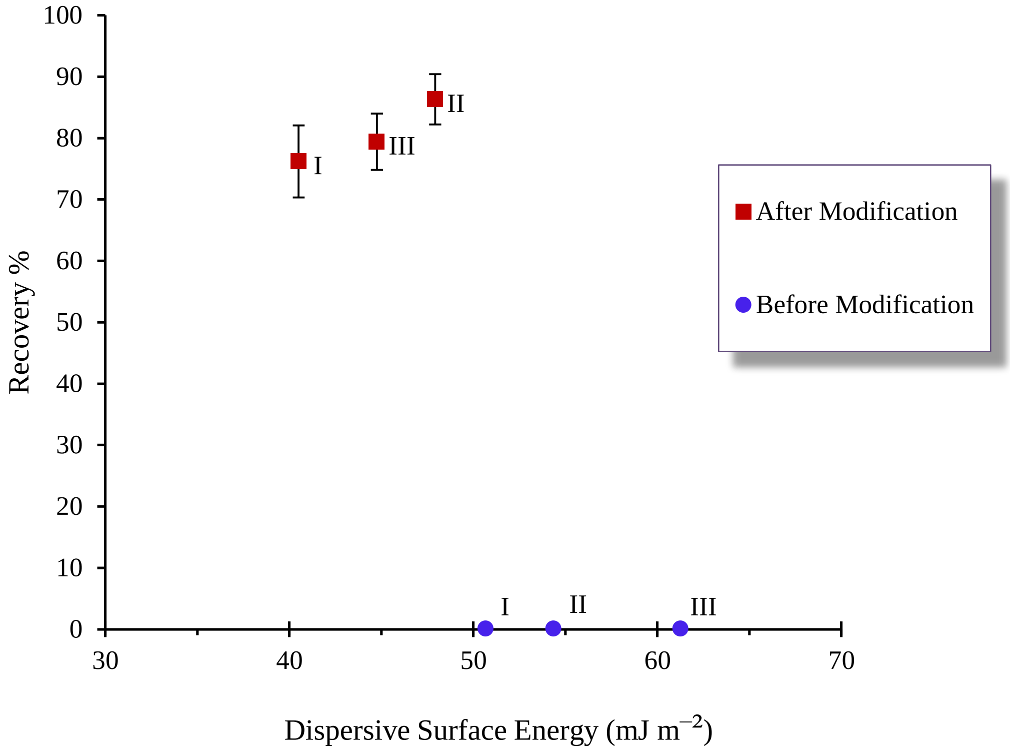

Figure 4.2. The recovery of quartz versus the dispersive surface energy at 5% surface coverage. The points I, II, and III refer to Quartz I, Quartz II, and Quartz III, respectively. Error bars represent 95% confidence interval.

Figures 4.3-4.8 show the profiles of total surface energy (γ^T), dispersive component of surface energy (γ^D), and specific (acid-base) component of surface energy (γ^{SP}) for Quartz I, Quartz II and Quartz III, pre and post modification. It can be clearly observed that the surface energy decreases as a function of surface coverage, and there is a notable difference between minimum and maximum dispersive values for the samples prior to treatment (Figures 4.3, 4.5 and 4.7). To reiterate, the surface energy difference as more probe is injected into the column is due to the high energy sites on the surface being taken up first by the probe molecules; with increasing surface coverage, the molecules are adsorbed by the sites that are energetically more stable. In other words, at infinite dilution, the retention time was dominated by the most energetic surface sites. As the injection concentration increased, the probe molecules occupied more lower energy surface sites. The detected retention times and subsequent surface energy values presented a larger percentage of the surface, and as the surface coverage increased, the less energetic sites were taken up. Therefore, for more energetically heterogeneous surfaces, the larger decrease in surface energy values was observed when going from low surface coverages to high surface coverages. In contrast, in the case of modified samples, the surface energy values remained nearly constant across the entire surface coverage range, which means the surface is energetically homogeneous. Therefore, the untreated quartz is energetically more active and more heterogeneous than the modified quartz which, in general, has lower surface energy and less variation of surface sites (Figures 4.4, 4.6 and 4.8).

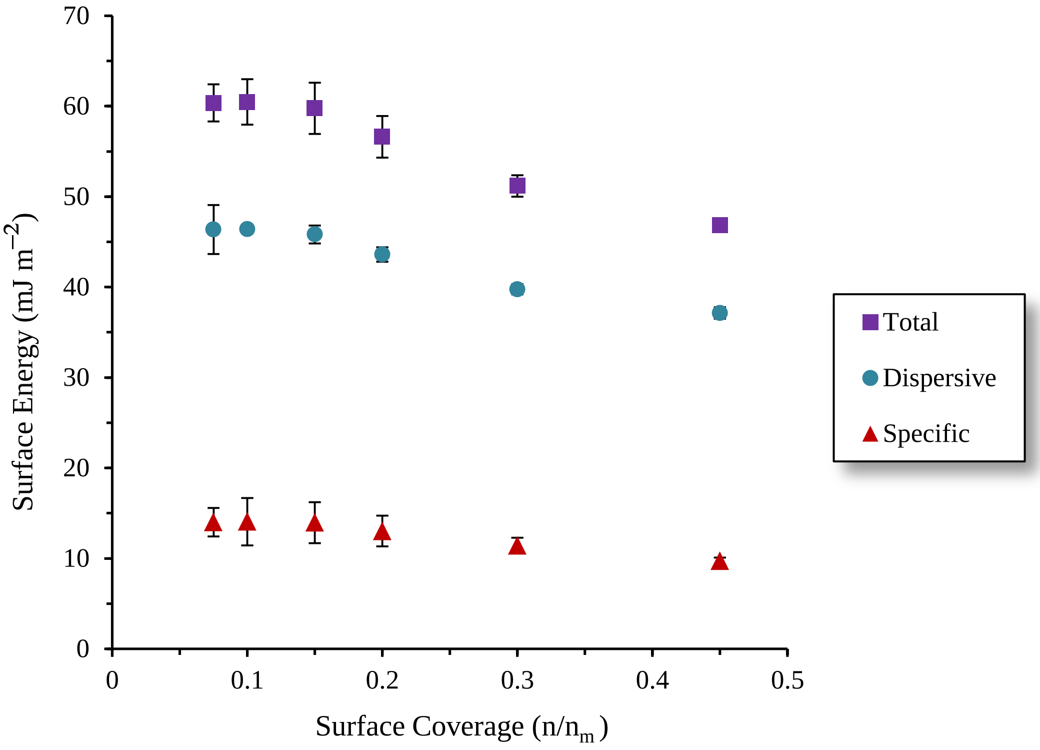

Figure 4.3. Surface energy profiles of untreated Quartz I. Error bars represent 95% confidence intervals.

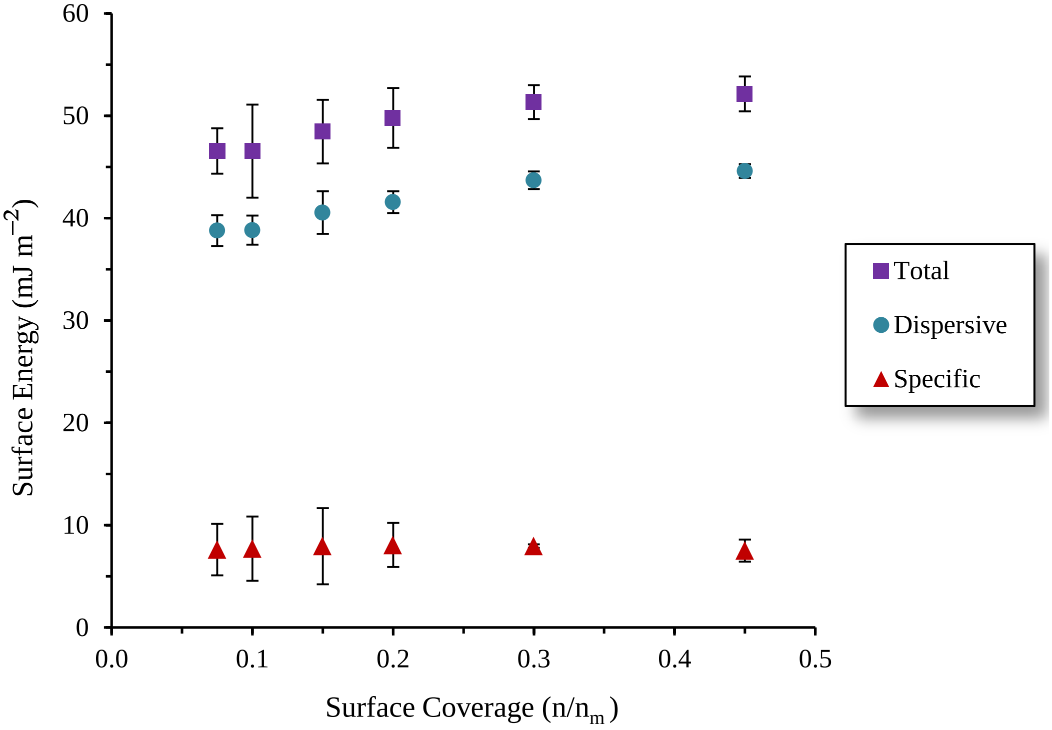

Figure 4.4. Surface energy profiles of treated Quartz I. Error bars represent 95% confidence intervals.

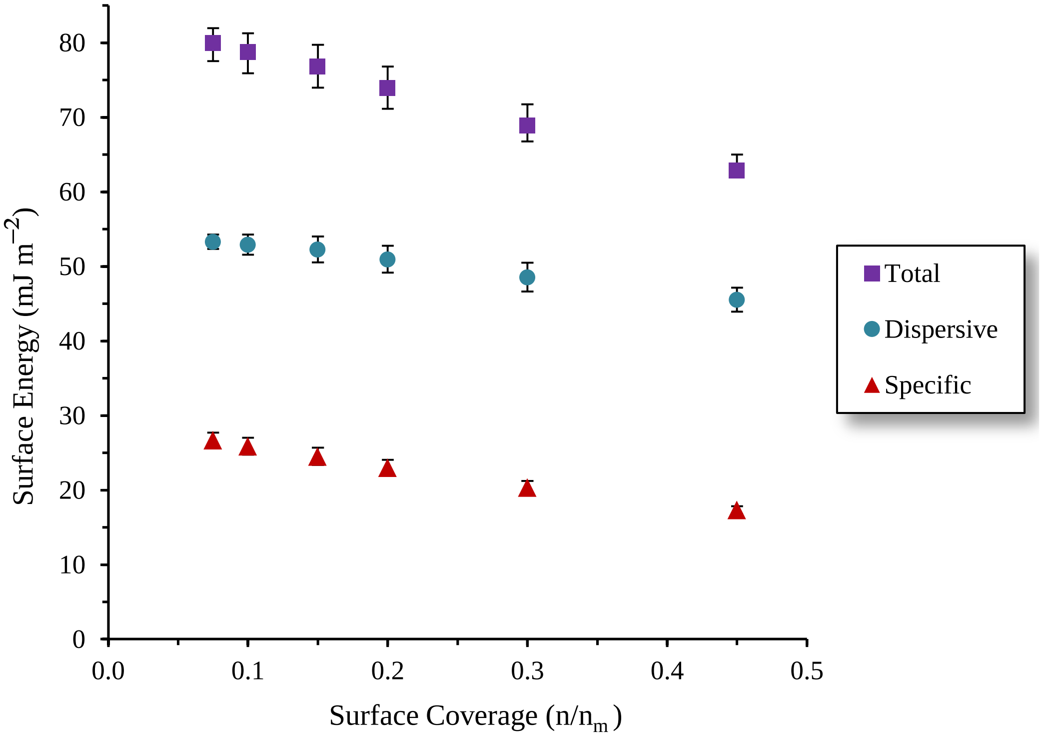

Figure 4.5. Surface energy profiles of untreated Quartz II. Error bars represent 95% confidence intervals.

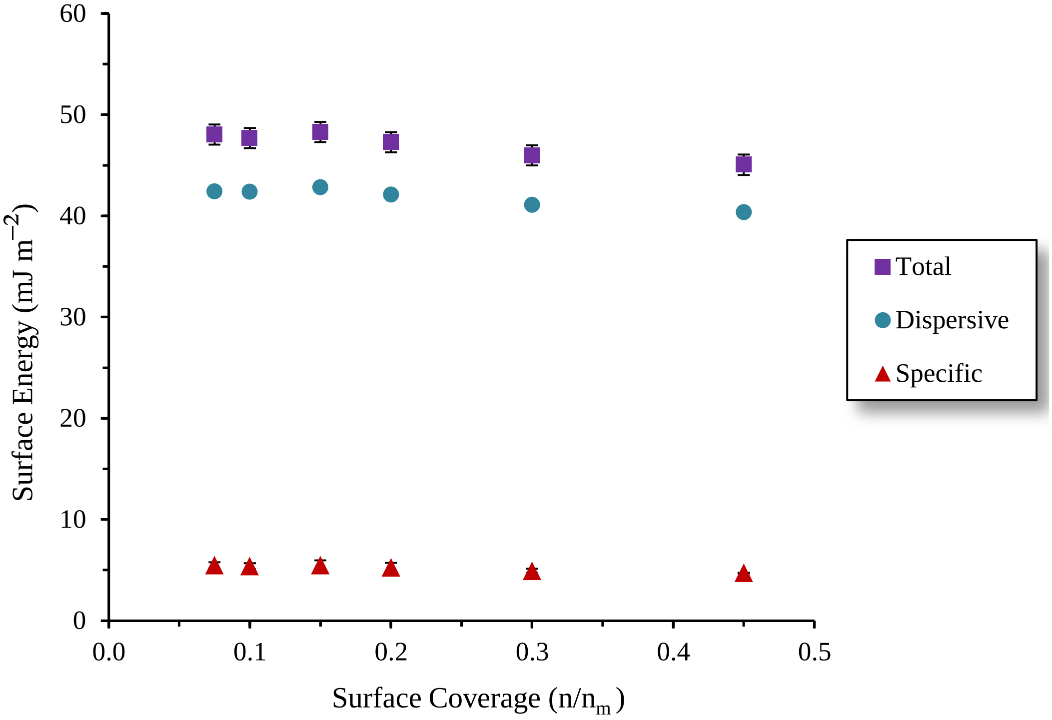

Figure 4.6. Surface energy profiles of treated Quartz II. Error bars represent 95% confidence intervals.

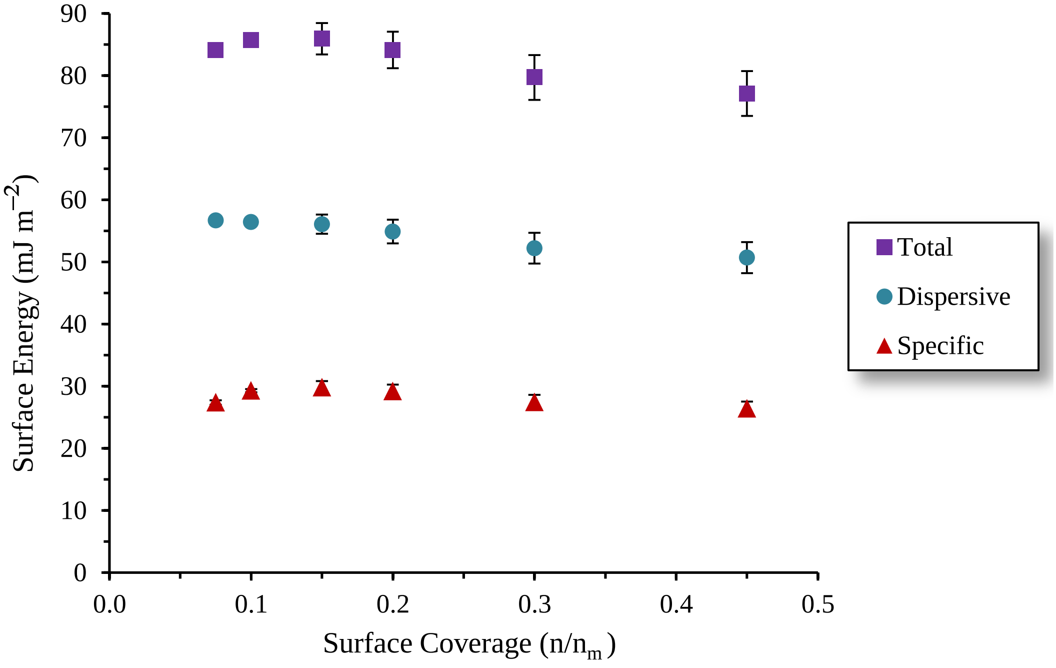

Figure 4.7. Surface energy profiles of untreated Quartz III. Error bars represent 95% confidence intervals.

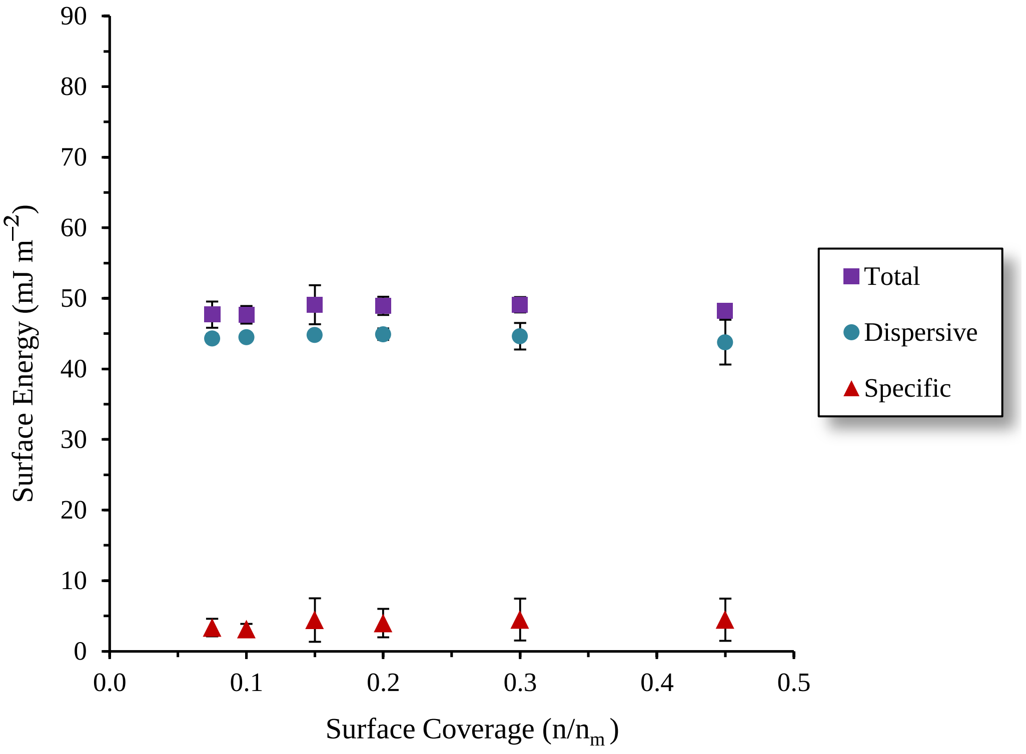

Figure 4.8. Surface energy profiles of treated Quartz III. Error bars represent 95% confidence intervals.

Figures 4.9, 4.10 and 4.11 represent the correlation between surface coverage, work of adhesion to water and hydrophilicity for three quartz samples before and after the treatment with DDA. The hydrophilicity was calculated using Equation 4-3 proposed by Ho *et al.* [16].

$$Hydrophilicity = \frac{\gamma^{SP}}{\gamma^{T}} \qquad (4-3)$$

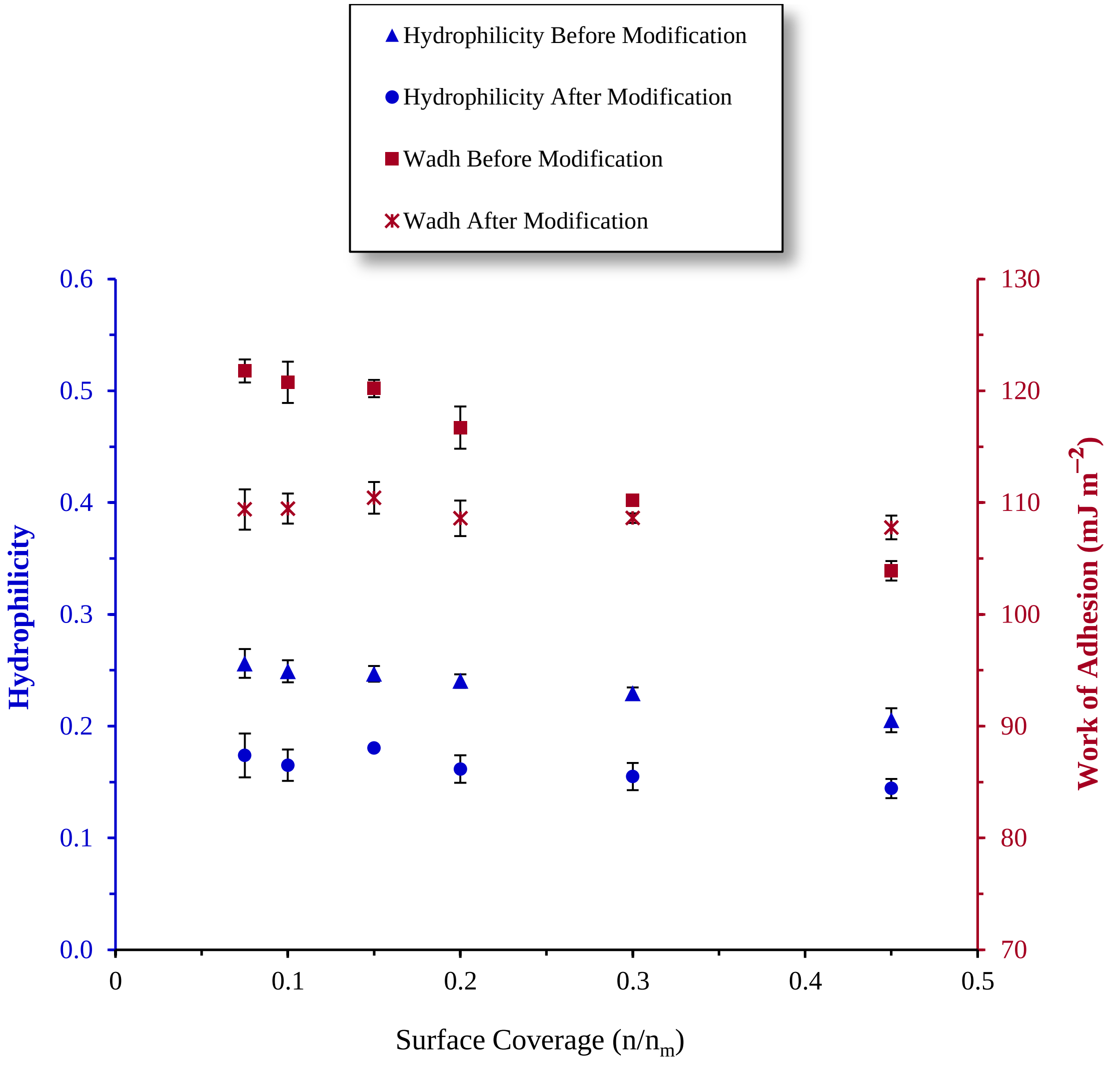

Figure 4.9. Hydrophilicity and work of adhesion profiles as a function of surface coverage for Quartz I before and after modification. Error bars represent 95% confidence intervals.

Higher hydrophilicity and W_{adh} of the samples before modification is in agreement with the high affinity of quartz to water. Also, the trend of hydrophilicity that decreases with increasing fractional surface coverage shows that at low surface coverage, the sites that are taken up by the probe molecules are the most hydrophilic, and as going forward, the lower energy sites that are more hydrophobic are occupied. For modified quartz, which has a more homogeneous surface, the values are lower with less variation.

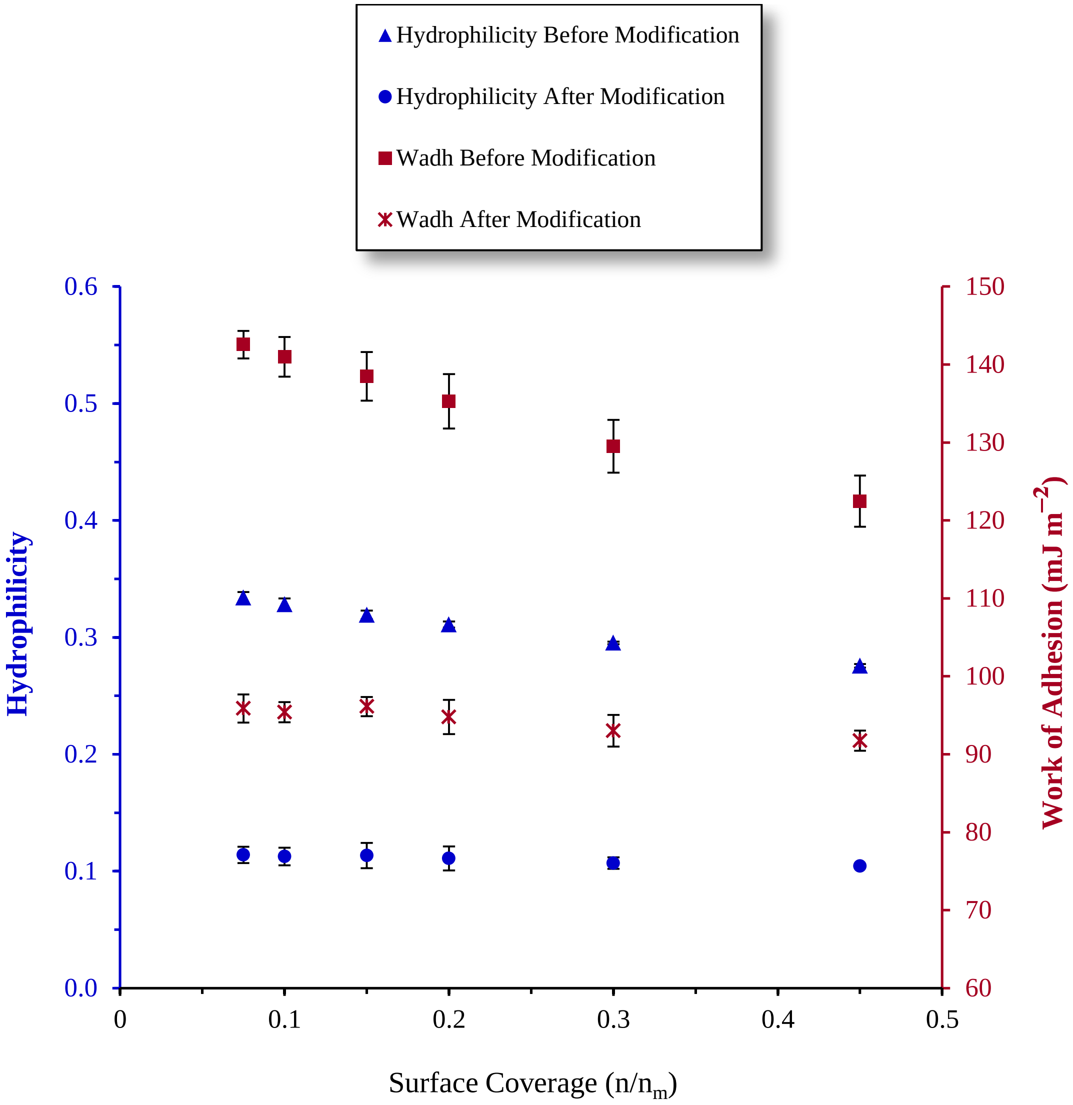

Figure 4.10. Hydrophilicity and work of adhesion profiles as a function of surface coverage for Quartz II before and after modification. Error bars represent 95% confidence intervals.

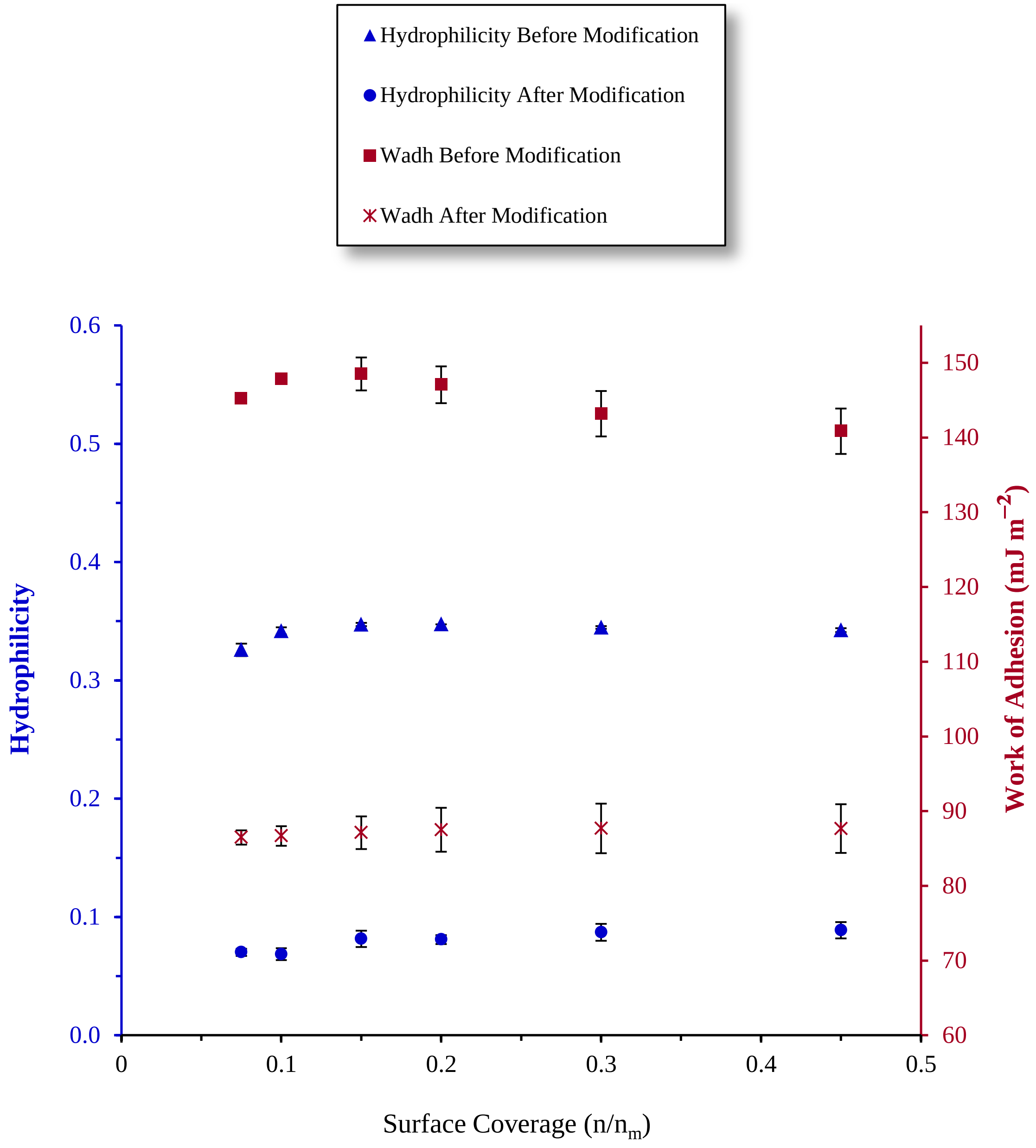

Figure 4.11. Hydrophilicity and work of adhesion profiles as a function of surface coverage for Quartz III before and after modification. Error bars represent 95% confidence intervals.

4.4. Conclusions

Inverse gas chromatography (IGC) has been shown to have the capability to determine the thermodynamic properties of quartz at different sizes, pre- and post-conditioning. Relating the hydrophobicity and flotation of minerals to the surface energy can be observed from combining the results of IGC and microflotation experiments. The dispersive and specific surface energy of the quartz samples were measured and compared. Moreover, the obtained values for surface energetics, work of adhesion, and hydrophilicity do, in general, agree with flotation recovery. The following chapter extends this initial investigation into applying IGC to flotation by investigating a common sulphide mineral, pyrite, treated with a xanthate collector at different pH.

References

[1] M. Yudin, B. Hughes, Surface energy of solids, Physical Review B, 49-8 (1994) 5638-5642.

[2] S.S. Ali, J.Y. Heng, A. Nikolaev, K.E. Waters, Introducing inverse gas chromatography as a method of determining the surface heterogeneity of minerals for flotation, Powder Technology, 249 (2013) 373-377.

[3] A. Voelkel, Physicochemical measurements (inverse gas chromatography), in: C. Poole (Ed.) Gas Chromatography, Elsevier, 2012, pp. 477-494.

[4] A. Voelkel, Inverse gas chromatography: characterization of polymers, fibers, modified silicas, and surfactants, Critical Reviews in Analytical Chemistry, 22-5 (1991) 411-439.

[5] P.P. Ylä-Mäihäniemi, J.Y. Heng, F. Thielmann, D.R. Williams, Inverse gas chromatographic method for measuring the dispersive surface energy distribution for particulates, Langmuir, 24-17 (2008) 9551-9557.

[6] E. Kokkoli, C.F. Zukoski, Surface pattern recognition by a colloidal particle, Langmuir, 17-2 (2001) 369-376.

[7] K. László, E. Tombácz, K. Josepovits, Effect of activation on the surface chemistry of carbons from polymer precursors, Carbon, 39-8 (2001) 1217-1228.

[8] G.M. Dorris, D.G. Gray, Adsorption of n-alkanes at zero surface coverage on cellulose paper and wood fibers, Journal of Colloid and Interface Science, 77-2 (1980) 353-362.

[9] J. Schultz, L. Lavielle, C. Martin, The role of the interface in carbon fibre-epoxy composites, The Journal of Adhesion, 23-1 (1987) 45-60.

[10] J. Schultz, L. Lavielle, Interfacial properties of carbon fiber-epoxy matrix composites, in: Inverse Gas Chromatography Characterisation of Polymers and Other Materials, ACS Symposium Ser, ACS Publications, 1989, pp. 185-202.

[11] P. Nikolopoulos, D. Sotiropoulou, Wettability between zirconia ceramics and the liquid metals copper, nickel and cobalt, Journal of Materials Science Letters, 6-12 (1987) 1429-1430.

[12] D. Sotiropoulou, P. Nikolopoulos, Work of adhesion in ZrO_2-liquid metal systems, Journal of Materials Science, 28-2 (1993) 356-360.

[13] A.C. Partridge, G. Smith, Flotation and adsorption characteristics of the hematite-dodecylamine-starch system, Canadian Metallurgical Quarterly, 10-3 (1971) 229-234.

[14] A. Partridge, G. Smith, Small-sample flotation testing: a new cell, Trans. Inst. Min. Metall. (Sect. C), 80 (1971) 199-200.

[15] X. Wang, J. Liu, H. Du, J. Miller, States of adsorbed dodecylamine and water at a silica surface as revealed by vibrational spectroscopy, Langmuir, 26-5 (2009) 3407-3414.

[16] R. Ho, S.J. Hinder, J.F. Watts, S.E. Dilworth, D.R. Williams, J.Y. Heng, Determination of surface heterogeneity of D-mannitol by sessile drop contact angle and finite concentration inverse gas chromatography, International Journal of Pharmaceutics, 387-1 (2010) 79-86.

CHAPTER 5

IGC ANALYSIS OF MINERALS: PYRITE WETTABILITY

Abstract

Inverse gas chromatography (IGC) is a powerful technique for characterising the physicochemical properties of a wide variety of materials. The behaviour of minerals in the flotation process is directly related to their wettability, which can be described by surface free energy. The previous Chapter introduced the potential of analysing mineral surfaces, and relating this to flotation. This Chapter extends this into investigating a common sulphide (pyrite) conditioned with a collector at different pH values. The adsorption of copper and xanthate on hydrophilic pyrite, prepared under different conditions, was studied using X-ray photoelectron spectroscopy (XPS) and IGC. Microflotation experiments were also conducted to determine flotation recovery. The XPS analyses confirmed the presence of copper(I) and xanthate compounds on the surface of treated samples. The surface energy and work of adhesion to water decreased, while the flotation recovery increased due to treatment. IGC has been shown to have the capability of characterizing mineral surfaces, pre- and post-treatment. It enabled the observation of the changes in physicochemical properties of pyrite surface due to surface modification at different conditions. Moreover, combining the microflotation recovery of the samples with IGC results confirmed the correlation between surface energy and flotation response.

5.1. Introduction

The separation of minerals by selective flotation is driven by surface chemistry, namely the affinity of a surface to water or an air bubble. This is controlled by the surface energy of the particle. Surface characterisations of minerals have been extensively studied using various techniques. However, surface free energy is not a directly measured characteristic and can be calculated through different methods and theories [1-4] . Inverse gas chromatography (IGC) is a powerful characterisation tool which has been used in various industries, most commonly pharmaceutical and polymer, to investigate diverse properties such as miscibility, solubility and crystallinity (see Chapter 3). It has recently been introduced to mineral processing, being applied to flotation by determining the surface energy and wettability of minerals [5, 6]. Surface energy is one of a variety of physicochemical properties that can be accurately determined using IGC. Dispersive (γ^D) and specific (γ^{SP}) components of surface energy are calculated through interactions of a solid surface with nonpolar and polar organic solvents, respectively. The sum of the dispersive and specific components represents the total solid surface energy. Due to the direct correlation between surface energy and work of adhesion, IGC is a powerful tool for investigating the wetting behaviour of a material. This work of adhesion is a measure of the strength of the affinity between two materials, and for a solid-liquid system can be defined by Fowkes' equation [7]:

$$W_{adh} = 2 \cdot \sqrt{\gamma_S^D \cdot \gamma_L^D} \qquad (5-1)$$

Fowkes mainly investigated two-phase systems and only the dispersion interactions, which are connected to London forces, were considered. However, Owens & Wendt [8] have suggested the nondispersive component of the intermolecular interactions between materials to be included as geometric mean of the nondispersive (polar) components. Therefore, the work of adhesion between a solid and a liquid is calculated as [9]:

$$W_{adh} = 2 \cdot \sqrt{\gamma_S^D \cdot \gamma_L^D} + 2 \cdot \sqrt{\gamma_S^{SP} \cdot \gamma_L^{SP}} \qquad (5-2)$$

where γ_S^{SP} and γ_L^{SP} are polar components of surface free energy of the solid and liquid molecule (mJ m^{-2}), respectively.

IGC can also be applied as a surface mapping technique by determining the distribution of different energy sites on a solid surface, which provides comprehensive information on the surface, known as energetic homogeneity and heterogeneity. A typical IGC instrument consists of a column, which is a capillary glass tube filled with the sample, a reservoir containing organic solvents, called probes, and a detector. Probe vapours are passed through the column using an inert gas such as helium. Adsorption onto and desorption from the sample leads to a retention of the probe in the column, and the retention time is determined by a detector. From a series of IGC measurement with different probes, polar and nonpolar, a wide range of physicochemical properties can be calculated.

Pyrite (FeS_2) is the most abundant sulfide mineral, frequently occurring as a gangue in association with minerals of economic value, such as sphalerite, chalcopyrite, galena and precious native metals such as gold [10]. Flotation recovery is based on the ability of certain chemicals, such as collectors and activators to modify the surface properties of minerals. The presence of metal ions can have a detrimental or beneficial effect on the flotation of sulphide minerals, through either depression or activation of minerals. The adsorption of copper(II) (activator) and xanthate (collector) onto pyrite surfaces has been shown to have a significant impact on the froth flotation recovery [10-24]. Ideally, in industrial flotation of minerals, copper containing minerals are recovered to the concentrate first; however, it is possible that Cu ions released from these minerals adsorb onto the pyrite surface, and pyrite flotation remarkably improves in the presence of xanthate collector since both $Cu^{(I)}S$ and $Cu^{(II)}$xanthate are hydrophobic [22]. The adsorption processes may proceed through different mechanisms and different species can be produced at surface upon these mechanisms. However, an investigation of the mineral surface in a flotation pulp in the presence of various reagents is very complicated and a variety of traditional and modern methods have been proposed to evaluate behaviour of mineral particles in flotation separation.

In this work, pyrite samples were conditioned with common flotation reagents, and the effect of the treatment on the sample surface was also investigated using X-ray photoelectron spectroscopy (XPS) and IGC. XPS is the most commonly used spectroscopic method for quantitatively determining chemical information and elemental components of materials surface. It also gives information about the ionisation energies of a particular electron in a particular atom. In this method, the sample is exposed to soft X-ray of known energy which causes surface atom ionisation and the energy of the released photoelectrons is then measured. The outcome of XPS analysis is a spectrum of emission intensity as a function of binding energy (BE) of the electrons which identify the surface elements and their concentration. In addition, the flotation behaviour of the mineral samples was investigated through microflotation experiments.

5.2. Methodology

5.2.1. Materials and Preparation

High purity pyrite was obtained from Ward's Scientific (USA) (originally from Peru). The pyrite was dry-crushed, ground, sieved, and a -75 +53 μm size fraction was collected for the experiments. Potassium amyl xanthate (KAX 51) was obtained from Prospect Chemicals (Canada). The xanthate compound was purified by dissolving in acetone, recrystallizing by petroleum ether and filtering out the precipitation. The purified KAX 51 was stored under petroleum ether.

The alkanes used in the surface energy experiments were decane, nonane, octane and heptane, and the polar probe molecules were toluene and dichloromethane. All chemicals used were of HPLC grade (>99.5% purity), purchased from Sigma–Aldrich (USA).

The activation of pyrite surface was conducted in a 10^{-4} M copper sulfate ($CuSO_4$) solution for 30 minutes. Then samples were washed with reverse osmosis water, and conditioned in 10^{-4} M KAX 51 solution for 10 minutes. Similarly, non-activated pyrite samples were also conditioned in a xanthate solution. A series of samples were also prepared by only conditioning pyrite in deionised water. The activation and conditioning were carried out at different pH values, detailed in Table 5.1. The pH of the each solution was adjusted using potassium hydroxide and hydrochloric acid, and monitored throughout the activation and conditioning reaction.

Table 5.1. The pH values of sample preparation reactions.

Sample	Cu-Activation pH	Xanthate-Treatment pH
Pyrite	–	–
*P3	–	–
*P7	–	–
*P10	–	–
X3	–	3
X7	–	7
X10	–	10
Cu3X3	3	3
Cu3X7	3	7
Cu3X10	3	10
Cu7X3	7	3
Cu7X7	7	7
Cu7X10	7	10
Cu10X3	10	3
Cu10X7	10	7
Cu10X10	10	10

* Samples P3, P7 and P10 were conditioned only in water at pH 3, 7 and 10, respectively.

5.2.2. Measurements

Surface energy measurements were carried out using a Surface Energy Analyser, SEA (Surface Measurements System Ltd., UK) at finite dilution (FD-IGC). The chromatography columns were presilanised glass tubes of 30 cm in length, with an outer diameter of 6 mm and an inner diameter of 4 mm. The sample powder was packed into the column and 5 min vertical tapping was applied to give a consistent packing density. Helium was selected as carrier gas at a flow of

10 ml min^{-1} and methane was used for dead volume corrections. The columns were preconditioned with the carrier gas at 30 °C for 60 min to remove any physisorbed water. All measurements were carried out at 30 °C and 0% RH. The experiments were run a minimum of three times for each sample. The data were analysed using Cirrus Plus Analysis Software (Surface Measurements System Ltd., UK). The retention time from the peak maximum was used to calculate the retention volume and to determine the surface energies; the Schultz method was employed for the dispersive components, and the specific components were obtained using the Della Volpe scale.

BET surface area of the samples was determined using Surface Area and Porosity Analyser (Micromeritics TriStar, USA). The N_2 sorptions were measured at 77 K and the samples were degassed under N_2 for approximately 2 h at 300 °C prior to the analysis.

X-ray photoelectron spectroscopy (XPS) measurements were performed using K-Alpha surface analysis system (Thermo Scientific) with an AlKα X-ray source (1489.6 eV), applying a 400 µm diameter beam spot. In order to avoid charging on the surface, a flood gun was used to shoot the samples with low energy electrons during the experiments. The collected data was processed using Avantage Data Processing software (Thermo Fisher Scientific). The binding energy (BE) was calibrated using the background hydrocarbon C 1s binding energy of 284.8 eV; no binding energy correction was necessary for this study. The samples were dried in a vacuum oven and transferred to a vacuum desiccator before being transferred into the XPS analysis chamber.

Flotation was conducted through microflotation experiments using a modified Hallimond tube (34.6 cm in height, 3.3 cm outer diameter and 2.6 cm inner diameter), as shown in Figure 5.1. The samples (1 g for each test) were conditioned with reverse osmosis water for 5 min. The suspension was then transferred to the microflotation cell and the volume was adjusted to 180 ml. During the microflotation tests, constant stirring was maintained by use of a magnetic stirrer to keep the particles in suspension. High purity nitrogen was used as the flotation gas at a flow rate of 40 mL min^{-1} to prevent any further oxidation while flotation tests were undergoing, and the recovered material was collected for one min after the first bubbles arrived at the surface of the suspension. The microflotation experiments were run seven times for each condition.

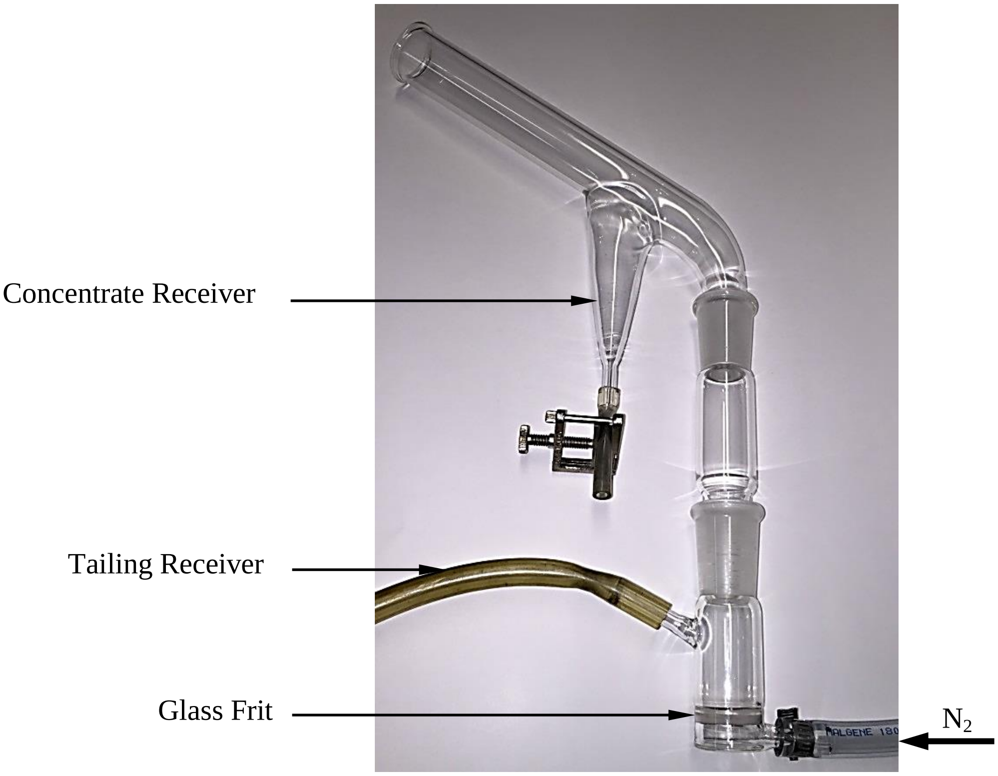

Figure 5.1. Microflotation cell.

5.3. Results and Discussion

5.3.1. X-Ray Photoelectron Spectroscopy (XPS) Measurements

The atomic composition of pyrite surfaces, prior to and post activation and conditioning, as determined by XPS, are given in Table 5.2. Cu 2p was detected on the surface of all pyrite samples at different concentrations. Copper 2p composition was higher for the activated samples and the value depended on the preparation condition. XPS C 1s, O 1s, S 2p, Fe 2p and Cu 2p high resolution spectra of samples were collected and compared. The spectrum of C 1s of the untreated pyrite was fitted into three components; a dominant peak at around 285 eV and two small signals at around 286 eV and 288 eV, which are attributed to hydrocarbon contamination

[25]. Unfortunately, it was impossible to use these spectra to distinguish xanthate signals from those of the contamination.

Table 5.2. Atomic concentration (atomic percentage)
of the elements measured on the pyrite surface by XPS.

Sample	**Atomic %**			
	Cu 2p	**Fe 2p**	**S 2p**	**O 1s**
Pyrite	1.43	8.81	33.10	22.14
P3	1.40	9.94	33.25	23.98
P7	2.41	6.83	28.35	32.33
P10	1.45	10.30	35.34	27.61
X3	1.56	9.13	29.27	27.96
X7	2.11	9.41	27.9	24.24
X10	2.90	11.30	35.32	23.59
Cu3X3	2.38	12.15	38.29	22.08
Cu3X7	1.79	11.78	33.05	27.87
Cu3X10	2.11	12.11	35.18	25.30
Cu7X3	2.69	10.57	34.94	25.72
Cu7X7	2.84	7.01	27.70	29.92
Cu7X10	3.91	6.93	28.11	25.52
Cu10X3	2.26	11.25	39.26	21.82
Cu10X7	4.88	12.94	25.60	31.83
Cu10X10	4.30	10.06	26.59	25.30

The Cu 2p spectra showed two couple peaks at approximately 932 eV and 934 eV, which are attributed to the presence of Cu(I) species in the sulfide lattice [22, 25-28] and Cu(II) species

[26-29], respectively. Two split spin-orbit components also present at approximately 20 eV (Δ_{metal} = 20 eV) from the former ones, *i.e.* 952 eV and 954 eV. The absence of Cu(II) shake-up satellites around 942 eV rules out the presence of copper hydroxide on the sample surface [30] and the spectra did not change significantly with different preparation conditions.

Table 5.3 summarises binding energies of O 1s, S 2p and Fe 2p components of X-ray photoelectron spectra of the sample surfaces. The spectra themselves are available as supplementary information in Appendix. The O 1s specification components resulting from oxidation of mineral surface could be seen in the spectra of all samples. The O 1s peak of the untreated and treated samples was composed of three signals. The main peak at around 531 eV (signal B) is mainly contribution of sulfate (SO_4^{-2}) [28], hydroxide (OH) [15, 25, 28, 30] and sulfoxy [30] species due to oxidation of the surface. The other component at binding energies around 530 eV (signal C) corresponds to FeOOH, $(FeOH)_2$ [27] or oxide type oxygen [19, 25]. The band at around 533 eV (signal A) can be attributed to adsorbed water [25, 27, 30]. The O 1s spectra from Cu-activated and xanthate-treated samples consisted of the same three components. However, the xanthate-treated samples indicated a noticeable increase in the intensity of signal A, as a result of the presence of a new oxygen atom due to the formation of the xanthate species on the pyrite surface [27, 28].

The S 2p high resolution spectra were composed of two doublets centred at approximately 162 eV (signal D) and 168 eV (signal B). The second signals (A and C) were closely spaced spin-orbit components (Δ = 1.2 eV), appearing at approximately 163 eV and 169 eV. Doublet C-D is attributed to pyritic sulphur [15, 19, 25, 30], elemental sulphur or xanthate polysulfide species [22, 27, 30] and oxidised sulphur (S2-2) [19, 26, 29]. Doublet A-B confirms the presence of sulfoxy species such as sulfate (SO_4^{2-}) or thiosulfate ($S_2O_3^{2-}$) [22, 25, 28-30]. The latter was also confirmed by the O 1s signal at around 531 eV. The binding energy values of S 2p for pyritic sulphur and surface xanthate sulphur are very similar [19, 27, 31], and surface oxidation does not typically make remarkable changes on the proportion of sulfides in similar environments [25]. However, from high resolution spectra for Cu-activated and xanthate-treated samples, the ratio of the signal at around D to the signal B was significantly higher than the signal observed for untreated pyrite. This is interpreted to be the result of S_2^{2-} oxidation to S^{2-} or S_n^{2-} upon the adsorbed Cu(II) reduction to Cu(I) [22, 26, 29] and/or the presence of xanthate species since the adsorption of xanthate inhibits the oxidation of pyrite surface [28, 32]. As a result, compared to untreated pyrite and the sample only treated in acidic or basic water, the signals S 2p-A and -B for activated and treated samples were of very low intensity and sometimes one or both of them almost disappeared.

Table 5.3. XPS binding energies (eV) of high resolution photoelectron spectra.

Sample	**O 1s**			**S 2p**				**Fe 2p**		
	A	**B**	**C**	**A**	**B**	**C**	**D**	**A**	**B**	**C**
Pyrite	533.58	531.68	529.88	169.88	168.68	163.88	162.68	720.08	*710.90	707.28
P3	533.68	531.68	530.18	169.88	168.78	163.68	162.68	719.98	–	707.18
P7	533.58	531.58	529.98	169.98	168.68	163.68	162.58	720.08	*710.88	707.28
P10	532.98	531.58	529.88	169.88	168.58	163.78	162.68	719.98	711.08	706.98
X3	533.18	531.58	529.98	–	*168.88	163.68	162.48	719.78	–	706.98
X7	533.38	531.68	530.08	*169.88	*168.68	163.78	162.68	719.98	*711.18	707.18
X10	533.38	531.78	530.08	–	–	163.78	162.58	719.88	710.88	707.08
Cu3X3	533.18	531.68	529.88	–	–	163.88	162.68	719.78	–	707.08
Cu3X7	533.28	531.58	529.98	–	*168.58	163.68	162.48	719.98	–	707.18
Cu3X10	533.18	531.58	529.98	–	*168.58	163.58	162.48	719.78	710.88	706.98
Cu7X3	533.28	531.58	529.78	–	*168.68	163.68	162.58	719.88	–	707.08
Cu7X7	533.08	531.48	529.98	–	*168.48	163.68	162.48	719.88	*710.68	707.08
Cu7X10	532.98	531.48	529.88	–	*168.28	163.58	162.38	719.98	711.18	707.18
Cu10X3	532.88	531.48	530.08	–	–	163.68	162.48	719.78	–	706.98
Cu10X7	532.48	531.28	529.78	169.88	168.48	163.68	162.38	719.68	710.98	706.88
Cu10X10	532.68	531.48	529.88	–	–	163.68	162.58	719.78	710.78	706.98

* Very low intensity.

The Fe 2p high resolution spectra of all samples could be fitted into two components. The dominant peak at the lowest binding energy of around 707 eV (signal C) is attributed to pyritic iron [15, 22, 25, 26, 29, 30], and the signal at around 720 eV (signal A) shows the split spin-orbit components of Fe 2p (Δ_{metal} = 12.9 eV). The signals A and C were not considerably influenced by treatment and the spectra exhibited no difference between the pyrite surface before and after activation and conditioning. However, for some samples, there was a broader peak at around 710 eV (Signal B), which was attributed to ferric oxide/hydroxide [22, 25, 26, 29, 30]. The latter may be formed due to immersion of pyrite into the non-acidic solution during activation and/or conditioning since its intensity changes with pH variations [27].

5.3.2. Microflotation

The flotation recoveries of the samples are given in Table 5.4. As expected, pyrite had a negligible flotation response, and the samples conditioned in water at pH 3 and 7 showed little difference from untreated pyrite. The flotation recovery of pyrite was influenced by Cu-activation and xanthate-conditioning. However, the changes in floatability were different, depending on the sample preparation condition.

5.3.3. Inverse Gas Chromatography (IGC)

Dispersive (γ^{D}) and specific (γ^{SP}) components of surface energies obtained from IGC experiments are presented in Table 5.4. The untreated pyrite has the highest surface free energy of all samples. Comparing surface free energies, the results generally indicate that the surface modifications, regardless of preparation condition, lower the total surface energy of pyrite. These changes occurred due to effects on the dispersive and/or specific surface free energy depending on the activation and/or conditioning reaction pH. This leads to the conclusion that polar sites of the pyrite surface were also influenced due to the surface changes, and the affected interactions were of both dispersive (nonpolar) and specific (polar) types.

There were no significant differences in the surface energies between untreated pyrite and that conditioned in water alone at pH 3 and pH 7. However, the Cu-activated and xanthate-treated samples showed a significant change in surface energies. As shown in Table 5.4, the changes in surface energies are in good agreement with the changes in flotation recovery, which indicates changes in hydrophobicity of the pyrite. The lowest change in the surface free energy was observed for the sample conditioned in water at pH 3 (P3) which also showed a very low flotation recovery (5%). Among the Cu-activated samples, the sample activated at pH 3 and treated with xanthate solution at pH 10 (Cu3X10) showed the highest surface energy and lowest flotation recovery; meaning that this is not a process that would lead to a marked increase in the hydrophobicity of pyrite. In contrast, the lowest surface energy was of the sample activated with copper at pH 7 and then conditioned with xanthate at pH 10 (Cu7X10), having the greatest flotation recovery among all samples tested (86%).

Table 5.4. Surface energies and flotation recovery percentages of pyrite samples.
The upper and lower boundaries are obtained from a 95% confidence interval estimate.

Sample	**γ^D (mJ m^{-2})**	**γ^{AB} (mJ m^{-2})**	**γ^+ (mJ m^{-2})**	**γ^-(mJ m^{-2})**	**Flotation Recovery (%)**
Pyrite	52.19 ±1.4	9.56 ±0.4	3.81±0.1	5.99±0.3	2 ±0.3
P3	52.77 ±2.4	7.81 ±0.6	2.78±0.2	5.48±0.3	5 ±0.3
P7	49.36 ±2.8	9.38 ±0.7	3.47±0.3	6.34±0.2	6 ±0.2
P10	43.59 ±1.8	8.52 ±0.5	2.86±0.2	6.34±0.3	20 ±0.4
X3	41.30 ±2.4	5.14 ±0.6	1.60±0.1	4.12±0.3	41 ±1.1
X7	39.39 ±3.4	6.16 ±0.9	2.01±0.3	4.71±0.5	72 ±1.0
X10	37.53 ±2.9	5.75 ±0.8	1.91±0.3	4.33±0.4	78 ±0.7
Cu3X3	43.13 ±2.8	4.20 ±0.8	4.28±0.5	1.03±0.2	41 ±0.7
Cu3X7	40.53 ±1.5	6.24 ±0.4	1.85±0.1	5.26±0.1	45 ±0.9
Cu3X10	53.11 ±2.7	4.93 ±0.7	1.90±0.3	3.20±0.3	14 ±0.5
Cu7X3	43.04 ±2.3	4.25 ±0.6	1.19±0.3	3.79±0.2	36 ±0.5
Cu7X7	37.03 ±2.3	6.88 ±0.6	2.20±0.3	5.37±0.2	65 ±1.3
Cu7X10	32.93 ±2.1	6.89 ±0.5	2.07±0.1	5.73±0.3	86 ±0.8
Cu10X3	39.84 ±2.8	5.98 ±0.7	1.85±0.3	4.82±0.3	46 ±1.0
Cu10X7	39.00 ±1.6	7.11 ±0.4	2.28±0.4	5.53±0.1	60 ±0.7
Cu10X10	39.04 ±1.7	5.77 ±0.4	1.94±0.1	4.30±0.4	76 ±0.8

In order to report a more concrete parameter for the evaluation of flotation behaviour of materials, the work of adhesion between water and solid was also determined (shown in Figure 5.2). Work of adhesion to water is a measure of the wettability and directly related to the surface free energy (Equation 5-2). The higher surface energy means the greater work of adhesion and the greater affinity to water (more hydrophilic surface) and therefore a decrease in flotation recovery. Figure 5.2 clearly demonstrates the relationship between the work of adhesion to water and flotation recovery of the pyrite samples. As would be expected, the most hydrophilic sample among all the samples with 2% flotation recovery had the highest value for the work of adhesion. The trend of the plot matched the expectations from the surface energetics of the samples since lower flotation recovery reflected a higher work of adhesion to water. As the work of adhesion decreased (*i.e.*, the wettability decreased), the flotation recovery of samples increased. The most hydrophobic sample with the work of adhesion to water of 86.07 mJ m^{-2} showed, as mentioned previously, the greatest flotation recovery and the lowest surface energy of all samples (γ^{T}_{Cu7X10} = 39.82 mJ m^{-2}).

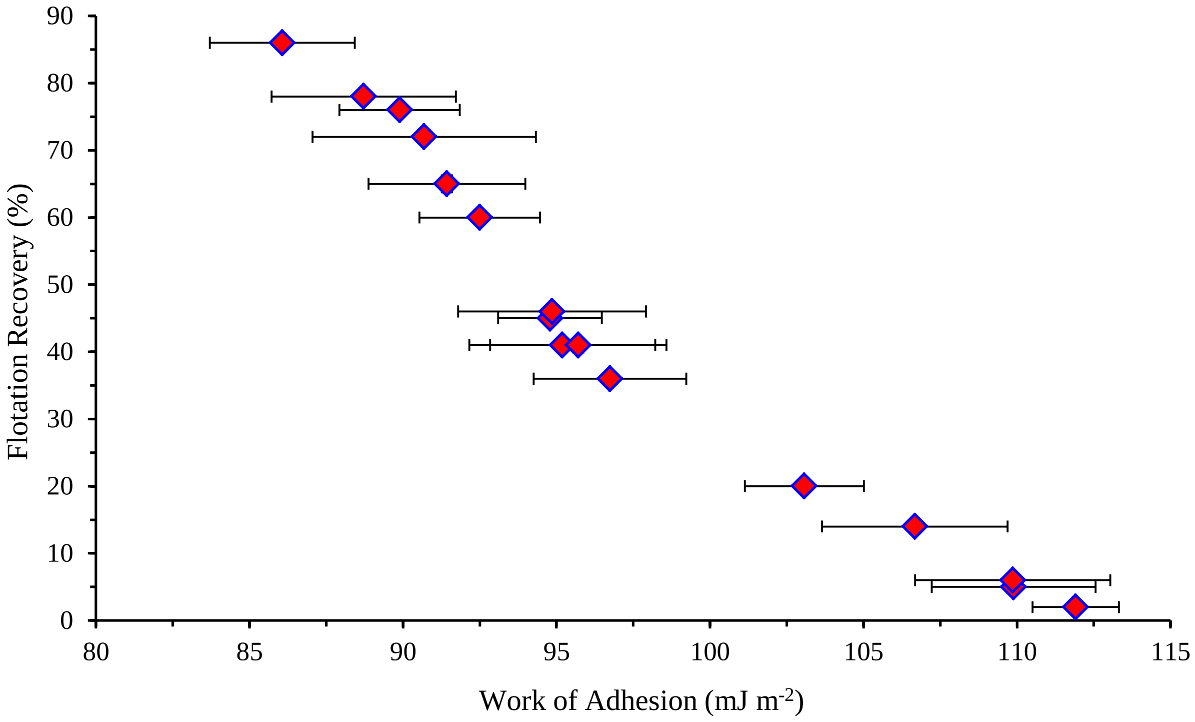

Figure 5.2. Flotation recovery versus work of adhesion to water for the pyrite samples. Error bars represent 95% confidence intervals.

5.4. Conclusions

IGC has been shown to be a useful technique in studying the effect of the surface treatment on the hydrophobic nature of pyrite. The presence of copper and xanthate at the sample surfaces was supported from Cu 2p, O 1s, S 2p and Fe 2p high resolution spectra through XPS analyses. Both dispersive and specific components of surface free energy of pyrite were affected due to treatment procedures: copper-activation and xanthate-conditioning. IGC was able to distinguish between untreated and treated pyrite and also to differentiate between differently activated and conditioned samples, with various degrees of hydrophobicity on the basis of the surface thermodynamic changes. The changes in surface properties after treatment at certain conditions have shown to effectively decrease surface free energy, which led to the increment of flotation recovery. The higher flotation recovery corresponds to lower surface energy values, which further supported by work of adhesion obtained from IGC experiments.

In conclusion, this study has given an indication that the prediction of flotation recovery of minerals may be possible by the measurement of surface free energy and work of adhesion to water by using inverse gas chromatography (IGC). This is an area that should be investigated further, with bench scale tests and plant trials. The following chapter includes the study of the surface energetics of concentrates and tailings from the flotation of a sulphide ore in a Denver flotation cell.

References

[1] R. Hartmann, J.A. Sirviö, R. Sliz, O. Laitinen, H. Liimatainen, A. Ämmälä, T. Fabritius, M. Illikainen, Interactions between aminated cellulose nanocrystals and quartz: Adsorption and wettability studies, Colloids and Surfaces A: Physicochemical and Engineering Aspects, 489 (2016) 207-215.

[2] D. Janssen, R. De Palma, S. Verlaak, P. Heremans, W. Dehaen, Static solvent contact angle measurements, surface free energy and wettability determination of various self-assembled monolayers on silicon dioxide, Thin Solid Films, 515-4 (2006) 1433-1438.

[3] E. Chibowski, L. Hołysz, On the use of Washburn's equation for contact angle determination, Journal of Adhesion Science and Technology, 11-10 (1997) 1289-1301.

[4] E. Chibowski, L. Holysz, Use of the Washburn equation for surface free energy determination, Langmuir, 8-2 (1992) 710-716.

[5] M. Rudolph, S.C. Chelgani, K. Meier, R. Hartmann, The energy of interactions between bubbles and particles–specific surface free energy distributions and microflotation, in: The 7th International Flotation Conference (Flotation '15), Cape Town, South Africa, 2015.

[6] S.S. Ali, J.Y. Heng, A. Nikolaev, K.E. Waters, Introducing inverse gas chromatography as a method of determining the surface heterogeneity of minerals for flotation, Powder Technology, 249 (2013) 373-377.

[7] F.M. Fowkes, Attractive forces at interfaces, Industrial & Engineering Chemistry, 56-12 (1964) 40-52.

[8] D.K. Owens, R. Wendt, Estimation of the surface free energy of polymers, Journal of Applied Polymer Science, 13-8 (1969) 1741-1747.

[9] J. Schultz, M. Nardin, Theories and mechanisms of adhesion, in: A. Pizzi, K.L. Mittal (Eds.) Handbook of Adhesive Technology, Revised and Expanded, Marcel Dekker, Inc., New York, USA, 2003.

[10] A.P. Chandra, L. Puskar, D.J. Simpson, A.R. Gerson, Copper and xanthate adsorption onto pyrite surfaces: Implications for mineral separation through flotation, International Journal of Mineral Processing, 114 (2012) 16-26.

[11] T.K. Dichmann, J. Finch, The role of copper ions in sphalerite-pyrite flotation selectivity, Minerals Engineering, 14-2 (2001) 217-225.

[12] T. Khmeleva, D.A. Beattie, T. Georgiev, W.M. Skinner, Surface study of the effect of sulphite ions on copper-activated pyrite pre-treated with xanthate, Minerals Engineering, 16-7 (2003) 601-608.

[13] T. Khmeleva, W. Skinner, D.A. Beattie, T. Georgiev, The effect of sulphite on the xanthate-induced flotation of copper-activated pyrite, Physicochemical Problems of Mineral Processing, 36 (2002) 185-195.

[14] C. O'Connor, C. Botha, M. Walls, R. Dunne, The role of copper sulphate in pyrite flotation, Minerals Engineering, 1-3 (1988) 203-212.

[15] A. Naveau, F. Monteil-Rivera, E. Guillon, J. Dumonceau, XPS and XAS studies of copper(II) sorbed onto a synthetic pyrite surface, Journal of Colloid and Interface Science, 303-1 (2006) 25-31.

[16] A. Chandra, A. Gerson, A review of the fundamental studies of the copper activation mechanisms for selective flotation of the sulfide minerals, sphalerite and pyrite, Advances in Colloid and Interface Science, 145-1 (2009) 97-110.

[17] A. Zouboulis, K. Kydros, K. Matis, Adsorbing flotation of copper hydroxo precipitates by pyrite fines, Separation Science and Technology, 27-15 (1992) 2143-2155.

[18] S. Voigt, R. Szargan, E. Suoninen, Interaction of copper(II) ions with pyrite and its influence on ethyl xanthate adsorption, Surface and Interface Analysis, 21-8 (1994) 526-536.

[19] K. Laajalehto, J. Leppinen, I. Kartio, T. Laiho, XPS and FTIR study of the influence of electrode potential on activation of pyrite by copper or lead, Colloids and Surfaces A: Physicochemical and Engineering Aspects, 154-1 (1999) 193-199.

[20] E. Pecina, A. Uribe, F. Nava, J. Finch, The role of copper and lead in the activation of pyrite in xanthate and non-xanthate systems, Minerals Engineering, 19-2 (2006) 172-179.

[21] E.T. Pecina, E. Orrantia, A. Uribe, Impact of copper and lead on the activation of pyrite in the presence of thiol collectors, International Journal of Materials and Product Technology, 27-1 (2006) 116-123.

[22] S. He, D. Fornasiero, W. Skinner, Correlation between copper-activated pyrite flotation and surface species: Effect of pulp oxidation potential, Minerals Engineering, 18-12 (2005) 1208-1213.

[23] C. Hicyilmaz, N. Emre Altun, Z. Ekmekci, G. Gokagac, Quantifying hydrophobicity of pyrite after copper activation and DTPI addition under electrochemically controlled conditions, Minerals Engineering, 17-7 (2004) 879-890.

[24] C.A. Prestidge, W.M. Skinner, J. Ralston, R.S.C. Smart, Copper(II) activation and cyanide deactivation of zinc sulphide under mildly alkaline conditions, Applied Surface Science, 108-3 (1997) 333-344.

[25] G. Fairthorne, D. Fornasiero, J. Ralston, Effect of oxidation on the collectorless flotation of chalcopyrite, International Journal of Mineral Processing, 49-1-2 (1997) 31-48.

[26] C. Weisener, A. Gerson, An investigation of the Cu(II) adsorption mechanism on pyrite by ARXPS and SIMS, Minerals Engineering, 13-13 (2000) 1329-1340.

[27] R. Szargan, S. Karthe, E. Suoninen, XPS studies of xanthate adsorption on pyrite, Applied Surface Science, 55-4 (1992) 227-232.

[28] M. Deng, D. Karpuzov, Q. Liu, Z. Xu, Cryo-XPS study of xanthate adsorption on pyrite, Surface and Interface Analysis, 45-4 (2013) 805-810.

[29] C. Weisener, A. Gerson, Cu(II)adsorption mechanism on pyrite: an XAFS and XPS study, Surface and Interface Analysis, 30-1 (2000) 454-458.

[30] A. Boulton, D. Fornasiero, J. Ralston, Characterisation of sphalerite and pyrite flotation samples by XPS and ToF-SIMS, International Journal of Mineral Processing, 70-1 (2003) 205-219.

[31] I. Kartio, K. Laajalehto, E. Suoninen, S. Karthe, R. Szargan, Technique for XPS measurements of volatile adsorbed layers: application to studies of sulphide flotation, Surface and Interface Analysis, 18-12 (1992) 807-810.

[32] R.S. Smart, J. Amarantidis, W.M. Skinner, C.A. Prestidge, L. La Vanier, S.R. Grano, Surface analytical studies of oxidation and collector adsorption in sulfide mineral flotation, Scanning Microscopy, 12-4 (1998) 553-583.

CHAPTER 6

INVERSE GAS CHROMATOGRAPHY FOR BENCH SCALE FLOTATION OF SULPHIDE ORE

Abstract

Inverse gas chromatography (IGC) is receiving increasing attention due to its high precision and ease of application to determining various characteristics of a wide variety of materials of different shapes and morphologies. This Chapter details an experimental investigation into of the application of the IGC technique to the flotation of sulphide minerals. It follows on from the single mineral analyses detailed in Chapters 4 and 5 by analysing an ore. Rather than giving the surface energy, the trends associated with the various concentrates and tailings are described. Bench scale flotation experiments of a nickel-copper sulphide ore were conducted in a Denver flotation cell. The concentrates were collected at different times, and the recovery as a function of time was determined by inductively coupled plasma spectroscopy (ICP). The IGC analyses were carried out on the timed concentrates, as well as the final tailings, in order to evaluate the correlation between surface energetics and flotation response of the ore particles. The results indicated that the floatability of sulphide minerals was directly related to the surface energy of the particles. Both dispersive and specific components of surface free energy increased by increasing the necessary time for the particles to be floated, which was consistent with the obtained values for the work of adhesion to water. The significance of particle size and its consequences in surface energy-flotation response relationship was also observed.

6.1. Introduction

Sulphide ores are important sources for various precious metals, most importantly gold, silver and platinum. They also contain industrially valuable base metals as sulphides, such as copper (chalcopyrite, $CuFeS_2$), lead (galena, PbS) and zinc (sphalerite, ZnS). Pentlandite ($(Fe, Ni, Co)_9S_8$) [1, 2] and molybdenite (MoS_2) are the most important nickel and molybdenum sulphide minerals, respectively [3]. Chalcopyrite, with chemical composition of $CuFeS_2$ can be found in most sulphide ore deposits. Although its copper content is not as much as other copper bearing minerals such as cuprite (Cu_2O) and chalcocite (Cu_2S), it has been the principal source of copper for thousands of years due to its wide distribution in large quantities [3]. Non valuable sulphide minerals such as pyrite (FeS_2) and pyrrhotite ($Fe_{(1-x)}S$ where $x = 0\text{-}0.2$) are considered as gangue sulphides. The ore deposits can also be associated with non-sulphide gangue, such as feldspar ((K, Na, Ca)(SiAl)4O8 with a Si/Al ratio 1 to 3), quartz (SiO_2), magnetite (Fe_3O_4), albite ($NaAlSi_3O_8$), anorthite ($CaAl_2Si_2O_8$), cordierite ($(Mg, Fe)_2Al_3(Si_5AlO_{18})$), dolomite ($Ca, Mg(CO_3)_2$), rhodonite ($(Mn, Ca, Fe, Mg)SiO_3$), calcite ($CaCO_3$), talc ($Mg_3Si_4O_{10}(OH)_2$) and chromite ($(Fe, Mg, Al)Cr_2O_4$) [4-9]. The most common method of sulphide ore concentration is froth flotation.

In order to achieve an efficient separation of minerals through flotation, the surfaces of the desired minerals must be altered to obtain the necessary hydrophobicity, which leads to a strong bubble-particle interaction. In order to render the mineral hydrophobic, reagents called collectors are added. Depressants may be added in order to reduce the hydrophobic nature of unwanted minerals. The development of sulphide flotation over many years has shown that sulphide mineral wettability is affected by various factors, such as surface treatment conditions, pH, electrochemical potential, chemical alteration of the surface in the pulp, galvanic interactions between different sulphide minerals, the presence of other particles and grinding by-products and wide range of particle sizes [10, 11]. In addition, sulphide minerals are highly prone to surface oxidation, which can result in both hydrophobic surfaces (rich in sulphur) and hydrophilic surfaces (rich in oxide/hydroxide). Therefore, the relative proportion of these species on the chemically altered surface is a key factor in flotation [11-13]. Brito e Abreu & Skinner [12] showed that the hydrophobizing effect of a collector on the coarser particles can be different from fine and intermediate sizes, resulting in a heterogeneity in hydrophobicity. Also, due to hydrodynamic effects, the contact angle threshold for being recovered was higher for the fine and coarse particles than the intermediate sizes. Depending on the collector concentration, hydrophobicity may or may not overcome the hydrodynamic effects of the particle size [12].

Inverse gas chromatography (IGC) is a well-established characterisation technique for research into the physicochemical properties of materials such as surface energy. Surface energy, which can be accurately measured by using IGC, describes the affinity of materials to water, or other solvents, which is directly related to the flotation behaviour. The correlation between surface energy and floatability of pure minerals has been evaluated, and it has been suggested the particles with lower surface energy have more tendencies to attach to air bubbles and hence, they are more hydrophobic than the particles with more energetic surfaces [14, 15].

Following previous studies that confirmed the capability of inverse gas chromatography (IGC) for determining the surface energetics of pure minerals (Chapters 4 & 5), in this chapter, a nickel-copper sulphide ore was examined. The concentrates and tailings from bench scale flotation tests were characterised in order to evaluate the relationship between surface characteristics and flotation behaviour.

6.2. Methodology

6.2.1. Materials

The nickel-copper sulphide ore was obtained from Vale's Discovery Hill ore body (Voisey's Bay mine, Newfoundland & Labrador, Canada). The ore was crushed in Marcy jaw crusher (Svedala Industries, Inc., USA), ground in a laboratory disc vibrating mill (T100 Siebetechnik, Germany) sieved using a Ro-Tap Sieve Shaker (Tyler, USA), and a -106 µm size fraction was collected for this study. Potassium amyl xanthate (PAX) was obtained from Prospect Chemicals (Canada). The xanthate compound was purified by dissolving in acetone, recrystallizing by petroleum ether and filtering out the precipitation. The purified PAX was stored under ethylene ether. The alkanes used in the surface energy experiments were decane, nonane, octane and heptane, and the polar probe molecules were toluene and dichloromethane. All chemicals used were of HPLC grade (>99.5% purity), purchased from Sigma–Aldrich (USA).

6.2.2. Experimental

6.2.2.1. Flotation

Flotation was conducted in a 1.2 L Denver flotation cell with an impeller rotation speed of 1200 rpm. For each test, a 33% (solids by mass) pulp was prepared by adding 1 L of tap water to 500 g of the sulphide ore. The pH of water was adjusted to 9.5 using calcium hydroxide ($Ca\ (OH)_2$) prior to the test. Aeration (3 L min^{-1}) was conducted for 15 minutes in order to oxidise and depress pyrrhotite. Potassium amyl xanthate (PAX) was added (140 g t^{-1}) as the collector and conditioned for 2 min. As the frother, 3 drops of Dowfroth 250C was used and the pulp was conditioned for 1 more minute. Air was introduced and kept at a constant flow rate of 3 L min^{-1}. The concentrates were collected for 0.5, 1, 2 and 4 minutes (for a total of 7.5 min) of flotation; hereafter called C1, C2, C3 and C4, respectively. Tap water and lime were used throughout the experiments as required to keep the pulp level and pH constant (pH 9.5) as the concentrate overflowed. The concentrate and tailings fractions were filtered and dried in an oven to at 80 °C, then weighed, homogenised and sampled for characterisation analyses. The flotation experiments repeated 5 times (series A to E).

6.2.2.2. Particle Size Analysis

In order to investigate the influence of particle size on the surface free energy flotation response of sulphide ore components, the feed, concentrates and tailings were split into size fractions of -38 µm, -75 +38 µm, and -106 +75 µm. These were obtained by wet screening at 38 µm, followed by dry screening.

6.2.2.3. Inductively Coupled Plasma Spectroscopy

Inductively coupled plasma atomic emission spectroscopy (ICP-AES) was used to determine the element content in the samples. The analyses were conducted using a Thermo Scientific iCAP 6000 series ICP Spectrometer (USA). The samples were prepared by dissolving approximately 0.1 g of finely ground minerals in a mixture of hydrochloric acid and nitric acid in a molar ration of 3/1 (aqua regia). Due to difficulties in digesting silicate minerals, in order to determine the silicon (Si) contents, another series of samples were dissolved in hydrofluoric acid (HF) first, and then in aqua regia. Then the samples were heated up to 95 °C for 2 hrs. For the major elements, 1% diluted solutions were also prepared by adding 4% (v/v) nitric acid. Both concentrated and diluted samples were analysed by ICP-AES.

6.2.2.4. Powder X-Ray Diffraction

To identify and characterise mineral constituents, powder X-ray diffraction (PXRD) analyses were conducted on the finely ground samples using a Bruker D8 Discovery X-Ray Diffractometer (USA), equipped with a Co-tube as the X-ray radiation source ($\lambda = 1.79$ Å)

6.2.2.5. Inverse Gas Chromatography

IGC experiments were conducted using a Surface Energy Analyser, SEA (Surface Measurement System Ltd., UK). The samples were packed in IGC columns which were 30 cm presilanised glass tubes with an outer diameter of 6 mm and an inner diameter of 4 mm. Helium and methane were used as carrier gas and dead volume corrector, respectively at a flow rate of 10 mL min^{-1}. All measurements were carried out at 30 °C and 0% RH. The columns were preconditioned with the carrier gas at 30 °C for 30 min prior the analyses to remove any physisorbed water. The experiments were run a minimum of three times for each sample. The data were analysed using the Cirrus Plus Analysis Software (Surface Measurements System Ltd., UK). The retention time from the peak maximum was used to calculate the retention volume and to determine the surface energies, Schultz method was employed for the dispersive components, and the specific components were obtained using the Della Volpe scale at 5% surface coverage.

6.3. Results and Discussion

6.3.1. Flotation

The mass recovery curves, constructed from the information collected during five flotation experiments (series A to E) are presented in Figure 6.1. The data confirms a good reproducibility of the experiments and indicates a fairly similar mass recovery in each floated product (7.6% in C1, 7.3% in C2, 10.0% in C3 and 11.5% in C4).

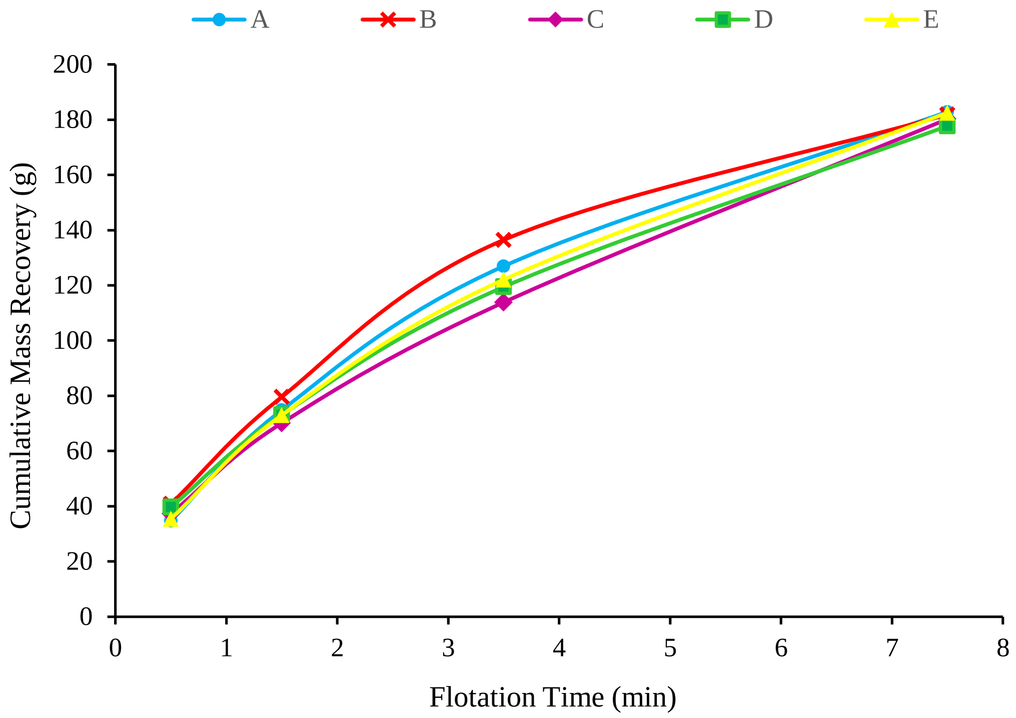

Figure 6.1. Cumulative mass recovery as a function of flotation time.

6.3.2. Inductively Coupled Plasma Spectroscopy (ICP)

The results of the ICP analyses are summarised in Table 6.1, from which the grade-recovery curve (Figure 6.2.a) and kinetics graph (Figure 6.2.b) for copper and nickel were generated based on the mass recovery of flotation. The results are consistent with previous flotation studies conducted with the Voisey's Bay ore [1], showing faster kinetics for the flotation of chalcopyrite than that of pentlandite. Figure 6.2.b shows the recovery of copper and nickel as a function of time. The elemental content indicates that flotation was more selective towards the copper mineral (chalcopyrite), which has the highest content in concentrate C1. Iron and nickel are found at higher concentrations in the final products, which is in agreement with the low kinetics of nickel indicated by the flotation kinetics. The silicate bearing elements (Al, Mg and Ca), along with Si, are found mostly in the tailings, which is consistent with the expected silicate minerals' hydrophilicity and the collection mechanism of PAX [3].

Table 6.1. Elemental composition (Wt%) of the samples.

Samples	**Fe**	**S**	**Si**	**Al**	**Mg**	**Ni**	**Cu**	**Ca**	**Co**
Feed	24.95	14.33	12.55	2.13	2.04	1.51	1.20	0.93	0.06
C1	37.13	27.30	5.05	0.98	1.16	2.46	9.33	0.58	0.11
C2	37.78	25.45	6.00	1.18	1.43	2.94	4.03	0.59	0.13
C3	41.43	25.51	5.14	1.15	1.25	3.10	1.14	0.65	0.17
C4	42.11	26.64	5.28	1.22	1.17	2.78	0.36	0.62	0.12
Tailings	17.55	6.49	16.16	2.62	2.40	0.62	0.09	1.21	0.03

C1, C2, C3 and C4 refer to concentrates collected for 0.5, 1, 2 and 4 min, respectively.

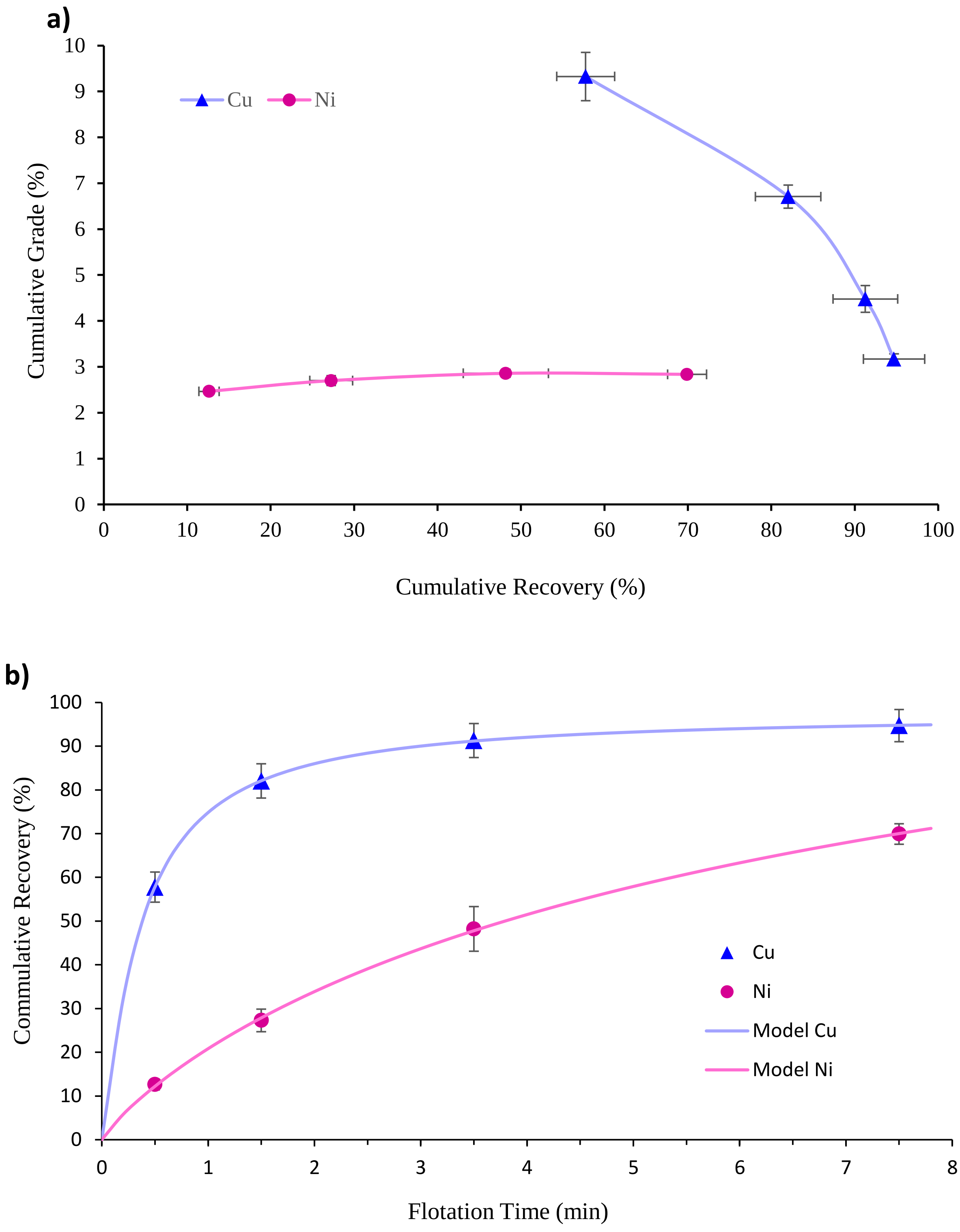

Figure 6.2. The grade-recovery (a) and kinetic (b) curves for copper and nickel. Error bars represent 95% confidence interval.

6.3.3. Powder X-Ray Diffraction (PXRD)

The powder X-ray diffraction patterns for the sulphide ore, timed concentrates and tailings from the flotation test are shown in Figure 6.3. The diffractograms corresponds to multiple phases, confirming the presence of multiple minerals in the ore: albite/anorthite, pyrrhotite, pentlandite, chalcopyrite, forsterite, magnetite and cordierite. The peaks are normalised and the relative intensities reflect the relative content of minerals in the patterns of different samples. Four characteristic peaks of chalcopyrite revealed that a high portion of chalcopyrite floated during the first minute, and most of the pyrrhotite started to float after 1 min, indicating the more hydrophobic surface for these two minerals relative to the other exposed species. Chalcopyrite was not detected in the concentrate after 4 min flotation, neither in the tailings. This was confirmed by Cu content values from ICP analysis (Table 6.1). Pentlandite was floated, but evenly throughout the flotation experiments. The Ni grade-recovery curve (Figure 6.2.a) suggests the same conclusion. There was no detectable amount of magnetite in the first three concentrates. Minor amounts were observed in the concentrate after 4 min flotation, with it mostly reporting to the tailings. Meanwhile, albite/anorthite reported almost exclusively to the tailings.

6.3.4. Particle Size Analysis

The fraction size percentages of the feed, concentrates and tailings are summarised in Table 6.2. Approximately 50% of the feed contained particles finer than 38 μm, and twice as much the medium size as coarser particles. The tailings showed approximately the same relative percentages. Compared to the concentrates, the tailings had a much higher percentage of the coarser particles and a lower content of fine material.

Table 6.2. The fraction size of the feed and flotation products.

Size Fraction (μm)	**Mass%**					
	Feed	**C1**	**C2**	**C3**	**C4**	**Tailings**
-106 +75	14.1	5.3	2.8	4.1	7.4	16.6
-75 +38	31.6	26.0	19.5	21.3	29.4	35.2
-38	54.2	68.7	77.7	74.6	63.2	48.1

C1, C2, C3 and C4 refer to concentrates collected for 0.5, 1, 2 and 4 min, respectively.

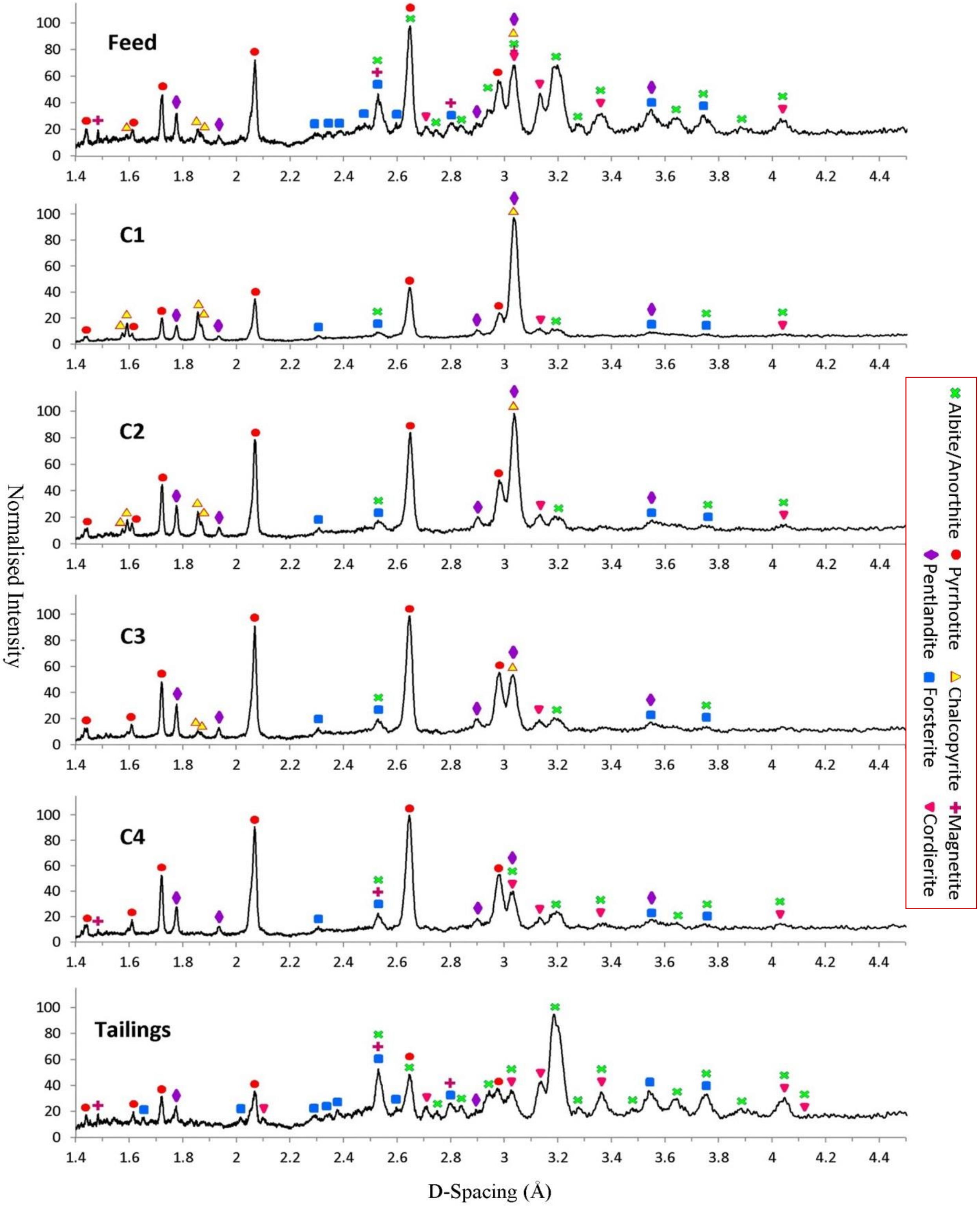

Figure 6.3. The PXRD patterns for the sulfide ore, timed concentrates and tailings. C1, C2, C3 and C4 refer to concentrates collected for 0.5, 1, 2 and 4 min, respectively.

6.3.5. Inverse Gas Chromatography (IGC)

The plot of the total surface energy for the concentrates and tailings obtained from IGC experiments are depicted in Figure 6.4. It can be observed that the total surface energy of the all concentrates was directly correlated to the time of collection. The first floating materials, which were expected to contain the most hydrophobic species, showed the lowest surface energy. As the collection time increased, the surface energy of the concentrates increased, indicating the particles with higher surface energy had fewer tendencies to float. Accordingly, the tailings were expected to show the highest surface energy among all samples since their particles did not float at all and stayed in the liquid phase. However, as can be seen in Figure 6.4, the surface energy value for the tailings decreased significantly. Moreover, it can be seen from this diagram that both dispersive (solid bars) and specific (shaded bars) contributions to the total surface energy showed the same trend as the total surface energy, meaning the decrease in surface energy for the tailings is due to a decrease in both dispersive and specific components of surface free energy.

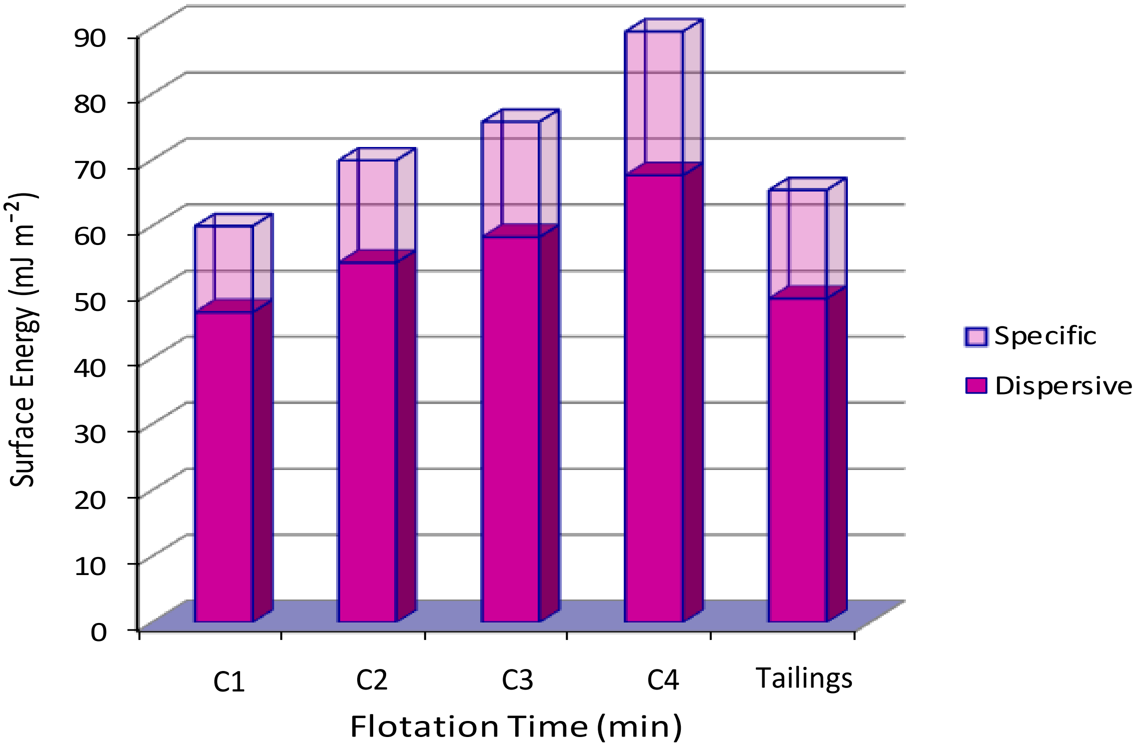

Figure 6.4. The plot of the dispersive (solid) and specific (shaded) contributions to the total surface energy of the timed concentrates and tailings.

The work of adhesion (W_{adh}) values, which also obtained from IGC measurements, supported the results from surface energy values (Figure 6.5). The W_{adh} to water is a measure of hydrophobicity and it was observed that the first floated species had lower W_{adh}, showing less affinity to water. The less hydrophobic species which floated later had higher W_{adh} values. However, for the tailings, which were expected to contain the most hydrophilic components of the sulphide ore, the W_{adh} decreased significantly, similar to the trend observed in the case of surface energy.

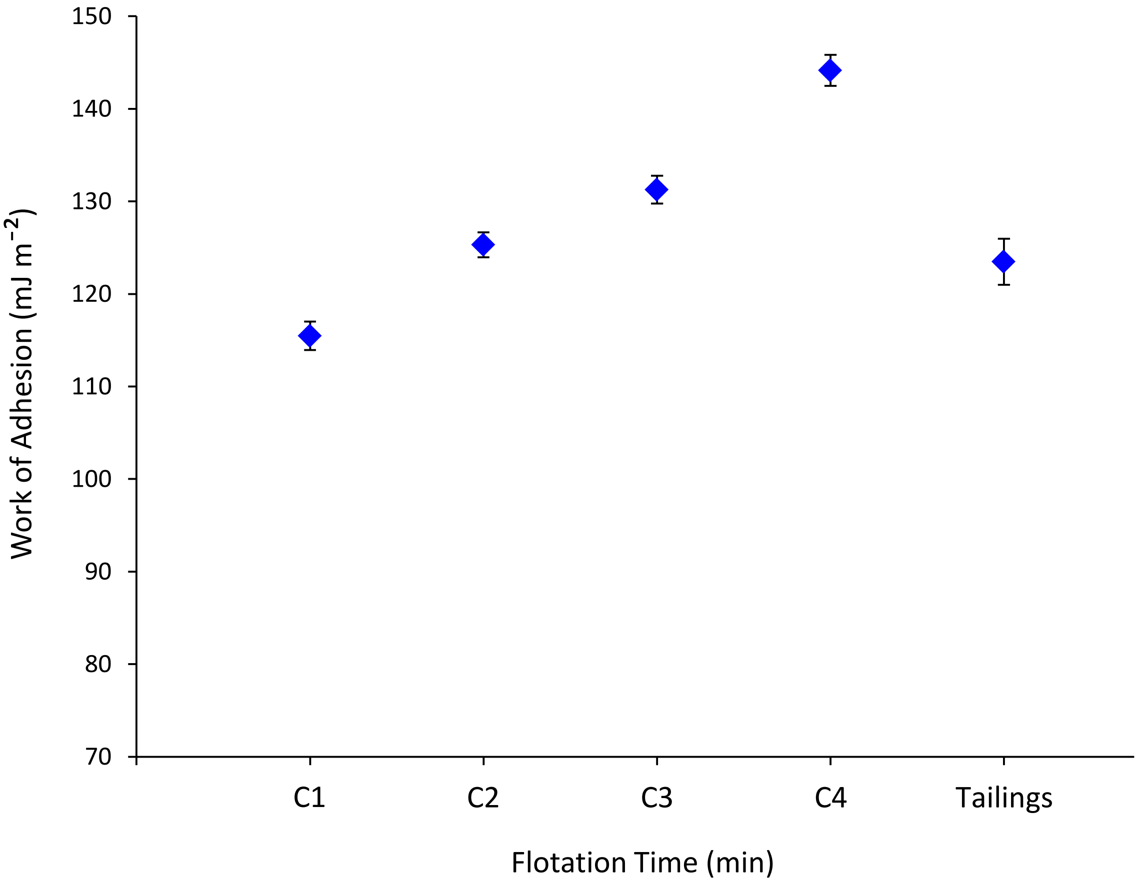

Figure 6.5. The plot of the work of adhesion (W_{adh}) of the timed concentrates and tailings. Error bars represent 95% confidence interval.

As was seen in the results of size analysis (Table 6.2), the concentrates and tailings contained different size distribution. Regarding the particle size effects on flotation recovery, which was discussed in the introduction of this chapter, different size fractions require different hydrophobicity threshold to be floated. Also, the broad distribution of surface energies makes the interpretation of the flotation behaviour and its correlation to the surface energetics complicated. This can be an explanation for the discrepancy of the lower surface energy of the tailings despite a higher wettability. In addition, residual reagents such as the xanthate collector may have remained in the tailings sample tested, thus giving a reading of “free” xanthate.

6.4. Conclusions

The applicability of surface free energy measurements to flotation process of sulphide minerals was considered in some detail. The feed, concentrates and tailings obtained from the flotation of a sulphide ore in a Denver cell were characterised using different analytical techniques. The XRD patterns of the samples confirmed the first concentrates contained more hydrophobic minerals, and the more hydrophilic species floated later or did not float at all. The surface free energy analyses of the samples revealed that the particles floated earlier showed lower values of surface energy than the particles with less floatability. As the flotation time increased, the particle surfaces were showed to be more energetic. In addition, the values of the work of adhesion to water, as a measure of hydrophobicity, was also calculated by IGC, were consistent and increased with flotation time of the concentrates. Therefore, the flotation separation of sulphide minerals is highly controlled by the relative hydrophobicity of mineral particles in a pulp, and the difference in floatability time is correlated to the difference in the surface free energy of particles. The surface free energy and work of adhesion for tailings, however, decreased to a level less than some concentrates. This is attributed to the coarser contents of the tailings since the surface free energy value is controlled by the size of the particles as well. However, this is not a genuinely independent correlation, and the particle size effect cannot be separated from the other effects such as morphology and crystal habits over the surface free energy. This observation brings new insight to the interpretation of the flotation response of the species of a natural ore in which the observed behaviour can be due to overlapping important parameters, as well as more questions to be answered in future studies.

References

[1] C. Marion, A. Jordens, C. Maloney, R. Langlois, K.E. Waters, Effect of microwave radiation on the processing of a Cu-Ni sulphide ore, The Canadian Journal of Chemical Engineering, 94-1 (2016) 117-127.

[2] A. Buckley, R. Woods, Surface composition of pentlandite under flotation-related conditions, Surface and Interface Analysis, 17-9 (1991) 675-680.

[3] B.A. Wills, J.A. Finch, Wills' Mineral Processing Technology: An Introduction to the Practical Aspects of Ore Treatment and Mineral Recovery, 8th ed., Butterworth-Heinemann, 2015.

[4] A. Lynch, The behaviour of minerals in sulphide flotation processes, with reference to simulation and control, Journal of the South African Institute of Mining and Metallurgy, 74 (1974) 349-361.

[5] S. Chehreh Chelgani, B. Hart, TOF-SIMS studies of surface chemistry of minerals subjected to flotation separation–A review, Minerals Engineering, 57 (2014) 1-11.

[6] T. Barrett, S. Cattalani, W. MacLean, Volcanic lithogeochemistry and alteration at the Delbridge massive sulfide deposit, Noranda, Quebec, Journal of Geochemical Exploration, 48-2 (1993) 135-173.

[7] J. Miller, N.A. Khalek, C. Basilio, H. Shall, K. Fa, K. Forssberg, M. Fuerstenau, S. Mathur, J. Nalaskowski, K. Rao, Flotation chemistry and technology of nonsulfide minerals, in: M. Fuerstenau, G. Jameson, RH Yoon (Eds.) Froth Flotation: A Century of Innovation, SME, New York, 2007, pp. 465-466.

[8] H. Wolter, F. Seifert, Mineralogy and genesis of cordierite-anthophyllite rocks from the sulfide deposit of Falun, Sweden, Lithos, 17 (1984) 147-152.

[9] I.R. Morrison, Geology of the Izok massive sulfide deposit, Nunavut Territory, Canada, Exploration and Mining Geology, 13-1-4 (2004) 25-36.

[10] C. Prestidge, J. Ralston, Contact angle studies of particulate sulphide minerals, Minerals Engineering, 9-1 (1996) 85-102.

[11] R.S. Smart, J. Amarantidis, W.M. Skinner, C.A. Prestidge, L. La Vanier, S.R. Grano, Surface analytical studies of oxidation and collector adsorption in sulfide mineral flotation, Scanning Microscopy, 12-4 (1998) 553-583.

[12] S. Brito e Abreu, W. Skinner, ToF-SIMS-derived hydrophobicity in DTP flotation of chalcopyrite: Contact angle distributions in flotation streams, International Journal of Mineral Processing, 98-1 (2011) 35-41.

[13] R. Hayes, D. Price, J. Ralston, R. Smith, Collectorless flotation of sulphide minerals, Mineral Procesing and Extractive Metallurgy Review, 2-3 (1987) 203-234.

[14] S.S. Ali, J.Y. Heng, A. Nikolaev, K.E. Waters, Introducing inverse gas chromatography as a method of determining the surface heterogeneity of minerals for flotation, Powder Technology, 249 (2013) 373-377.

[15] M. Rudolph, S.C. Chelgani, K. Meier, R. Hartmann, The energy of interactions between bubbles and particles–specific surface free energy distributions and microflotation, in: The 7th International Flotation Conference (Flotation '15), Cape Town, South Africa, 2015.

CHAPTER 7

CONCLUSIONS

7.1. Conclusions

The main research objective of this dissertation was to determine the surface energetics of minerals using inverse gas chromatography (IGC) and investigate the correlation between the surface energy and flotation behaviour of minerals. This may contribute to transferring the use and application of such measurements from fundamental flotation studies to practical flotation applications as well as enhancing our understanding of the consequences of surface modification upon mineral flotation.

Inverse gas chromatography (IGC), as a new technique in mineral processing, has been successfully applied to characterise the surface physicochemical properties of minerals (quartz and pyrite) and a real ore (nickel-copper sulphide) in detail. It has been demonstrated how the coupling of surface energy analysis and flotation may contribute to a better understanding of flotation behaviour, as well as the elucidation of the consequences of the modification upon the surface properties of minerals.

The main conclusions that can be drawn from the individual studies are:

- The variation of surface energetics of quartz upon treatment with dodecylamine (cationic collector for quartz) was evidenced by IGC. The correlation between surface energetics and the flotation behaviour of the mineral was clearly observed from microflotation experiments. Both dispersive (γ^D) and specific (γ^{SP}) components of surface free energy decreased as the floatability increased upon surface modification with the collector.

- It was shown that the surface of quartz can be inhomogeneous and the adsorption sites on its surface may not be identical, leading to energetically heterogeneous surfaces. This means that there is a notable difference between surface free energy values, and thus a single value for surface free energy is not necessarily representative of the entire surface of a mineral. The surface energetic heterogeneity profile of quartz, provided by IGC, delivered a description of the distribution of adsorption energies on the mineral surfaces, pre- and post-treatment. The accurate measurement of surface free energy at different surface coverages can be used as an energy map of the mineral surface. However, the surface treatment of quartz with the collector resulted in more energetically homogeneous surfaces, as well as decreasing the total surface free energy of the mineral.

- Copper activation of pyrite, and subsequent xanthate adsorption on the activated surfaces under different conditions was examined using IGC and X-ray photoelectron spectroscopy (XPS) methods. The response of the non-activated surface of pyrite to the adsorption of amyl xanthate at different pH values was also studied to give a baseline for comparison. The combination of surface energy from IGC with microflotation tests, indicated that the activation and treatment of pyrite surface altered the surface energetics of pyrite, and the changes were reflected in flotation behaviour. The Cu-activation at pH 7 and following xanthate-treatment at pH 10 generated a sample with the highest flotation recovery among all examined pyrite samples. Through IGC experiments, this sample was observed to have the lowest surface free energy. Generally, the more energetic surfaces showed less flotation recovery. Meanwhile, the work of adhesion to water (W_{adh}) values was in good agreement with flotation recovery. The samples with greater W_{adh}, having more affinity to water, were those with lower flotation recovery.

- Nickel-copper sulphide ore flotation behaviour was studied using a Denver flotation cell. Timed samples of concentrate and tailings were collected and analysed. X-ray diffraction (XRD) analyses indicated that chalcopyrite floated first, then pyrrhotite, and magnetite and Albite/Anorthite almost did not float during 4 minutes. Surface energetic examinations indicated that the surface free energy was the lowest for the first samples, which were collected 30 s of flotation experiments, and then increased for next samples with longer flotation time. This result supports, and may explain the fact that, in practice, the most energetically stable particles floated first and as the particles became energetically more active, their tendencies to float declined. However, both dispersive and specific components surface energy of the tailings decreased significantly, which is tentatively attributed to a higher percentage of coarser particles in tailings relative to the concentrates.

7.2. Contributions to Original Knowledge

This is the first systematic study of the application of IGC technique to mineral flotation. Through studying the surface characteristics of minerals using different methods, the capability of IGC in accurately determining surface energetics of mineral particles was evidenced. The reliability of this method for evaluating the surface wettability was investigated by a comparative study between the work of adhesion to water, obtained from the surface energy analyses, and flotation behaviour of the particles.

The concept of surface energy heterogeneity was investigated using IGC on the surface of minerals. It was shown at different levels of surface coverage, various adsorption sites with different surface energies are involved in the adsorption phenomenon. Therefore, different values of surface energy are obtained at different surface coverages. On the basis of this observation, it was proposed and proved that the surface energy of minerals becomes more homogeneous after the surface treatments.

The present work assembles surface energy information acquired from IGC, as a promising technique, with appropriate flotation data to advance the understanding of flotation mechanisms. This may lead to transferring the IGC applications from fundamental floatability studies to practical implementations such as additional functions in flotation models and simulations, in order to control strategies for improving flotation performance.

7.3. Recommendations for Future Work

While this thesis has demonstrated the potential of predicting flotation behaviour of minerals using the IGC technique, many opportunities for extending the scope of the present work remain. Some interesting directions for further studies include the following:

- The suggested relationship between the surface energy and wettability can be evaluated by the extension of the work to other minerals, as well as evaluating how the adsorption of depressants influences the surface free energy and surface energy heterogeneity of minerals.

- In-depth exploration of the impact of surface treatments on surface energetics; it would be helpful to establish the optimal conditions for surface treatments of minerals using surface energy measurements, and to determine if the same results are obtained from their flotation response.

- Further research could also be conducted to determine the effectiveness of grinding methods, particle size and shape, physical heterogeneities and surface roughness on the surface free energy, measured using IGC.

- It would be a worthwhile endeavour to investigate the effect of more than one determinative parameter on the surface energetics of minerals, simultaneously.

- More methodological work is needed on how to predict flotation recovery, through flotation kinetics in a controlled flotation process, with knowing particle size, bubble size, reagent concentrations, hydrodynamic conditions and surface free energy of the particles.

APPENDIX

The XPS high resolution spectra of O 1s, S 2p and Fe 2p for pyrite samples (Chapter 5).

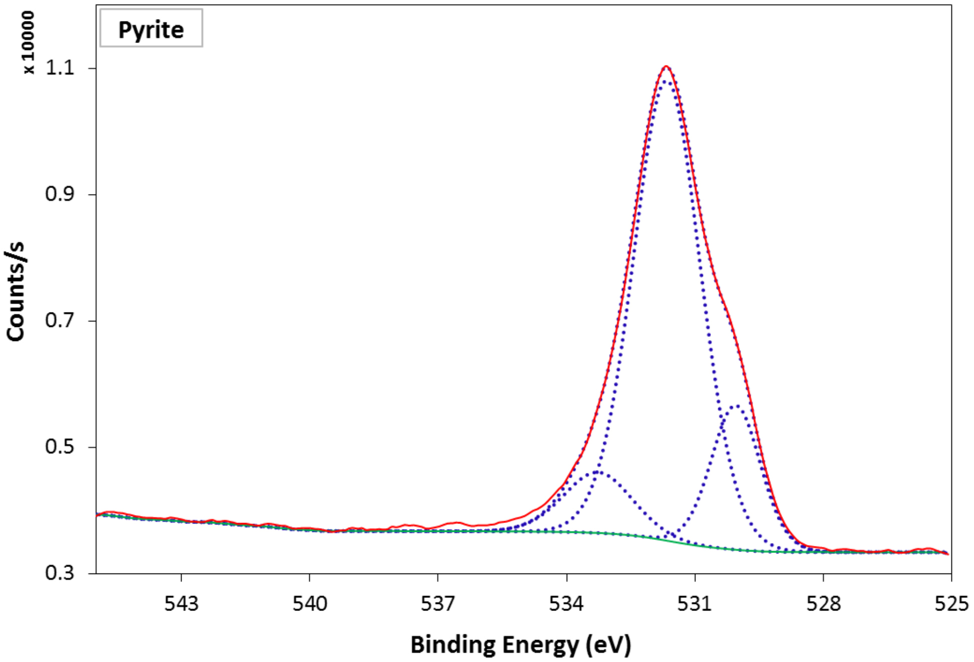

Figure A1. O 1s XPS high resolution spectrum of untreated pyrite.

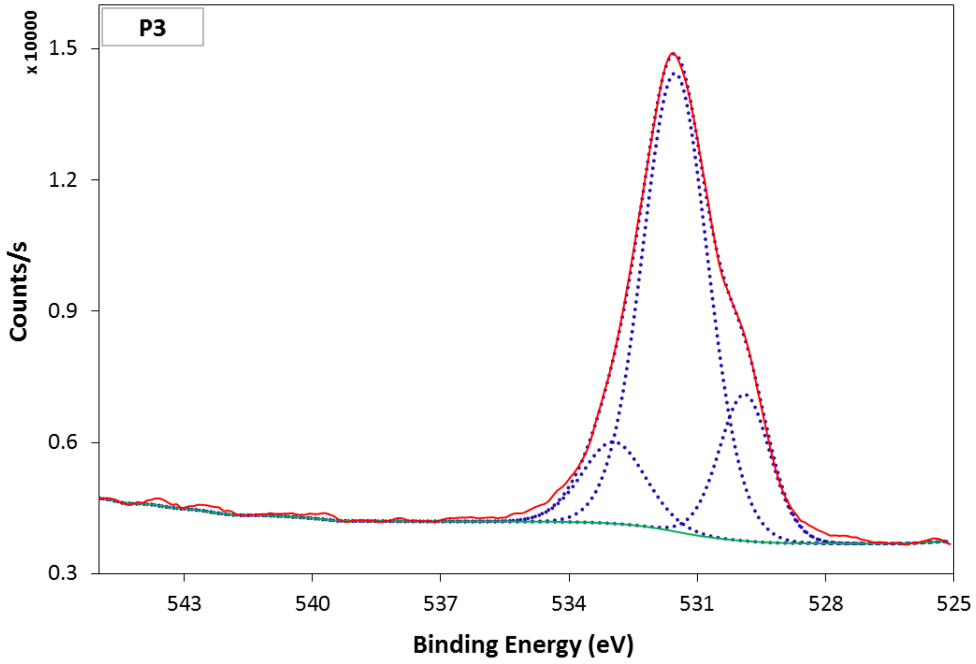

Figure A2. O 1s XPS high resolution spectrum of pyrite, treated in water at pH 3.

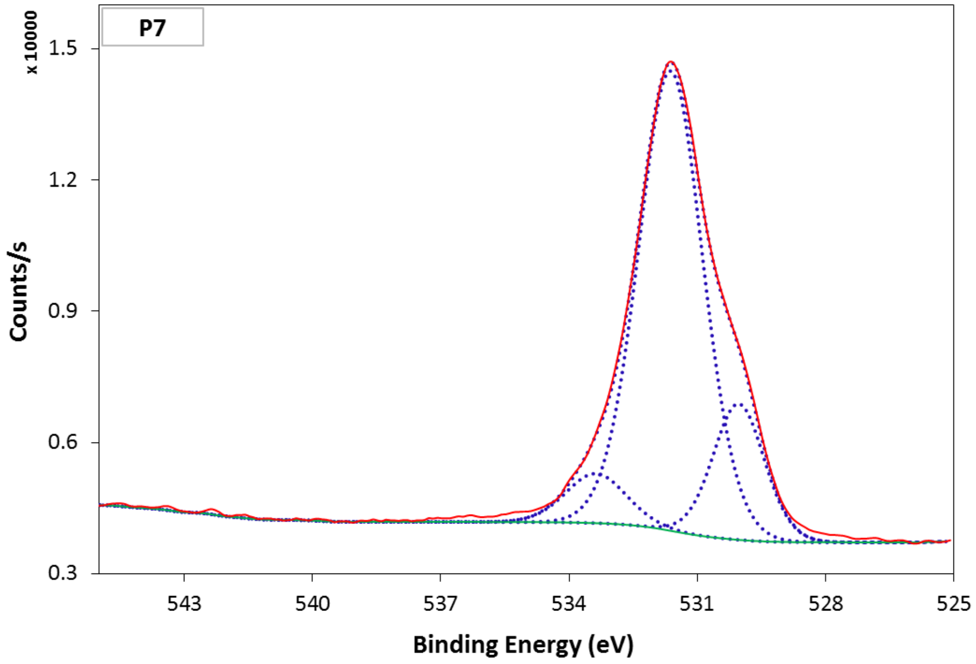

Figure A3. O 1s XPS high resolution spectrum of pyrite, treated in water at pH 7.

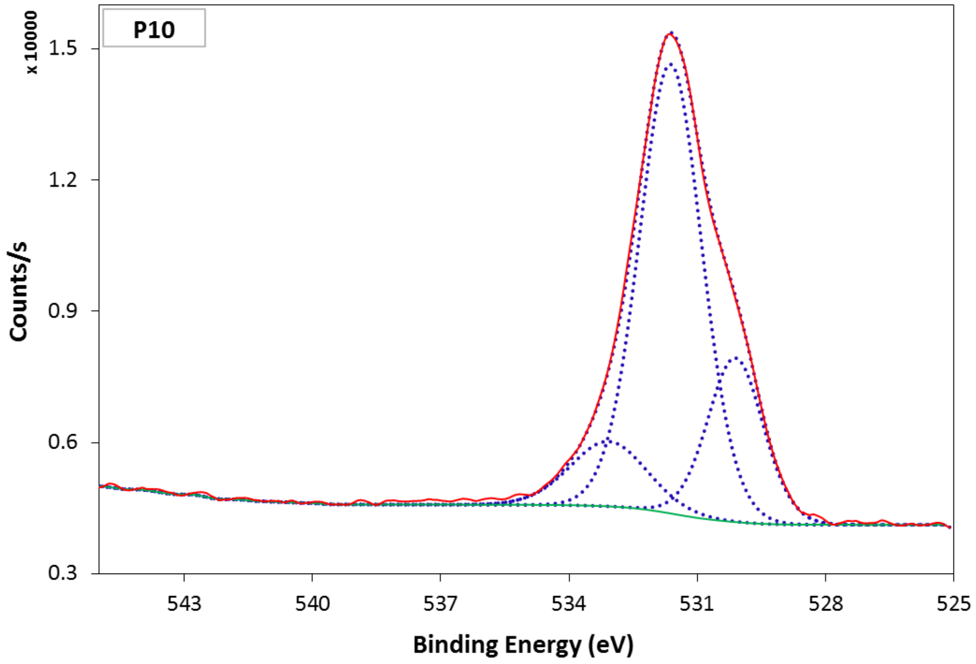

Figure A4. O 1s XPS high resolution spectrum of pyrite, treated in water at pH 10.

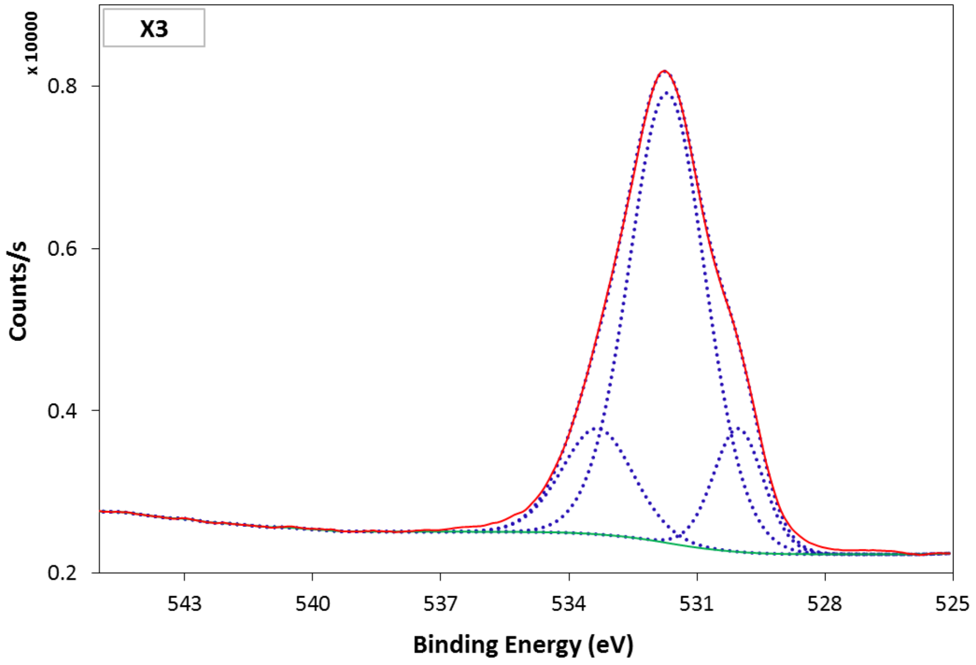

Figure A5. O 1s XPS high resolution spectrum of pyrite, conditioned with xanthate at pH 3.

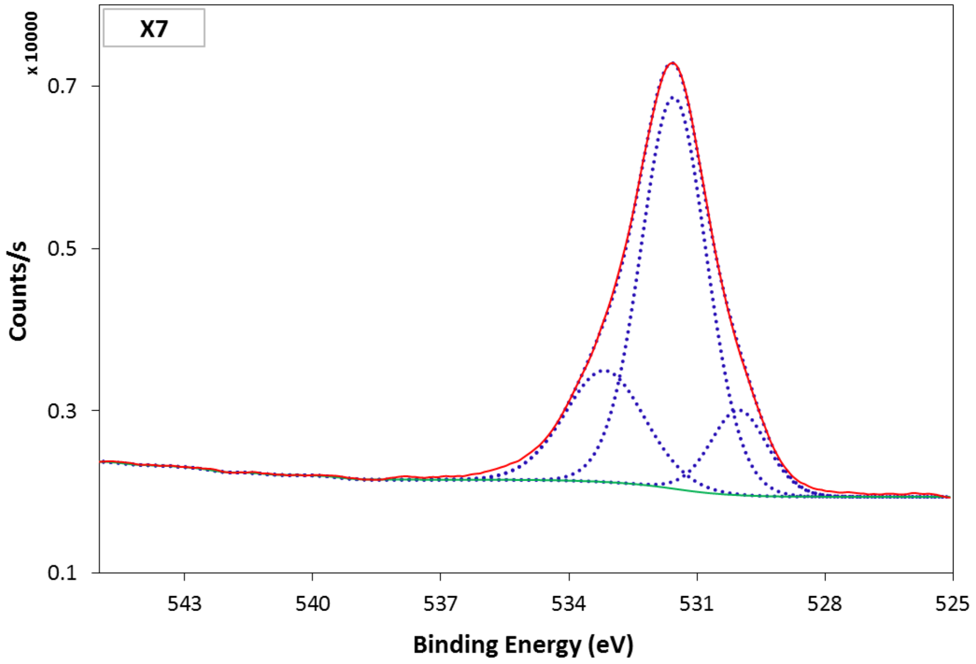

Figure A6. O 1s XPS high resolution spectrum of pyrite, conditioned with xanthate at pH 7.

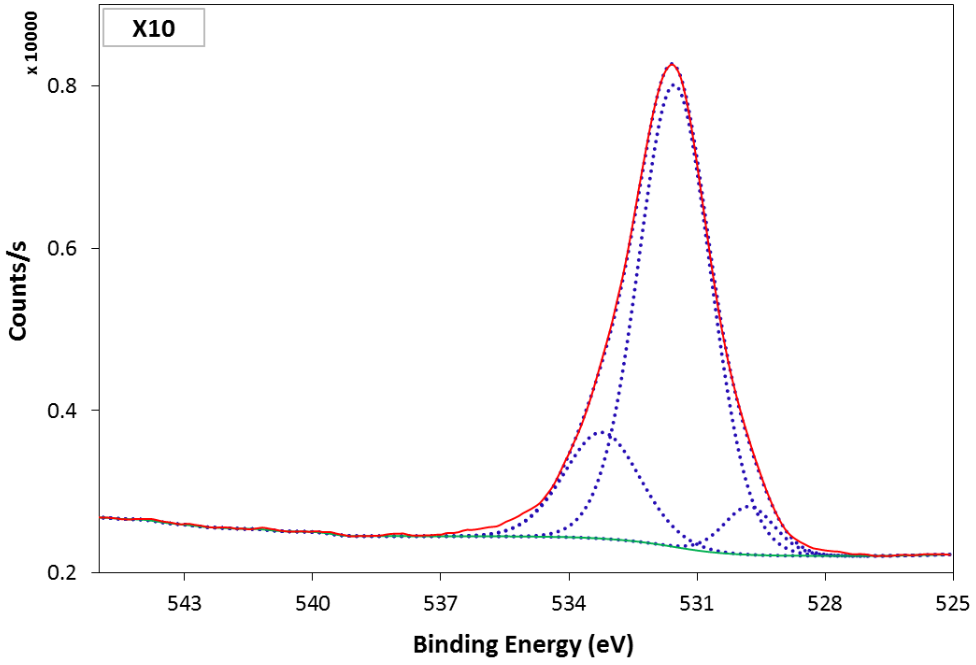

Figure A7. O 1s XPS high resolution spectrum of pyrite, conditioned with xanthate at pH 10.

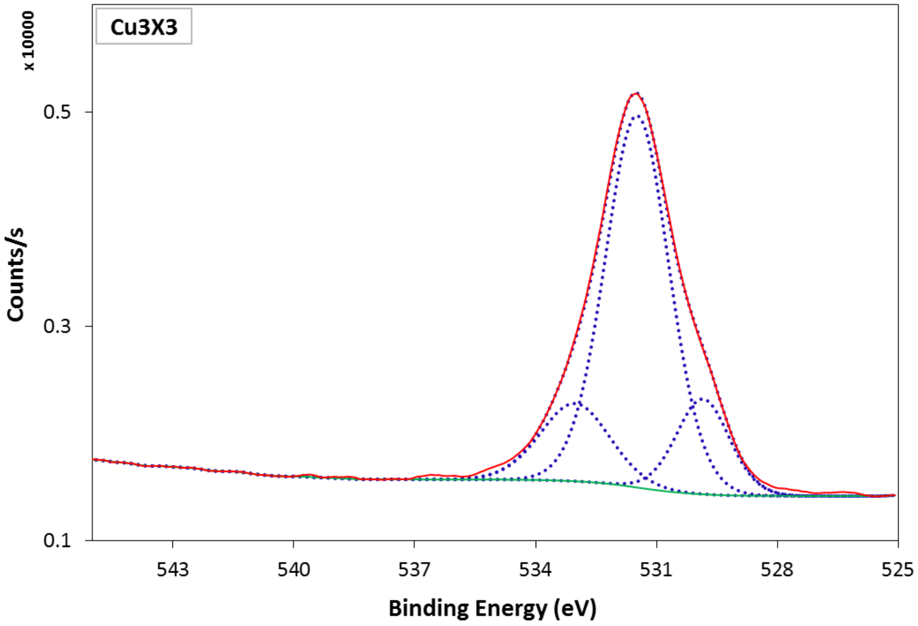

Figure A8. O 1s XPS high resolution spectrum of pyrite, activated with copper and conditioned with xanthate at pH 3.

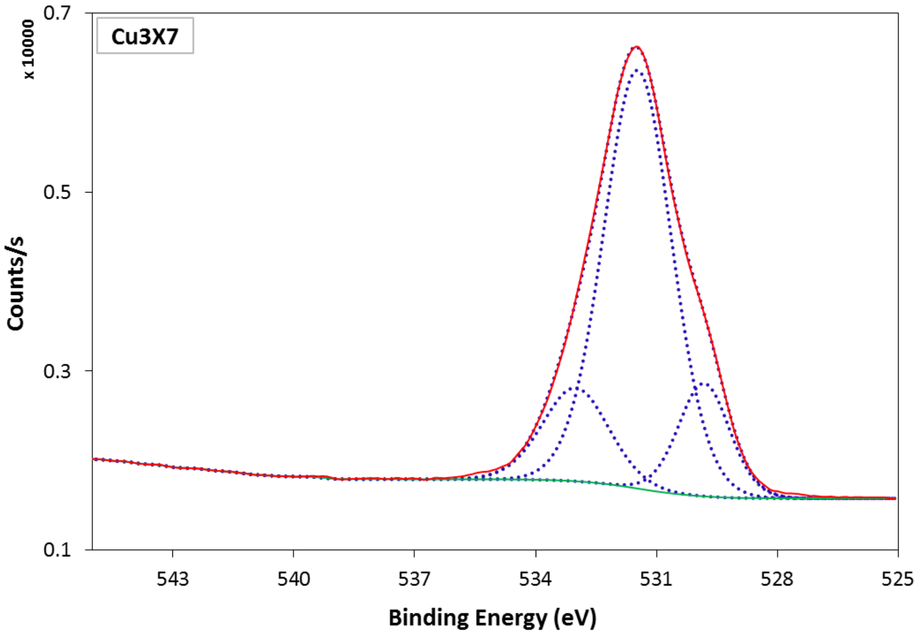

Figure A9. O 1s XPS high resolution spectrum of pyrite, activated with copper at pH 3 and conditioned with xanthate at pH 7.

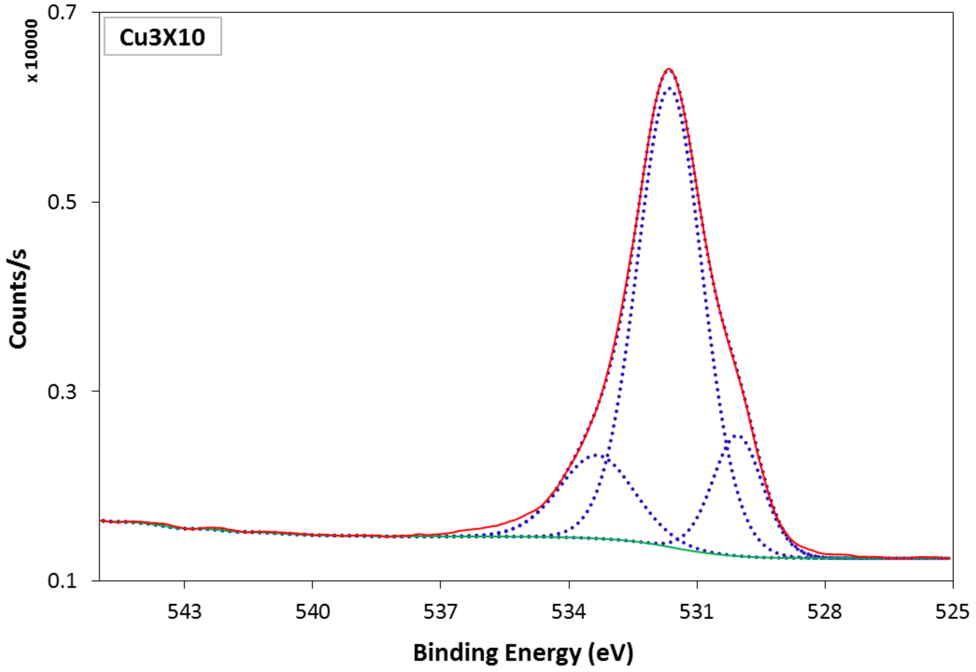

Figure A10. O 1s XPS high resolution spectrum of pyrite, activated with copper at pH 3 and conditioned with xanthate at pH 10.

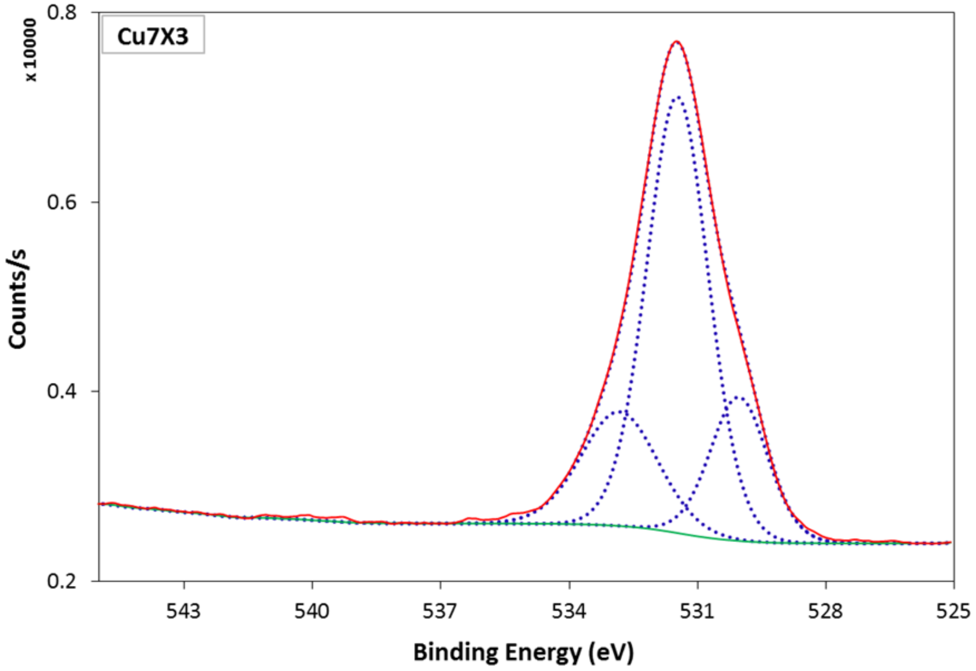

Figure A11. O 1s XPS high resolution spectrum of pyrite, activated with copper at pH 7 and conditioned with xanthate at pH 3.

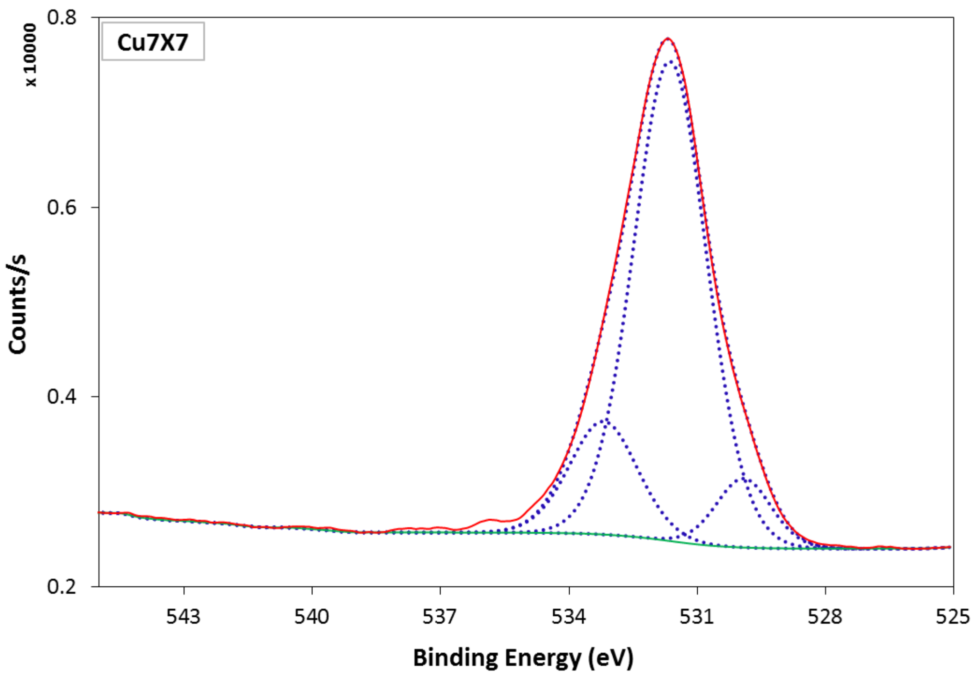

Figure A12. O 1s XPS high resolution spectrum of pyrite, activated with copper and conditioned with xanthate at pH 7.

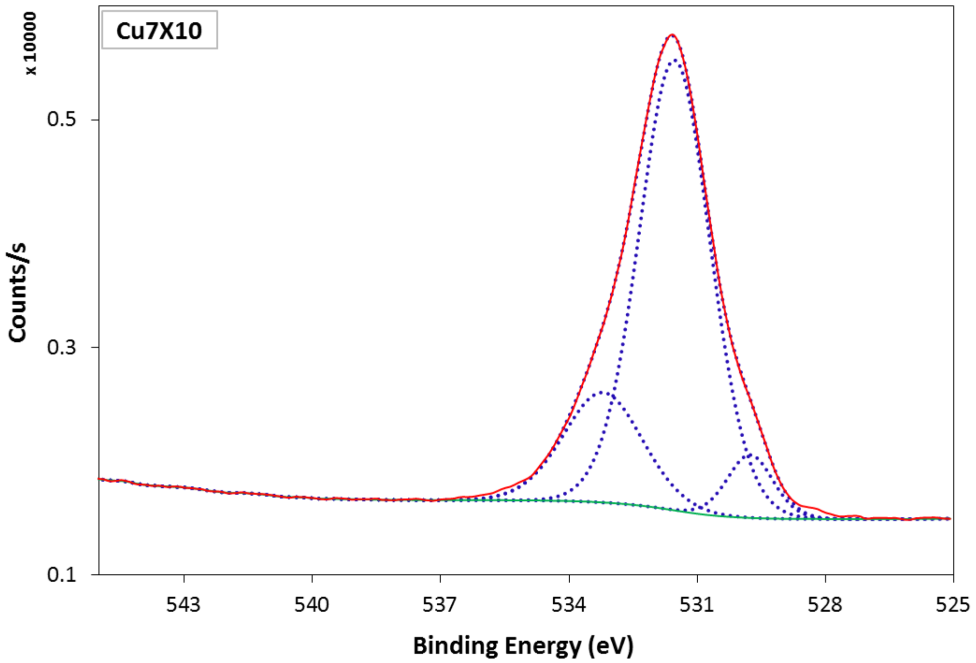

Figure A13. O 1s XPS high resolution spectrum of pyrite, activated with copper at pH 7 and conditioned with xanthate at pH 10.

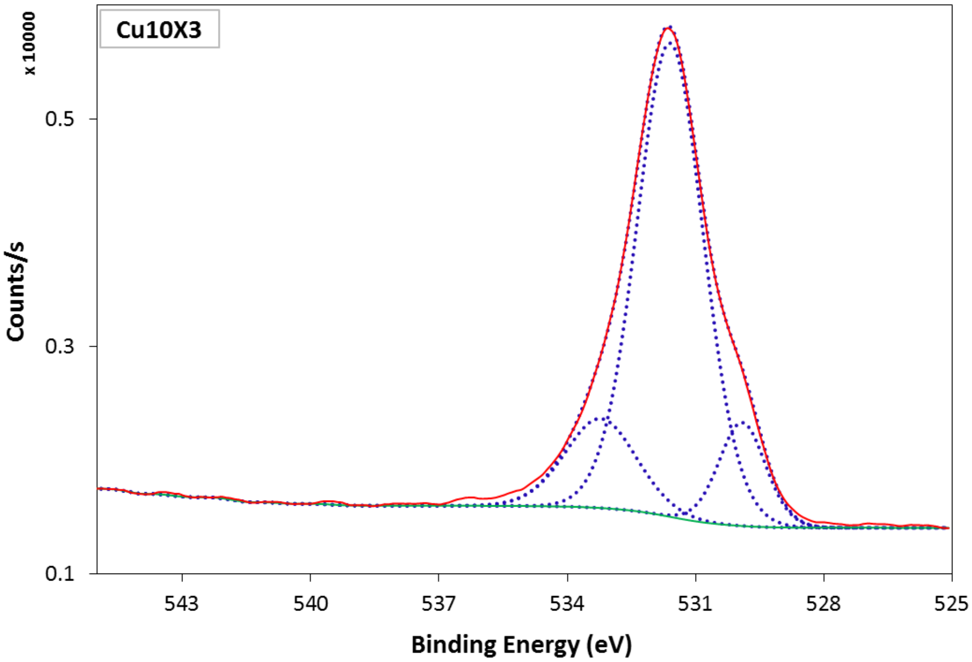

Figure A14. O 1s XPS high resolution spectrum of pyrite, activated with copper at pH 10 and conditioned with xanthate at pH 3.

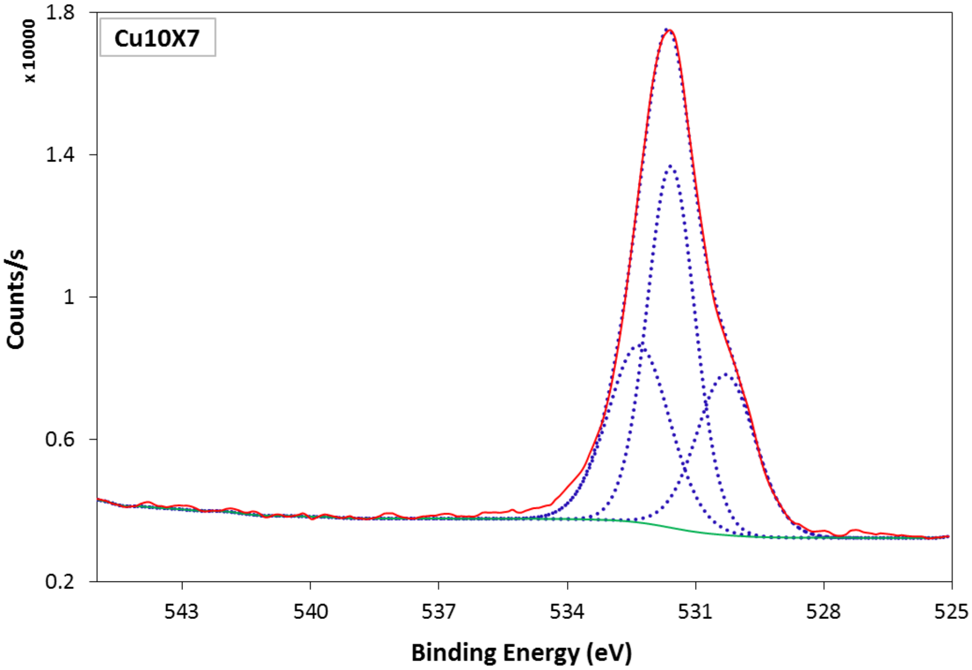

Figure A15. O 1s XPS high resolution spectrum of pyrite, activated with copper at pH 10 and conditioned with xanthate at pH 7.

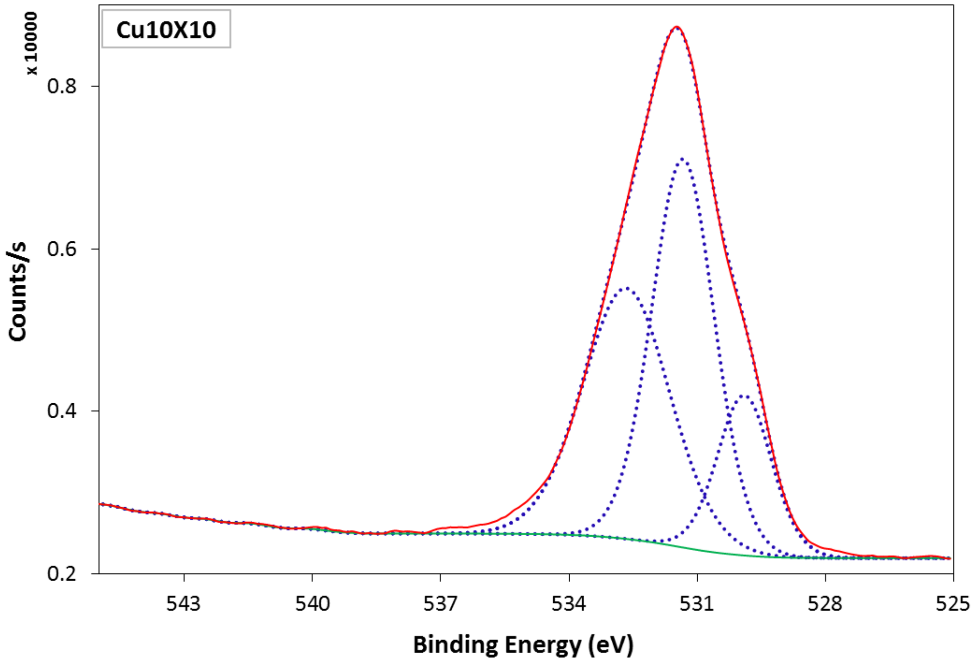

Figure A16. O 1s XPS high resolution spectrum of pyrite, activated with copper and conditioned with xanthate at pH 10.

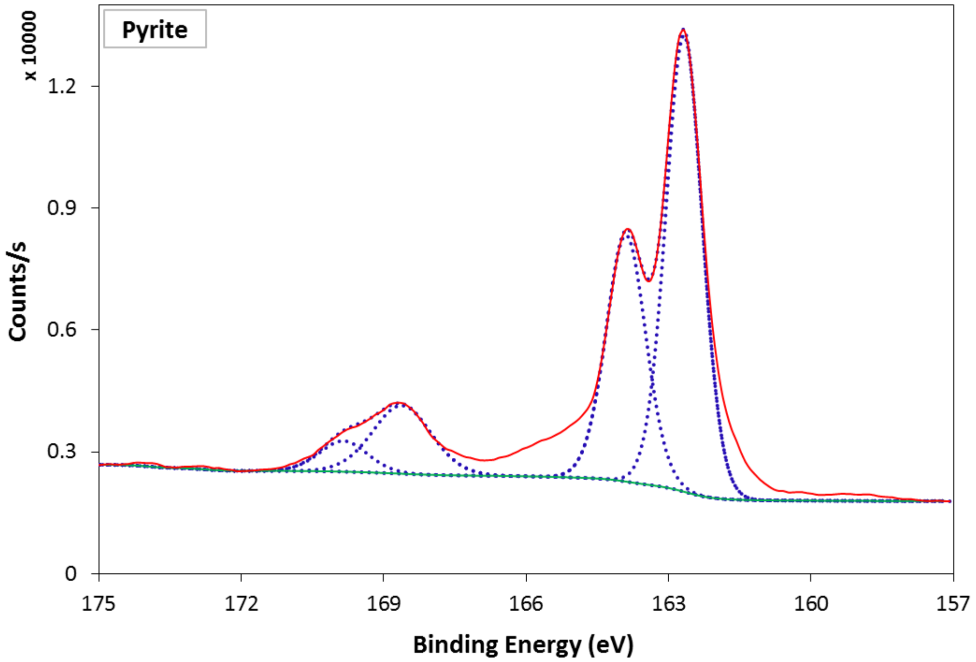

Figure A17. S 2p XPS high resolution spectrum of untreated pyrite.

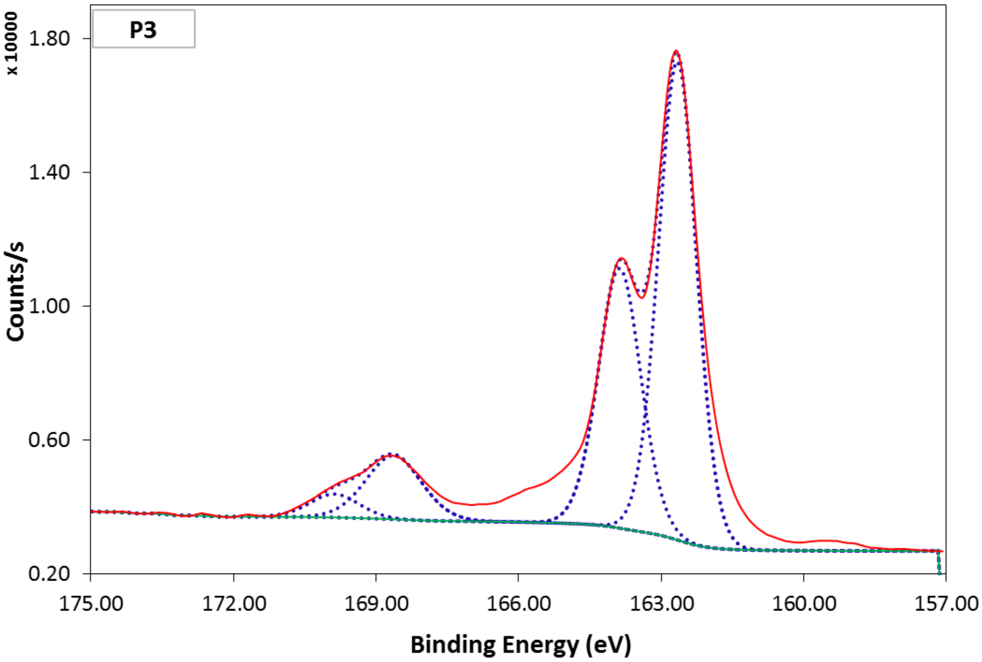

Figure A18. S 2p XPS high resolution spectrum of pyrite, treated in water at pH 3.

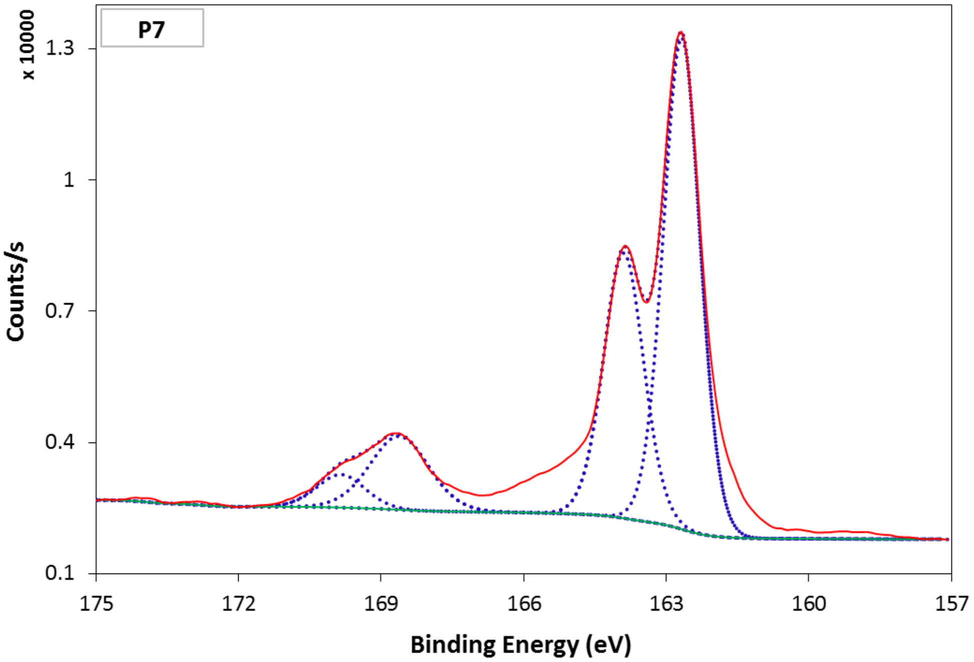

Figure A19. S 2p XPS high resolution spectrum of pyrite, treated in water at pH 7.

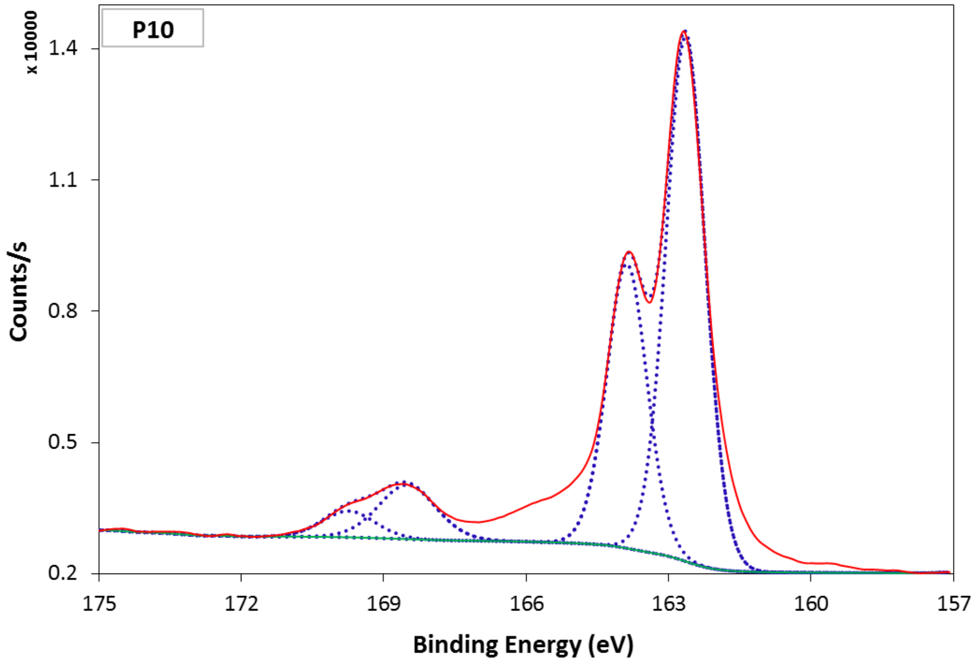

Figure A20. S 2p XPS high resolution spectrum of pyrite, treated in water at pH 10.

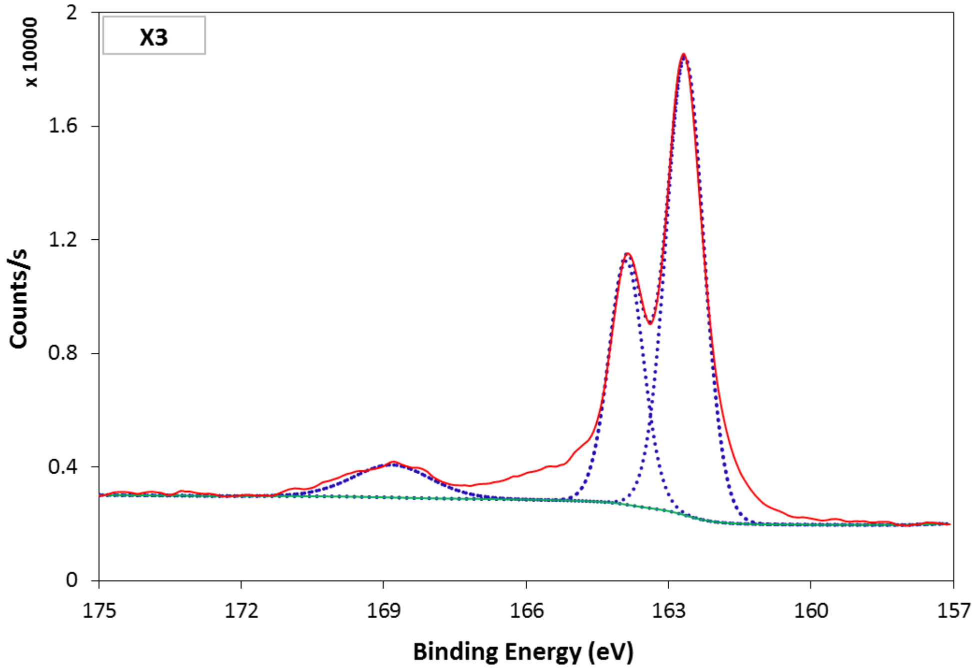

Figure A21. S 2p XPS high resolution spectrum of pyrite, conditioned with xanthate at pH 3.

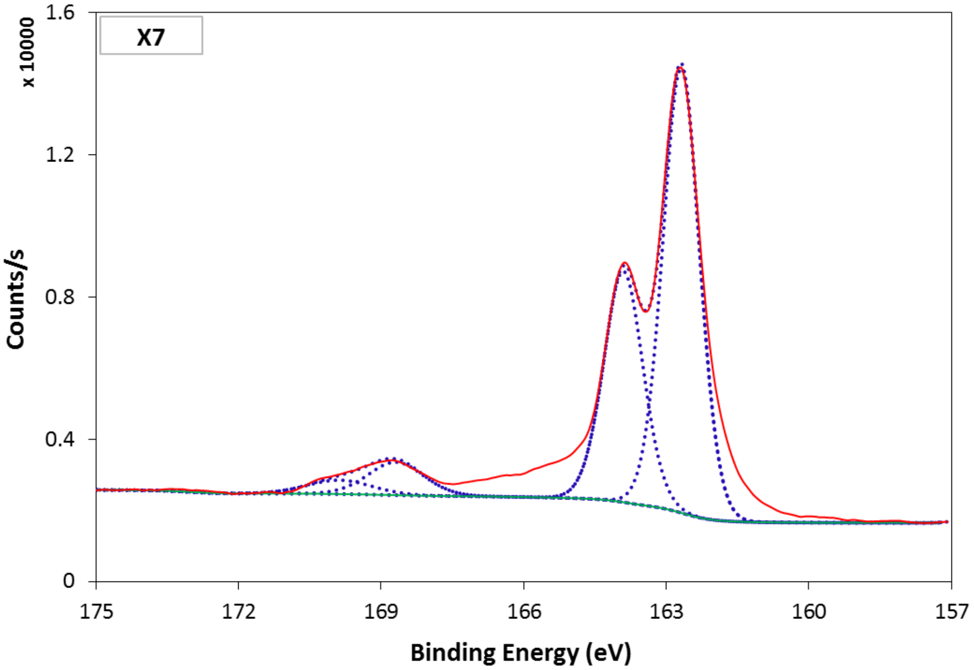

Figure A22. S 2p XPS high resolution spectrum of pyrite, conditioned with xanthate at pH 7.

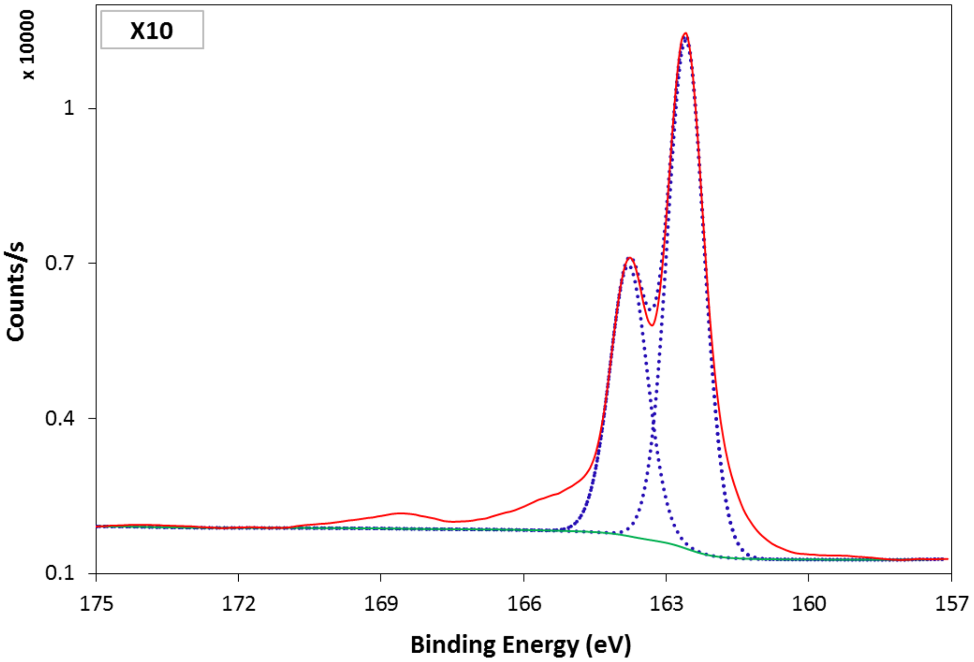

Figure A23. S 2p XPS high resolution spectrum of pyrite, conditioned with xanthate at pH 10.

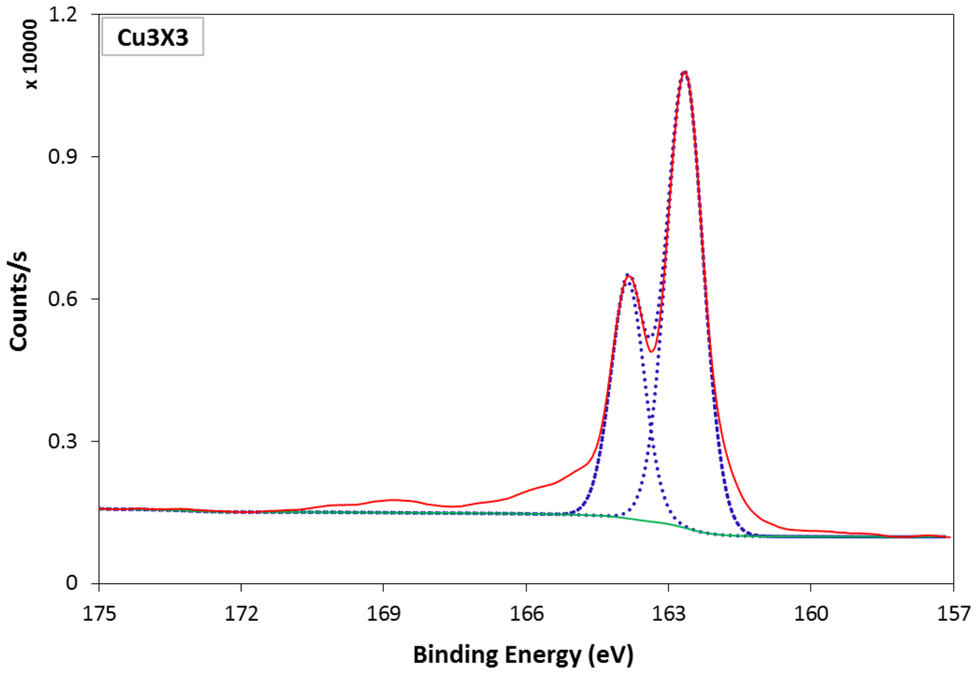

Figure A24. S 2p XPS high resolution spectrum of pyrite, activated with copper and conditioned with xanthate at pH 3.

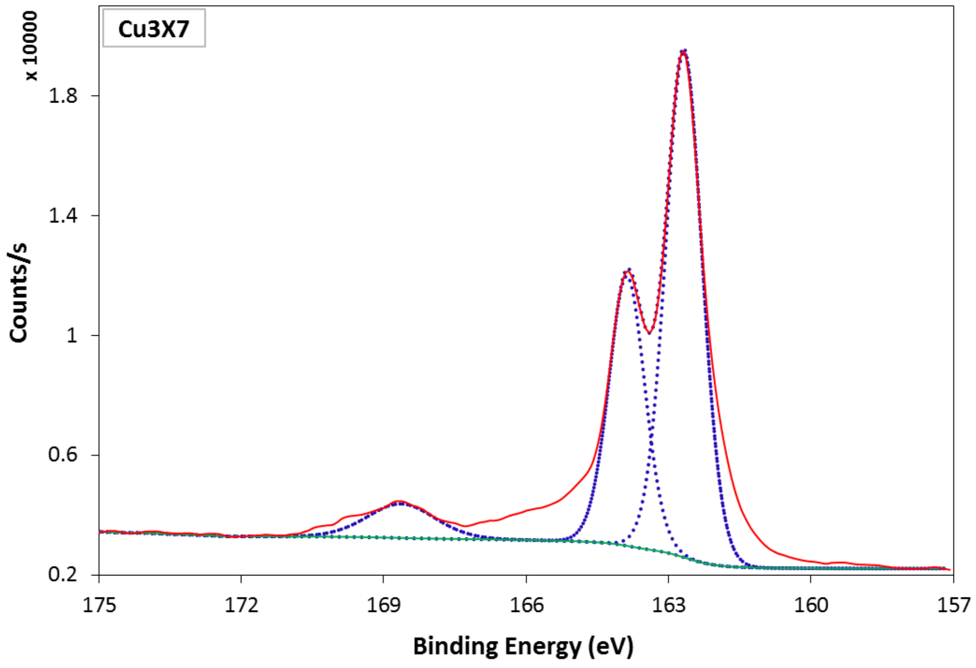

Figure A25. S 2p XPS high resolution spectrum of pyrite, activated with copper at pH 3 and conditioned with xanthate at pH 7.

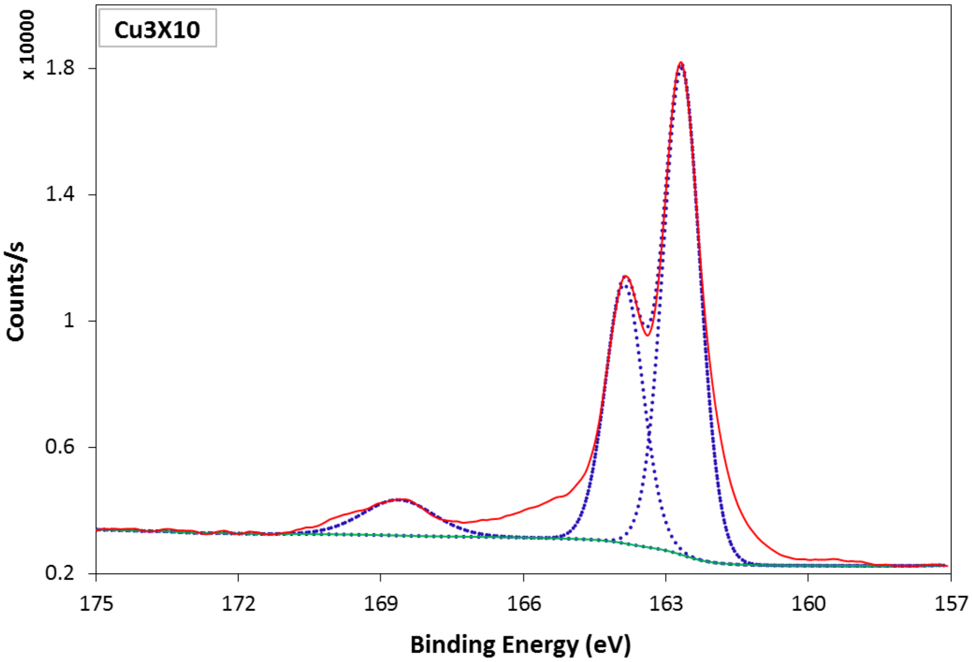

Figure A26. S 2p XPS high resolution spectrum of pyrite, activated with copper at pH 3 and conditioned with xanthate at pH 10.

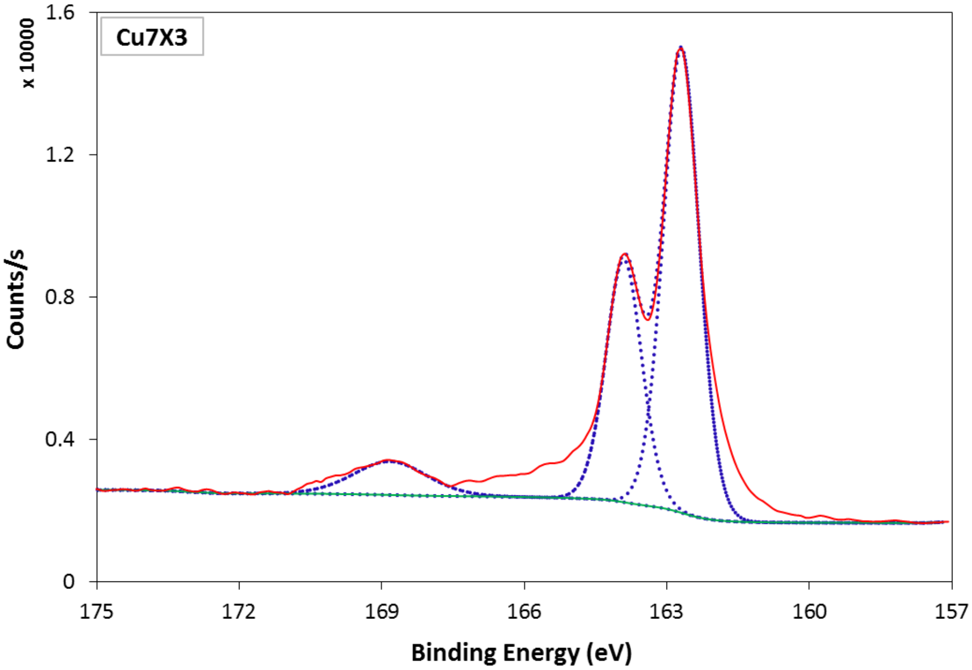

Figure A27. S 2p XPS high resolution spectrum of pyrite, activated with copper at pH 7 and conditioned with xanthate at pH 3.

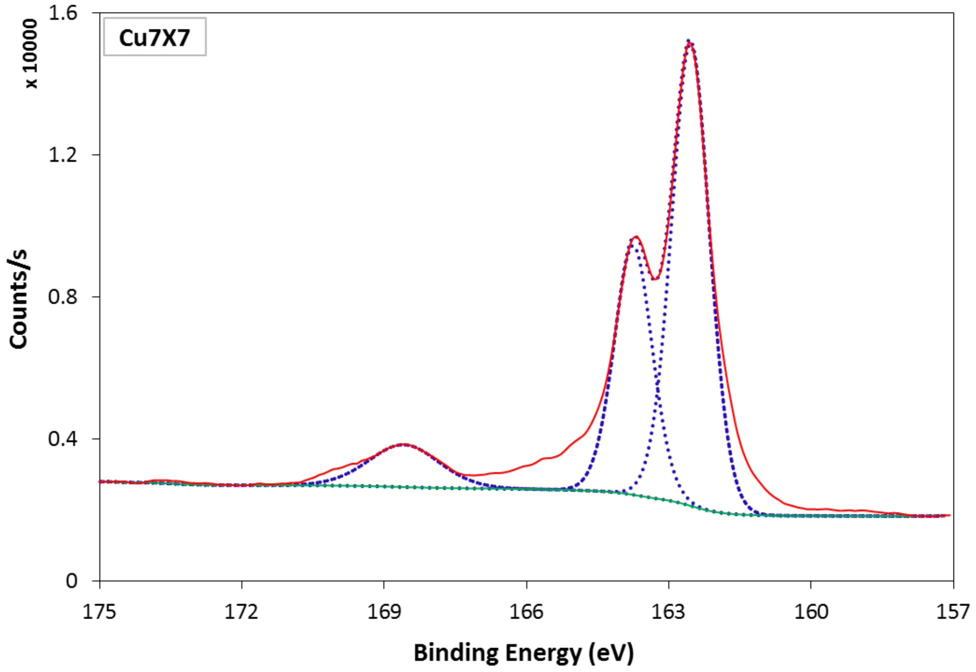

Figure A28. S 2p XPS high resolution spectrum of pyrite, activated with copper and conditioned with xanthate at pH 7.

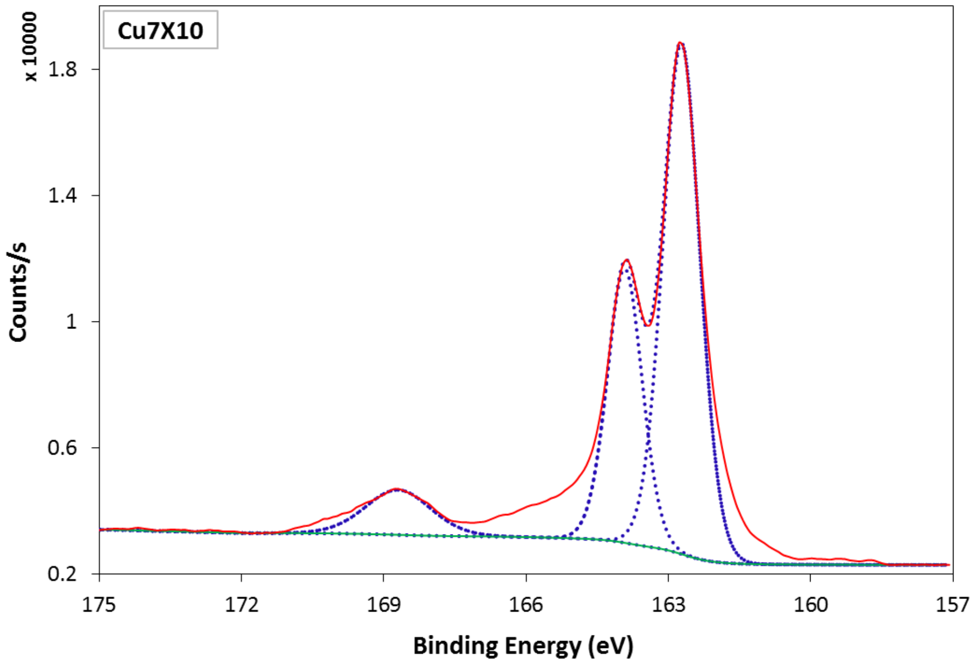

Figure A29. S 2p XPS high resolution spectrum of pyrite, activated with copper at pH 7 and conditioned with xanthate at pH 10.

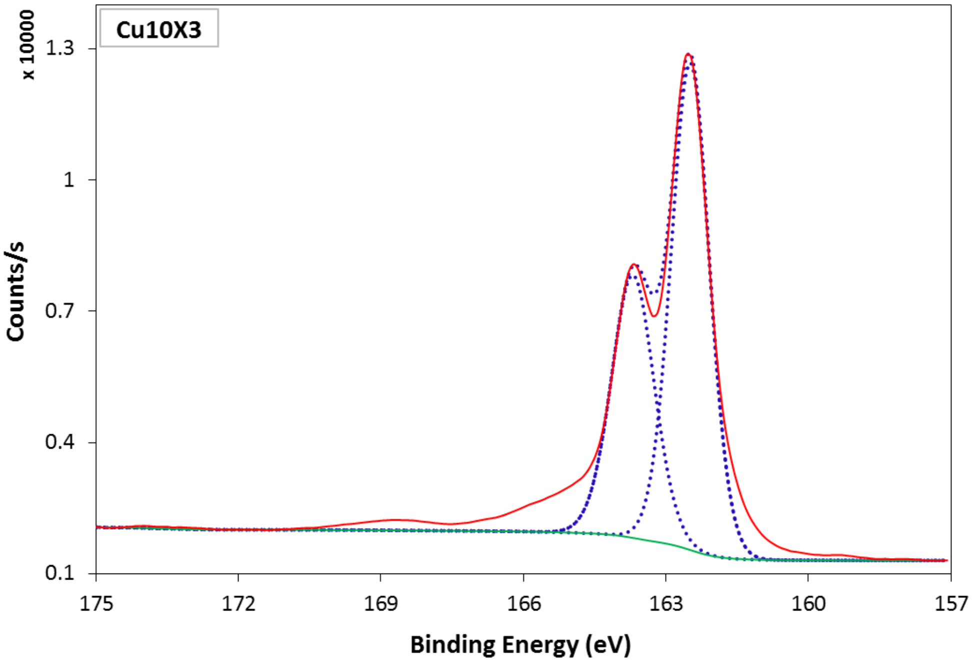

Figure A30. S 2p XPS high resolution spectrum of pyrite, activated with copper at pH 10 and conditioned with xanthate at pH 3.

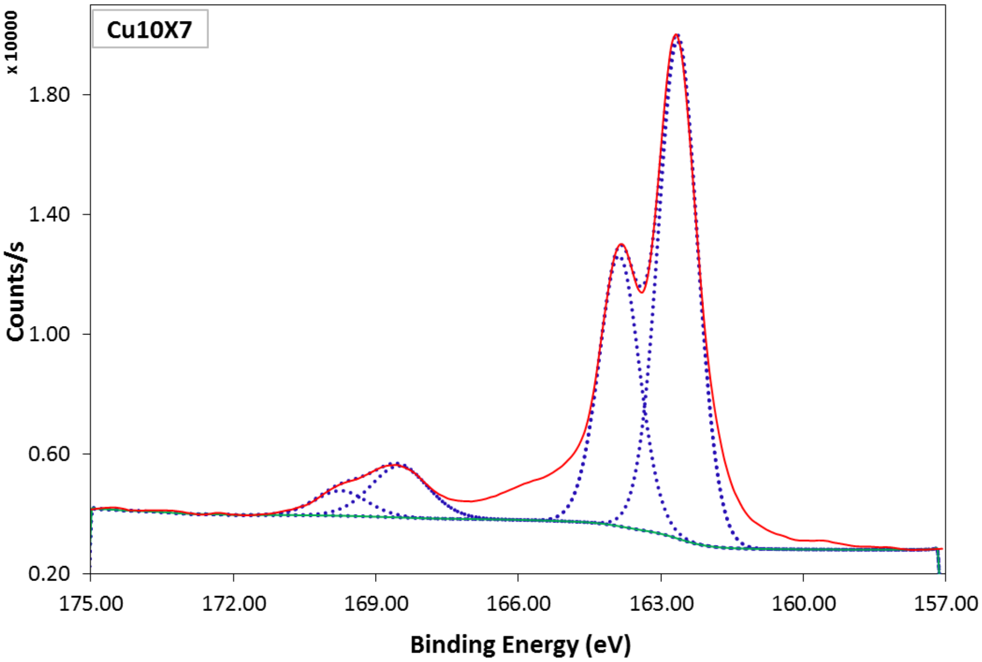

Figure A31. S 2p XPS high resolution spectrum of pyrite, activated with copper at pH 10 and conditioned with xanthate at pH 7.

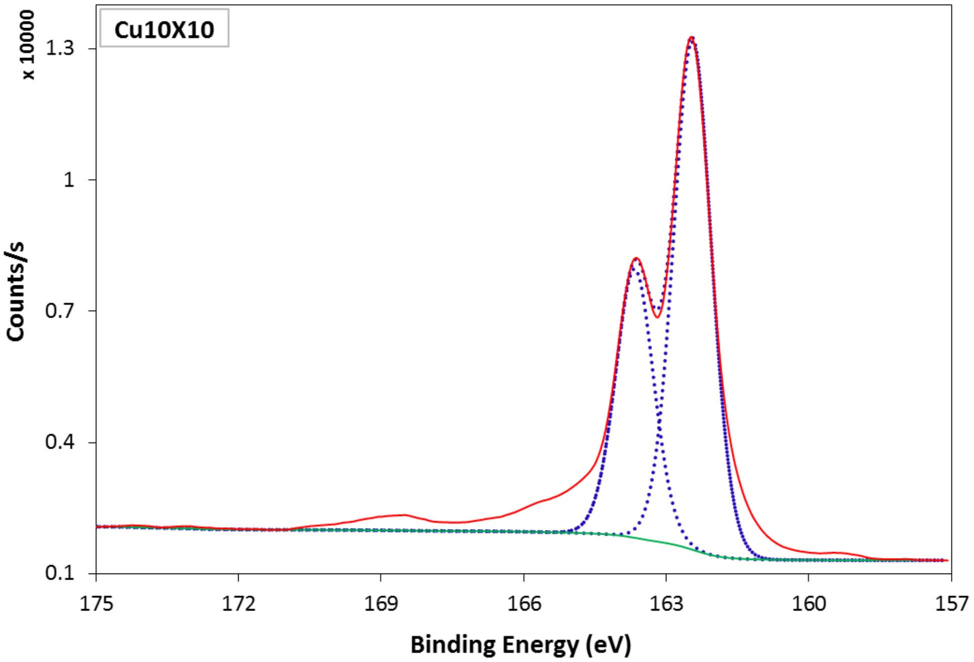

Figure A32. S 2p XPS high resolution spectrum of pyrite, activated with copper and conditioned with xanthate at pH 10.

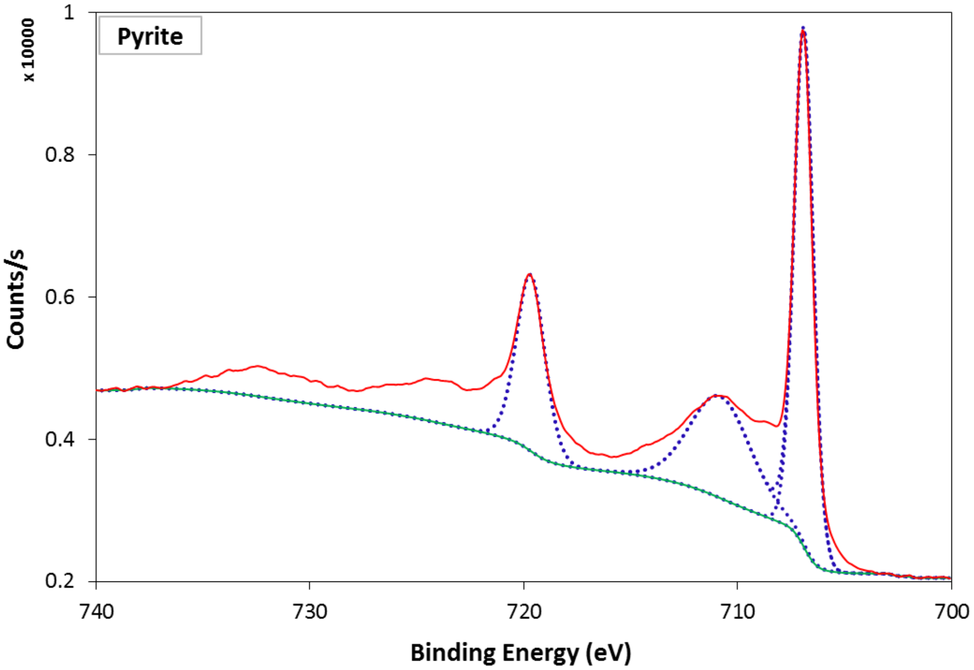

Figure A33. Fe 2p XPS high resolution spectrum of untreated pyrite.

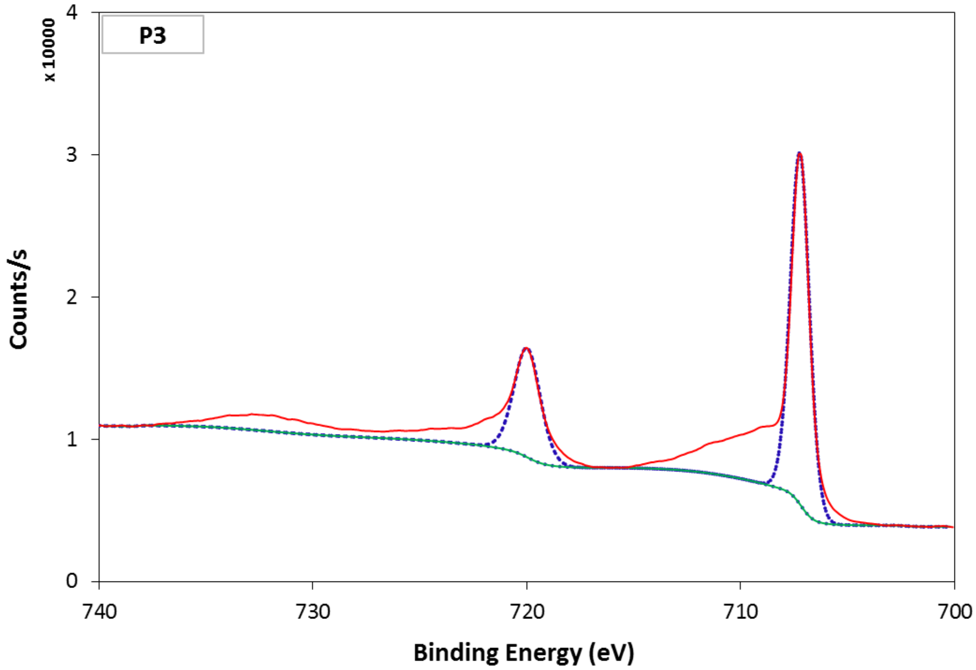

Figure A34. Fe 2p XPS high resolution spectrum of pyrite, treated in water at pH 3.

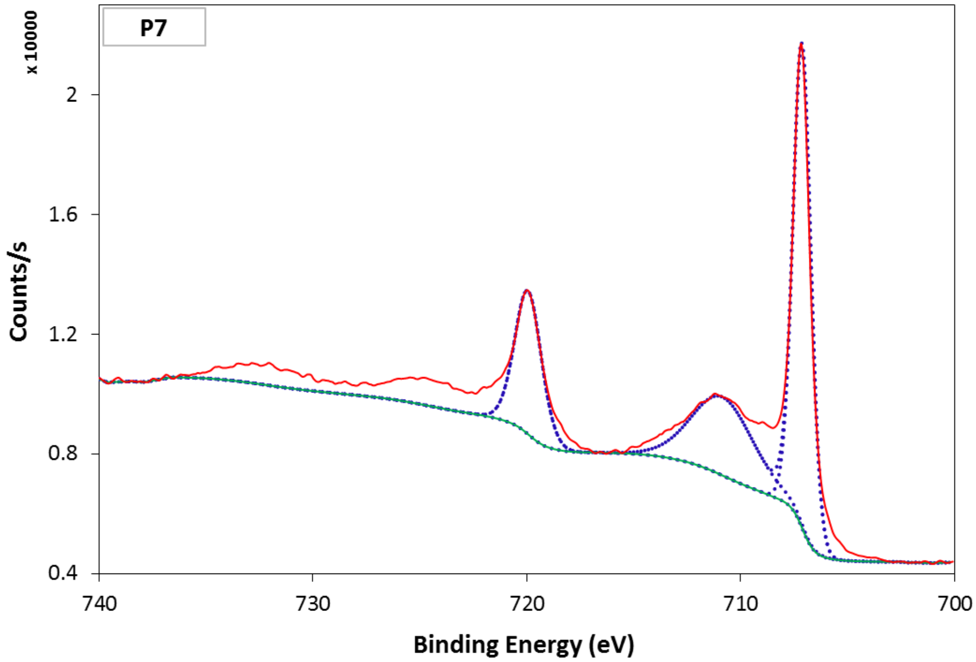

Figure A35. Fe 2p XPS high resolution spectrum of pyrite, treated in water at pH 7.

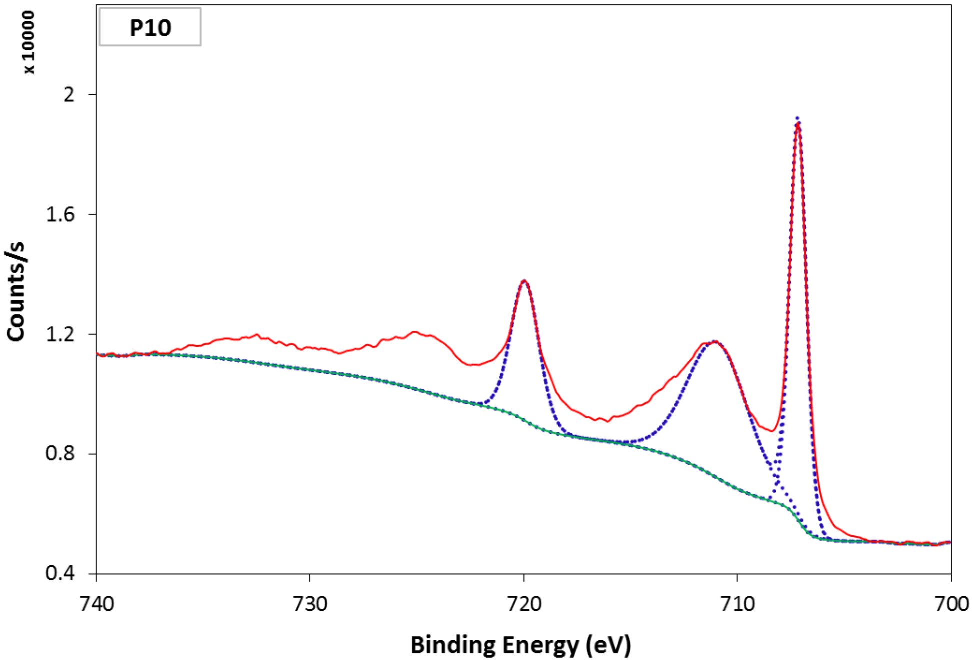

Figure A36. Fe 2p XPS high resolution spectrum of pyrite, treated in water at pH 10.

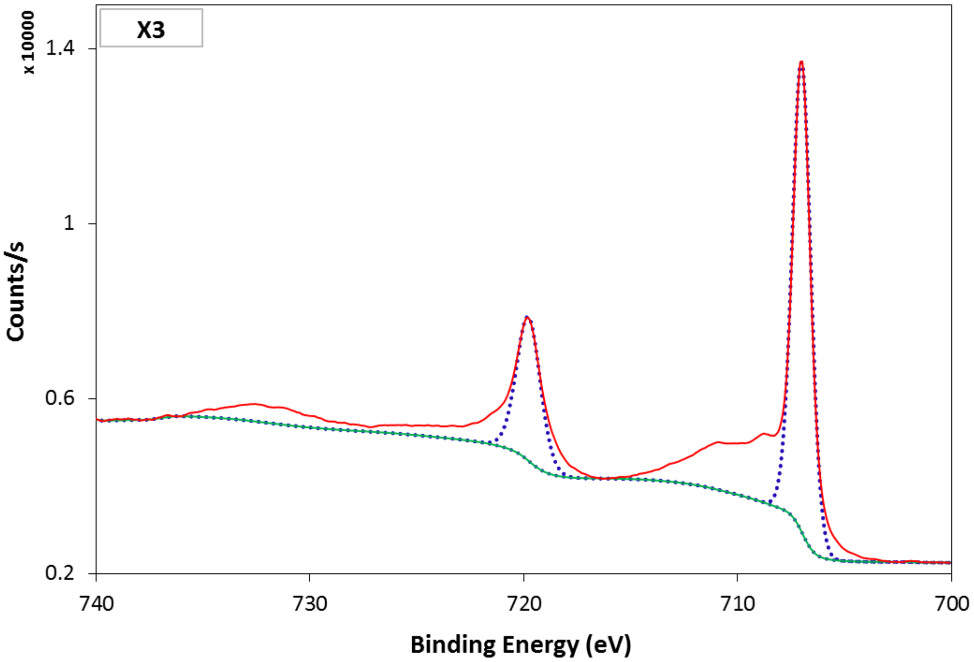

Figure A37. Fe 2p XPS high resolution spectrum of pyrite, conditioned with xanthate at pH 3.

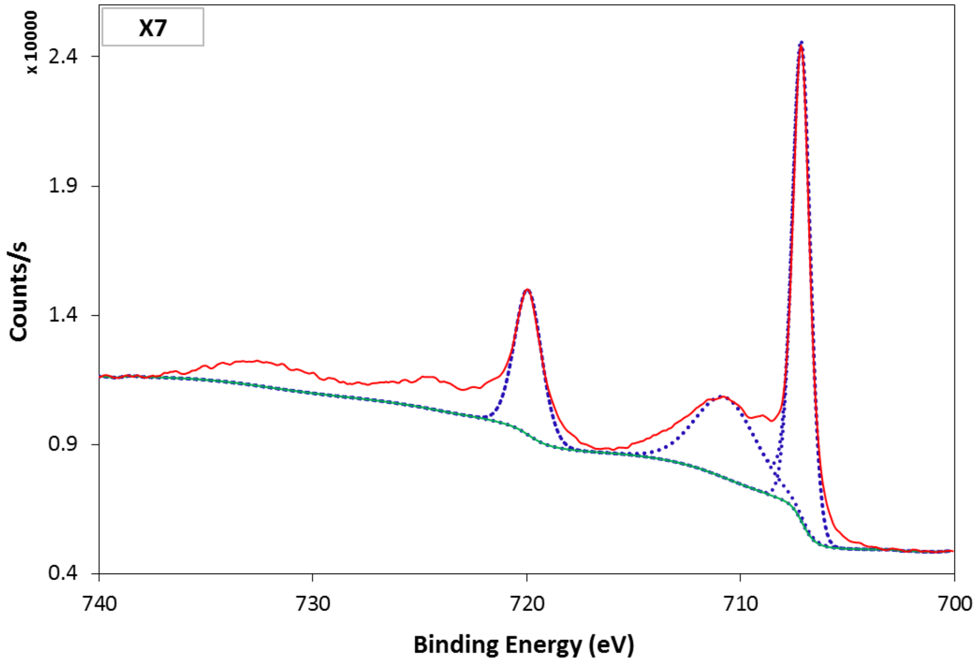

Figure A38. Fe 2p XPS high resolution spectrum of pyrite, conditioned with xanthate at pH 7.

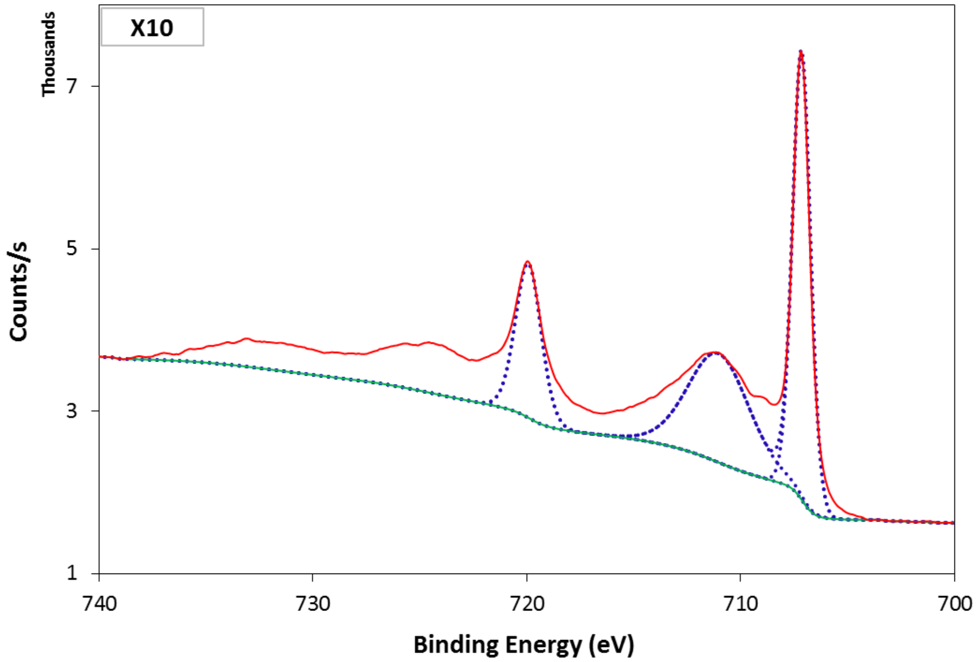

Figure A39. Fe 2p XPS high resolution spectrum of pyrite, conditioned with xanthate at pH 10.

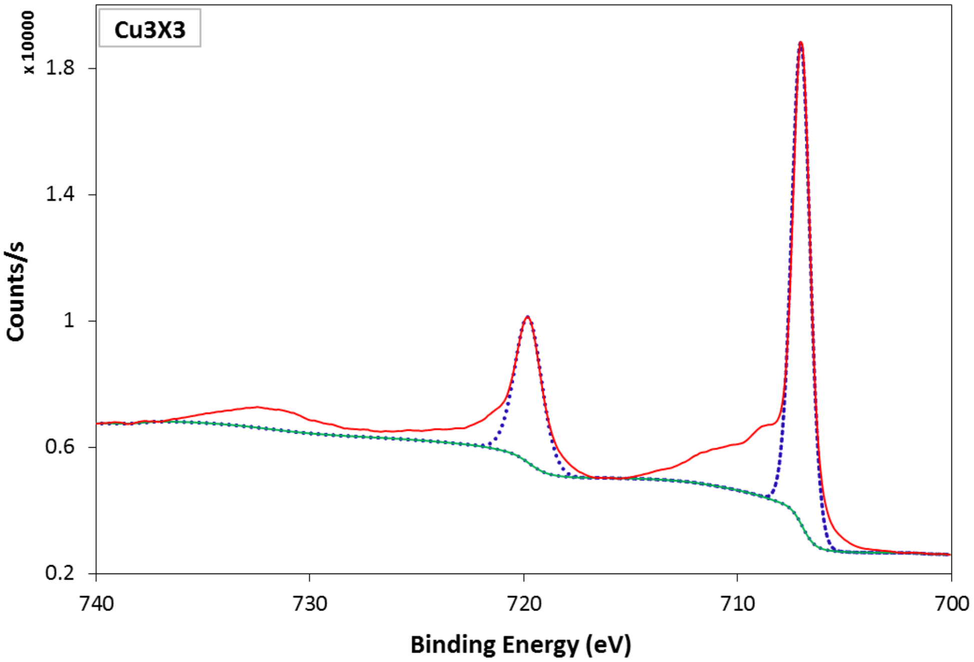

Figure A40. Fe 2p XPS high resolution spectrum of pyrite, activated with copper and conditioned with xanthate at pH 3.

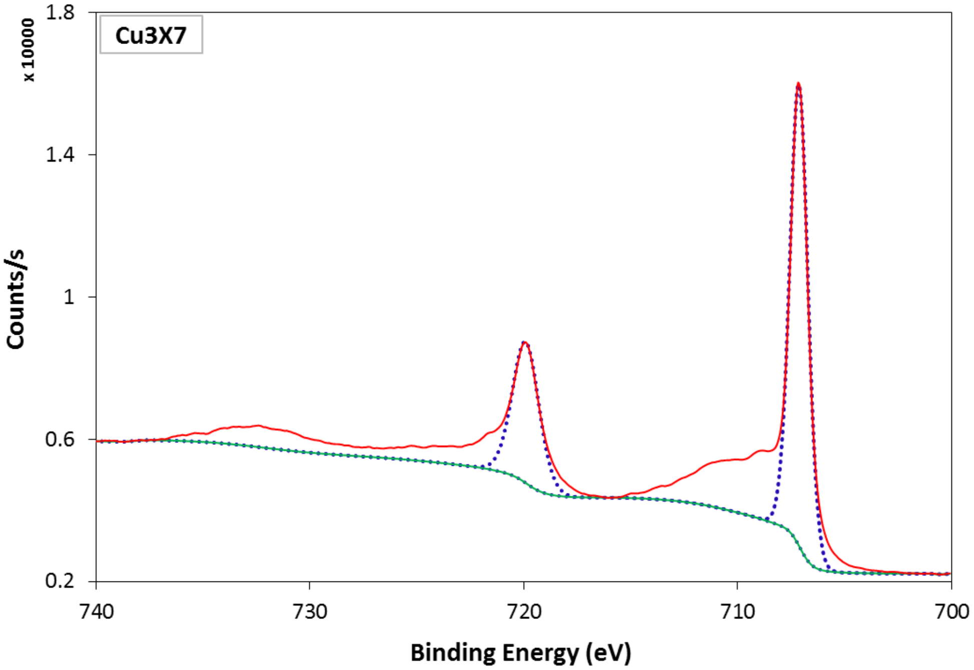

Figure A41. Fe 2p XPS high resolution spectrum of pyrite, activated with copper at pH 3 and conditioned with xanthate at pH 7.

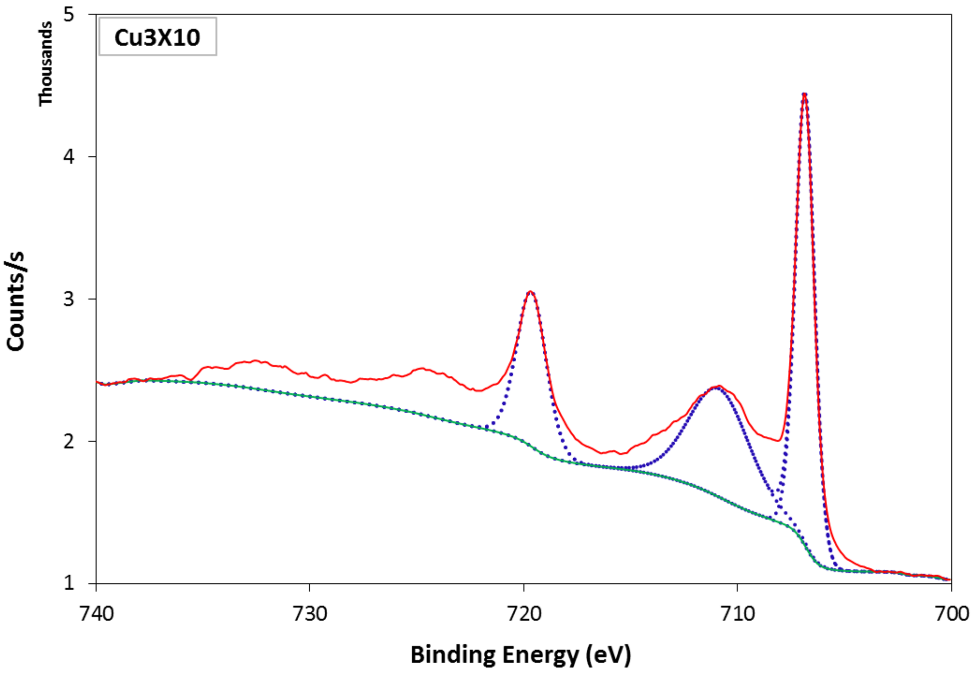

Figure A42. Fe 2p XPS high resolution spectrum of pyrite, activated with copper at pH 3 and conditioned with xanthate at pH 10.

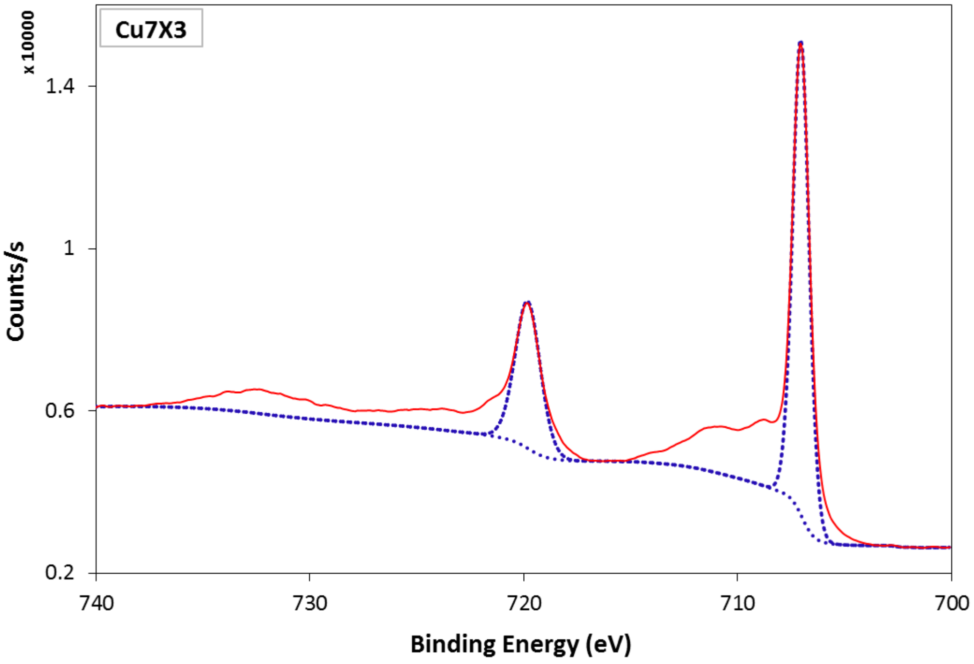

Figure A43. Fe 2p XPS high resolution spectrum of pyrite, activated with copper at pH 7 and conditioned with xanthate at pH 3.

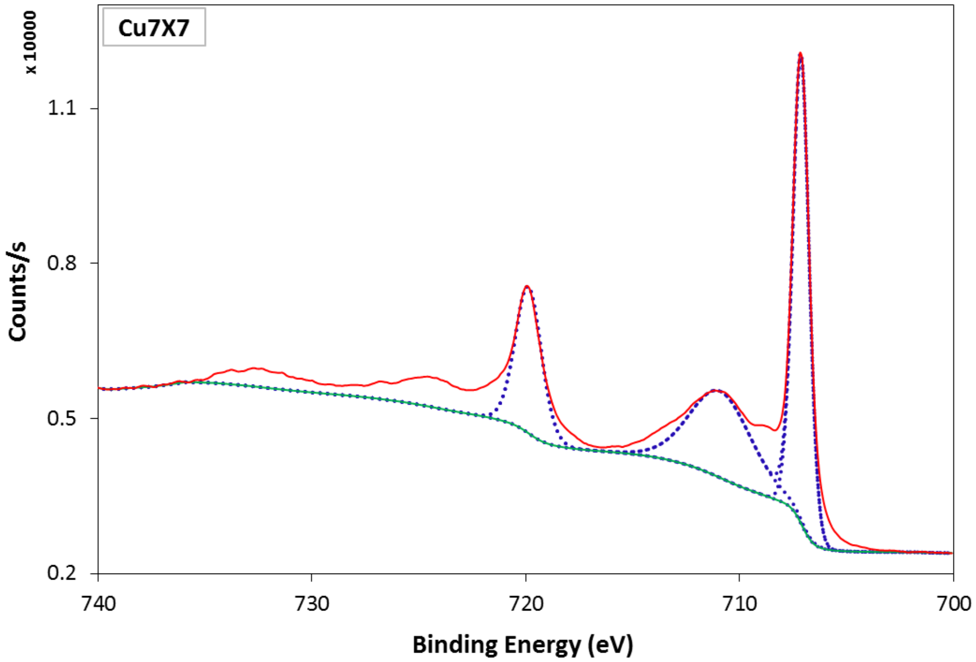

Figure A44. Fe 2p XPS high resolution spectrum of pyrite, activated with copper and conditioned with xanthate at pH 7.

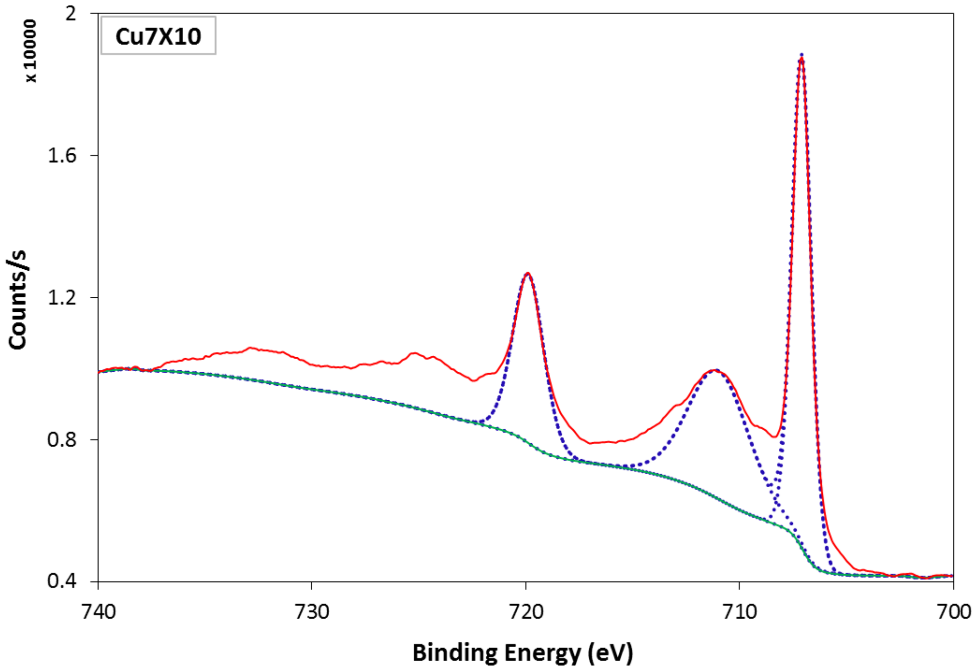

Figure A45. Fe 2p XPS high resolution spectrum of pyrite, activated with copper at pH 7 and conditioned with xanthate at pH 10.

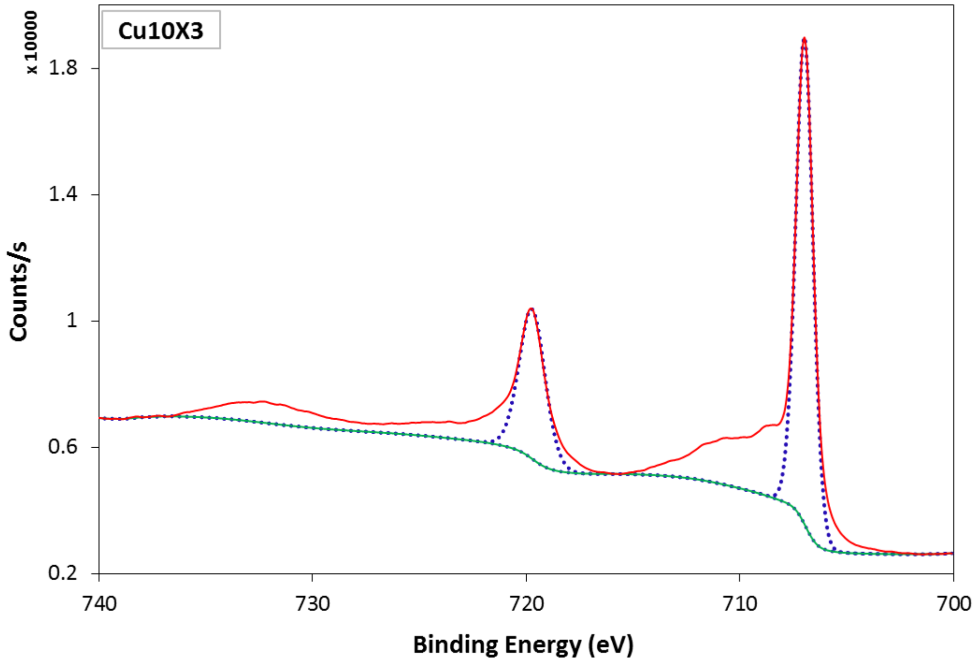

Figure A46. Fe 2p XPS high resolution spectrum of pyrite, activated with copper at pH 10 and conditioned with xanthate at pH 3.

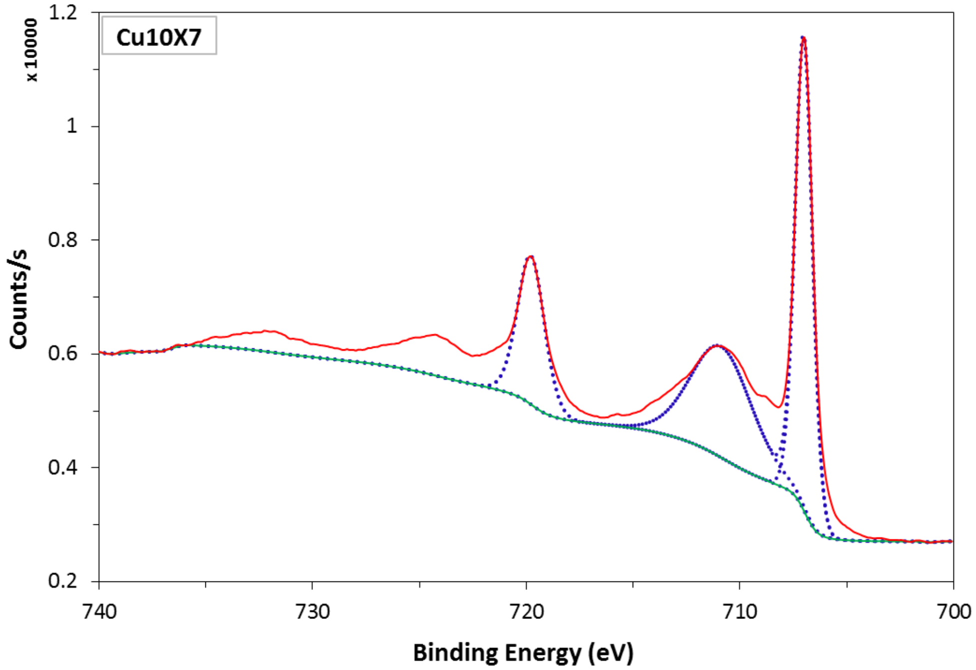

Figure A47. Fe 2p XPS high resolution spectrum of pyrite, activated with copper at pH 10 and conditioned with xanthate at pH 7.

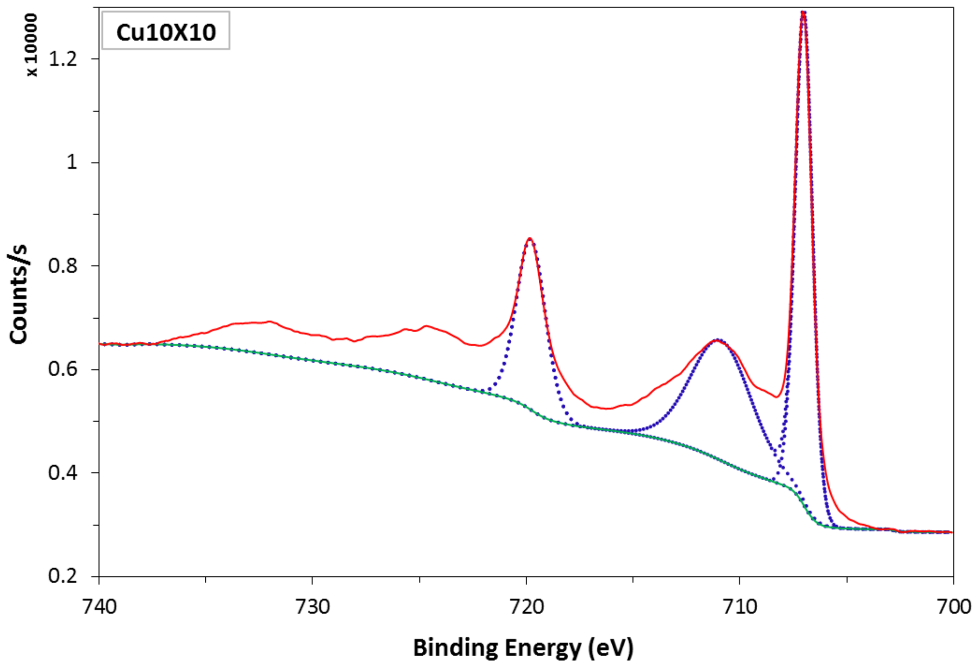

Figure A48. Fe 2p XPS high resolution spectrum of pyrite, activated with copper and conditioned with xanthate at pH 10.s